NTNU
Innovation and Creativity

Large-scale wind power integration in Nordland

Tarjei Benum Solvang

Master of Science in Energy and Environment
Submission date: June 2007
Supervisor: Olav B Fosso, ELKRAFT

Norwegian University of Science and Technology
Department of Electrical Power Engineering

Problem Description

The thesis will focus on challenges related to integration of large scale wind power in Nordland, Norway. It is planned to build two wind farms located at Sleneset and Sjonfjellet. The performance of these wind farms should be investigated under different operating conditions.

The following activities must be included in the study:

Establish a steady-state and dynamic grid model of the system

Investigate if it is possible to operate these wind farms with maximum generation in different system configurations.

Transformer tap changers can be an important element in voltage and reactive power control in systems. The influence of these components in the grid should be investigated.

The system impact of alternative wind farm control strategies should be investigated.

These activities are partly a continuation of the project work done in 2006. However, based on the experiences with the existing model, it is found necessary to re-establish the network model to better capture the characteristics of the network for the dynamic system simulation.

Assignment given: 15. January 2007
Supervisor: Olav B Fosso, ELKRAFT

Preface

This master thesis has been written at the Department of Electrical Engineering at the Norwegian University of Science and Technology (NTNU) during the spring of 2007. It is mandatory and has been carried out during the 10th semester of the master study. This thesis represents the end of the master study.

The project is a continuation of a steady-state analysis performed by Norsk Systemplan og Enøk AS (NORSEC) for Nord-Norsk Vindkraft AS (NNV). This project deals with dynamic problems regarding large-scale wind power integration in Nordland. The theme of this project is closely related to a project performed during the autumn of 2006. The earlier project can, from an educational point of view, be considered as a pre-project to this project.

I would like to thank Norsk Systemplan og Enøk AS at Fauske, for letting me work with my project there for some weeks during the spring of 2007, and for guidance during the work.

I would also like to thank SINTEF Energiforskning AS and especially Trond Toftevaag, for providing me with important technical data and for helpful discussions and guidance during all of the phases of this project. Without the frequent correspondence between Trond Toftevaag and the SIMPOW support-team in Västerås Sweden, the result would not have been the same.

In addition, I would like to thank my subject teacher Prof. Olav B. Fosso for important help and guidance during all the phases of this project.

Trondheim 19. June 2007

Tarjei Benum Solvang

Abstract

Introduction

Nord-Norsk Vindkraft AS is planning to build two wind farms in Nordland, Norway. The wind farms are located at Sleneset and Sjonfjellet. The planned total installed power is 653 MW.

An important part of the planning phase is to perform steady-state and dynamic analyses, to simulate the impacts from the wind farms on the existing power system in the area. The steady-state analysis is performed by Norsk Systemplan og Enøk AS (NORSEC). The project presented in this master thesis is part of the dynamic analysis.

Research objective

The overall objective for this project is to illustrate the dynamic impacts from the wind farms on the existing power system and the differences in impact depending on the various control strategies being used.

The following elements are included in the assignment:

- Establish a steady-state and dynamic grid model describing the power system in question.
- Determine whether the wind farms are able to reach full production during different configurations without reaching an unacceptable operating state.
- Examine the impact from and behaviour of transformers with load tap changers.
- Illustrate the differences between different control modes in the wind farm connection point.

Report outline

This report can roughly be divided into three sections. The first section consists of chapter 2 and 3. Here, a short presentation of the power system in the area and the specific wind farms is given. Background theory considered to be relevant for the analyses performed is also included. The aim of this section is to provide the reader with information which can be helpful when reading the results and conclusions.

The second section is chapter 4. This section describes the modelling of the power system models used in the simulations in this project. A description of the basic steady-state model employed in the steady-state analysis is also provided. This section is included to explain the choices and assumptions which are made for this project, and the methods which are used. Thus, this part of the thesis illustrates how the results are obtained.

The third section consists of chapter 5, 6 and 7. In this section the simulated scenarios are described, the most important results are presented and the results of the simulations are discussed. The discussion ends with the conclusions that are to be drawn from this project and some recommendations for further work.

Modelling

The model used in this project is established by converting the steady-state model used in the steady-state analysis from Netbas to SIMPOW. The time in the steady-state model is set to January 2009.

The steady-state model is then expanded by introducing aggregated doubly-fed induction generators for power production in the wind farms. For some of the simulations, a static VAR compensator is inserted at Bardal.

The dynamic model is established by introducing a dynamic description of the components in the steady-state model. Due to lack of dynamic data, typical values are used for some of the components.

Results and conclusions
The comparison between the power flows from the basic model provided by NORSEC and the initial converted SIMPOW model show small differences in reactive power flow. These differences were, however to be expected, due to changes made when converting the model from Netbas to SIMPOW but are not considered important for the conclusions to be drawn from the project.

Simulations describing an increase in wind power production from 50% to 100% are performed on the dynamic model describing the grid between Salten and Tunnsjødal. The timeframe of increase varies depending of the objective for the specific case.

The simulations performed on the dynamic model indicate a need for reactive power compensation between the wind farms and the connection point at Nedre Røssåga. Without reactive power compensation on the radial connection, the wind farms are not able to reach full wind power production without breaching either voltage or thermal limits. This is the case even if local compensation is added at the wind farms.

With an SVC in voltage control placed at Bardal, the wind farms are able to reach full power production without violating any specified limits. The SVC maintains acceptable voltage levels within the radial. However, the amount of imported reactive power at the connection point increases during the production increase. This causes a depression in voltage in the rest of the grid.

If the SVC at Bardal is set to control the reactive power flow in the connection point, simulations indicate that the amount of reactive power drawn from the main grid can be considerable reduced. This, however, results in a larger need for reactive power production within the radial. A larger reactive power production increases the voltages. Without voltage control at the wind farms or voltage regulation by load tap changers, the simulations show that the voltage at the generator terminals increases above 1.05 pu.

Simulations demonstrate that tap-operations in the transformer at the connection point between the main grid and the wind farm radial increases the amount of imported reactive power. This takes place when the SVC operates in voltage control. The need for reactive power production within the radial is then reduced. The tendency is the same whether voltage control is introduced at the wind farms or not.

When the SVC operates in reactive power control and no voltage control is present at the wind farms, tap-operations from the same transformer result in an increase in reactive power production within the radial. However, if voltage control is included at the wind farms, tap-operations at the connection point will decrease the reactive power production. This is because in voltage control the wind farms are consuming reactive power in order to maintain a specified terminal voltage.

The results from the simulations indicate that the number of tap-operations from the transformer at the connection point is reduced when the SVC at Bardal operates in reactive power control compared to when it operates in voltage control. However, no wind models based on statistics are introduced in this project. It is therefore uncertain to what extent a similar result would be obtained under more realistic conditions.

All the simulations show that when the production from the wind farms increases, the voltages in the grid outside the radial decreases. This is due to increased reactive losses. The decrease is largest when the SVC at Bardal operates in voltage control due to reactive power drawn by the radial connection. The area in the main grid with the largest decrease is located between the connection point at Nedre Røssåga and Trofors.

Further work
This project is only a part of the necessary dynamic analyses that have to be carried out in the planning phase for the wind farms at Sleneset and Sjonfjellet. A natural continuation of this project could be to perform analyses in a light load situation, and analyses of the system's response to disturbances. Wind models obtained from statistical wind data should also be included in future dynamic analyses.

Table of contents

1 Introduction

1.1 Motivation

Due to good wind conditions in northern Norway, several wind farms are planned in the region. However, the situation in the power system in this region is characterized by a surplus of both power and energy. The power produced by wind power will therefore mainly be transported out of the region.

The introduction of considerable amounts of new power production into a power system can result in challenges regarding voltage levels, thermal limits and stability. A fluctuating power source like wind power introduces additional challenges connected to reactive power compensation, fluctuations in active and reactive power and control strategies. It is therefore necessary to do thorough steady-state and dynamical analyses to map the impacts of the planned new production on the existing power system.

This master thesis concentrates on challenges related to the introduction of two wind farms in Nordland, Norway.

1.2 Background

Nord-Norsk Vindkraft AS (NNV) plan to erect two wind farms located in Nordland. The wind farms are located at Sleneset and Sjonfjellet. An important part of the planning phase is to perform steady-state and dynamic analyses to map the impacts the wind farms have on the rest of the power system.

The steady-state analysis is performed by Norsk Systemplan og Enøk AS (NORSEC) for Nord-Norsk Vindkraft AS.

The model used in this project is based on the steady-state model developed by NORSEC.

1.3 Research Objective

The initial aim of this project was to perform dynamic analyses on the power system between Salten and Tunnsjødal when the planned wind power production is introduced to the system. However, many of the required analyses for planned wind farms falls under the term dynamic analyses. Therefore it was chosen to split the objective into minor but, more concrete objectives. The objectives examined in this project are described below.

The first objective of this project is to establish a dynamic grid model describing the power system in question, including a dynamic description of the wind farms. This will give the possibility to perform the desired dynamic analyses. The established dynamic model should be such that it could provide the basis for possible future analyses beyond the scope of this project. In order to be able to perform dynamic analyses, a basis steady-state model is needed. This model should be based on the model employed in the steady-state analysis.

The second objective is to determine whether the wind farms are able to operate with maximum generation and whether additional reactive power compensation is needed. The aim is to keep the system within specified limits during the simulations.

Transformers with load tap changers can be an important factor in order to maintain acceptable voltages within a power system. However, they can also cause large problems in highly loaded grids. Therefore an aim of this project is to evaluate the behaviour of transformers with load tap changers related to the wind farms.

It is stated in the guidelines concerning requirements for grid connection of wind power plants that a wind power plant should be able to operate in two different control modes. An objective of this project is therefore to illustrate the differences between these two control modes and how they affect the rest of the power system in different ways.

Some of the analyses could perhaps have been performed on a smaller dynamic model without loosing credibility regarding the results. However, since the steady-state model is of a certain size, it was decided to use the same model for the dynamic simulations. This will improve the ability to compare the results obtained from the steady-state calculations with the results of the dynamic calculations.

1.4 Report Outline

This thesis is written with the intention to guide the reader chronologically through the project and to present the performed work in a form which gives good readability and overview over the obtained results. Below follows a description of the different parts of this thesis.

In chapter 2 a short description of the project in question is given. The power system included in the model and the two planned wind farms are presented. A presentation of the planned grid connection is also given.

Chapter 3 presents the background theory considered relevant for this project. More theory related to power system analysis and wind power production could have been included. However, even though the locations of the wind farms are different, this project can be considered a continuation of a project performed by the author during the autumn of 2006. That project was to a larger degree a literature study. The theory presented there is also relevant for the analysis performed in this project. The project report written for the pre-project is included in Appendix E of this project.

In chapter 4 the modelling of the steady-state and dynamic model is presented. This chapter includes a description of the steady-state model used in the steady-state analysis performed by NORSEC. It includes a description of the initial established steady-state SIMPOW model together with a comparison of the two steady-state models. The expansions made to the initial steady-state model and the modelling of the dynamic model is presented here. Problems encountered during the establishing of the SIMPOW models are also described.

A description of the simulated scenarios and a presentation of obtained results are given in chapter 5. The simulations are split in different cases, each describing a specific situation. The various cases are again gathered in sections describing similar cases. In order to improve the readability of the results, a short discussion is contained in this chapter. Including a detailed discussion chapter after the presentation of the results was therefore considered unnecessary.

In chapter 1, a general discussion and a summary of the most important results is given.

In the final chapter, the conclusions to be drawn from the work that has been carried out in this project and recommendations for further work are presented.

In order to further illustrate the work that has been performed in this project, some test simulations are placed in appendix. This includes test simulations illustrating the behaviour of the doubly-fed induction generator and test simulations describing the performance of two dynamic load tap changer regulators.

Calculations performed during the establishing of the model are placed in appendix along with the input values of the different regulators used.

Due to the size of the model, a lot of different parameters are monitored during the simulations. Not all of these responses are considered to be important for the discussion. Therefore, diagrams describing these responses are placed in an electronic appendix. This is also the case for model files and output files.

1.5 Prerequisites, Assumptions and Simplifications

A number of prerequisites, assumptions and simplifications are made during the course of this project. Most of them are presented at relevant locations in the report. However, some are inherited from the steady-state analysis and are not listed elsewhere than here. In order to provide an overview over the different prerequisites, assumptions and simplifications, a short listing is given below.

1.5.1 General

- This project does not include traditional stability analyses, like studies investigating small-signal stability and transient stability.
- The grid connection alternative obtained from the steady-state analysis is the only grid connection alternative investigated.
- The power exchange towards Sweden is disregarded.
- The power exchange towards north at Salten is considered constant.

1.5.2 Modelling and Simulations

- Simulations are only performed with both of the wind farms built and operational.
- The largest generator alternative is chosen for Sjonfjellet, resulting in a total wind farm capacity of 428 MW.
- Simulations are only performed on one type of generator in the wind farms. However, this generator can operate in different modes.
- Simulations are only performed on a heavy load situation in the grid.
- Standardized parameters are used as dynamic data for synchronous generators.
- A DC excitation system is used for voltage regulation of the synchronous generators.
- Only transformers in the radial connection towards the wind farms are equipped with dynamic load tap changer regulators.
- The connection point between the wind farms and the rest of the grid is considered to be at Nedre Røssåga.

2 Presentation of Power System and Wind Farms

2.1 Today's Grid

The main grid in the area treated in this project consists of voltage levels at 300 kV and 420 kV. Between Tunnsjødal and Nedre Røssåga there are two transmission lines at 300 kV. At Nedre Røssåga the voltage level is transformed up to 420 kV, and from Nedre Røssåga, one 420 kV transmission line goes north to Balsfjord in Troms. North of Balsfjord the main grid is at 132 kV. The grid analysed in this project does not go further north than the region of Salten in Nordland. [1] [2]

The regional grid between Tunnsjødal and Salten is mainly at a 132 kV voltage level. However, some parts are at a 66 kV level. The map below shows the regional and main grid between Helgeland and the southern part of Salten. [2]

Figure 2.1: Main and regional grid between Tunnsjødal and Salten, from [2]

In the area between Tunnsjødal and Salten there is normally a large surplus of both power and energy. Total installed power capacity is 2862 MW, while the total available power capacity during the winter is 2335 MW. The capacity is quite evenly distributed between the two regions of Helgeland and Salten. [2]

The main part of the production is concentrated in large hydro power plants located in Kobbelv, Svartisen, Nedre Røssåga, Øvre Røssåga and Kolsvik. The load in the area is approximately 1346 MW with the largest part located in Helgeland. The largest consumers are Straumen (Elkem Salten), the city of Bodø, Rana (Mo Industripark) and Mosjøen (Elkem Aluminium). [2]

The distribution between production and load in the area is shown in Figure 2.2.

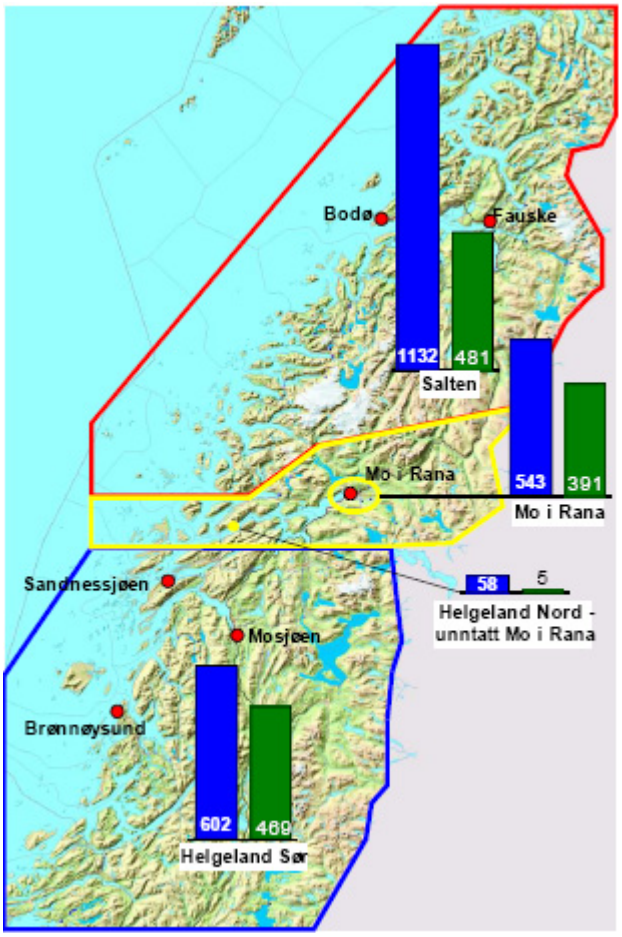

Figure 2.2: Distribution of production and load within the area, from [2]

The blue columns show the maximum available power capacity during the winter, while the green columns show the maximum measured load. All numbers are in MW. [2]

2.2 Sleneset Wind Farm

One of the two planned wind farms analysed in this project is located at Sleneset in Lurøy municipality in Nordland. For this wind farm, an application for concession has already been sent to the relevant authorities. [3]

According to the application, the wind farm will have a total capacity of 225 MW divided on either 75 wind turbines with 3 MW capacity, or 50 wind turbines with 4.5 MW capacity. A final decision regarding the size of the turbines will not be made until the final investment decision. This is due to the on-going development of wind turbine technology and the uncertainty of the time-frame for the project. [3]

The geographical location of the wind farm at Sleneset is shown in Figure 2.3.

Figure 2.3: Location of the wind park at Sleneset, from [3].

Preliminary calculations estimate an energy production of 675 GWh each year, provided a capacity of 225 MW. [3]

For further information regarding this wind farm, see [3].

2.3 Sjonfjellet Wind Farm

The other planned wind farm treated in this project is located at Sjonfjellet in the municipalities Nesna and Rana in Nordland County. This wind park is at an earlier stage of planning than Sleneset. So far, only a notification of the planning has been published. [4]

A preliminary assessment suggests that it would be possible to build approximately 120 wind turbines with a capacity of 3 MW each at Sjonfjellet. This would give a total capacity of 360 MW and an energy production of approximately 1100 GWh each year. Another possibility would be to increase the size of the turbines to 4.5 MW. These larger turbines will require longer distance between them. Considering the park area and wind conditions, it would then be possible to build up to 95 wind turbines. This would give a total capacity of 428 MW and a yearly energy production of 1300 GWh. [4]

The geographical location of the wind farm at Sjonfjellet is shown in Figure 2.4.

Figure 2.4: Location of the wind park at Sjonfjellet, from [4]

A final decision regarding the size of the turbines has not been taken for this project either. Such a decision will not be made until the final investment decision. As for the farm at Sleneset, this is due to the on-going development of wind turbine technology and the uncertainty of the time-frame for the project. [4]

For further information regarding this wind farm see [4].

2.4 Grid Connection of Wind Farms

A prerequisite for the building of these wind farms is that they are connected to already existing parts of the regional or main grid. Between the wind farms and these connection points, new transmission lines have to be built or already existing ones have to be reinforced. There are several different alternatives for grid connection. These are listed in [3] and [4].

A preliminary steady-state analysis performed by NORSEC concludes that the best economical solution is to connect both of the wind farms to the 300 kV grid in Nedre Røssåga. [2]

Figure 2.5 shows the planned route for the transmission lines and power cables. The planned route is marked in red. A single line diagram which includes voltage levels and distances are given in Figure 5.1 in chapter 5.

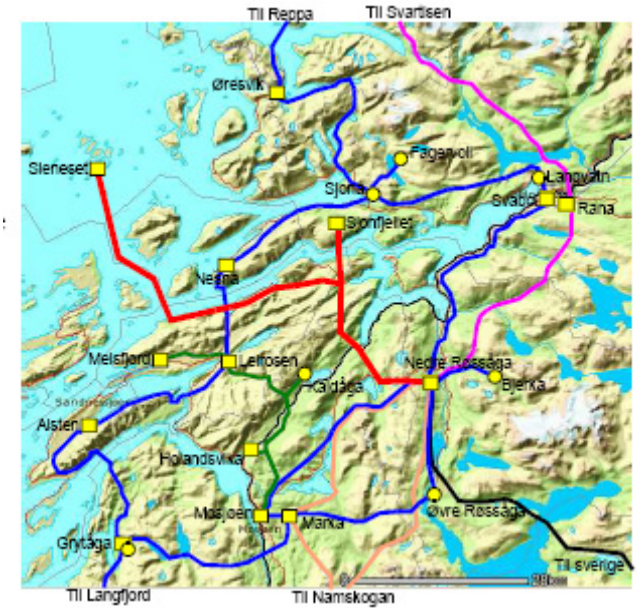

Figure 2.5: Grid connection for Sleneset and Sjonfjellet, from [2]

A prerequisite for this alternative is that both of the wind farms are built. [2]

For a more detailed description of the grid connection see [2].

3 Theory

3.1 Introduction

As mentioned in chapter 1, the project described in [5] can in many ways be considered a pre-project to the project dealt with in this report. The latter concentrates more on the establishing of a grid model and simulations related to this, whereas a grid model was already in place for the pre-project and it was therefore to a larger degree a literature study. Theory describing power transmission, component characteristics, voltage and reactive power control, voltage stability and rules and regulations are presented in [5]. These topics are also relevant for the studies performed in this project. However, they are not presented here. The project report from the pre-project is included in Appendix E.

In addition, this project treats some subjects not included in the pre-project. Background theory regarding these elements is therefore included in the following sections.

3.2 Load Tap Changers

3.2.1 Introduction

The introduction of distributed production in the power grid results in a different power flow and voltage distribution compared with a traditional power grid with centralized production. It can be expected that this will result in new working conditions for transformers with load tap changers, especially if the power source is a fluctuating source like wind power. Transformers with load tap changers play a major part in both the modelling and the simulations done in this project. This chapter therefore describes aspects around transformers with load tap changers.

Almost all equipment used in a power system is designed for a particular voltage level, the rated voltage. If the system voltage deviates from this rated value, the performance of the device can be affected and its life expectancy might be reduced. This is a good reason for controlling the voltages in a power system. [6]

Another reason for controlling the voltages in a power system is that reactive power flows depend highly upon line-end voltages. Reactive power flows contribute, as well as active power flows, to line losses. By adjusting voltage levels to minimize reactive power flows, losses can be minimized. [6]

Common ways to control voltages in a power system are [6]:

- Excitation control of generators.
- Switched shunt capacitors and/or reactors. Step or continuous control.
- Synchronous condensers.
- Transformers with load tap changers.

Excitation of synchronous generators, switched shunt capacitors and reactors and synchronous condensers are described in [5] and are therefore not included in this report.

In the following section a description of transformers with load tap changers is presented. The impact of load tap changers in a power system is also included.

3.2.2 Description

The purpose of voltage control with regulating transformers is to compensate for load variations and events in the transmission system to keep the voltage level at the consumers within specified limits. [7]

The transformer performs voltage control by changing its turns ratio. This is done by placing taps on one or more windings of a transformer. This normally allows the ratio to vary in the range of ±10% to ±15%, with steps of 1% to 3%. There are two types of tap changing transformers: Off-load tap changing or under-load tap changing (the latter is referred to as LTC in this report). [8]

Transformers with off-load tap changers needs to be de-energized before tap changing can take place. Tap changing of such transformers are therefore limited to voltage regulation due to long-term variations. This can be load growth, system expansion or seasonal changes. LTC-transformers however, are used for more frequent regulation. These can, as the name signals, be used as voltage regulation without de-energizing the transformer. Normally, such regulation has been on a daily basis. [8]

The tap changing in LTC-transformers is automatic and operated by motors which respond to relays set to hold voltage at a prescribed level. The frequency of tap changes per day is minimized in order to prolong the life expectancy of the transformer. [9] According to [7], wear on the tap changers is the most common reason for transformer maintenance today. The reduction of tap changer operations is therefore highly desirable.

The focus of this project, and as a consequence also in this description, is on under-load tap changing transformers. Many of the same principles are however also applicable for off-load tap changers.

A sketch describing the principle of a transformer equipped with a tap changer is described in Figure 3.1.

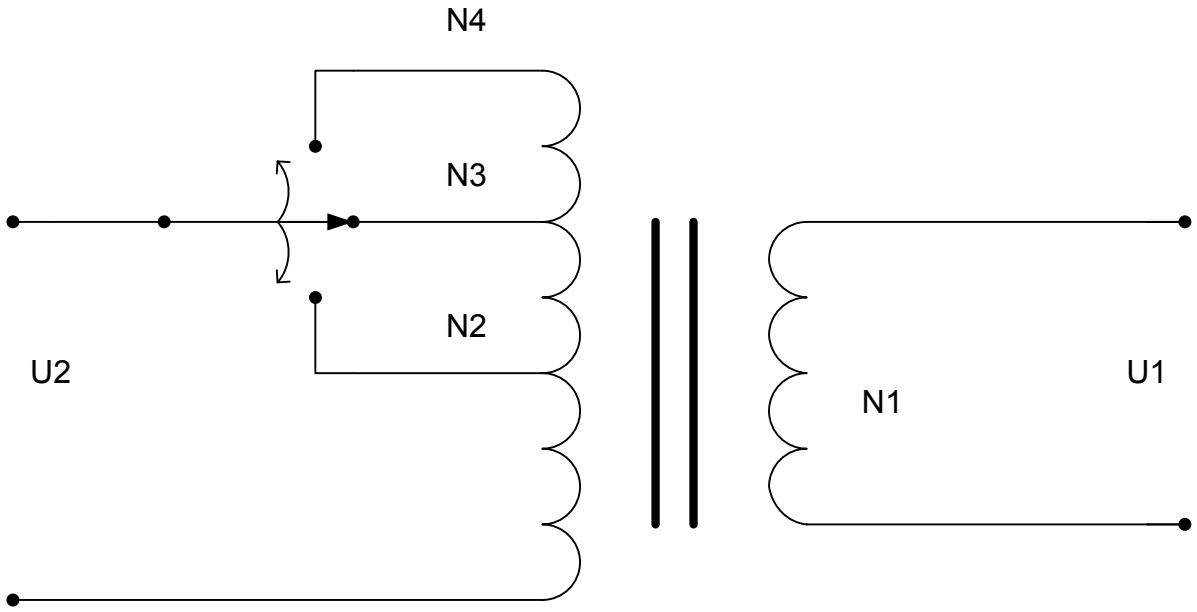

Figure 3.1: Principle of transformer with load tap changer

The voltage as a function of turns ratio will be as described by equation (3.1) [6].

$$U_1 = \frac{N_1}{N_N} \cdot U_2 \tag{3.1}$$

N_N represents the actual number of turns connected on the tap side.

3.2.3 Regulation by LTC-transformers

The theory for this section is mainly taken from [10]. If information is obtained from other sources it is specified.

In a radial grid the voltage regulation performed by LTC-transformers is often shared between 2 or 3 transformers connected in series from the main grid to the distribution grid. The tap changer is then normally located on the high-voltage side of the transformer. This is mainly because the high-voltage side has the lowest current.

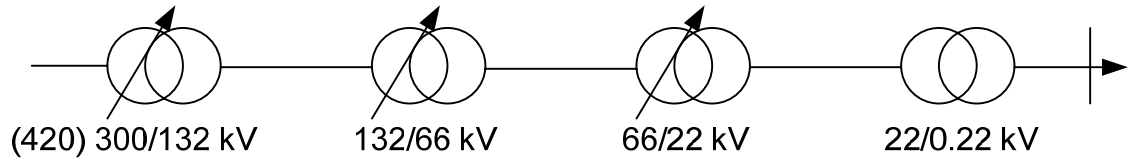

Figure 3.2: LTC-transformers at different voltage levels, based on [10]

The need for tap changing can come from different causes:

- The loads in the distribution grid have changed and therefore also the voltage distribution.
- The voltage in the main grid have changed, and thereby the voltages all the way down to the consumer.

In the first case, the change in voltage will be largest at the consumer. It will therefore only be the LTC-transformer on the lowest voltage level who will regulate. This is the desirable solution.

In the second case, the load tap changers at the different voltage levels might start to regulate at the same time. They will all then step in the same direction, and the result will be an overshoot in voltage at the lowest level. This causes more tap changing operations in order to get the voltage back to an acceptable level.

Since loads are often voltage sensitive, an overshoot will increase the loading on the transmission system. If the system is already operating close to its transfer or stability limits increased loading is highly undesirable. [7]

In order to avoid such problems, coordinated control of LTC-transformers is needed in a power system. [7]

Coordinated control of transformers with under-load tap changers is performed by adjusting parameters in the voltage regulator. In all voltage regulators connected to LTC-transformers there are at least 3 parameters that can be tuned:

- Desired voltage level, U_B
- Allowed voltage difference, ΔU
- Time delay, T

The allowed voltage difference, ΔU, is the maximum allowed difference in voltage in one direction between the measured voltage value and the desired voltage value before regulation is implemented. The distance in voltage from the maximum to the minimum allowed voltage value is called the dead band or insensitivity area. The dead band is therefore two times larger than ΔU.

The time delay, T, is the time between the registration of an unacceptable voltage value and the implementation of regulation.

In principle, both of the latter parameters can be used in order to obtain the desired selectivity between LTC-transformers at different levels. However, if the dead band is adjusted to create the desired selectivity, the dead band in the lowest voltage levels will be large, and this will result in a lower voltage quality for the consumers. Adjustment of the time delay is therefore the most common way to achieve the desired selectivity.

The setting of the allowed voltage difference in the voltage regulator decides how much the voltage will deviate from the reference value. The theoretic limit for this insensitivity is when the dead band equals the step size of the transformer. This is illustrated in Figure 3.3b. If the measured voltage is reduced to the lower limit, the voltage regulator will increase the voltage to the upper limit. This will result in an unstable situation. As a consequence, a prerequisite for stable regulation is that the dead band is larger than the step size of the transformer. A small difference between the dead band and the step size will result in a small difference between the end voltage value and the desired voltage value. However, the number of tap-operations will increase.

A common recommendation from suppliers of power system transformers is to set the dead band to 1.6 times the step size of the transformer. This is illustrated by Figure 3.3a.

Figure 3.3: Sensitivity-settings for the transformer regulator, based on [10]

If the same sensitivity is chosen for transformers at all voltage levels in a radial connection the selectivity will to a large degree be controlled by the time delays. However, since transformers can have different step sizes and since it will be incidental where within the dead band the different transformers is located at the time of a voltage depression, time delays will not control the selectivity completely.

Desired selectivity by adjusting the time delays is obtained by increasing the time delay from the highest voltage levels and down to the lowest levels. The highest voltage levels should have a time delay to prevent the regulator to respond to temporary changes in voltage. The increase in time delay between the different voltage levels should be large enough to allow a regulator to complete the tap-operation before another regulator starts to operate.

A recommended setting of the time delays at different voltage levels is to have a time delay of 30 seconds at the highest voltage level and 60 seconds at the next level. If a third level exists, this level can have a time delay of 120 seconds.

Most voltage regulators have a possibility to set the time delay in two different modes. The time delay can either be dependent or independent of the measured deviation in voltage. If the time delay is dependent of the voltage difference, an inverse time-characteristic is deployed. It will then react faster to larger voltage changes. However, during rapid depressions in voltage at the highest levels, the selectivity between the different levels can be poor. This can cause an unnecessary number of tap-operations and an overshoot in voltage at the lower levels. A basic sketch describing the two settings of a voltage regulator for a load tap changer is provided in Figure 3.4.

Constant time delay provides the best selectivity between the different levels. The most important thing during swift voltage depressions is however to restore the voltage at the consumer level. Time dependent time delays are therefore recommended.

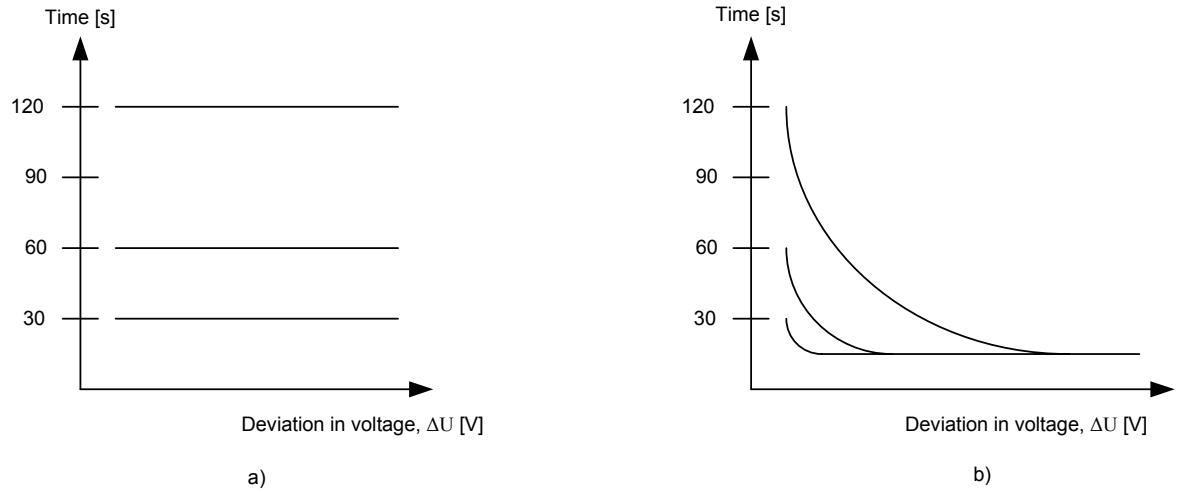

Figure 3.4: Possible different settings for the time delay, based on [10]

It should be noted that the recommended settings presented in this chapter applies for load tap changers connected in series in a radial connection. If the grid is looped, the conditions become advanced and detailed calculations are needed in order to provide the desired selectivity. Under such conditions, adjustment of time delays can also be used to obtain selectivity. A detailed description of how load tap changer regulators should be adjusted in looped power grids is not included here, since it is not treated in the simulations in this project.

3.2.4 LTC-transformers in Stability Studies

Transformers with load tap changers can play a major part during a voltage collapse. This could be illustrated by an example of a heavily loaded power system:

If a disturbance, for instance a disconnection of a transmission line, causes a depression in voltage throughout the system, transformers with load tap changers will eventually try to restore the voltages on the lower voltage levels. With each tap-operation, the resulting increment in load on the transmission lines in the highest levels will increase the active and reactive line losses. This will then cause a greater drop in voltage. Each tap-operation will lead to an increase in the reactive power output of the generators in the system. Eventually, generators will reach their maximum field current limits. This will transfer the generator's share of reactive loading to other generators leading to the overloading of more generators. Such a process can lead to a voltage collapse. [8]

3.2.5 Parallel LTC-transformers

Transformers with load tap changers can be used to regulate the reactive power flows in a power system. This can be illustrated by a simple example from [11]. Two ideal transformers are connected in parallel. One (T_a) has a turns ratio of 1/n and the other (T_b) has a turns ratio of 1/n'. A single line diagram describing this configuration is shown in Figure 3.5. The base voltages are equal to the voltage ratio of the first transformer.

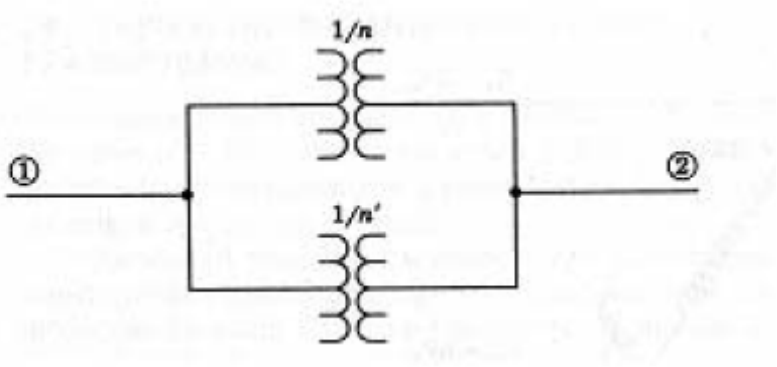

Figure 3.5: Single line diagram of parallel transformers, from [11]

The equivalent circuit is shown in Figure 3.6. An ideal transformer with turns ratio 1/t takes care of the off-nominal turns ratio of the second transformer. The base voltages are determined by the turns ratio of the first transformer. This configuration could be interpreted as two parallel transmission lines with a regulating transformer in one line.

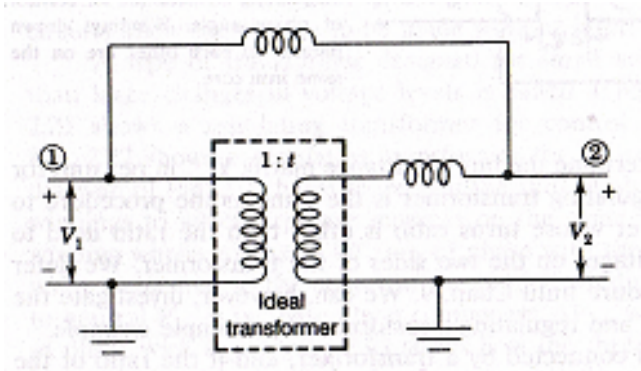

Figure 3.6: Equivalent circuit of parallel transformers, from [11]

In order to illustrate the result of such a situation, values are introduced. The parallel transformers are supplying a load of 0.8 + j0.6 pu at a voltage V_2 of $1.0 \angle 0^{\circ}$ pu. The transformers have an impedance of j0.1 pu. Transformer T_a has a turns ratio equal to the base voltages, while transformer T_b has a turns ratio 1.05 times of T_a, with a step up towards the load.

An approximate solution for this example can be found by accepting that Figure 3.7 is the equivalent circuit of this example when S is closed. The voltage, ΔV, is in the branch of the equivalent circuit of transformer T_b and is equal to t -1 pu. This means that T_a is providing a voltage ratio 5% higher than T_b. When the switch is open ΔV will create a circulating current. If the assumption that only a small fraction of I_{circ} will go through the load when the switch is closed is accepted, the superposition principle can be applied to ΔV and the voltage source. This is considered to be a valid approximation since the difference in impedance is considerable.

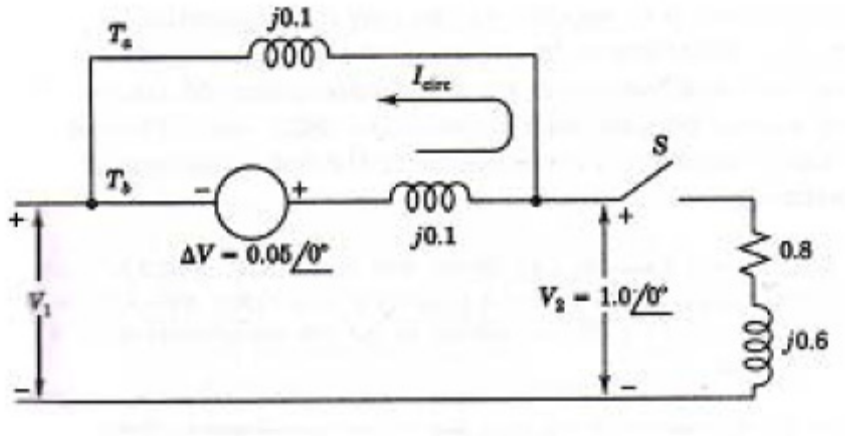

Figure 3.7: Approximated equivalent circuit of parallel transformers, from [11]

The following equations calculate the power flow through the transformers:

$$I_{load} = \frac{1.0}{0.8 + j0.6} = 0.8 - j0.6\,pu \tag{3.2}$$

Due to ΔV:

$$I_{circ} = \frac{0.05}{j0.2} = -j0.25\,pu \tag{3.3}$$

With ΔV short-circuited the load current will be divided equally in the two paths. The total approximated current will then be:

$$I_{T_a} = 0.4 - j0.3 - \left(-j0.25\right) = 0.4 - j0.05\,pu \tag{3.4}$$

$$I_{T_b} = 0.4 - j0.3 + \left(-j0.25\right) = 0.4 - j0.55\,pu \tag{3.5}$$

This gives the following distribution of power flow:

$$S_{T_a} = 0.4 + j0.05\,pu \tag{3.6}$$

$$S_{T_b} = 0.4 + j0.55\,pu \tag{3.7}$$

This shows that the largest reactive power flow will go through the transformer with the higher tap setting. The real power flow is divided equally. [11]

3.2.6 LTC-transformers in SIMPOW

In SIMPOW, transformers with load tap changers can operate in two different modes. They can operate in either discrete or continuous mode. If the step size is not specified, the transformer will operate in continuous mode. It can then control the turns ratio to any real value between the minimum and maximum limit. If the step size is specified, the transformer will operate in discrete control and can only regulate in steps. [12] Transformers with load tap changers operate in discrete mode in this project.

In the steady-state calculation the LTC-transformer will regulate the turns ratio in order to obtain the specified desirable voltage. If the transformer is in discrete mode, and the exact specified voltage value is not possible to achieve, the closest possible step is chosen. [12]

Unless specified dynamic regulators are included in the dynamic model, load tap changers will not regulate during dynamic simulations. A description of two different dynamic load tap changer regulators is given in Appendix B.

3.3 Doubly-Fed Induction Generator

3.3.1 Introduction

A short description of doubly-fed induction generators is already included in [5]. However, as doubly-fed induction generators are used to model the power production from the wind farms at Sleneset and Sjonfjellet, a more extensive description was required for this report. This is presented below. Different fault ride-through configurations are described to illustrate that even though the DFIG model in SIMPOW has limited fault ride-through capabilities, other possible solutions exists.

Wind turbines can either operate at fixed speed or variable speed. A fixed-speed wind turbine is directly connected to the grid, while a variable-speed wind turbine is controlled by power electronic equipment. There are several advantages connected to the use of variable-speed turbines compared with fixed speed. For instance, mechanical stress and acoustic noise can be reduced. The variable-speed turbine also often gives the ability to control active and reactive power. [13]

The major wind turbine manufactures show a tendency to develop new and larger wind turbines. These large wind turbines are all based on variable-speed operation with pitch control. The generators in these turbines are either direct-driven synchronous generators or doubly-fed induction generators.

The number of variable-speed wind turbines with doubly-fed induction generators (DFIGs) connected to national power systems has increased in the recent years, and they are today commonly used by the wind turbine industry. The main reason for this is that they have a good ability to supply power at a constant voltage and frequency, while the rotor speed varies. Results from the study in [13] show that compared with an active-stall fixed-speed wind turbine (using two fixed speeds) or a full-power-converter direct-driven wind turbine, the energy production from a DFIG wind turbine is approximately the same. Though, compared with a traditional fixed-speed induction generator the DFIG can deliver some percentage units more. [13] [14]

However, other studies state that the differences are larger. According to [36] the energy output can be up to 60% larger from a wind turbine with DFIG-technology compared with a traditional fixed-speed system with a cage rotor induction generator.

Another advantage with the doubly-fed induction generator is that the power electronic converter only has to handle about 20-30% of the turbines rated power. This means reduction of costs and losses compared with a full-scale converter which has to be used with a direct-driven synchronous generator. The size of the converter in a doubly-fed induction generator decides the variable-speed range. This is often between -30% to +30% slip. Due to mechanical strain and converter rating, a wind turbine will normally not operate outside this region. The turbine is kept within this speed-range by the turbine blade control and the electrical torque control. [13] [15]

3.3.2 Description

A popular configuration for wind turbines with a doubly-fed induction generator is illustrated in Figure 3.8.

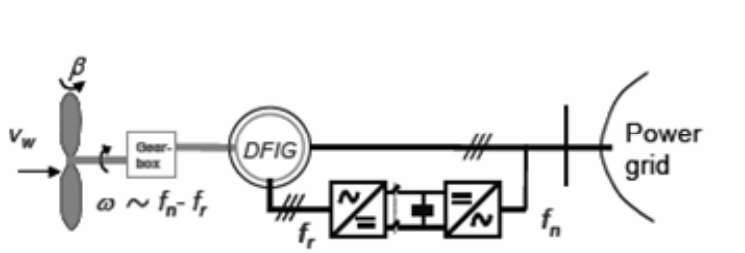

Figure 3.8: Configuration for a wind turbine with a DFIG, from [37]

The stator in a DFIG is directly connected to the grid, while the rotor is connected via slip rings to the power electronics converter.

A DFIG-technology where external rotor resistances are controlled also exists. However, this solution results in unnecessary dissipation of energy in the external rotor resistances and there is no possibility to control the reactive power. [13]

The power electronics converter is a back-to-back converter with a DC-link capacitor in between. The capacitor works as energy storage and keeps the voltage variations in the DC-link small. The machine-side converter can control the torque or the speed of the generator. It can also control the power factor at the stator terminals. The main objective for the grid-side converter is to keep the DC-link voltage constant. [13]

Figure 3.9 shows the equivalent circuit of a doubly-fed induction generator. Magnetizing losses are included. The circuit is valid for steady-state calculations. [13]

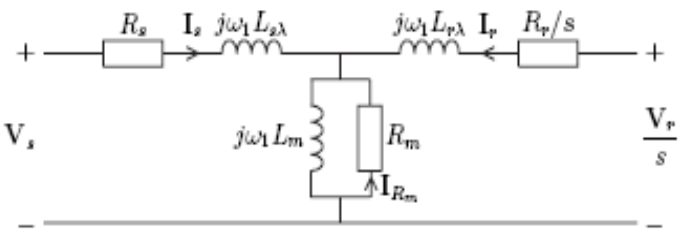

Figure 3.9: Equivalent circuit of the DFIG, from [13]

An important notation is that if the rotor voltage, V_r is short-circuited, the equivalent circuit becomes identical with the equivalent circuit of an ordinary squirrel cage induction machine. The equivalent circuit of a squirrel cage induction machine is shown in [5].

3.3.3 Fault Ride-Through Capabilities

Due to the increase in size of planned wind turbines and wind farms, the turbines behaviour during grid disturbances becomes increasingly important. Newly developed grid codes, defines fault scenarios that the wind farms should be able to ride through. This implies that normal power production should be restored once the nominal grid voltage has been recovered. [13]

Wind farms connected to the regional or main grid in Norway have to consider guidelines for which faults the wind farms should be able to ride through. These are specified in [16]. Guidelines regarding simulations performed in this project are described in section 3.4.

Doubly-fed induction generators connected to the grid today are traditionally disconnected if large voltage sags are to appear. This is done in order to protect the power electronic equipment from high fault currents. [17]

A traditional way to protect the rotor side circuit during voltage sags is to short-circuit the rotor windings with a thyristor crow-bar. The thyristor crow-bar is enabled when the rotor current or power increases above a specified limit. The crow-bar is connected to the windings of the rotor until the stator is disconnected from the grid. The crow-bar recovers to the pre-fault condition when the rotor currents die out. A DFIG-configuration with a crow-bar made of a diode bridge with a thyristor is shown in Figure 3.10. [17]

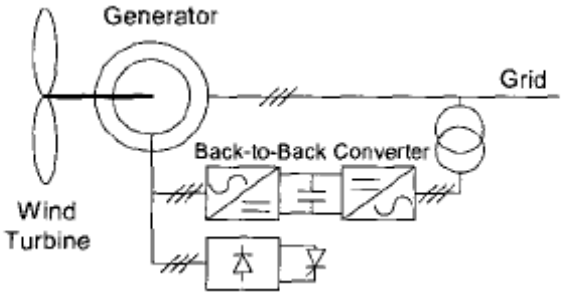

Figure 3.10: DFIG with diode bridge crow-bar, from [17]

This configuration is however not suitable for new grid codes demanding fault-ride through capabilities. A number of different modifications has therefore been suggested to improve the fault-ride through capabilities of the DFIG. [17]

A configuration described in Figure 3.11 shows a solution where the high current in the rotor is limited by thyristor controlled by-pass resistors. This solution is recommended in [18] as a way to improve the fault ride-through capabilities of a DFIG. However, according to [17] the size of the resistors is critical, and the configuration is not preferable for long-time sags in voltage.

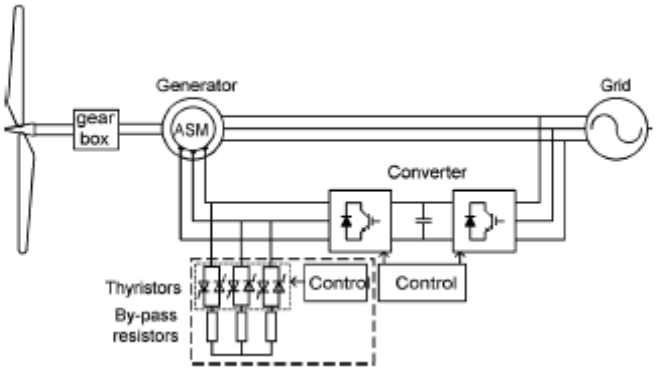

Figure 3.11: DFIG configuration with by-pass resistors, from [18]

Another suggested solution is to design the converter devices for a higher current rating. This will allow the converter to stay connected longer without connecting the crow-bar. Anti-parallel thyristors are placed in each phase between the stator and the grid acting as an AC voltage controller to isolate the stator from the grid when the grid voltage recovers after a disturbance. However, the thyristors are kept conducting during normal operation and thereby reducing the system efficiency. This solution is also not suitable for long-time voltage sags. This configuration is shown in Figure 3.12. [17]

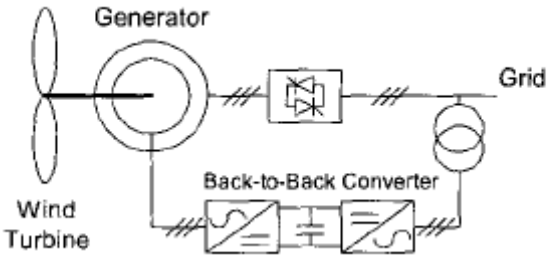

Figure 3.12: DFIG configuration with series antiparallel resistors, from [17]

A DFIG configuration recommended in [17] is to add a 3-phase series-connected converter between a conventional DFIG and the grid. This will work as a dynamic voltage restorer and thereby improve the fault-ride through capability. The series converter will also be able to add other benefits like reactive power compensator, series active filter and electronic isolator. However, it should be noted that this is a more complicated configuration. [17]

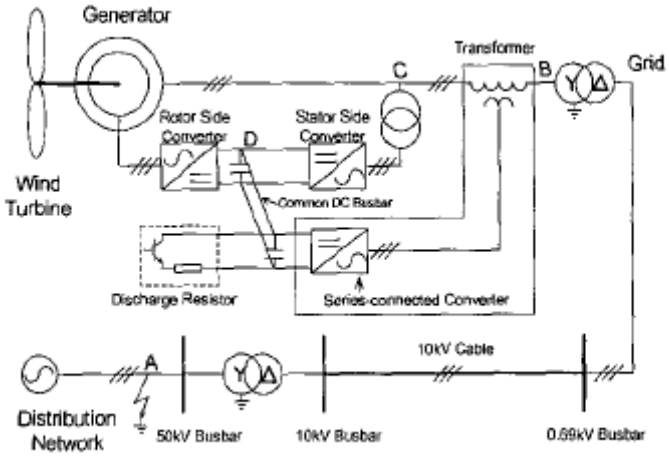

Figure 3.13: DFIG configuration with one series-connected voltage source converter, from [17]

3.3.4 The DFIG Model in SIMPOW

There are several different configurations describing different versions of the doubly-fed induction generator. An overview over how a wind turbine with a DFIG is described in SIMPOW is given below. The theory used for this section is mainly obtained from [19].

A specific model describing a wind turbine with a doubly-fed induction generator is included in SIMPOW. The intended use for this model is for system analysis of power flows and electromechanical transients in an electrical system. It can be used for both symmetrical and unsymmetrical calculations. Harmonics are neglected in the model because they normally have second order effect on active and reactive power. Active and reactive power affects the node voltages and speed and angles of rotating components in the system. The validity of the DFIG-model is therefore limited to the fundamental frequency components of voltages and currents. The electrical state in the AC system is assumed to be sinusoidal. The AC voltages and currents are therefore described by phasors. During transient conditions, the phasors will vary in time. The model is written for transient conditions. The model for steady-state is obtained by neglecting all time derivatives.

The DFIG in SIMPOW is modelled as an induction machine with a wound rotor. The rotor has slip rings for external rotor circuits. Between the grid and the rotor slip rings there is a frequency converter. This converter consists of a machine-side converter and a grid-side converter. Between these converters, an intermediate DC-system is located.

The converter is transferring real power from the rotor to the grid when the generator operates at negative slip. At positive slip, the real power is transferred from the grid to the rotor. The real power transfer is controlled by the speed control. The aim of this controller is to operate at the most efficient rotation speed related to the wind speed as possible. The generator is modelled as detailed as possible while the frequency converter is modelled as a voltage source transferring the real power without losses between the grid and the rotor slip rings.

A pitch control system is also included in the model. This system shall operate at high wind speeds, at strong wind variations or at high power production. Pitch control is used to capture less wind power by turning the blades.

Another feature of the DFIG model is that the machine-side converter has the ability to consume or produce reactive power. By the use of this feature, the DFIG can control the power factor at its terminals to unity. This is the default control strategy. Another possible control strategy is to control the AC-voltage at the terminal by adjusting the reactive power production from the machine-side converter.

If large voltage changes at the DFIG terminals were to occur, the frequency converter is disconnected and the crow-bar resistor is connected into the external rotor circuit. This is done in order to protect the frequency converter from high currents. If the voltage returns to a value within the specified limits in the crow-bar control system, the frequency converter can be reconnected after a specified time delay.

3.3.4.1 Modules

The DFIG model in SIMPOW includes six modules. A sketch of the modules and their interaction is shown in Figure 3.14.

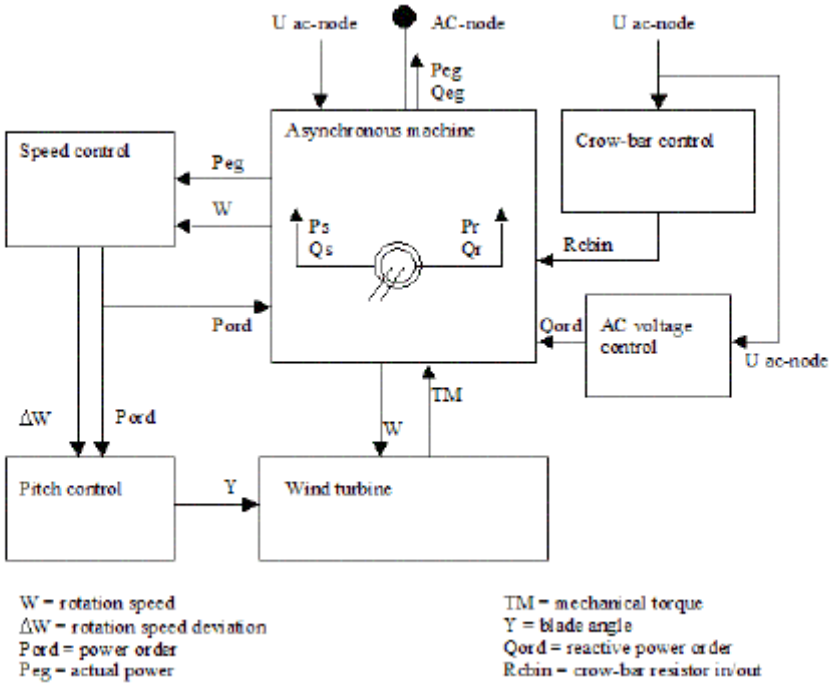

Figure 3.14: DFIG model with modules, from [19]

The model of the asynchronous generator consists of a wound rotor induction generator, a simplified model of the frequency converter and a crow-bar resistance.

The wind turbine calculates the mechanical torque based on equation (3.8).

$$T_m = \frac{P_m}{\omega} = \frac{0.5 \cdot C_p \cdot \rho \cdot \pi \cdot R^2 \cdot v_w^3}{\omega \cdot S_N} \tag{3.8}$$

Where:

T_m = Mechanical torque in pu.

ω	=	Rotation speed of the wind turbine in pu
C_P	=	Rotor power coefficient in pu
ρ	=	Air density in pu
R	=	Length of blades in m
ν	=	Wind speed in m/s
S_N	=	Rated power of the DFIG in MVA

Further description of the equations and input values describing the asynchronous generator is given in [19].

The speed control system gives the power order to the DFIG and the pitch control. A block diagram describing the speed control regulator is shown in Figure 3.15.

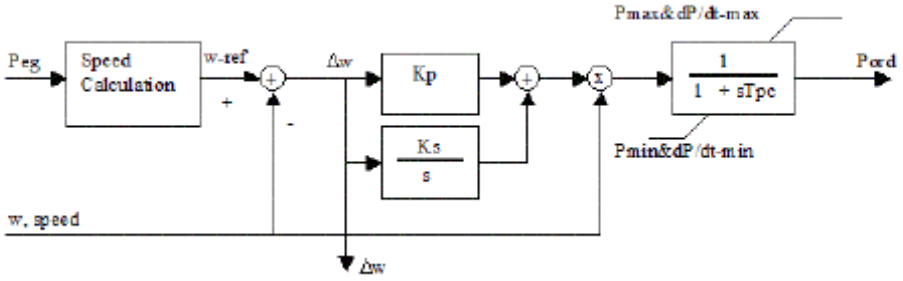

Figure 3.15: Block diagram for the speed control, from [19]

The real power generation and the speed are the input values for the regulator. From the actual real power generation a speed reference is calculated. The difference between this calculated speed and the speed reference goes into the PI-type regulator. The output is then multiplied with the speed and this gives the power order. The power order response is filtered.

The pitch control calculates the blade angle. This angle controls the captured wind power or the mechanical torque of the wind turbine. The block diagram for this regulator is shown in Figure 3.16.

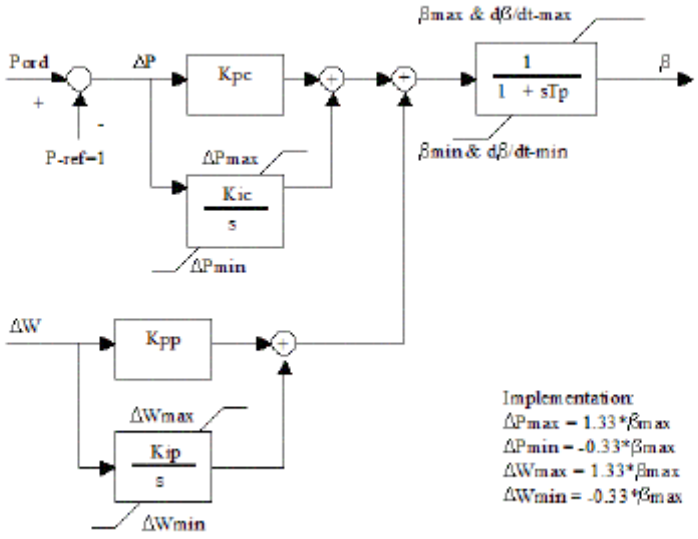

Figure 3.16: Block diagram for the pitch control, from [19]

The input to this regulator is the power order and the speed deviation obtained from the speed control. The power order is compared with a power reference. This difference and the speed deviation go into two separate PI-type regulators. The outputs are added and the sum is the blade angle. Before the angle response is sent to the wind turbine it is filtered with limitations in both size and derivatives.

The crow-bar resistor status, R_{cbin}, is obtained from the crow-bar control This status controls the connection and disconnection of the crow-bar resistor in the machine model. The only input for this regulator is the bus voltage of connected bus. If this voltage violates the maximum or minimum voltage limits set for the regulator, the value of the R_{cbin} is switched from zero to one. This means that the crow-bar resistor is connected.

The block diagram for the crow-bar resistor control is shown in Figure 3.17. The user might specify a time delay before the status change is sent to the machine.

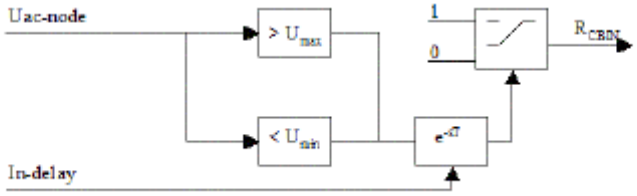

Figure 3.17: Block diagram for crow-bar resistor control, from [19]

The AC voltage control regulator is only used if the DFIG is using the voltage control strategy. Otherwise the regulator is blocked. In this regulator the reactive power order, Q_{ord}, is obtained. The reactive power order controls the reactive power production or consumption in the external rotor circuit.

A block diagram for the AC voltage control regulator is given in Figure 3.18.

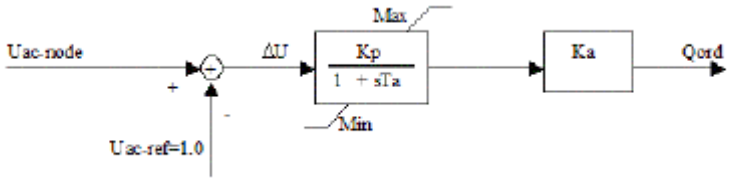

Figure 3.18: Block diagram for AC voltage control regulator, from [19]

The input for the regulator is the voltage of the connected bus. The voltage is compared with a specified reference. The voltage deviation goes through a PI-type regulator with maximum and minimum limits.

Further details regarding the calculations done in these regulators during simulations are described in [19].

3.4 Rules and Regulations

A thorough review of the different relevant regulations, rules and guidelines concerning grid connection of a wind farm was presented in [5]. Thus, only a short description of some of the guidelines that are especially relevant for the studies performed in this project is presented below.

This chapter is based on information collected from the guide for system demands for installations connected to the regional and main grid in Norway. [16] The statements presented there are guidelines for which requirements a grid connected wind farm should fulfil.

3.4.1 Operation During Deviations in System Voltage

The following guidelines for demands for wind farms are stated in [16] when there is a deviation in system voltage:

- No reduction in active power production if there is a deviation in the system voltage of less than ±10%.
- Wind farms should be able to operate with a power factor within the area cos φ = ±0.91 referred to the connection point of the wind farm for system voltages within ±10% of normal voltage.
- At system voltages below 90% of normal value, a reduction of reactive power production is accepted. The allowed reduction is proportional to the voltage reduction if power electronics are used and squared to the voltage reduction if shunt capacitors are used.

At special needs, additional requirements can be asked for.

3.4.2 Control of Reactive Power

Wind farms are required to have the capability to regulate voltage or reactive power in the connection point.

The regulator must have the ability to operate in two different control modes:

- Set point for power factor or reactive power.
- Voltage regulation with controllable set point for voltage and reactive droop.

Normally, voltage regulation shall be utilized. VAR or power factor regulation should not be implemented unless it is agreed upon by the system operator.

3.4.3 Operation during Faults or Abnormal System Voltages

There are several guidelines for demands regarding operation during faults or abnormal system voltages given in [16]. Of these guidelines, only the ones dealing with symmetrical faults for wind farms connected to voltage levels at 132 kV or above are presented here.

According to [16], a wind farm should be able to deliver reactive power equal to the maximum reactive capability for 10 seconds at system voltages down to 70% of normal voltage.

A wind farm should remain connected during a given three-phase symmetrical fault with a failed reconnection which results in a dip in voltage referred to wind farm connection point. The voltage during the given fault and after reconnection is presented in Figure 3.19.

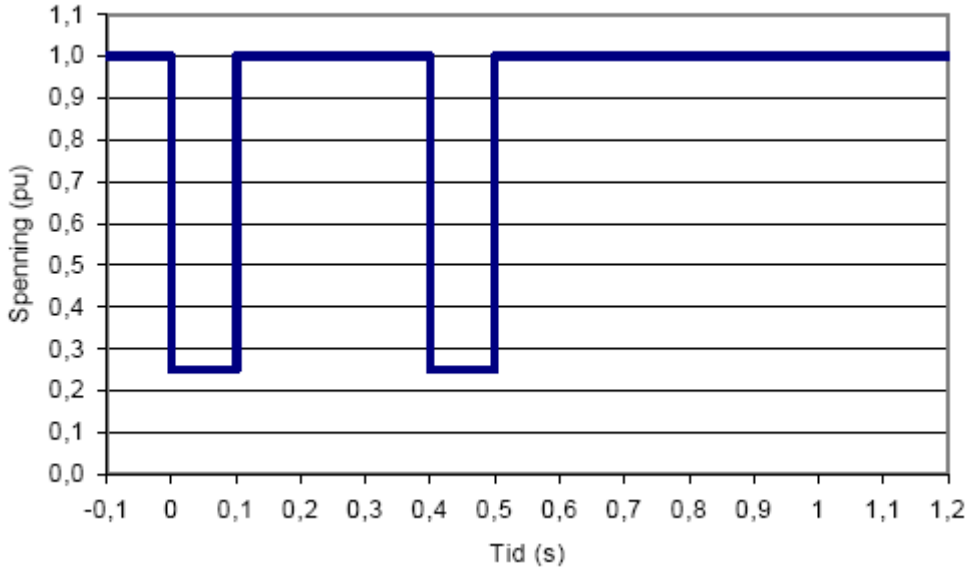

Figure 3.19: Voltage characteristic at wind farm connection point during grid fault, from [16]

At grid faults that give approximately symmetrical voltage changes referred to the wind farm connection point, the wind farm should remain connected as long as the voltage is above the voltage characteristic presented in Figure 3.20.

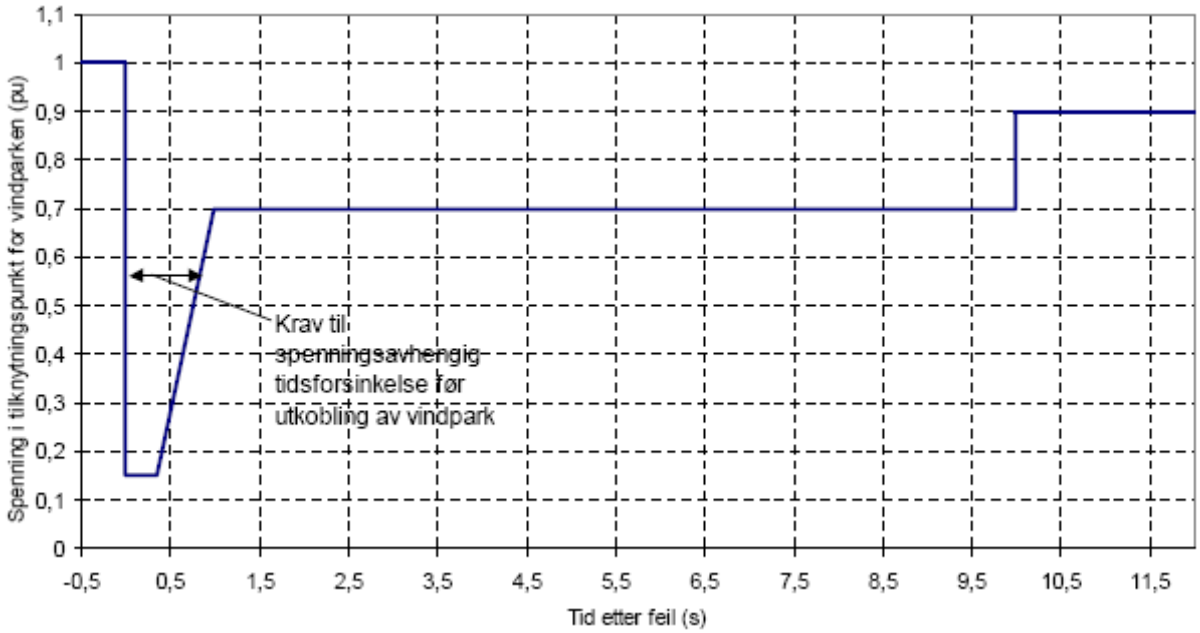

Figure 3.20: Voltage characteristic at the wind farm connection point at which the wind farm should remain connected, from [16]

3.5 Voltage Control and Power Factor Control

In this project, simulations are performed with compensation devices in both voltage control and power factor control. This is done to illustrate some of the differences between the two control methods. This chapter therefore outlines the relevant theory regarding voltage and VAR/power factor control. The theory is mainly taken from [20]. Whenever other sources are used it is specified.

The theory in this chapter is taken from sources which describes different control methods for synchronous machines. In this project, the voltage and reactive power compensation in the wind farm radial is performed by static VAR compensators (SVCs). SVCs are particularly designed for transmission voltage regulation and are traditionally faster than excitation systems in synchronous generators. However, with respect to the effects on the transmission system, many of the same principles will apply. [21]

Continuously acting automatic voltage regulators (AVRs) have been used as a standard in power systems for over 50 years. [21] By regulating the terminal voltage of generators, the transmitted voltage is maintained in a stable manner. A drop in the system voltage will result in a boost in produced reactive power. In a synchronous generator, this is performed by a boost in the field current supplied to the generator. An excitation system cannot control the terminal voltage and the VAR output independently. Therefore, a controller which holds the produced VARs constant or the power factor constant might defeat the purpose of the voltage regulator.

A voltage controller can be equipped with a secondary VAR or power factor controller. If this is the case, the voltage reference of the voltage regulator's voltage adjuster will receive automatic commands to raise or lower the voltage reference in order to maintain a constant steady-state level of VARs or power factor. This voltage adjuster is typically slow-acting and will thereby result in a smooth and controllable adjustment. A simplified block diagram describing a typical system with a VAR or power factor controller is given in Figure 3.21.

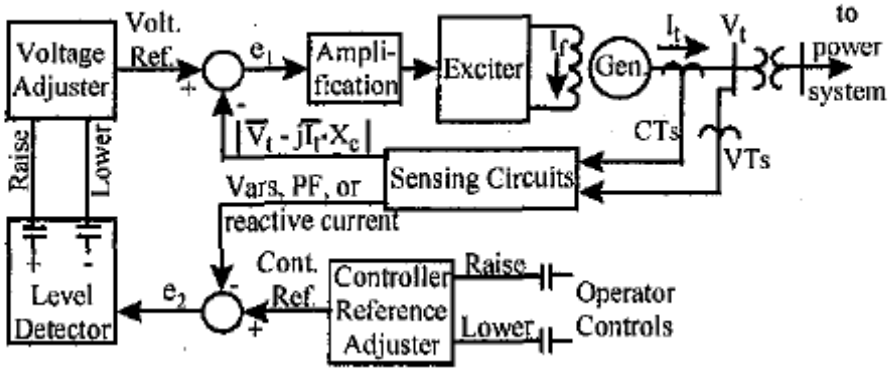

Figure 3.21: Simplified block diagram of voltage regulator with a VAR/PF controller, from [20]

It should be noted that this block diagram describes a regulator for a synchronous machine. A description of the primary voltage regulator and secondary VAR regulator for a SVC is given in chapter 4.3.4.

The controller reference adjuster provides a controller reference signal, much like the voltage adjuster provides a voltage reference signal. This signal can be slowly adjusted by the operator if needed. The controller reference signal is compared with an actual measured value. The measured value can be of either of VARs, the power factor or reactive current. The

difference between the measured value and the reference value creates an error signal. Depending on the size of the error signal, the level detector indicates to the voltage adjuster whether the voltage reference should be raised or lowered. A small dead band is often included in the level detector to prevent the voltage adjuster to act on minor variations in reactive power.

The regulator will respond to transient changes in the terminal voltage as a normal voltage regulator. If a sudden disturbance causes a change in terminal voltage from the reference voltage, the voltage regulator will provide the desired transient compensation in order to recover from such a disturbance. However, if the disturbance is sustained or arises over a longer period of time, the controller has sufficient time to adjust the voltage reference according to the change in VARs, power factor or reactive current rather than voltage.

There is a simpler type of VAR or power factor regulator than the one described above. This regulator provides direct feedback control of VARs, power factor or reactive current. A simplified block diagram describing this regulator is given in Figure 3.22.

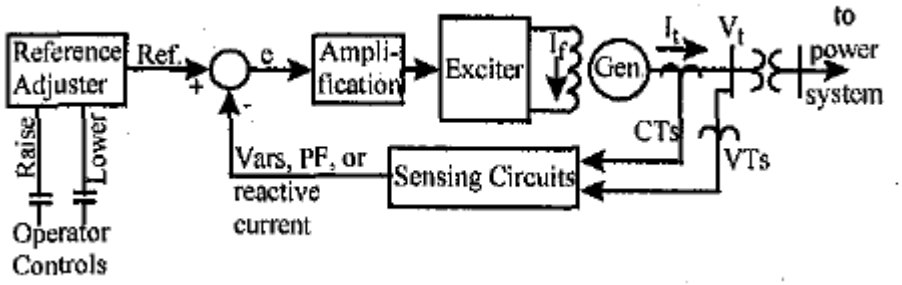

Figure 3.22: Simplified block diagram for VAR/PF regulator, from [20]

During transient disturbances, this type of regulator will typically not provide any boosting of the excitation system output in response to a reduction in voltage, neither momentarily nor in steady-state. This type of regulator is most often used for excitation control of synchronous motors.

In steady-state simulations performed in [20] the consequences of a depression of system voltage are examined with various types of excitation controls. The results show that with VAR or power factor control, no steady-state voltage support is provided. Similar results are expected in situations where the steady-state system voltage is increased due to a disturbance.

The conclusions derived from the simulations performed in [20] are that voltage control should be implemented in as many synchronous machines as possible in order to support the system voltage. VAR or power factor control should generally not be specified or utilized in machines intended to provide voltage support. However, a regulator which provides VAR or power factor control might be feasible as long as the voltage is within a reasonable normal band. It should be noted that extreme care must be taken to assure that mixing different control strategies does not cause control instabilities or other problems.

4 Modelling of the System

4.1 Introduction

The purpose of this project is to analyse some of the impacts that the planned wind farms at Sleneset and Sjonfjellet have on the existing power grid. The steady-state power flow analysis is performed in Netbas by NORSEC [2]. However, dynamic simulations can not be performed in Netbas. In order to be able to analyse the dynamic responses in the grid, a dynamic model is needed. The steady-state Netbas model is therefore converted into a steady-state model in SIMPOW. This works as a basis for the dynamic SIMPOW model.

In order to receive valid results from the dynamic simulations, it is important that the steady-state model, which is the foundation for the dynamic model, is correct. In addition, some expansions and changes are done to the steady-state SIMPOW model compared to the Netbas model in order to adapt the steady-state model to the dynamic simulations. These changes to the model are also done to better illustrate some of the challenges regarding wind power integration.

This chapter presents the basis Netbas model and the initial and expanded SIMPOW model.

Firstly, a short description of the steady-state Netbas model is given.

Secondly, a description of the initial steady-state SIMPOW model is presented. Some of the problems encountered during the modelling are also briefly reported upon. To ensure that the converted model somewhat corresponds to the Netbas-basis, the power flow from the two models are compared.

Thirdly, the expansions to the initial steady-state model are described. As the various dynamic simulations require different configurations in the steady-state model, not all expansions to the model are included in all simulations. Several different steady-state models are therefore needed.

Finally, a presentation of the dynamic model is included in the chapter. As for the steady-state model, some of the dynamic components described in this chapter are not included in all of the simulations.

4.2 The Netbas Model

4.2.1 Description

The model used for the simulations in this project is based on a Netbas model describing the power grid between Tunnsjødal in Nord-Trøndelag and Salten in Nordland. The time in the model is set to January 2009. The data is collected from the Netbas database at NORSEC. Prior to the steady-state analysis, the database was updated with information from SKS Nett, Helgelandskraft, NTE and Statnett. [2]

The reference bus is located in Tunnsjødal. It represents the interface with the power system to the south of Tunnsjødal. The power flow towards this bus will depend on the level of production and load in the analyzed area.

The interface towards north is represented by a constant active power flow. This power flow is based on hourly measurements made by Statnett. [2]

At Nedre Røssåga there is a 220 kV transmission line towards Ajaure in Sweden. This line has a maximum transmission capacity of 400 MW. According to [22], the power flow in this line will not be significantly affected by new wind power production in Northern Norway. However, the planned wind farms at Sleneset and Sjonfjellet were not included in this analysis. [22]

The power flow in the connection towards Sweden is difficult to model since it depends on the level of production in both the Norwegian and Swedish power plants. In the Netbas model it is assumed that there is no exchange of power with Sweden through this transmission line. An export of power towards Sweden in this line will reduce the loading on the transmission lines towards south from Nedre Røssåga. [2]

Some key figures for the Netbas model are presented in Table 4.1.

Table 4.1: Model data

Description	Number
Nodes	691
Lines	618
2-winding transformers	117
3-winding transformers	17
Shunt capacitors	16
Loads	53
Generators	79

It should be noted that the number of nodes and transmission lines includes some circuit-breakers and connections between circuit-breakers and buses.

4.2.2 Special Conditions

The generators representing hydro power plants in the steady-state model from NORSEC are set to PQ-buses with no reactive power regulating capabilities. Instead, the regulating capabilities are summed up in fictitious regulating units placed at nodes where several real generators are connected. These regulating units are set to UP-buses with no active power production.

Some of the transmission lines in the area have a maximum temperature of 50ºC. The maximum allowed current is normally calculated from a temperature of 80ºC. This will result in a higher allowed current than what the lines can allow in reality. [2]

The maximum allowed current for lines with a maximum temperature of 50ºC is considered in both the static and dynamic analyses.

4.2.3 Variations in Voltage

According to Statnett, the voltage in this particular part of the 420 kV grid is normally between 415 kV and 420 kV. An alarm will sound if the voltage reaches over 430 kV or below 410 kV. [2]

In the 300 kV grid the voltage is usually between 295 kV and 300 kV. If the voltage comes above 310 kV or below 280 kV an alarm will sound. [2]

The voltages at the 22 kV, 66 kV, 132 kV and 220 kV level is allowed to vary approximately ±10% of the rated value. The maximum and minimum allowed voltages in the transmission system specified in the steady-state model used in the steady-state analysis are given in Table 4.2.

Table 4.2: Allowed voltage variations

Voltage level [kV]	Minimum voltage [kV]	Maximum voltage [kV]
22	20	24
66	60	72.5
132	120	145
220	220	250
300	280	310
420	410	430

The voltages in the regional and distribution grid are regulated by the use of load tap changers in transformers and the regulating units mentioned above.

4.3 The SIMPOW models

4.3.1 The SIMPOW Program

All of the simulations in this project are performed in the computer program SIMPOW. During the course of this project the software has been updated several times. However, all of the updates are part of SIMPOW version 10.2.110. This is the version used in this project. The updates mainly concern the model describing the doubly-fed induction generators.

A description of SIMPOW is given in [23], [12] and [5].

4.3.2 Initial Steady-State Model

The steady-state model is converted manually by importing from Netbas to SIMPOW through Microsoft Excel. Below follows a short description of the different components included in the steady-state model. The OPTPOW file for this model is given in Appendix E. For further details regarding the input parameters for the different grid components, see [12].

Some key figures for the SIMPOW model are presented in Table 4.3.

Table 4.3: SIMPOW model data

Description	Number
Nodes	597
Lines	502
Two-winding transformers	116
Three-winding transformers	17
Shunt impedances	16
Loads	53
Generators	69

The model consists of voltage levels between 420 kV and 0.24 kV. There is, however, only one node at 0.24 kV, and this is a transformer terminal without any load connected to it. The next voltage level above 0.24 kV is at 6 kV.

The number of nodes and lines in the SIMPOW model are reduced compared with the number in the Netbas model. The grid has been simplified by removing end nodes without any load or generation connected to them. If the end nodes are in the end of long transmission lines they can not automatically be removed because the transmission lines will generate reactive power, and this will impact the power flow. The end nodes removed in this model are connected to the grid with type 1 lines. These lines do not have any power flow through them.

The model is also reduced by removing connections with double buses. Double buses are important during real operations, but as long as the connections between them are short-circuited, they can be removed without reducing the credibility of the simulation results. Double buses combined with parallel transformers with load tap changers are also a source of loop-flows and numerical errors in a model. [24]

Problems regarding loop-flows will be further described below.

4.3.2.1 Lines

The transmission lines are in Netbas defined with total resistance, total reactance and total capacitance. This corresponds to a type 2 line modelling in SIMPOW. The inputs for a type 2 line in SIMPOW are resistance, reactance and susceptance. The total susceptance for a transmission line can be calculated by using equation (3.9).

$$B = 2\pi f \cdot C_d \tag{3.9}$$

The equivalent of a type 2 transmission line is shown in Figure 4.1.

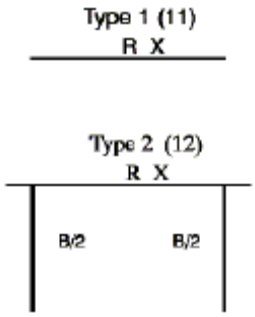

Figure 4.1: Line modelling in SIMPOW, from [23].

In the output file from Netbas, all connections between breakers and nodes are modelled as lines with an insignificant resistance and reactance. These lines are modelled as type 1 lines in the SIMPOW model. As mentioned above, a lot of these lines and nodes have been removed in order to create a grid which is better adapted to the purpose of these analyses.

4.3.2.2 Thermal limits

When the transmitted power across a transmission line increases, the phase current also increases, and the ohmic losses will augment proportional to the square of the current. The temperature in the conductor will then increase until the heat dissipation is in balance with the conductor heat loss. [6]

This change in temperature can cause severe permanent damage to the transmission line. For instance, high temperatures can cause non-reversible sag on the line or faster aging of isolation in power cables. Thermal capacity limits are therefore specified in order to prevent such damage. [6]

It is important to be aware of the thermal limits in the radial branch that connects the wind farms to the main grid. These limits can determine the maximum possible amount of power which can be transferred from the wind farms. However, it is also important to monitor lines outside the radial connection since it can be expected that increase in wind power production will create changes in the power flow throughout the grid.

In the steady-state calculations a message is posted if thermal limits are reached during the calculation. However, if thermal limits are reached during dynamic simulations no message is posted. It is therefore important to monitor transmission lines and power cables during dynamic simulations.

A single line diagram describing the grid from the wind farms to the connection point at Nedre Røssåga is given in Figure 5.1 in chapter 5.

The maximum allowed current in the transmission lines and power cables in the radial connection from Nedre Røssåga to the wind farms are given in Table 4.4. The maximum allowed current in the highest loaded line outside the radial is also given. This line is located between Øvre Røssåga and Marka. It is the only transmission line or power cable which is loaded above 90% of its full capacity in the steady-state calculations.

The line data is based on data given in the steady-state Netbas model.

Table 4.4: Maximum allowed current for monitored transmission lines and power cables

Between nodes	Type	Voltage [kV]	I_{MAX} [kA]
Bardal – N.Røssåga	Line	132	6.176
Sjo-Alt1_3 - #304656	Cable	132	1.160
Sjonfjell132A – Sjonfjell132B	Cable	132	1.160
#600095 - #304633-3662	Line	132	1.211
#304633-3662 - #304366	Cable	132	0.970
#304366 – Sleneset132O	Cable	132	0.990
Sleneset132O - Sleneset132V	Cable	132	0.715
#300763 - #300788	Line	132	0.560

The transmission line between Nedre Røssåga and Bardal can be expected to be the line in the radial with the highest power transfer. This is because the branches from the wind farms at Sleneset and Sjonfjellet meet at Bardal and unite to a mutual transmission line towards Nedre Røssåga. This line has a substantial larger maximum allowed current than the rest of the radial.

The power cable between node Sjo-Alt1_3 and node #304656 is located between Bardal and Sjonfjellet. As a consequence, only the power flow from Sjonfjellet will go through this line. Between these two nodes there are two identical power cables. This will reduce the loading of the cables. The transmission lines between Bardal and Sjonfjellet have the same maximum allowed current as the transmission line between Bardal and Nedre Røssåga. It can therefore be expected that the parallel power cables will be the dimensioning part of the connection between Bardal and Sjonfjellet.

Between Bardal and Sleneset there are two power cables and one transmission line in series. The power cable between node #304366-3662 and node #304366 is the part with the lowest thermal capacity. It can therefore be expected that this cable will be the highest loaded part of this connection.

The power cables at the 132 kV level within the wind farms are also important to monitor. The power cable within the wind farm at Sjonfjellet has the same thermal capacity as the parallel power cables in the connection towards Sjonfjellet. If the wind farm at Sjonfjellet was split into two parts with equal size it could be expected that the loading in this cable would be approximately the same as the loading in one of the two parallel cables. However, the wind farm at Sjonfjellet is split into one part of 185 MW and one part of 243 MW in the preliminary steady-state analysis. The part with 243 MW is located in the far end of the radial. It is likely that more than half of the production from Sjonfjellet will go through this power cable. The power cable within the farm at Sjonfjellet can therefore be more loaded than one of the parallel cables in the connection towards Sjonfjellet. This will however be influenced by the reactive power flows in the radial.

The power cable within the 132 kV level at Sleneset has a thermal capacity of more than half the capacity of the dimensioning cable towards Sleneset. The wind farm at Sleneset is divided into two equal parts with a capacity of 112.5 MW each. This cable should therefore be less loaded than the highest loaded power cable between Bardal and Sleneset. However this will also be influenced by the reactive power flow in the radial.

The power cables in the internal grid of the wind farms at a lower level than 132 kV are not evaluated in this project.

In [25] the following equation is given as a guide for calculating the current that should be tolerated in the line or power cable in question:

$$I_T \geq \frac{1}{\sqrt{3} \cdot U} \sum_{i=1}^{N_{wt}} S_{mc,i} \tag{3.10}$$

Where:

I_T = Maximum allowed current in the transmission line or power cable in question.

U = Lowest tolerated voltage value in the connection point of the line or cable.

$S_{mc,I}$ = Maximum allowed power production from wind turbine i.

N_{wt} = Number of wind turbines connected to the connection point.

If this rule were applied to the power cable between node #304633-3662 and node #304366 and the lowest tolerated voltage value were set to 118.8 kV, which is 0.9 pu the cable should be able to tolerate a current of 1.093 kA.

However, this equation is conservative, and the ability to tolerate currents is dependent of several factors [25]:

- Maximum production and thereby maximum current will occur at high wind speeds which will have a cooling effect, especially on transmission lines.
- Maximum production will seldom last in long periods.
- Maximum production will most often occur in cold periods.
- The voltage level can be increased during maximum production.
- All the wind turbines in a wind farm will seldom deliver maximum production at the same time.

A more thorough analysis, which also includes wind speed statistics, should be performed before a conclusion of whether the capacity of the power cables is sufficient can be taken. Such an analysis is not performed in this project.

4.3.2.3 Transformers

The model consists of 116 two-winding transformers. 75 of these are equipped with load tap changers (LTC). Compared with the Netbas model, one transformer has been removed. This was a transformer connected at the end of a radial line at Rognan.

For transformers with load tap changers, the maximum number of steps and the size of each step are specified. The desired voltage on the controlled side of the transformer is also specified. SIMPOW will then try to achieve this value during the steady-state power flow calculation. If this is not possible, the closest possible step is chosen. [12]

The load tap changers are set to control the voltages on the load side of the transformer. For most of the LTC-transformers this means that the tap changer is located on the side with the highest voltage. However, for 4 of the transformers, the tap changer is located on the low-voltage side. These transformers are located in Sjona, Oldereid, Sundsfjord and Grytåga. For all of these locations, the grid configuration is the same. An example from Sjona is shown in Figure 4.2. The large arrows represent connections with the rest of the power grid, while the small arrow represents the local load.

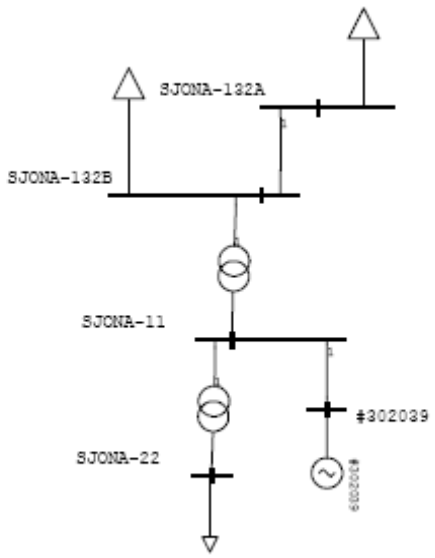

Figure 4.2: Grid configuration at Sjona

The regional grid at 132 kV is connected to a generator at 11 kV through a transformer. This transformer has a load tap changer located on the 132 kV side. At Sjona there is a local load at 22 kV. This load is connected to the grid through a transformer to the 11 kV node. The transformer between the 11 kV and the 22 kV level has a load tap changer located on the low-voltage side. This is done in order to control the voltage on the local load. In this configuration, it is important that the controlled voltage of the load tap changer matches the terminal voltage of the generator.

There are 17 three-winding transformers in the grid. 11 of these are equipped with load tap changers. The tap changers are located at the high-voltage sides of the transformer. This means at 420 kV, 132 kV or 66 kV.

The three-winding transformers are set to type A transformers in SIMPOW. This means that the short-circuit impedances are given. These impedances are recomputed into an equivalent Y and from there into an equivalent Δ within SIMPOW.

The phase shift from the high voltage side to the low-voltage side is set to zero for all transformers in the model.

More details about the modelling of transformers are given in [12] and [23].

4.3.2.4 Loads

The loads in the grid are defined by their active and reactive power consumption. They are set to be independent of the actual voltage on the node. This is a simplification which is made due to the lack of load data. A representation where the load is totally independent of the voltage can be considered to be a conservative scenario [9]. For instance, during a depression in voltage, the load will increase the drawn current in order to maintain the same power consumption.

It should be noted that even though the loads are independent of voltage changes in OPTPOW, they are dependent with the squared of the voltage in DYNPOW. For further details, see [19].

4.3.2.5 Power generation

As mentioned above, the hydro power generators in the Netbas model are set to PQ-buses and the regulating capabilities are represented by fictitious regulating units.

In order to move the voltage regulation to the generators, the fictitious regulating units are removed. This will give a deviation in reactive power flow, losses and voltages between the Netbas and SIMPOW model.

The wind power plants are in Netbas are modelled as UP-nodes. This means that they can regulate the reactive power production in order to maintain a specified voltage. However, to avoid conflicts with the above LTC-transformers, the generators at Sleneset and Sjonfjellet are set as PQ-nodes in the SIMPOW model. The initial values for the active and reactive power production are taken from the calculated power flow values in Netbas.

The hydro power generators are set to UP-nodes. This will allow the possibility to observe the reactive production needed in each generator in order to keep acceptable voltages in the grid. Maximum and minimum allowed reactive power production is specified for each generator.

The production level and the initial set voltage for the generators are taken from the Netbas model.

4.3.2.6 Compensating units

There are 16 shunt capacitors in the model. They are connected into the grid at the 33 kV, 22 kV or 11 kV voltage level. None of the shunt capacitors are regulated in steps.

There are two static VAR compensators (SVC) located at Nedre Røssågå. Each has a maximum capacity of 80 MVAR. There are no specific data group for defining SVCs in OPTPOW. They are therefore set as UP-nodes with no active power production and a maximum and minimum limit for reactive power production.

As mentioned above, the wind power plants are defined as UP-nodes. Therefore no compensating units were included in Netbas to compensate for the reactive power consumption of the wind farms. Consequently, no compensating units are introduced connected to the wind farms in the initial power flow.

4.3.2.7 Initial steady-state power flow

Since the only basis for the establishing of the SIMPOW model is the Netbas model, an initial goal of this project is to compare the two static models. This will give an impression of the quality of the SIMPOW model. However, since some changes have been made during the conversion from Netbas to SIMPOW, it will neither be possible nor desirable to create an identical steady-state power flow.

To create a starting point in the new model, terminal voltages from the generators in Netbas are chosen as terminal voltages in SIMPOW. As reference voltages for the LTC-transformers in SIMPOW, voltages on the controlled nodes in Netbas are chosen.

All these locked voltage values creates problems regarding reactive power flow in the grid. Due to mismatches between terminal voltages for generators, and set voltages for closely placed LTC-transformers, many generators ends up at either minimum or maximum allowed excitation. This results in large reactive power flows in the grid. A large reactive power flow results again in large reactive losses in transmission lines and transformers. A reason for these mismatches is that the regulating units for reactive power are removed in SIMPOW. This creates a different reactive power flow and hence different voltages.

Another problem in the SIMPOW model occurs at locations with parallel LTC-transformers. At these locations, large loop-flows of reactive power are created. These large loop-flows then increase the reactive losses in the grid.

The reactive loop-flows linked to parallel transformers can be avoided by removing unnecessary nodes and defining a common node for both load tap changers to control. In this way the transformers will behave identically. This should not affect the simulation results compared with the Netbas model.

Some LTC-transformers which are not connected in parallel still are connected in loops in the grid. These are also a source of large reactive power loop-flows. In order to get rid of these loop-flows, the size of the controlled voltages for the load tap changers is altered. In all but one case this method is successful for removing the loop-flows.

At Nedre Røssåga there are two connections between the 300 kV grid and the 132 kV grid. One through a transformer that goes directly between the two levels and one that goes by the 220 kV level. The section in question is shown in Figure 4.3. The transformers between nodes #300399 and #300731 and between nodes NRØSSÅGA220 and #300736 have load tap changers.

Figure 4.3 show that a large reactive power flow is circling in the loop. This results in high reactive losses in the transformers. The controlled node has been set to NRØSSÅGA132A for both of the transformers, and the controlled voltage has been altered in order to reduce the reactive loop-flow. However, this is not sufficient to remove the loop-flow.

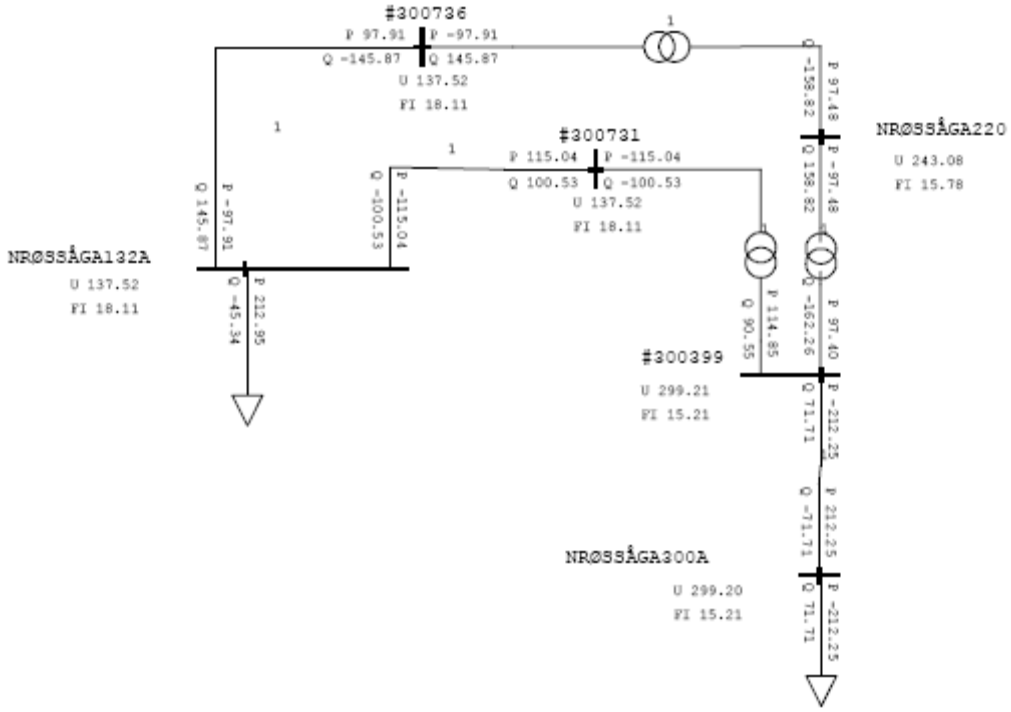

Figure 4.3: Grid configuration at Nedre Røssåga with two LTC-transformers.

To remove the loop-flow entirely, the load tap changer on the transformer between the 220 kV level and the 132 kV level is taken out of the model. This is shown in Figure 4.4. This is a simplification compared with the real grid. However, if the voltages or the power flow becomes unacceptable, regulation can be performed by adjusting the turns ratio manually.

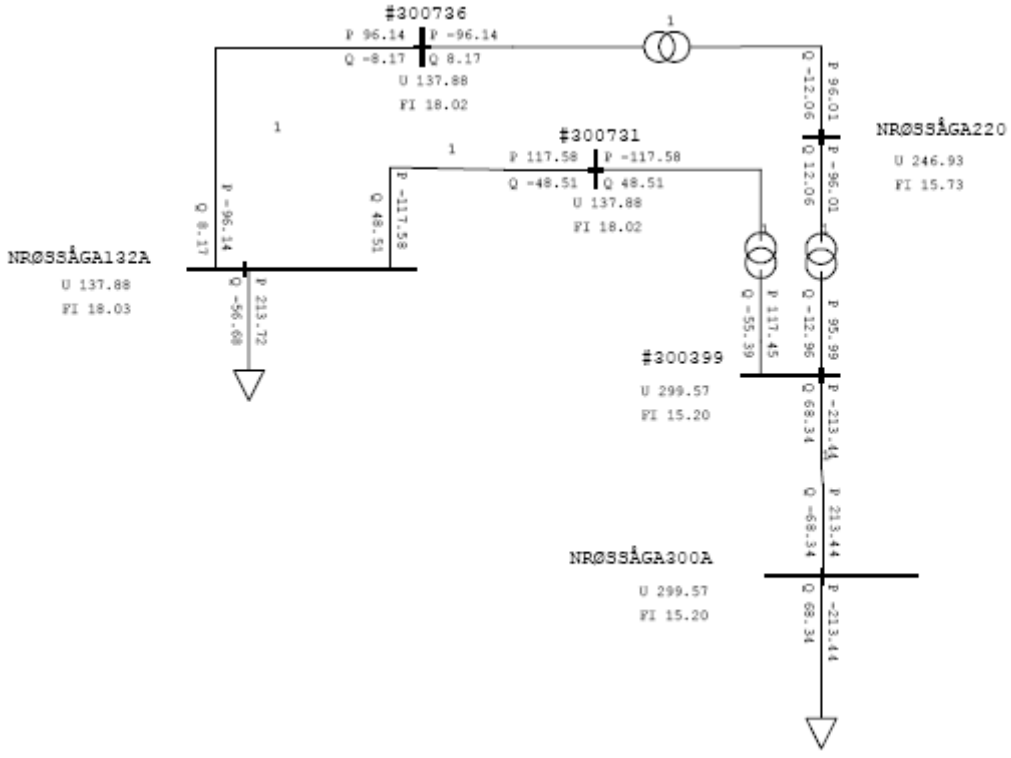

Figure 4.4: Grid configuration at Nedre Røssåga with one LTC-transformer.

Even if the loop-flows are removed, many generators in the model are still operating on the maximum or minimum limit for reactive power production. To get an impression of where the voltages are the most wrong, the limits for reactive power production for generators are removed. The terminal voltages are then adjusted to get the generators within their reactive power limits. After the reactive power production is adjusted within limits specified in the Netbas model, the limitations are reinserted in the SIMPOW model.

When adjusting the terminal voltage on a generator, the maximum allowed deviation from the nominal voltage is set to 5 %. This is based on the standard for voltage limits set by IEC in [26]. It states that a generator should normally have a terminal voltage between 0.95 and 1.05 pu at rated frequency. However, in practical applications and operations, the generator should be able to sometimes operate outside this specified area. Such incidents should nevertheless be limited in value, duration and frequency of occurrence. [26]

For other nodes in the grid, a voltage difference of 10% from the rated value is tolerated.

Some of the smaller generators are set back to PQ-buses. This is done to avoid conflicts with closely placed LTC-transformers. As mentioned above, the generator will end up at either maximum or minimum allowed reactive power production if there is a small mismatch between the specified terminal voltage and the controlled voltage of the transformer. The small generators are not supposed to provide the grid with major reactive support, which is why this simplification is made. The generators defined as PQ-nodes in OPTPOW are listed in the steady-state initial OPTPOW file given in Appendix E. This choice is supported by [17] where it is stated that small synchronous machines are the ones which justifiably could be set to have a constant power factor.

It is important to monitor the voltages at these generators if major changes are made to the steady-state model. If the terminal voltage becomes unacceptable, a resizing of the reactive power production might be necessary.

After all the efforts made in order to get all values in the grid within acceptable limits, there are still two generators that operate at the maximum reactive power limit and that have an unacceptable low terminal voltage. These two generators are located at Langvatn. The generators have a rated voltage of 11 kV. Directly above these generators there are two three-winding transformers without regulation. The transformers have a rated turn ratio of 142 kV / 10 kV. If this was an ideal transformer, without any losses, a rated voltage at the generator terminals would give a voltage of 156.2 kV or 1.18 pu in the regional grid. A lowering of the terminal voltage to 0.95 pu or 10.45 kV would give a voltage of 1.12 pu or 148.4 kV. The grid configuration is illustrated by Figure 4.5.

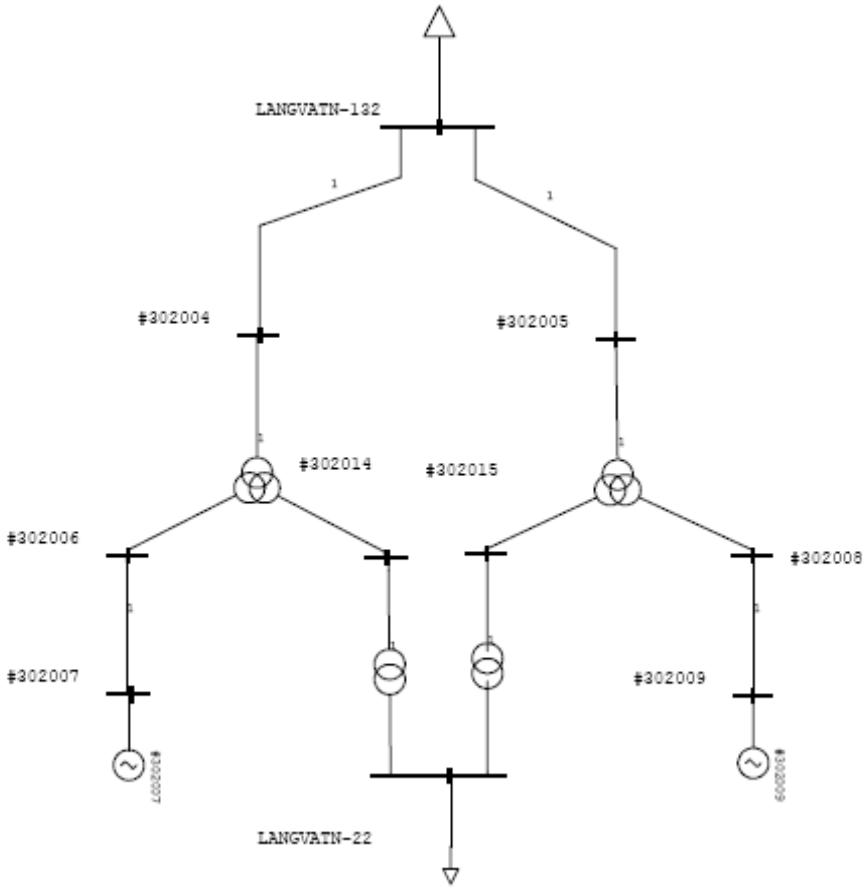

Figure 4.5: Grid configuration at Langvatn

As a compromise, a voltage lower than 0.95 pu on the generator terminals is tolerated. This is done to give an acceptable voltage on the high voltage side of the transformer. It should be noted that the voltage at the terminals of these generators in the Netbas model is below 0.9 pu.

The only node in the initial power flow that has a voltage outside the acceptable deviation of 10 % from the nominal value is a node at the 220 kV level at Nedre Røssåga. In the initial power flow the voltage at this node is at 1.121 pu or 246.6 kV. This is normally an unacceptable voltage deviation. However, the maximum allowed voltage at this level in Netbas is set to 250 kV. Therefore no attempt is being made to reduce this voltage.

The results from the initial steady-state power flow in SIMPOW are given in Appendix E.

Table 4.5 compares the results from the static power flow in SIMPOW with the results from the power flow in Netbas.

Table 4.5: Key results for steady-state power flow in SIMPOW and Netbas

Parameter	SIMPOW	Netbas	Difference	Difference in %(1)
Active prod. generators [MW]	1321.33	1321.54	-0.21	-0.02
Reactive prod. generators [MVAR]	204.62	177.66	26.96	15.18
Active prod. Ref bus [MW]	-940.32	-940.12	-0.20	-0.02
Reactive prod. Ref bus [MVAR]	61.64	82.73	-21.09	-25.49
Reactive prod. shunt cap. [MVAR]	244.33	242.99	1.34	0.55
Active grid losses [MW]	45.76	45.96	-0.20	0.44
Reactive grid losses(2) [MVAR]	252.34	224.05	28.29	12.63
Active load [MW]	1275.58	1275.58	0.00	0.00
Reactive load [MVAR]	196.60	196.60	0.00	0.00

(1) The value from Netbas is used as reference.

(2) The reactive losses in Table 4.5 include the generation of reactive power from transmission lines.

Table 4.5 shows that there is practically no variation in total active power flow and active losses between the two models. The biggest differences are in the reactive power flow. This was expected due to the removal of the regulating units mentioned above. When these centrally placed units are removed, the reactive power needed in the grid to maintain voltages has to be produced by generators elsewhere. This leads to a larger reactive power flow in the grid and larger reactive losses.

A more detailed comparison between the SIMPOW and Netbas model is shown in a Microsoft Excel sheet provided in Appendix E

It is possible that the deviation in reactive power flow between the two models can be reduced even more. A better solution might be found by adjusting the terminal voltages on UP-generators or by adjusting the reactive power production on PQ-generators. However, when the size of the model and the changes which are done are taken into account, the solution which is done here is considered to be adequate as a basis for further modelling.

4.3.3 Expansions to Initial Steady-State Model

As explained in the project description, a decision regarding which generator technology that shall be used in the wind farms has not been taken for any of the two wind farms. For this project it has been chosen to use doubly-fed induction generators (DFIG) for wind power generation. This is a more advanced and up-to-date technology than the traditional asynchronous generator. For more details regarding this type of generator and the modelling in SIMPOW, see chapter 3.3 and [19].

In the steady-state calculations, the doubly-fed induction generator is set to have a power factor of unity. This could be compared to other generator solutions with either no reactive power consumption or full reactive power compensation. This will create differences in the steady-state power flow compared to the representation used in the initial SIMPOW model,

and the Netbas model. There is not made an effort to obtain the same power flow as in the initial model.

The wind farm configuration used in the initial modelling is kept also after the introduction of the new generators. This means that the wind farms at Sleneset and Sjonfjellet are each represented by two aggregated generators and turbines. However, the generators are now connected to the grid at 0.69 kV. Between the 22 kV level and the 0.69 kV level, two new transformers are introduced in each farm. The losses between the 0.69 kV level and the 22 kV level will then also be included.

The aggregation of the two wind farms is a simplification. A consequence of this simplification is that all generators and turbines behave identically. This is nevertheless a way of representing wind farms that has already been extensively applied to power system analysis of large power systems. An advantage of making an aggregation is a reduction of the modelling and simulation time [27]. Whether or not this is a valid simplification depends on which simulations that shall be performed. In this project, no wind model based on statistic wind data is included, and the main focus is on the grid outside the internal grid of each farm. The simplification is therefore considered to be valid for this project.

The DFIG is defined under the data group "Asynchronous machines" in OPTPOW. Here, the steady-state electrical parameters for the generator are inserted. The electrical parameters used to describe the generators are based on data given in [14]. Compared with typical values listed in [13], these values are considered to be valid. The assumption that the pu values will be the same for aggregated generators as for a single generator has been made in this project.

In some of the cases in the simulations a static VAR compensator is added at Bardal. This SVC is in the steady-state model defined in the same way as the existing SVCs at Nedre Røssåga. However the size of this SVC is increased in the model in order to avoid that the SVC at Bardal becomes a limiting factor.

For some of the simulations, a secondary regulator is added in the SVC at Bardal. This regulator is included to control the reactive power flow in the connection point between the radial connection towards the wind farms and the main grid.

The secondary regulator added at the SVC at Bardal needs a transmission line to measure the reactive power flow. In order to compensate for the reactive losses in the transformer between radial towards the wind farms and the main grid at Nedre Røssåga, the monitored transmission line has to be on the high-voltage side of the transformer. Since there are several transmission lines connected to the node (Nedre Røssåga 300A) on the high-voltage side of this transformer, a new transmission line is inserted between the transformer and this node. This is a transmission line which all of the power flow between the main grid and the wind farm radial has to go through. The impedance of the line is set low in order to minimize the effect on the simulation results. The grid configuration at the connection point at Nedre Røssåga with the inserted line is described in Figure 4.6. The arrows represent connections to the rest of the grid.

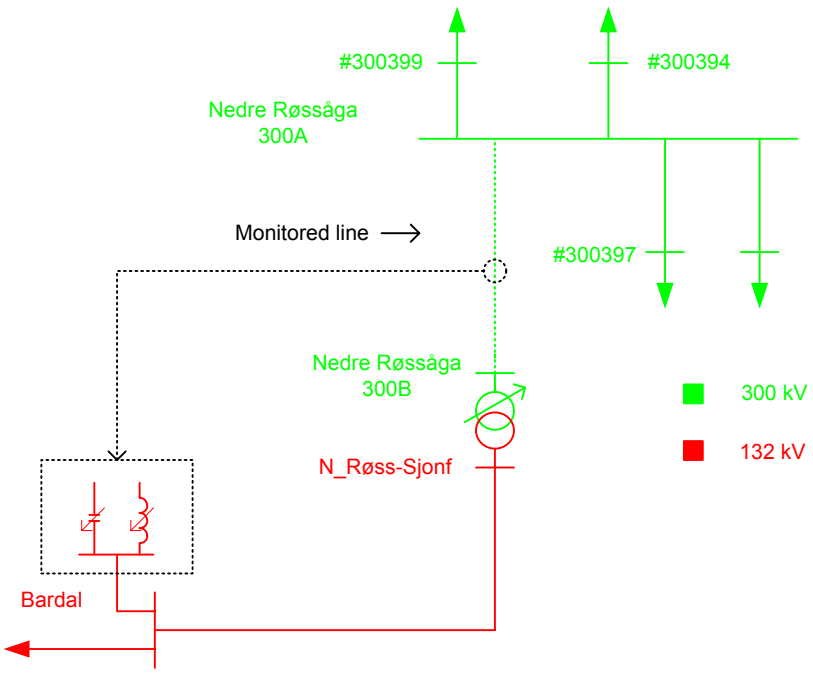

Figure 4.6: Grid configuration at connection point at Nedre Røssåga with monitored transmission line

A single line diagram describing the entire steady-state model is provided in Appendix E.

4.3.4 Dynamic Model

4.3.4.1 Synchronous machines

In the dynamic model the reference bus at Tunnsjødal is set as the reference machine.

The synchronous generators in the grid are set as type 2 generators. This means that they have one field winding, one damper winding in d-axis and one damper winding in q-axis. Saturation is included. Due to a lack of dynamic data, typical electrical parameters have been used for the synchronous generators in the grid. These parameters are derived from a comparison of typical parameters given in [28], [8] and [11] together with Trond Toftevaag at SINTEF Energiforskning AS. This is a simplification which will most likely result in a deviation in the dynamic response of the model compared with the real grid. The parameters for the synchronous machines are given in the dynamic model files provided in Appendix E.

During the set up of the dynamic model, several different voltage regulators are tested. Combined with the dynamic description of the doubly-fed induction generators, several of these voltage regulators create numerical difficulties in the simulations. These numerical difficulties are most likely connected to the SIMPOW description of the DFIGs. [29] It was therefore decided to change the voltage regulator of the synchronous machine to a regulator that does not create numerical problems during simulations. This is a DC excitation system.

A DC excitation system utilizes DC generators as sources of excitation power. The current is provided to the rotor of the synchronous machine through slip rings. The exciter can be driven by either a motor or by the shaft of the generator. [8]

It should be noted that DC excitation systems represent early excitation systems which have lost favour today. [8] Using them in the model can therefore cause deviations between the dynamic results and the real responses in the grid.

The block diagram for the voltage regulator used on the synchronous machines in the dynamic model is shown in Figure 4.7. [19]

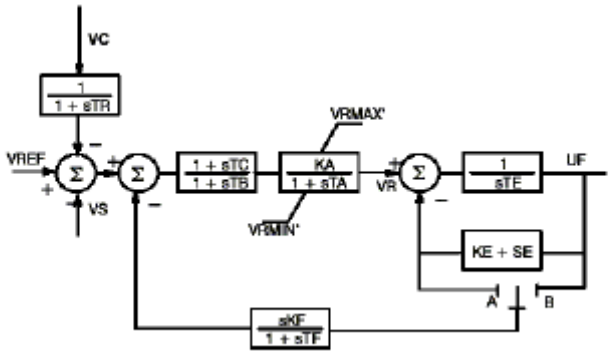

Figure 4.7: Block diagram for voltage regulator, from [19]

The input values for this regulator is given in Appendix D. The input values are provided by Trond Toftevaag at SINTEF Energiforskning AS. [30]

For further description of this regulator, see [19] or [23].

4.3.4.2 Static VAR compensators

The two SVC-facilities located at Nedre Røssåga are defined under the data group "SVC" in DYNPOW. The rated capacity is specified, and they are set to control the voltage at the associated node.

The regulator controlling the SVCs is a symmetrical static VAR compensator regulator (SVS). The regulator is equipped with a lead-lag network. Figure 4.7 shows the SVS regulator, while Figure 4.8 shows the lead-lag network. This regulator is identical to the one used in [5] and is provided by SINTEF Energiforskning AS.

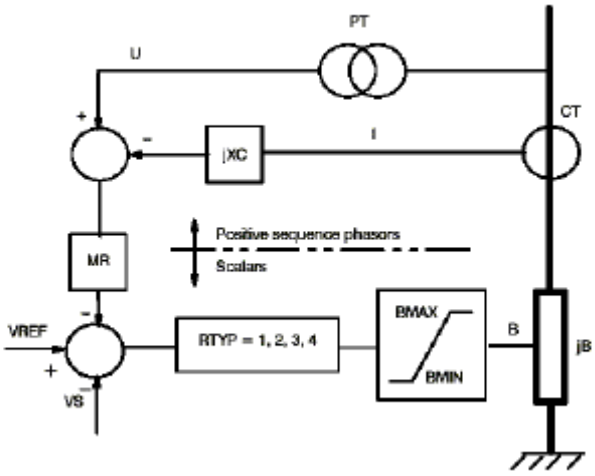

Figure 4.8: SVS regulator, from [19]

PT is a potential transformer. CT is a current transformer. MR represents a measuring rectifier. The parameters U, I, and B represent terminal voltage, current output and the susceptance of the SVC. The jXC block gives the reactive compensation degree. A negative value means that a droop in the bus voltage is created, proportional to the lagging current of the SVC. A positive value means a voltage rise. If the current is leading it will give the opposite sign. [19]

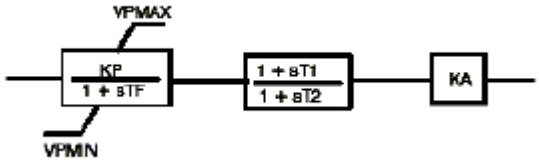

Figure 4.9: Lead-lag network for SVS regulator, from [19]

The SVC included at Bardal in some of the cases in the simulations is defined with the same regulators as the SVCs located at Nedre Røssåga. However, the proportional gain is set higher in some of the simulated scenarios. This is done to avoid a numerical problem caused by the combination of the regulator of SVC and the doubly-fed induction generators in power factor control. A lower proportional gain caused disconnection of the frequency converter in the DFIGs during high power production. [31]

The values of the different parameters for this regulator are given in Appendix D.

For further description regarding the SVS regulator, see [19] or [23].

The secondary regulator in the SVC at Bardal regulates the voltage reference in the SVC to keep a constant reactive power flow in a monitored transmission line. A block diagram describing this secondary regulator is shown in Figure 4.10.

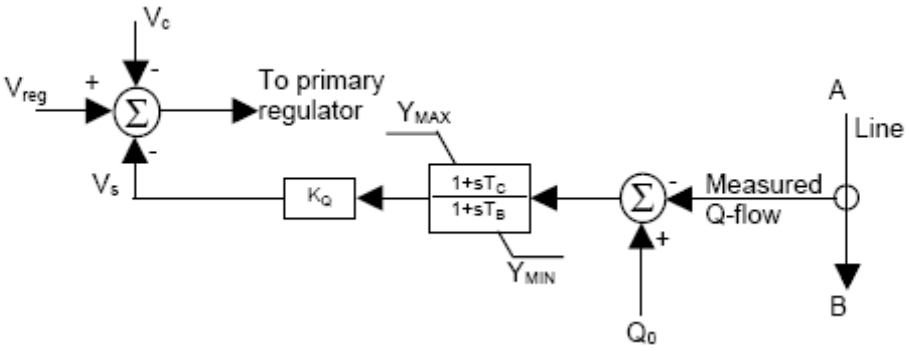

Figure 4.10: Block diagram for secondary regulator SVC at Bardal, from [32]

The regulator monitors the reactive power flow in the transmission line between A and B. This measured flow is compared with a reference value, Q_0, defined by the steady-state reactive power flow in the transmission line. If this difference is negative, reactive power is drawn from the main grid. The secondary regulator then increases the terminal voltage reference for the SVC. The SVC will then produce more reactive power. [32]

It should be mentioned that no dead band is implemented for this regulator. This will cause the regulator to act on small differences in the reactive power flow.

This secondary SVC regulator is provided by SINTEF Energiforskning AS. The values of the different parameters in the regulator are given in Appendix D.

4.3.4.3 Doubly-fed induction generators

The doubly-fed induction generators are described in the data group "ASYNCHRONOUS MACHINES" in DYNPOW. Here, a reference to the DSL-script "MACHDYN" must be made. In this script the dynamic equations describing the DFIG is located. The zero and negative sequence impedances for the DFIG are also defined in this data group.

The DFIG can be set to operate in three different control modes. It can be set to operate with unity power factor in the external rotor circuit or at the terminal bus. A third option is to control the terminal bus voltage. In the simulations in this project, the generators are set to operate with unity power factor at the terminal bus and in voltage control.

For each doubly-fed induction generator, a link to the respective wind turbine must be given. The wind turbine used in this project is a DSL-script designed for wind turbines. The turbines are aggregated in order to correspond with the aggregated generator. Hence, the two equivalent wind turbines representing a wind farm are scaled up from a single wind turbine. The base power of these turbines is N times the base power of a single turbine. N is the number of turbines in each aggregated turbine. The aggregation results in values that are not physically possible for a real turbine. The calculations done in order to aggregate the turbines are shown in Appendix C. The values used in this aggregation are based on an example turbine provided in [19]

The rotor power coefficient, C_p, is important to calculate the power output from the wind turbine. It is a function of the tip-speed ratio, λ, and the blade angle, β. It is common to present C_p as a function of λ for a specific blade angle. [19] An example of such curves is presented in Figure 4.11.

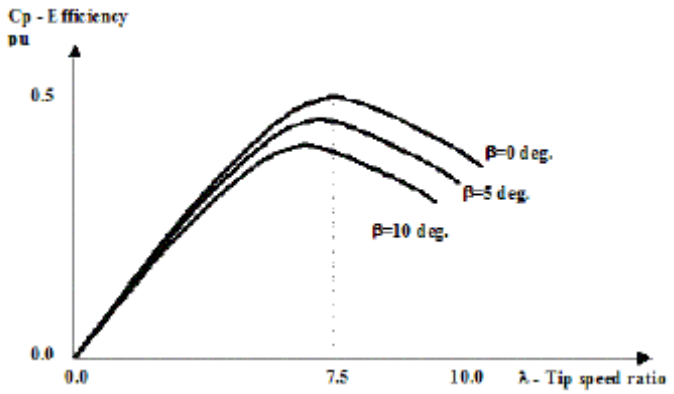

Figure 4.11: Example of Cpλ -curves for different blade angles, from [19]

In this project, it has been chosen to use the default C_p characteristics specified in [19]. This is done because a decision regarding what kind of turbine which is going to be used in the planned wind farms has not yet been taken. [3] [4]

The production of the wind farms is altered by referring to a table describing the wind speed during the simulated time. The default wind speed in DYNPOW is the wind speed corresponding to the level of production specified in OPTPOW.

A description of the DFIG model in SIMPOW and the different regulators included in this model is given in chapter 3.3.4. The input parameters in these regulators are given in Appendix D. Other input parameters in the doubly-fed induction generators are provided in the model files included in Appendix E.

As mentioned in section 3.3.3, the DFIG configuration with a crow-bar resistor is not able to meet the demanded fault-ride through capabilities specified in new grid codes. However, the DFIG SIMPOW model used is the only DFIG model included in SIMPOW. As described in [17], the fault-ride through capabilities will depend greatly on the chosen generator configuration. It will therefore be necessary to perform additional fault-analyses when a generator solution is chosen.

For further details regarding the dynamic modelling of the doubly-fed induction generators and the wind turbines, see [19].

4.3.4.4 Transformers

For some of the simulations, dynamic load tap changer regulators are used on the LTC-transformers in the wind farm radial. There are two available regulators in SIMPOW. One regulator is described in the SIMPOW manual [19] and the other is described in [33]. The latter is referred to as the "Beta-regulator".

Test simulations are performed on a small test grid in order to illustrate the differences between the two regulators. Descriptions of the transformer regulators and the results from the test simulations are given in Appendix B.

The test simulations indicate that the Beta-regulator is preferable for the simulations performed in this project.

The settings of the load tap changer regulators used in the simulations described in chapter 5 are based on the theory given in chapter 3.2. These settings can be found in Appendix E where the dynamic model files are included.

It should be noted that the Beta-regulator does not allow the time delay to depend on the voltage difference. Constant time delays are therefore employed.

5 Case Descriptions and Results

5.1 Introduction

In this chapter the simulations performed in this project are described and the results are presented. In order to improve the readability, a short discussion regarding the specific cases is included in the same section as the results are presented. A general discussion with less emphasis on detailed results is given in the next chapter.

To limit the size of this report, diagrams describing responses similar to responses presented in preceding diagrams or diagrams not considered to be important for the discussion are placed in Appendix E.

In all the simulations, the connection between the main grid and the radial towards the wind farms is considered to be the connection point. This is due to that the radial connection from the wind farms to Nedre Røssåga is planned exclusively for this project and does not exist in the grid today.

A single line diagram describing the grid configuration between Nedre Røssåga and the wind farms at Sjonfjellet and Sleneset is given in Figure 5.1.

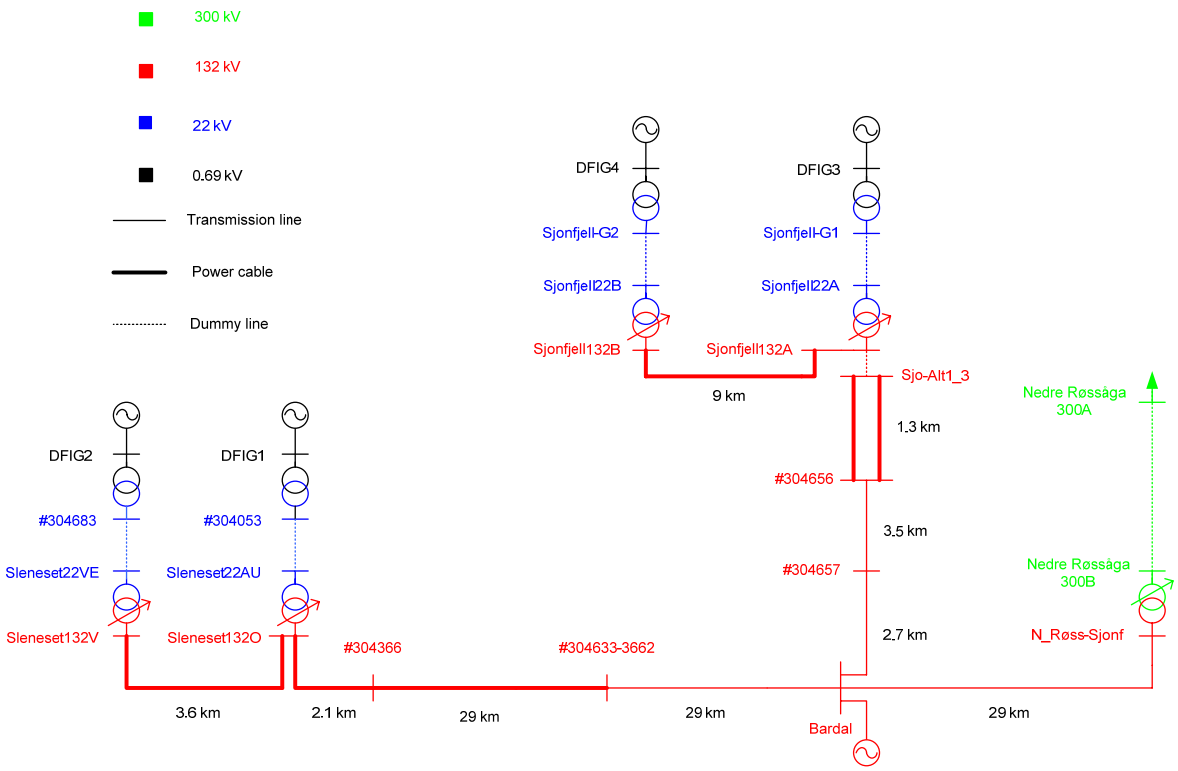

Figure 5.1: Single line diagram for radial connection between wind farms and connection point at Nedre Røssåga

5.1.1 Description of Cases

In this project, several different steady-state power flow scenarios and different dynamic scenarios are simulated. A specific description of the different cases is given at the start of each case. However, in order to provide a better overview of how the different steady-state

power flows is connected with the different dynamic scenarios, a short description is included here.

There are three different steady-state power flows used in the simulations. These are listed below.

1. Steady-state power flow based on the initial SIMPOW model. However, doubly-fed induction generators are inserted for wind power generation. These are set to have a power factor equal to 1 in the steady-state calculation. No reactive power compensation is added at Bardal.
2. Same as 1. However, an SVC is included at Bardal. The terminal voltage of the SVC is adjusted to minimize the reactive power exchange on the high voltage side of the transformer at Nedre Røssåga during the steady-state calculation.
3. SVC added at Bardal. However, the voltage level within the radial is lowered by lowering the terminal voltage of the SVC at Bardal and desired voltage of the regulating transformer at Nedre Røssåga. This results in a different reactive power flow in the connection point and a slightly different steady-state voltage in the main grid.

The connection between the different steady-state power flow scenarios used in the different dynamic cases are described in Table 5.1.

Table 5.1: Connection between steady-state power flow and dynamic case

Dynamic scenario	1.1	1.2	2.1	2.2	3.1	3.2	4.1	4.2	5.1	5.2	5.3
Steady-state scenario	1	2	1	2	2	2	3	2	3	2	2

5.2 Transmission Capacity

5.2.1 Introduction

When planning a wind farm at the end of a radial branch of the grid it is necessary to calculate the maximum amount of power that can possible be transferred into the main grid without reaching any unacceptable operating conditions. In order to find this amount, dynamic analyses with ramping of production are performed.

There are several factors which may decide the limit for maximum power transfer:

- Thermal limits in transmission lines
- Unacceptable voltages at generator terminals or in the grid
- Voltage stability limits

Generator characteristics and reactive power compensation will influence these limits. Theory regarding the DFIG generator is described in chapter 3.3. Theory about power transmission, reactive power compensation and voltage stability is described in [5].

Since a decision regarding the generator technology and the reactive power compensation to be used in the planned wind farms has not yet been taken, the maximum power transfer capacity is calculated for different solutions.

First, the doubly-fed induction generator is set to control the power factor at the terminals to unity. No further reactive power compensation is added. This could compare to other generator solutions where the reactive power consumption of the generators is fully compensated, or to a generator that does not draw reactive power from the grid, but have no voltage regulating capabilities.

The second step will be to install an SVC on the radial branch. This will compensate for the increased reactive power losses in the grid due to higher power transfers. The SVC is inserted at Bardal.

Finally, identical simulations are carried with the DFIG in voltage control mode. The DFIG in voltage control mode can be compared to other generating solutions with rapid voltage control at the generator terminals.

In all simulations, the crow-bar control regulator disconnects the frequency converter if the voltage at the DFIG terminals is below 0.9 pu or above 1.1 pu. This means that the voltage has to be between 0.621 and 0.759 kV. Whether this is a reasonable limit will depend on the design and robustness of the chosen generator. A maximum allowed voltage deviation of 10% from the nominal value is a normal standard in a power grid. However, during normal operating conditions a change in voltage of more than 5% on the generator terminals is considered to be unacceptable. [26]

In these first simulations, the increase in production is so fast that the influence from transformers with load tap changers is disregarded.

The starting point for all simulations is a steady-state power flow with approximately 50% production at both wind farms. The wind is then increased until the farms are at full production or unacceptable conditions occur.

The wind speed is calculated from the specified production level set in the steady-state simulation. By monitoring the values used in the pre-simulation, the initial wind speed can be found. The wind speeds are ramped almost identically for the four wind turbines. A small deviation is caused by a small deviation in wind speeds from OPTPOW.

Since there is a small difference in the initial wind speed for the four aggregated generators, four different tables are used to ramp the wind speed.

Normally the wind speed in two different wind farms will not be identical. However, these simulations are done in order to monitor the behaviour of the grid. A situation with high wind speeds in both farms will represent a worst case scenario regarding transmission capacity. Something which increases the likelihood of similar wind speed in the two wind farms is that they are located relatively close in distance. There is therefore a reason to believe that the correlation between them will be quite high.

5.2.2 Case 1.1 - DFIG in Power Factor Control Mode

5.2.2.1 Description

Case 1.1 represents a case where the doubly-fed induction generators are controlling the power factor at the generator terminals to unity.

The values obtained from the dynamic simulations are based on plotted values and might therefore cause some inaccuracies.

The basis for this case is that the wind farm at Sleneset is at 50% production and the wind farm at Sjonfjellet is at 48% production. The production is then increased by increasing the wind speed. The wind speed is increased from the initial wind speed obtained in OPTPOW towards a wind speed of 11 m/s in 50 seconds. The initial wind speed of the four aggregated wind turbines is between 9.26 and 9.38 m/s.

5.2.2.2 Power production

The simulations indicate that the first limit that is reached is the lower voltage limit at the terminals of the doubly-fed induction generators. It is the crow-bar regulator at DFIG4 at Sjonfjellet who disconnects the frequency converter first. This is shown in Figure 5.2. It shows the status of the crow-bar resistor for the four aggregated generators. The crow-bar resistor is activated at 33.385 seconds.

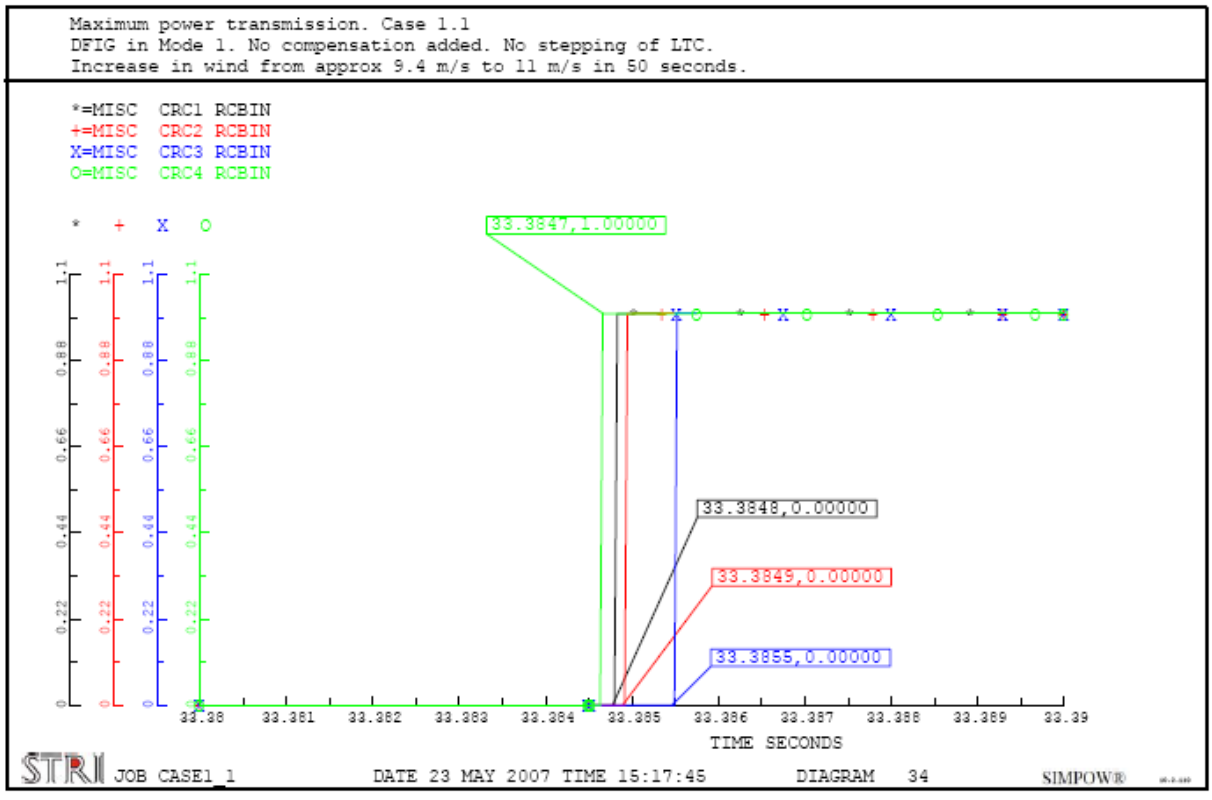

Figure 5.2: Status of crow-bar resistor, Case 1.1

As described in Appendix A, when the frequency converter is disconnected the generator starts to consume reactive power and thereby reduces the voltage further. This means that when one doubly-fed induction generator reaches its lower limit, it may cause the disconnection of the frequency converters of the other generators. However, in this case the terminal voltages of the DFIGs indicate that all of the generators would have reached their lower voltage limits eventually.

At the time the voltage reaches 0.9 pu at the terminals of DFIG4, the wind speed at turbine 4 is approximately 10.42 m/s and the production of the generator is at 154.2 MW. This equals a

production level of 63.5%. The active and reactive production of DFIG4 is shown in Figure 5.3.

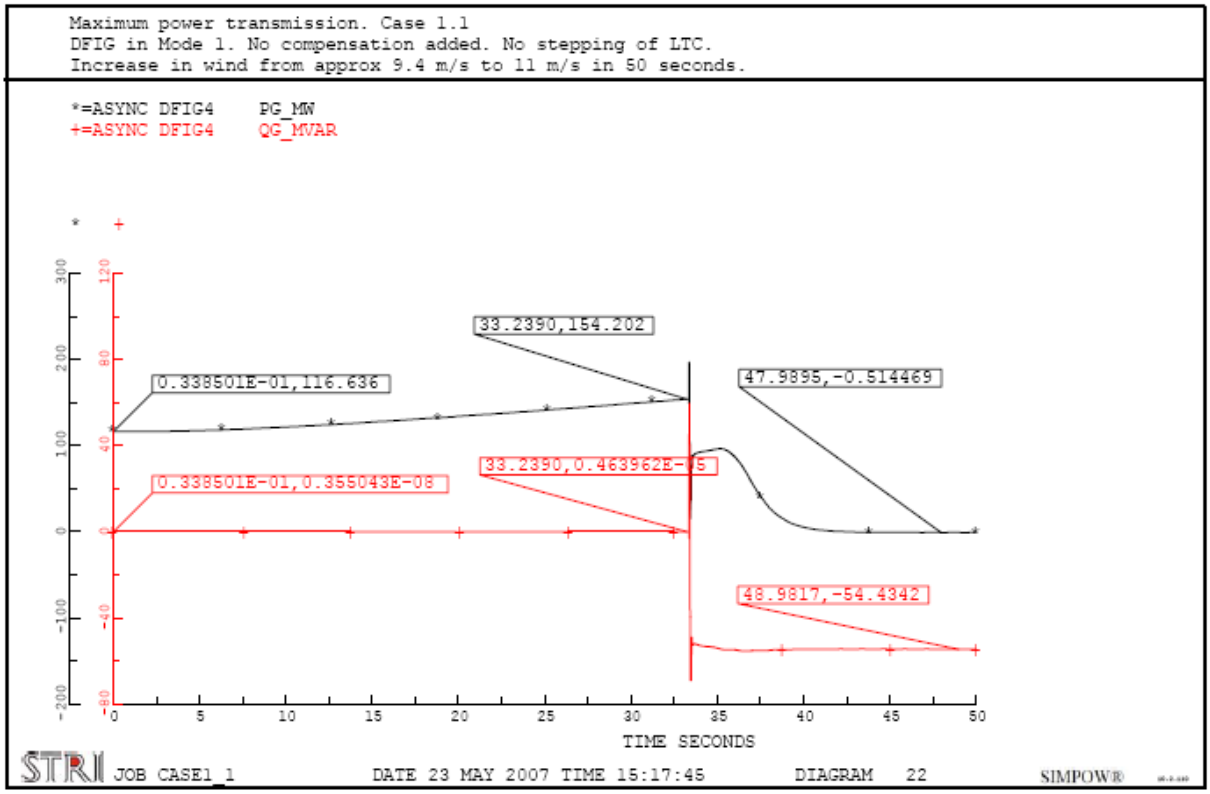

Figure 5.3: Active and reactive production from DFIG4, Case 1.1

The other aggregated generator at Sjonfjellet produces 117.4 MW when the frequency converter is disconnected. This is a production level of 63.5%. The generators at Sleneset both reach a production of 72.6 MW. This equals a production level of 64.5% of full production. The total production level reaches 63.8% of full production.

The reactive power produced in the radial connection containing the wind farms at Sleneset and Sjonfjellet is described in Table 5.2. It contains the reactive power produced by the doubly-fed induction generators and the reactive power imported at Nedre Røssåga. The total describes the reactive power consumed in the radial.

Table 5.2: Reactive power production when the frequency converters are disconnected, Case 1.1

Source	Reactive production at full active production [MVAR]
DFIG1	0
DFIG2	0
DFIG3	0
DFIG4	0
Imported at N.Røssåga	192.0
Total	192.0

5.2.2.3 Power flow

The active and reactive power flow at the connection point between the wind farms and the main grid at Nedre Røssåga is shown in Figure 5.4. It shows that for this particular increase in

production the reactive power drawn from the main grid increases from 49.2 MVAR to 192 MVAR.

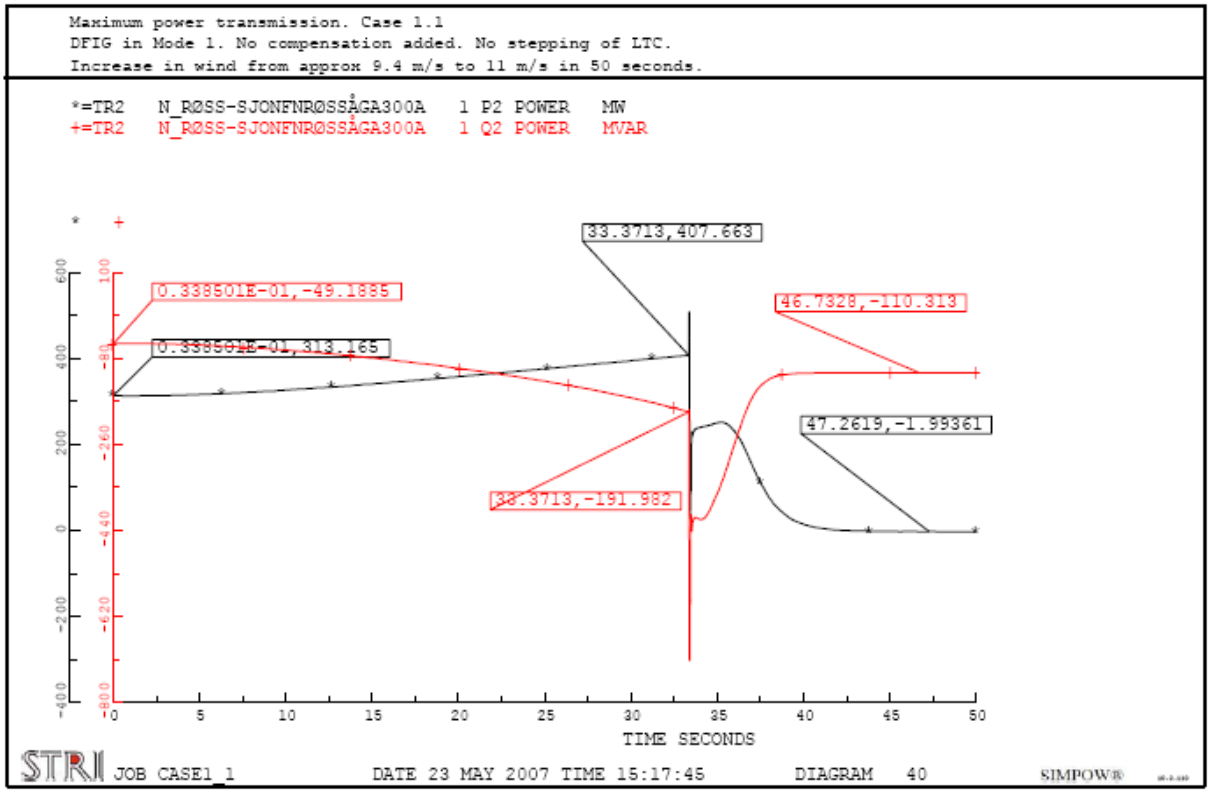

Figure 5.4: Active and reactive power flow through transformer at connection point at Nedre Røssåga, Case 1.1

Figure 5.5 shows the active and reactive power flow from the reference bus and into the grid. It illustrates the power flow between this model and the power system further south. From the starting point and to the disturbance occurs, the active power consumed by the reference bus increases from 939.7 MW to 1039.5 MW. This is an increase of 99.8 MW and implies that the entire increase in production from the wind farms is transported to the southern interface of the model. This was to be expected since the interface at Nedre Røssåga and Salten have a defined constant active power flow.

Figure 5.5 also shows that the reactive power drawn by the model augments. During the production increase at the wind farms the reactive power production of the reference bus increases from 60.0 MVAR to 138.4 MVAR. When the grid has stabilized after the disturbance, the reference bus has gone from producing reactive power to consuming reactive power. This is because of the reduced reactive losses in the grid due to less active power flow.

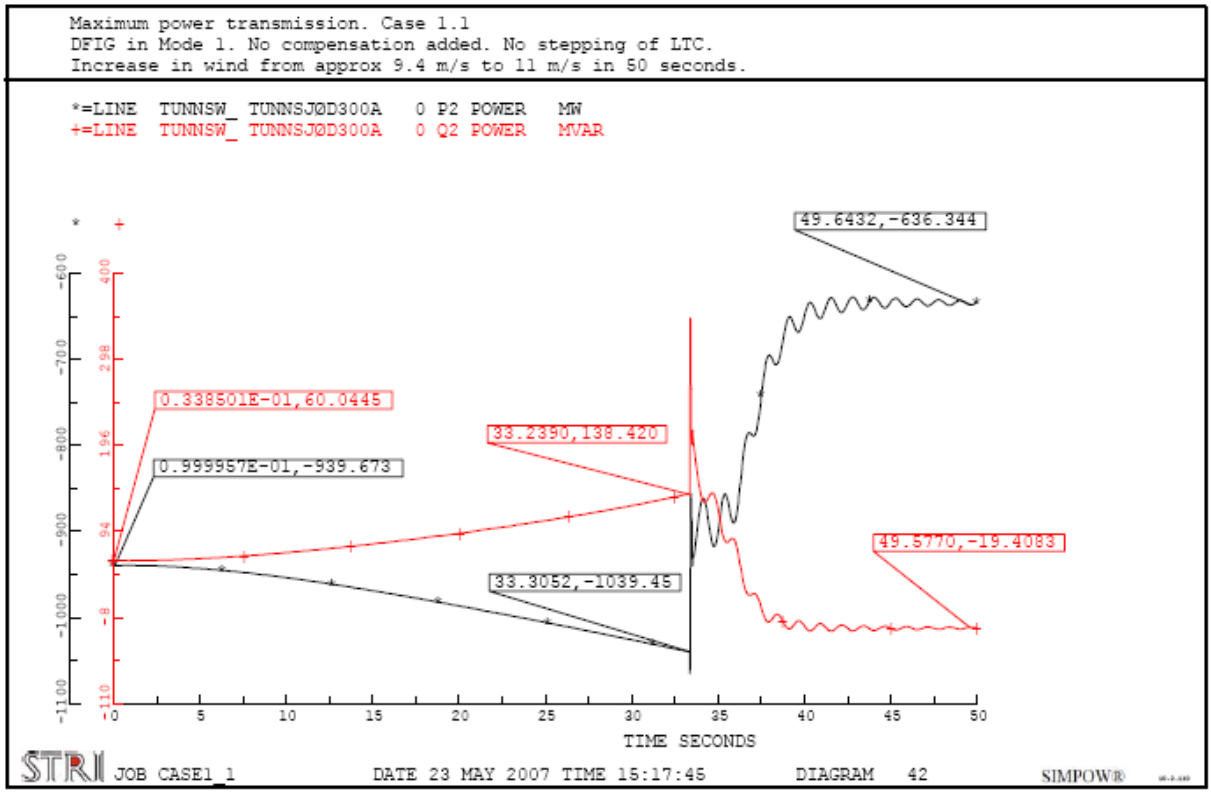

Figure 5.5: Active and reactive power flow from reference bus at Tunnsjødal, Case 1.1

5.2.2.4 Thermal limits

Table 5.3 shows the currents in the dimensioning lines and power cables between Nedre Røssåga and the wind farms at Sleneset and Sjonfjellet. It also illustrates the line outside the radial connection with the highest loading. This line is located between Marka and Øvre Røssåga.

Table 5.3: Line loading, Case 1.1

Line	I_{Limit} [kA]	$I_{63.8\% \text{ production}}$ [kA]	Loading [%]
Bardal – N.Røssåga	6.176	2.001	32.4
Sjo-Alt1_3 - #304656	1.160	0.661	56.9
Sjonfjell132A – Sjonfjell132B	1.160	0.756	65.2
#304633-3662 - #304366	0.970	0.687	70.8
Sleneset132O - Sleneset132V	0.715	0.344	48.1
#300763 - #300788	0.560	0.525	93.7

Table 5.3 shows that the power cable between node #304633-3662 and node #304366 has the highest loading in the radial when the frequency converters are disconnected. The loading is then at 70.8 % of full capacity. This cable is later only referred to as the power cable between Bardal and Sleneset. This is because it is the power cable in this connection with the lowest thermal capacity and therefore the most important to monitor.

The line with the highest loading in the grid is the transmission line between node #300763 and node #300788. This line has a loading of 93.7% of full capacity when the generators reach their lower voltage limit. However, the loading of this line is not heavily affected by the

increase in production from the wind farms. During this particular increase, the loading of the line increases with 0.6% of full capacity.

5.2.2.5 Voltage variations

The voltage at the terminals of DFIG4 is presented in Figure 5.6. The voltage never recovers above 0.621 kV (0.9 pu). The frequency converter therefore remains disconnected. As a result, the generator draws reactive power. Like in Case 1 in Appendix A, the pitch control regulates the blade angle in order to try to regulate the rotational speed. When β reaches its maximum angle of 27 degrees the mechanical torque is zero and the production goes to zero. The time lapse of the blade angle for the wind turbine of DFIG4 is shown in Figure 5.7.

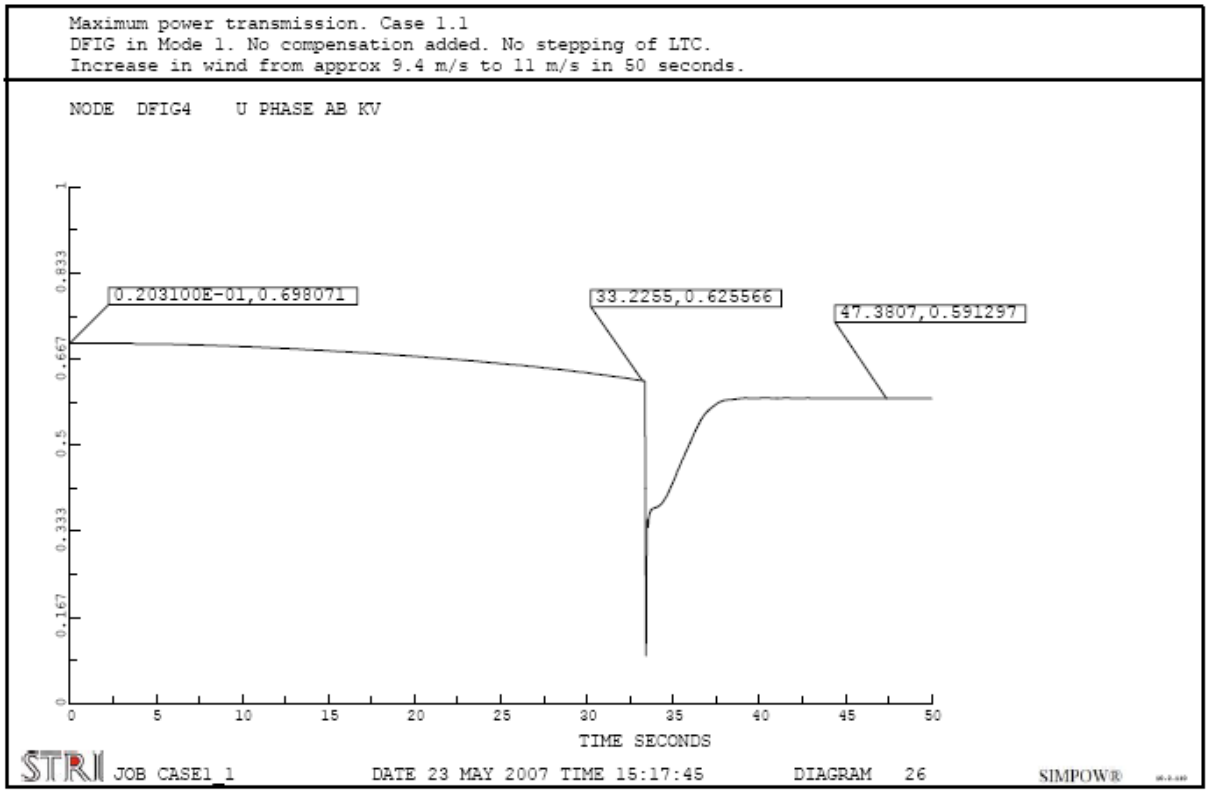

Figure 5.6: Voltage at terminals of DFIG4, Case1.1

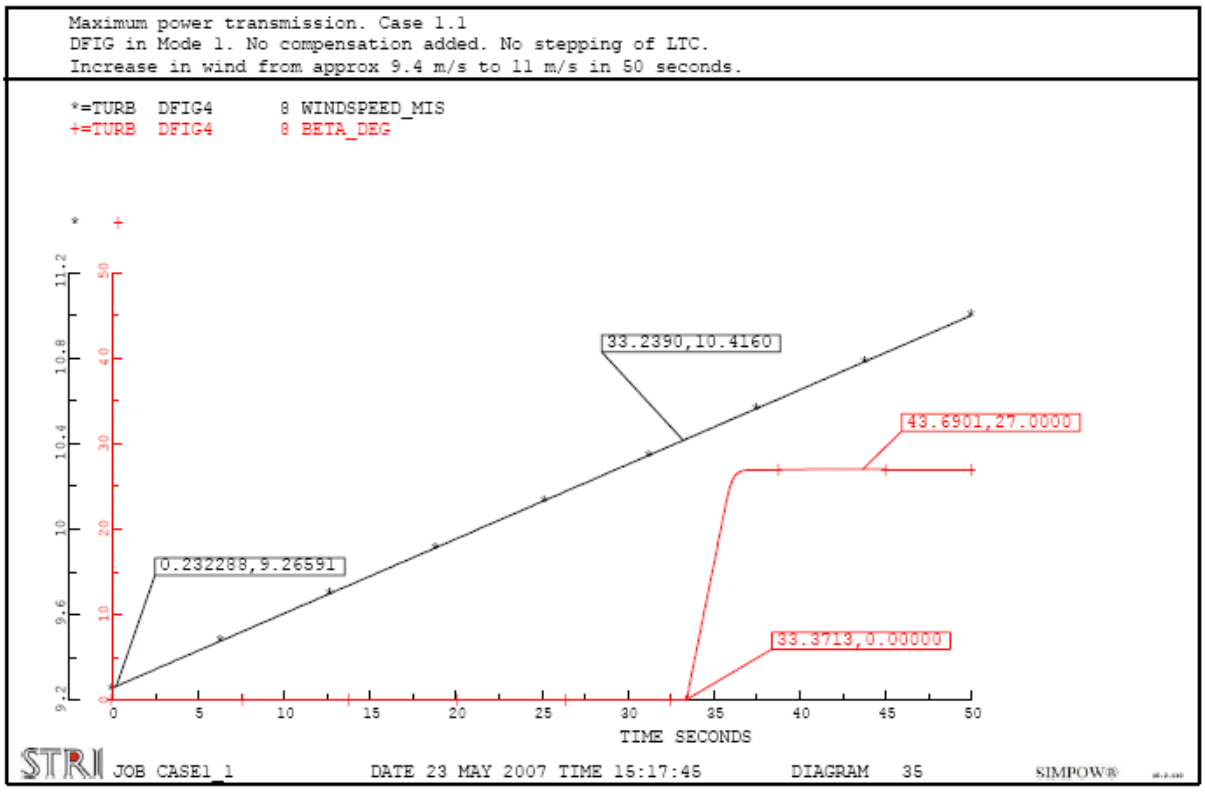

Figure 5.7: Windspeed and blade angle, Case 1.1

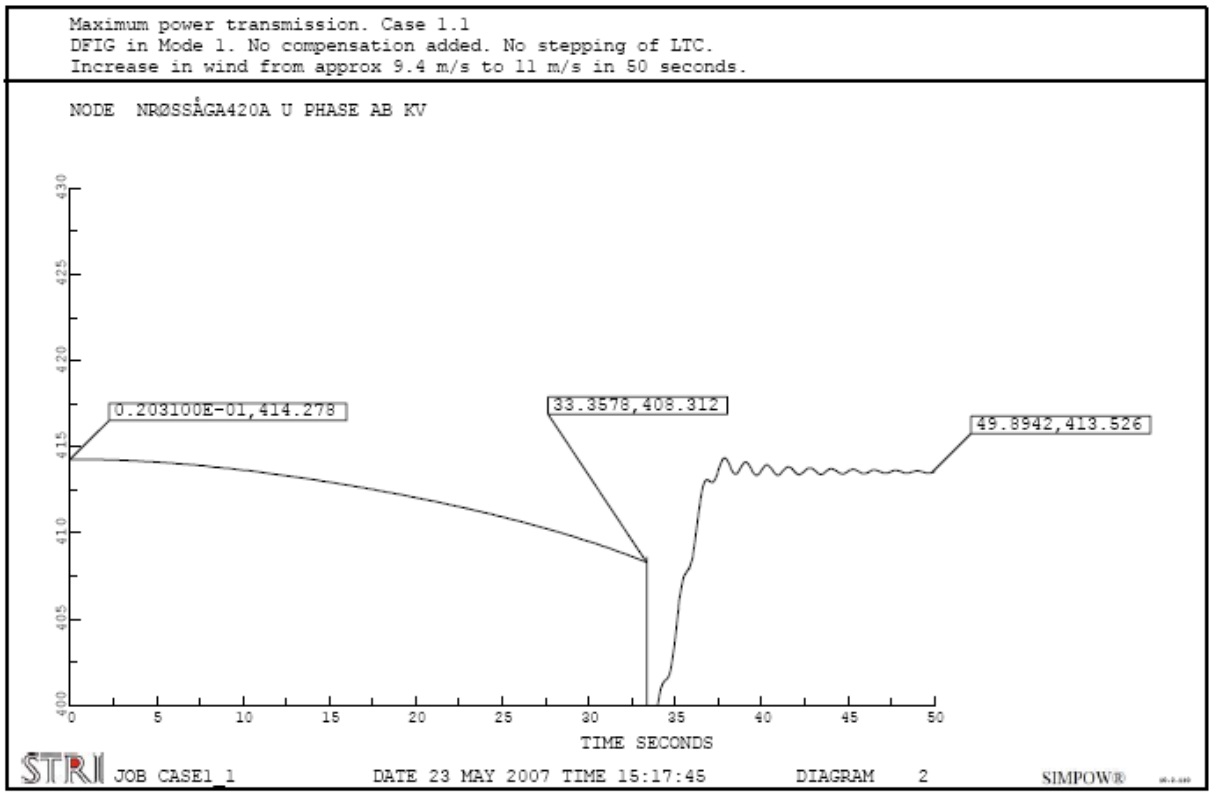

Figure 5.8: Voltage at 420 kV level at Nedre Røssåga, Case 1.1

Due to the production increase in the wind farms the voltages in the main grid decrease. The largest falls are at nodes in the wind farm radial and at nodes close to the connection point at Nedre Røssåga. The voltage at the 420 kV level at Nedre Røssåga is shown in Figure 5.8. Before the frequency converters are disconnected, the voltage is at 408.3 kV. As mentioned in

section 4.2.3, a voltage below 410 kV is not considered to be normal. An alarm would therefore go off if such a situation should occur.

The decrease in voltage due to the increased wind farm production is described in Table 5.4 for significant nodes in the grid. The voltage change describes the largest voltage change compared to the initial voltage. The maximum value voltage value during the production increase is at the start of the simulation. The minimum voltage while the generators are connected occurs at the instant just before disconnection of the frequency converters.

Table 5.4: Voltage change, Case 1.1

Node	Voltage level [kV]	Voltage at $P_{63.8\%}$ [pu]	Voltage change [%]
Salten	420	1.00	0.17
Rana420	420	0.98	-1.07
Nedre Røssåga	420	0.97	-1.42
Nedre Røssåga	300	0.98	-1.57
N_Røss-Sjonf	132	0.93	-6.01
DFIG1	0.69	0.90	-11.26
Trofors	300	0.99	-1.13
Majavatn	300	0.99	-0.82

5.2.2.6 General

Case 1.1 shows that the production reaches a level of 63.8% before the system reaches the specified lower voltage limit at the DFIG terminals. This is clearly not an acceptable situation.

In these simulations, it is focused on the conditions in the grid prior to the disconnection of the power electronics in the doubly-fed induction generators. This is done because the purpose of these simulations is to find the maximum possible production level at different generator settings and different compensating solutions. It should be noted that the grid seem to handle the loss of production from the wind farms without becoming unstable. However, the voltages at the DFIG terminals become unacceptable low. At the time when the frequency converters are disconnected there is a drop in voltage throughout the system. This drop might result in the trigging of protection devices or disconnection of other voltage sensitive components. This is not investigated further.

Responses considered not being important for the discussion is included in Appendix E. The output file from the steady-state power flow calculation along with the OPTPOW and DYNPOW files are also included in this appendix.

5.2.3 Case 1.2 – DFIG in Power Factor Control Mode and SVC at Bardal

5.2.3.1 Description

In Case 1.2 a Static VAR Compensator (SVC) is placed at Bardal. This is done in order to compensate for the increased reactive consumption in the transmission lines due to increased active production. The SVC is also introduced in the steady-state simulation. The controlled voltage is adjusted so that the reactive power flow at the connection point in Nedre Røssåga is minimized. This adjustment results in some unacceptable voltages in the grid, especially at the

420 kV level. The terminal voltage at some of the hydro power generators and the controlled voltages on some of the LTC-transformers between the main and regional grid are therefore adjusted in order to get an acceptable steady-state power flow. This will create a different power flow than the one used in Case 1.1.

The capacity of the SVC is set to 500 MVAR. This is done to avoid that the capacity of the SVC is the limiting factor.

Like in Case 1.1 the doubly-fed induction generators are controlling the power factor at the generator terminals to unity.

The values obtained from the dynamic simulations are based on plotted values and might therefore cause some inaccuracies.

The basis for this case is that the wind farm at Sleneset is at 50% production and the wind farm at Sjonfjellet is at 48% production. The production is then increased by augmenting the wind speed. The wind speed is increased from the initial wind speed obtained in OPTPOW to a wind speed of 13 m/s in 50 seconds. The initial wind speed of the four aggregated wind turbines is between 9.26 and 9.38 m/s. In order to let the system stabilize, the simulation is run for another 10 seconds after the wind speed has reached 13 m/s.

5.2.3.2 Power production

The results from the dynamic simulation demonstrate that the production at the wind farms increases from approximately 50% to 100% when the wind is increased from 9.4 m/s to 13 m/s. The responses for the doubly-fed induction generators show that the active production increases until the production limit is reached, while the reactive production is kept at zero. The production from DFIG1 is illustrated in Figure 5.9.

At approximately 30 seconds there is a change in the slope of the active power production. This change is due to the pitch controller. After 30 seconds, the pitch controller starts to regulate the blade angle in order to optimize the efficiency of the wind turbine. This will influence the slope of the power production, which again influences node voltages and reactive power flow. . Time plots showing the blade angle and the wind speed for the four aggregated wind turbines is given in Appendix E This pitch regulation is dependent on the wind speed, and will therefore occur in all cases where the wind speed is increased from 9.4 m/s to 13 m/s.

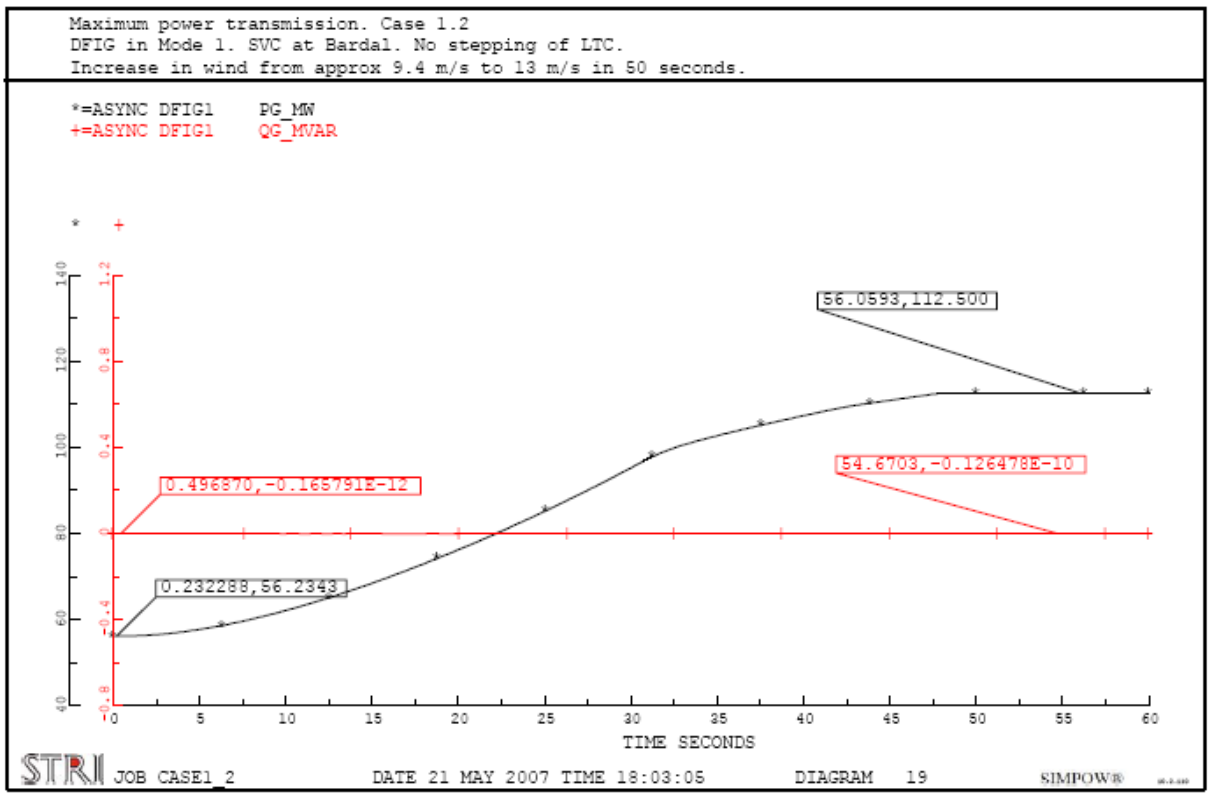

Figure 5.9: Active and reactive power production from DFIG1, Case 1.2

Figure 5.10 describes the reactive power production from the SVC at Bardal during the production increase in the wind farms. It shows that the reactive power production increases from 45.2 MVAR at 50% production to 334.8 MVAR at 100% production.

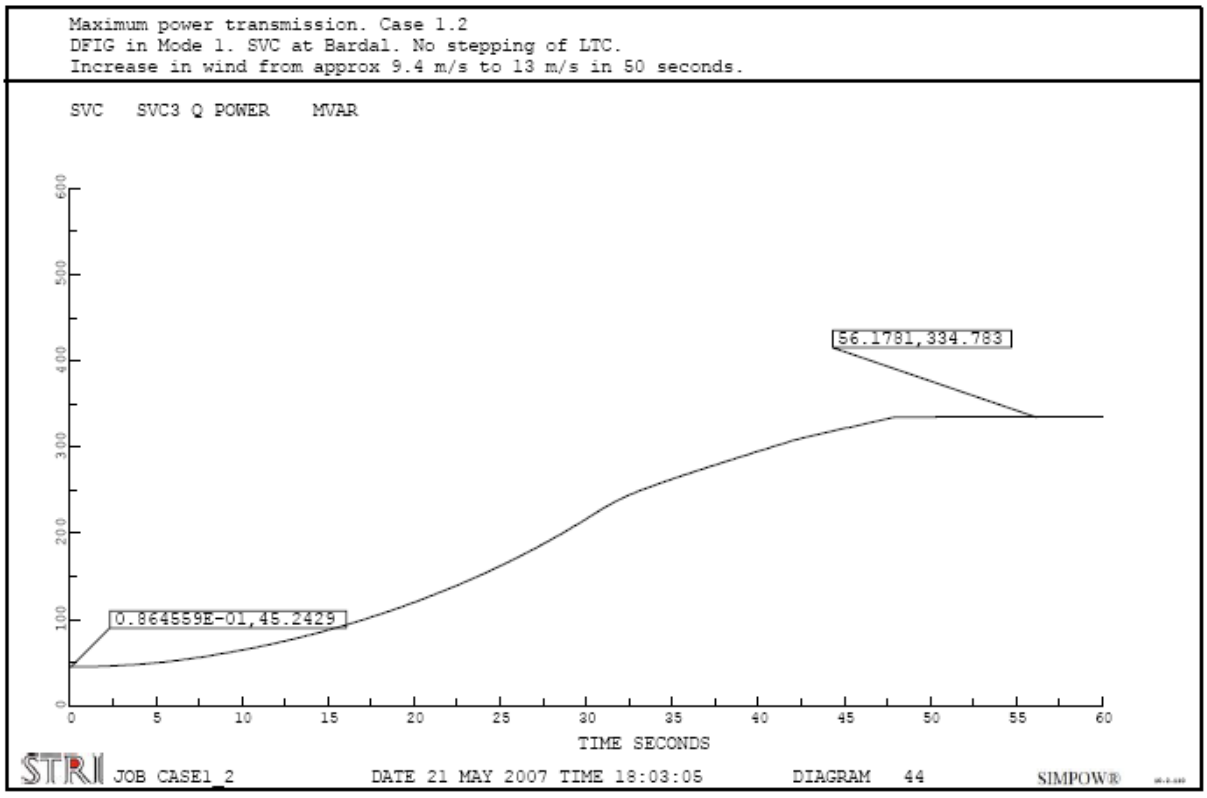

Figure 5.10: Reactive power production from SVC at Bardal, Case 1.2

The reactive power produced in the radial connection containing the wind farms at Sleneset and Sjonfjellet is described in Table 5.5. It contains the reactive power produced by the doubly-fed induction generators and the static VAR compensator at Bardal. In addition the reactive power imported at Nedre Røssåga is given. The row "Total" in the table indicates the total reactive power consumed in the radial.

Table 5.5: Reactive power production at full active power production, Case 1.2

Source	Reactive production at full active production [MVAR]
DFIG1	0
DFIG2	0
DFIG3	0
DFIG4	0
SVC3	334.8
Imported at N.Røssåga	115.7
Total	450.5

5.2.3.3 Power flow

The power flow through the transformer at the connection point at Nedre Røssåga is given in Figure 5.11. It shows that when the production in the wind farms is increased to full production, 115.7 MVAR is drawn from the main grid. The generators in the wind farms are, as shown in Figure 5.9, not consuming reactive power. The reactive power drawn from the grid is as a consequence due to increased reactive losses in lines and transformers.

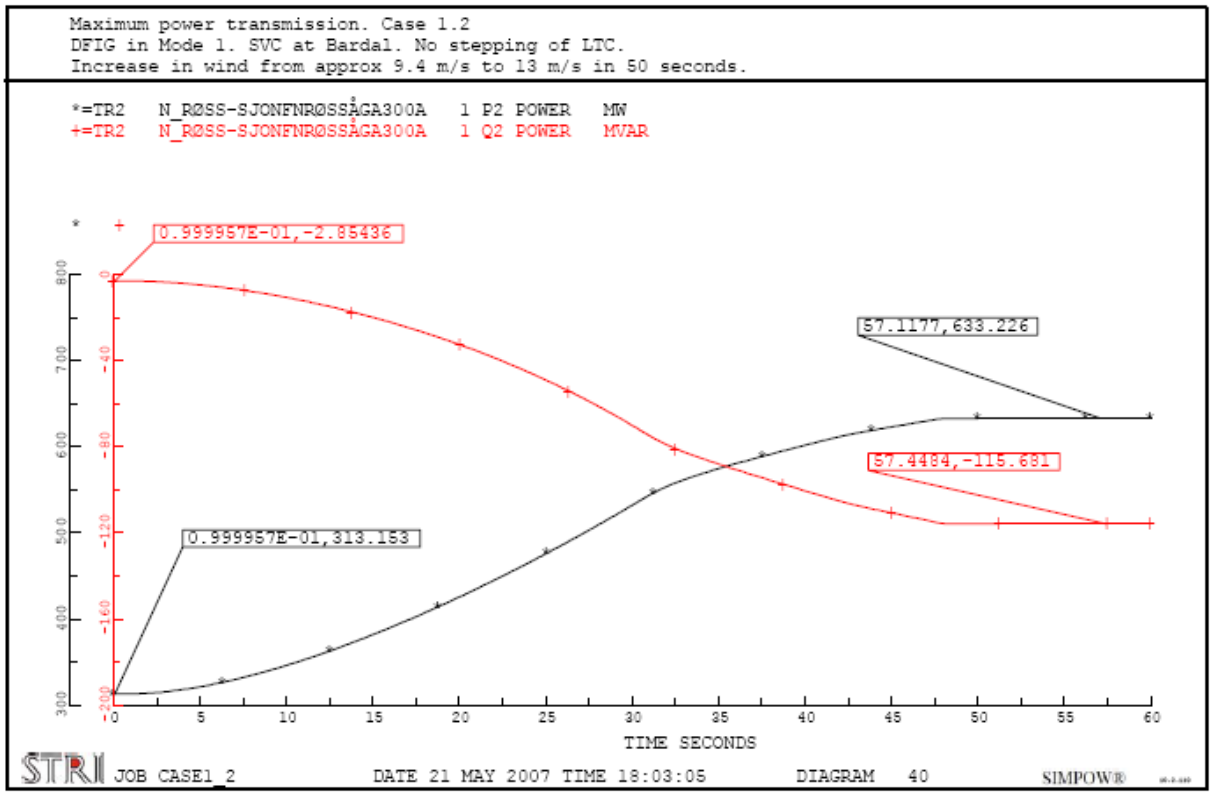

Figure 5.11: Active and reactive power flow through transformer at connection point at Nedre Røssåga, Case 1.2

Figure 5.12 shows the active and reactive power flow from the reference bus at Tunnsjødal. When the production in the wind farms are at 100%, the reference bus is consuming 1254.4 MW and producing 245.2 MVAR.

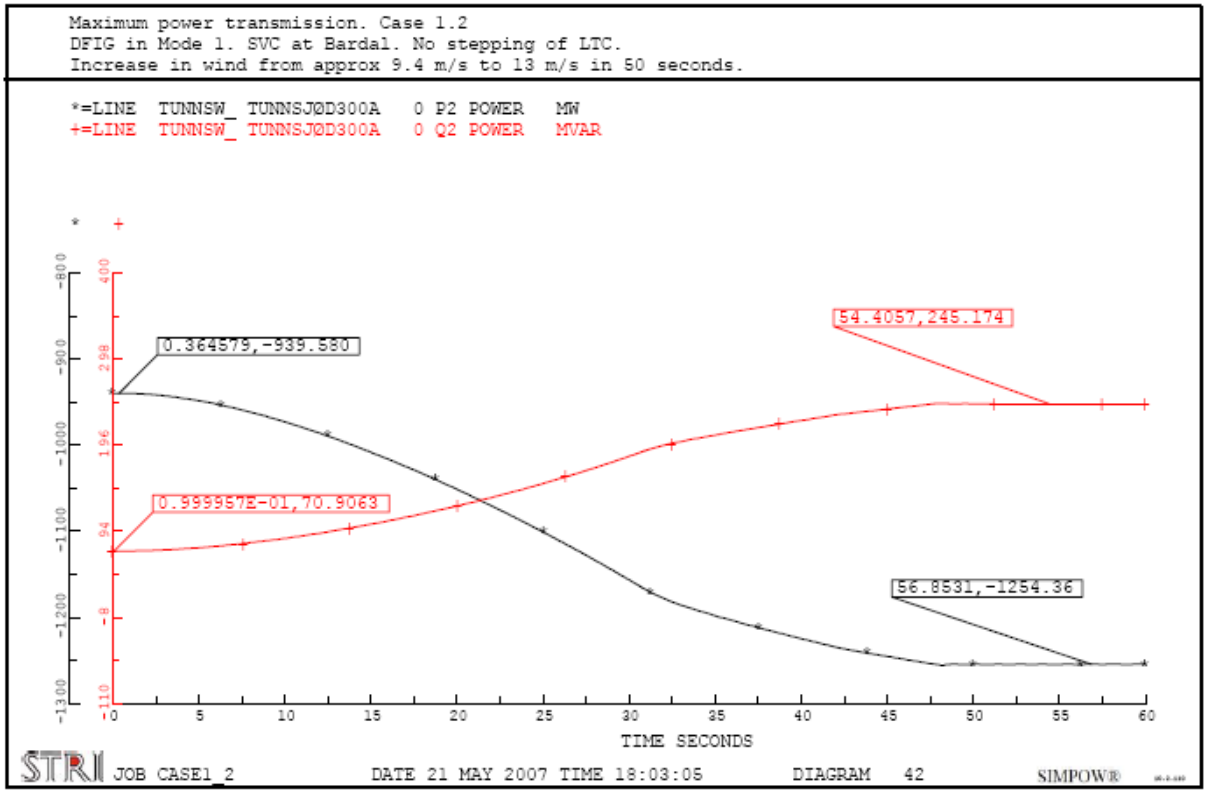

Figure 5.12: Active and reactive power flow from reference bus, Case 1.2

5.2.3.4 Thermal limits

Table 5.6 shows the currents in the dimensioning lines and power cables between Nedre Røssåga and the wind farms at Sleneset and Sjonfjellet. The table also present the line outside the radial connection with the highest loading. This line is located between Marka and Øvre Røssåga.

Table 5.6: Line loading, Case 1.2

Line	I_{Limit} [kA]	$I_{100\% \text{ production}}$ [kA]	Loading [%]
Bardal – N.Røssåga	6.176	2.924	47.3
Sjo-Alt1_3 - #304656	1.160	0.939	80.9
Sjonfjell132A – Sjonfjell132B	1.160	1.080	93.1
#304633-3662 - #304366	0.970	0.953	98.2
Sleneset132O - Sleneset132V	0.715	0.484	67.7
#300763 - #300788	0.560	0.526	94.0

Table 5.6 shows that the power cable between node Bardal and Sleneset has the highest loading during full production. The loading increases from 51.0% to 98.2%.

The transmission line between node #300763 and node #300788 has a loading of 94.0% during full production in the wind parks. However, this line is not affected by the production increase in the wind farms in the same way as the lines in the wind farm radial. During the

given production increase the loading in this line has an increase in loading of 2.5% of full capacity.

5.2.3.5 Voltage variations

The time plots for the voltages in the grid indicate that the decrease in voltage is largest at nodes close to the connection point at Nedre Røssåga. However, the voltage levels are acceptable at full production. The voltage level at the 132 kV side at the connection point at Nedre Røssåga is also at within acceptable limits during full wind power production.

An overview of the voltages in the radial connection between Nedre Røssåga and DFIG1 at Sleneset is given in Figure 5.13. The decrease in voltage due to the increase in power production is largest at the connection point, but all of the voltages are well within limits for what is acceptable. The voltage at Bardal is the most stable. This is because the SVC is located there.

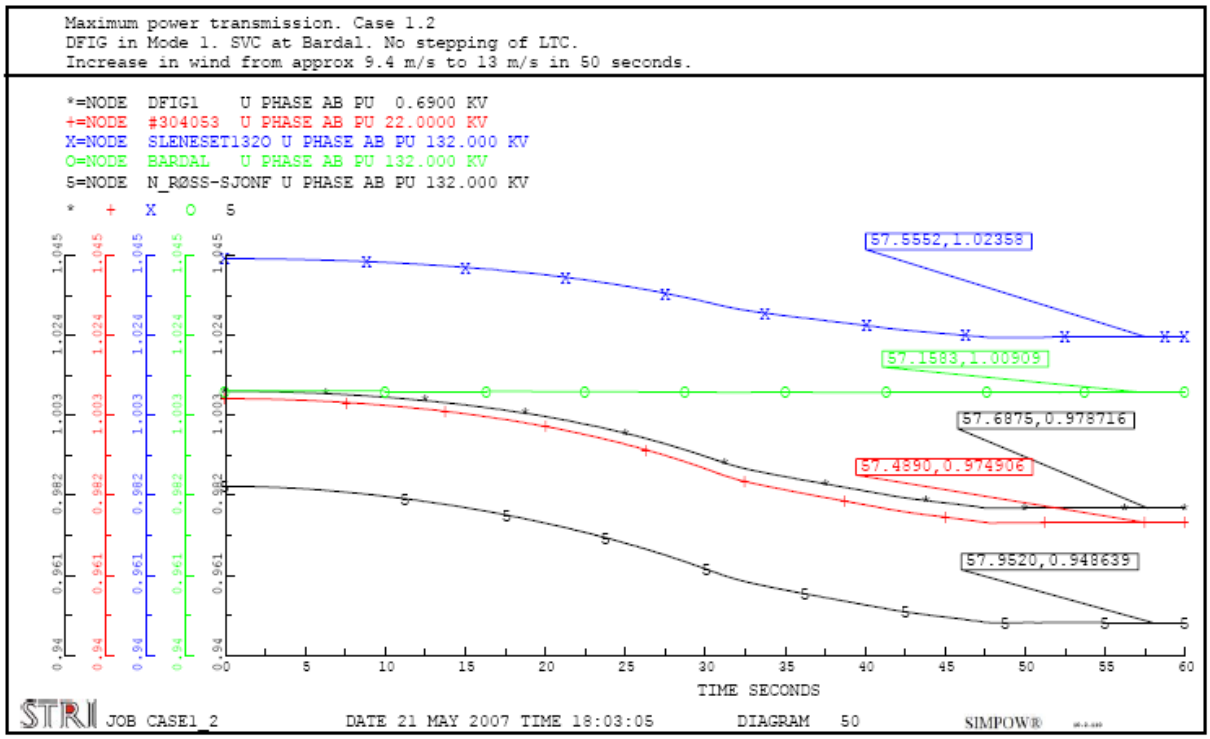

Figure 5.13: Voltages between DFIG1 at Sleneset and connection point at Nedre Røssåga, Case 1.2

The decrease in voltage due to the increased wind farm production for significant nodes in the grid is described in Table 5.7. The voltage change in the column "Voltage change" is calculated with the initial voltage as reference.

Table 5.7: Voltage change, Case 1.2

Node	Voltage level [kV]	Min / Max voltage [pu]	End voltage [pu]	Voltage change [%]
Salten	420	1.01 / 1.01	1.01	0.02
Rana420	420	1.00 / 1.01	1.00	-1.18
Nedre Røssåga	420	1.00 / 1.01	1.00	-1.57
Nedre Røssåga	300	0.98 / 1.00	0.98	-1.71
N_Røss-Sjonf	132	0.95 / 0.98	0.95	-3.57
DFIG1	0.69	0.98 / 1.01	0.98	-3.06
Trofors	300	0.98 / 1.00	0.98	-1.84
Majavatn	300	0.98 / 1.00	0.98	-1.51

5.2.3.6 General

Case 1.2 shows that the production in the wind farms increases from approximately 50% to 100% when the wind increases from approximately 9.4 to 13 m/s.

By placing a SVC at Bardal, the production is allowed to increase to 100% without reaching any specified limits for voltage or current.

The capacity of the SVC needs to be 335 MVAR in order to maintain the voltage at Bardal. When this is done, the wind farms also draw 116 MVAR from the main grid.

Due to increased reactive losses in the grid when active power production is augmented, the voltages in the grid decrease. Simulations done in Case 1.2 show that the voltage changes are largest closest to the connection point between the wind farm radial and the main grid at Nedre Røssåga.

Responses considered not being important for the discussion is included in Appendix E. The output file from the steady-state power flow calculation along with the OPTPOW and DYNPOW files are also included in this appendix.

5.2.4 Case 2.1 – DFIG in Voltage Control Mode

5.2.4.1 Description

In Case 2.1 the doubly-fed induction generators are set to control the voltage at the terminals to 0.69 kV. This implies that in order to maintain the terminal voltage, the generators have to produce reactive power when the production increases.

The values obtained from the dynamic simulations are based on plotted values and might therefore cause some inaccuracies.

The production increase used in Case 1.2 is also applied in this case.

5.2.4.2 Power production

The simulations show that the wind power production is increased from approximately 50% to 100% when the wind is increased to 13 m/s. In Figure 5.14 the active and reactive power production from DFIG1 is given.

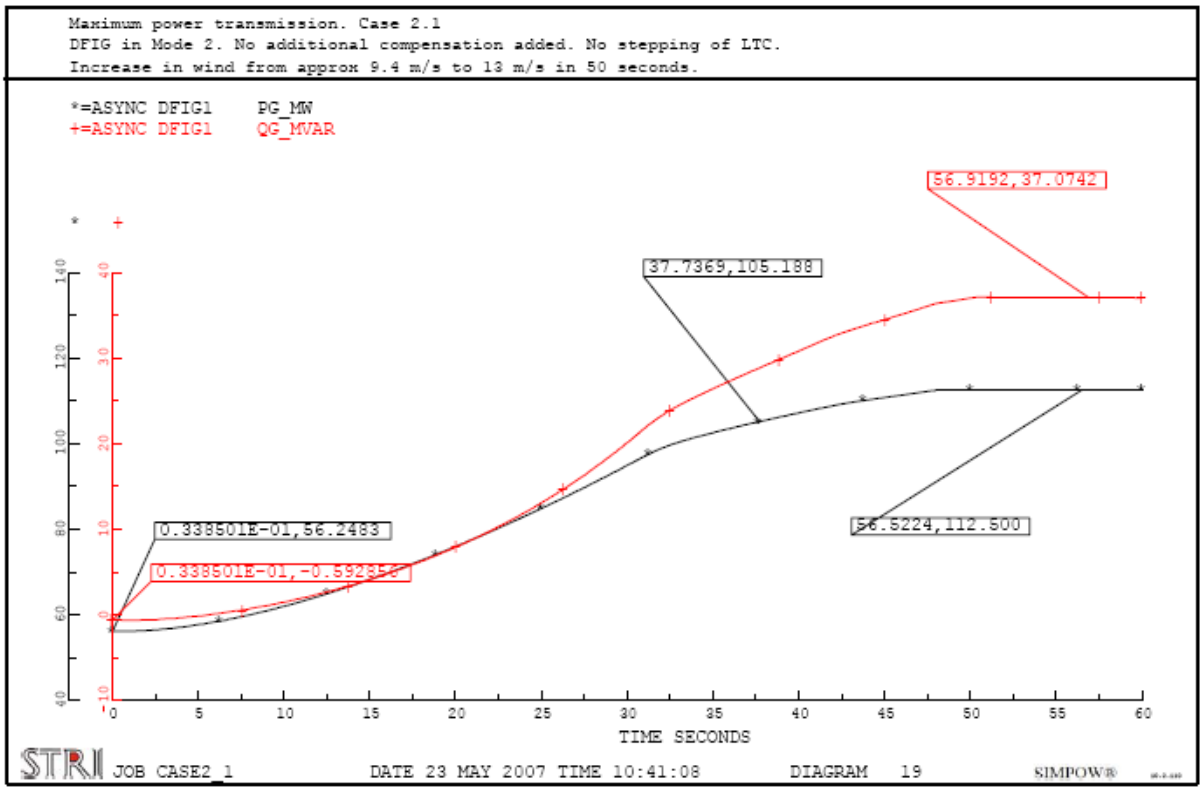

Figure 5.14: Active and reactive power production from DFIG1, Case 2.1

Figure 5.14 shows that the reactive power production is increased in order to control the voltage at the terminals when the active power production is increased. At full active production (112.5 MW), DFIG1 is also producing 37.1 MVAR.

The reactive power production of the doubly-fed induction generators at full active power production is presented in Table 5.8. The imported power at the connection point at Nedre Røssåga is also given. The total amount describes the reactive power consumed in the radial.

Table 5.8: Reactive power production at full active power production, Case 2.1

Source	Reactive production at full active production [MVAR]
DFIG1	37.1
DFIG2	36.1
DFIG3	84.4
DFIG4	89.3
Imported at N.Røssåga	283.8
Total	530.7

Whether or not it is possible to have doubly-fed induction generators with this amount of reactive power capacity is not investigated. However, it illustrates the amount of reactive power needed at the generator terminals in order to maintain a voltage of 0.69 kV during 100% production.

5.2.4.3 Power flow

The power flow through the transformer between the radial towards the wind farms and the main grid is given in Figure 5.15. It shows that when the production goes from 50% to 100%, the reactive power drawn from the main grid goes from 59.2 MVAR to 283.8 MVAR. This raise is only due to increased reactive losses in transmission lines and transformers.

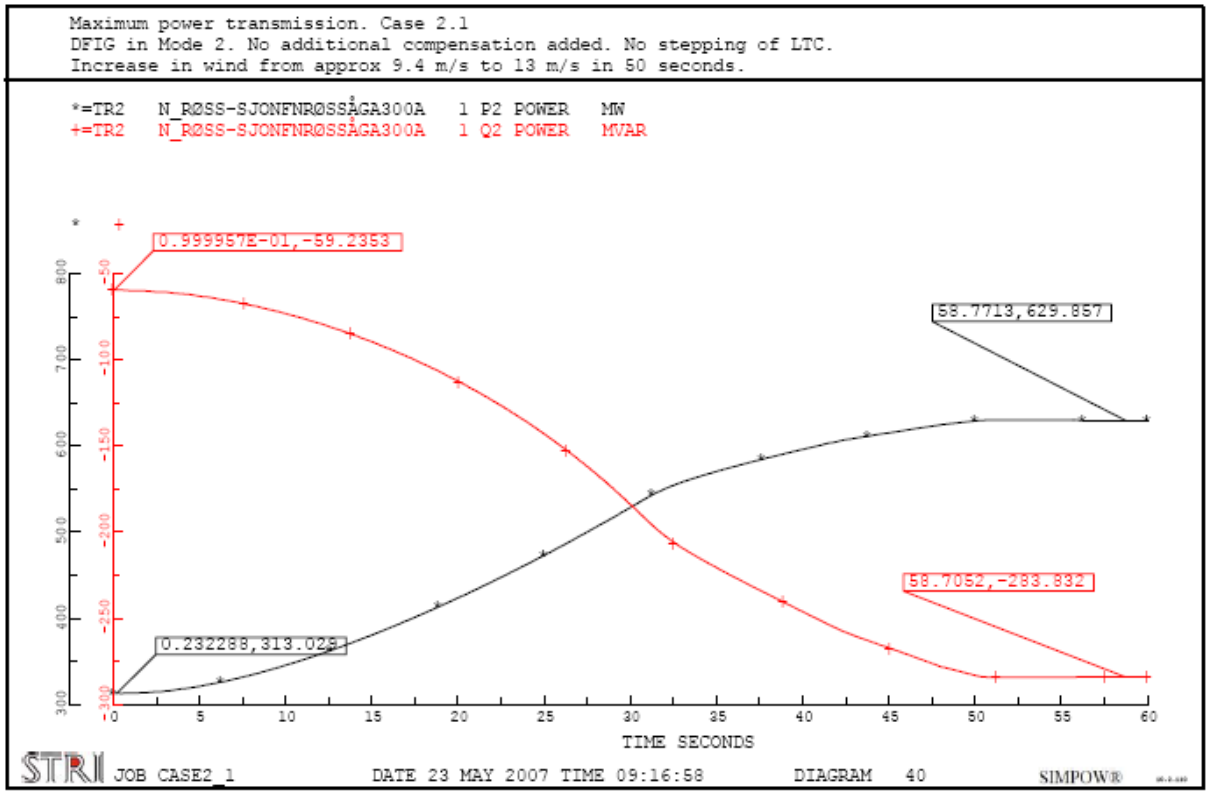

Figure 5.15: Active and reactive power flow through the transformer at the connection point at Nedre Røssåga, Case 2.1

The response for the reference bus shows that it consumes 1257.3 MW when the wind farms are at full production. The reactive power produced by the reference bus increases from 65.0 MVAR to 270.7 MVAR. The diagram illustrating the power flow from the reference bus is included in Appendix E.

5.2.4.4 Thermal limits

Table 5.9 shows the currents in the dimensioning lines and power cables between Nedre Røssåga and the wind farms at Sleneset and Sjonfjellet. It also describes the maximum current in the line outside the radial connection with the highest loading. This line is located between Marka and Øvre Røssåga.

Table 5.9: Line loading, Case 2.1

Line	I_{Limit} [kA]	$I_{100\% production}$ [kA]	Loading [%]
Bardal – N.Røssåga	6.176	3.118	50.5
Sjo-Alt1_3 - #304656	1.160	1.030	88.8
Sjonfjell132A – Sjonfjell132B	1.160	1.080	93.1
#304633-3662 - #304366	0.970	1.055	108.8
Sleneset132O - Sleneset132V	0.715	0.510	71.3
#300763 - #300788	0.560	0.530	94.6

It is the power cable between Bardal and Sleneset which has the highest loading during full production. The increase in current during the given production increase for this cable is given in Figure 5.16. The loading increases from 51.7% to 108.8%. This is an unacceptable operating situation.

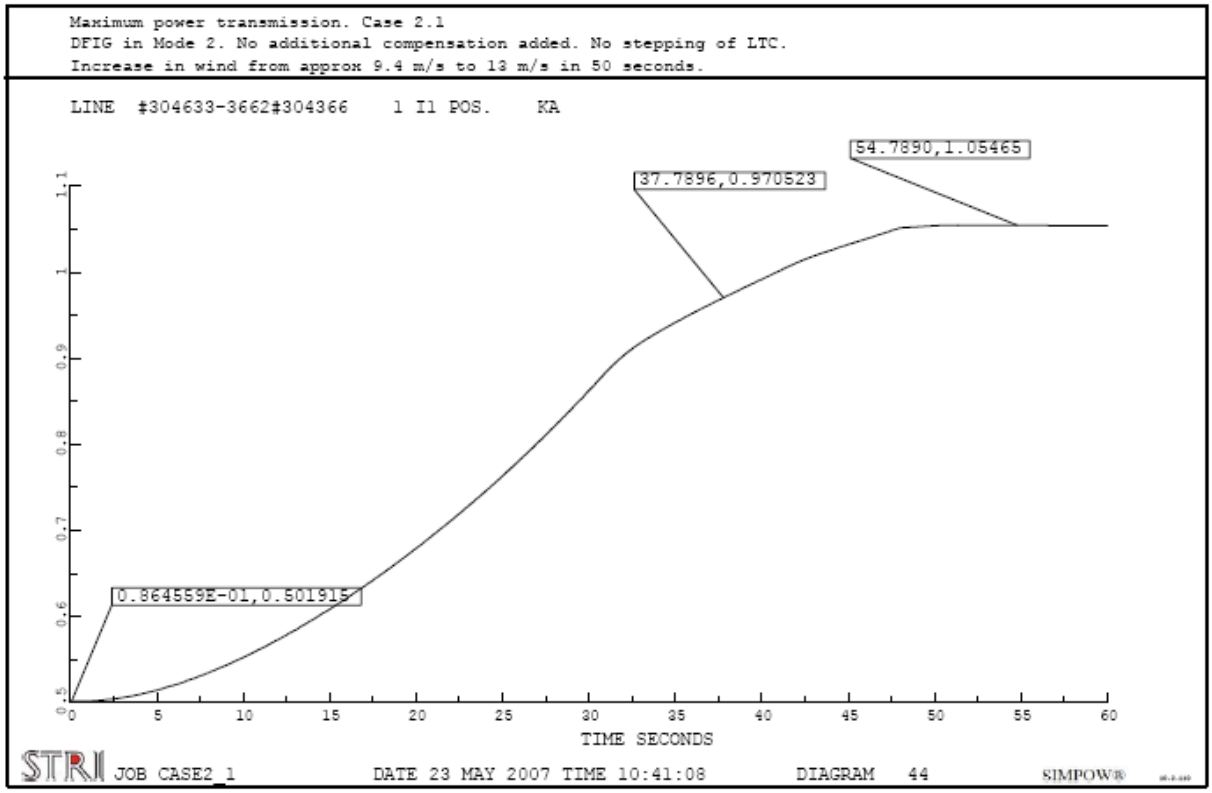

Figure 5.16: Highest loaded cable, Case 2.1

Figure 5.16 illustrate that the cable passes its thermal limit after 37.79 seconds. At that instant, the production from the wind farm at Sleneset has then reached 93.5% of full production. This can be seen from Figure 5.14.

It should be noted that the production at Sjonfjellet can reach rated capacity without reaching any thermal capacity limits. The total production can therefore reach 97.8% of full capacity.

5.2.4.5 Voltage variations

The voltage at the 132 kV side at Nedre Røssåga is given in Figure 5.17. It shows that the production increase in Case 2.1 causes the voltage to drop from 129.8 kV to 118.5 kV. A

voltage of 118.5 kV equals 0.898 pu and is below the normal allowed minimum value of 0.9 pu. This is therefore an unacceptable low voltage.

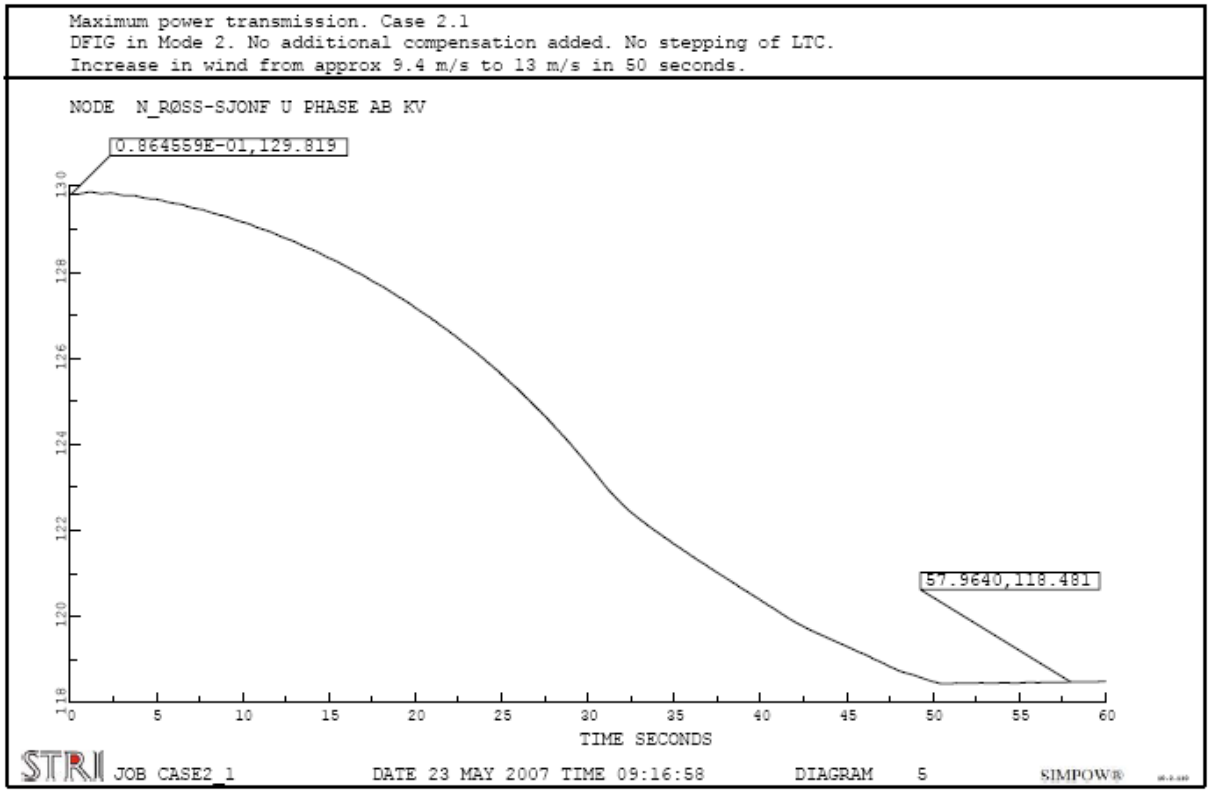

Figure 5.17: Voltage at connection point for wind radial at Nedre Røssåga, 132 kV level, Case 2.1

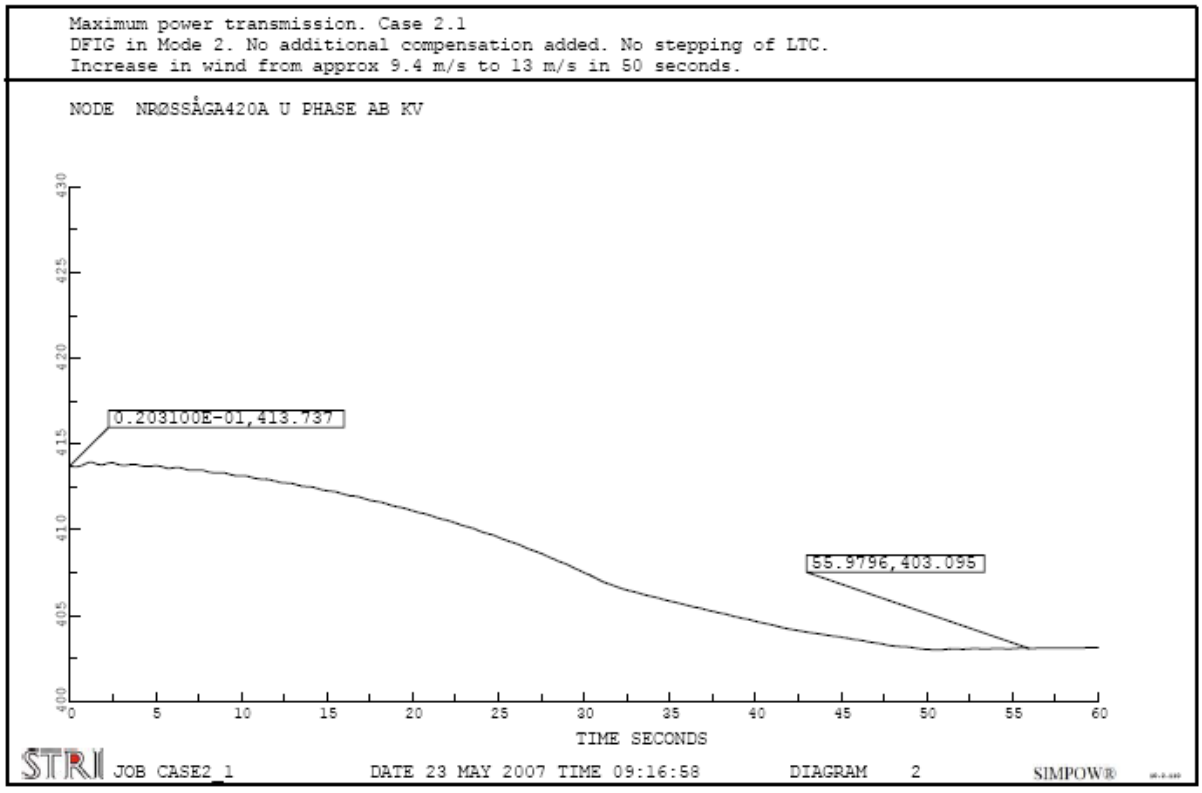

Figure 5.18: Voltage at 420 kV level at Nedre Røssåga, Case 2.1

Figure 5.18 describes the voltage in the 420 kV grid at Nedre Røssåga. The voltage decreases from 413.7 kV to 403.1 kV when the production in the wind farms increases from 50 to 100%. As mentioned in chapter 4.2.3, a voltage below 410 kV is considered to be an unacceptable low voltage in this grid.

An overview of the voltages in the radial connection between Nedre Røssåga and DFIG1 at Sleneset is given in Figure 5.19. The decrease in voltage due to the increase in power production is largest at the connection point in Nedre Røssåga. This is also the only node in the radial where the voltage becomes unacceptable low. The voltage at the terminals of the generator is the most stable. This is because it is the only node with voltage control.

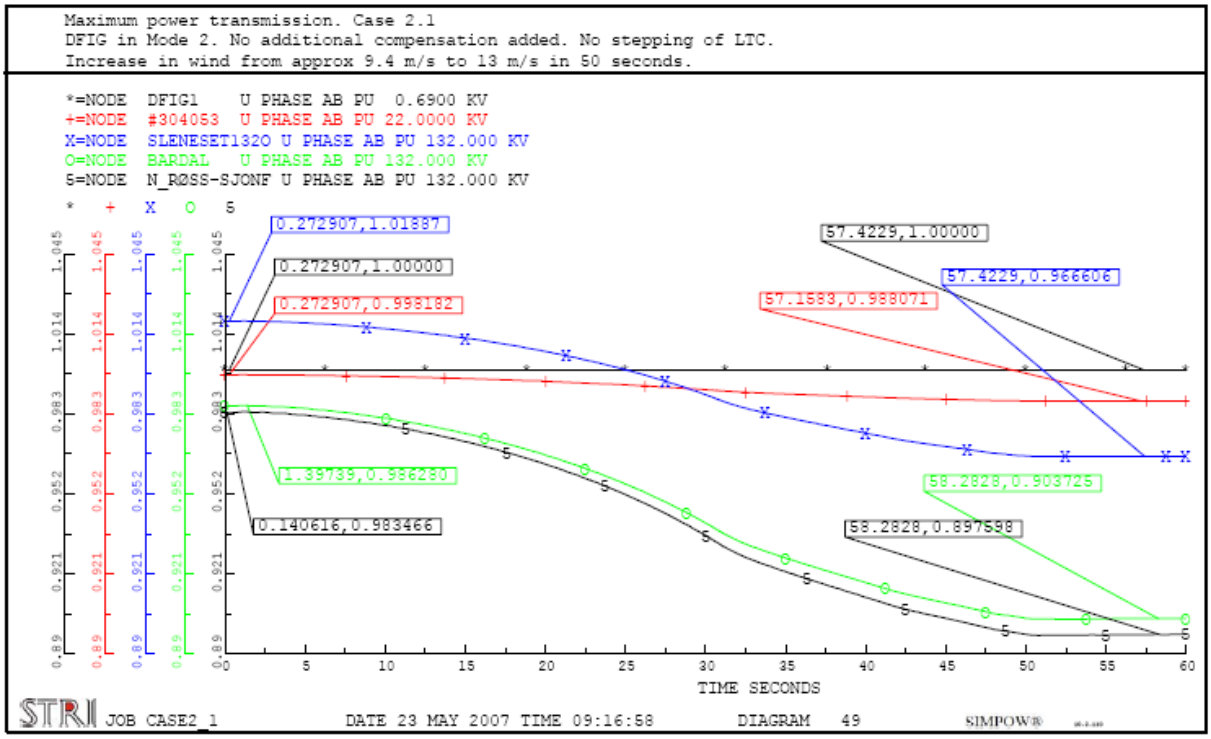

Figure 5.19: Voltages between DFIG1 at Sleneset and connection point at Nedre Røssåga, Case 2.1

The decrease in voltage due to increased wind farm production in Case 2.1 is given in Table 5.10 for significant nodes. The voltage change is calculated with the initial voltage as a reference.

Table 5.10: Voltage change, Case 2.1

Node	Voltage level [kV]	Min / Max voltage [pu]	Voltage at $P_{100\%}$ [pu]	Voltage change [%]
Salten	420	1.00 / 1.00	1.00	0.02
Rana420	420	0.97 / 0.99	0.97	-1.87
Nedre Røssåga	420	0.96 / 0.99	0.96	-2.53
Nedre Røssåga	300	0.97 / 1.00	0.97	-2.83
N_Røss-Sjonf	132	0.90 / 0.98	0.90	-8.59
DFIG1	0.69	1.00 / 1.00	1.00	-0.00
Trofors	300	0.97 / 1.00	0.97	-2.50
Majavatn	300	0.98 / 1.00	0.98	-1.93

5.2.4.6 General

Case 2.1 shows that the production in the doubly-fed induction generators increases to full production when the wind speed is ramped up to 13 m/s. Full production occurs before the wind speed reaches 13 m/s. Finding the exact wind speed that gives 100% production ill depend on the chosen wind turbine and is not an objective of this project.

Case 2.1 also shows that the power system handles such an increase in inserted power without any major disturbances during the simulated time. However, a power cable in the radial towards the wind farm at Sleneset has a loading of 108.8% during full production at Sleneset. A short temporary overloading of a power cable can sometimes be accepted in a power system, but it is normally not acceptable to have a power cable between a production source and the main grid which is overloaded if the production is at its rated value. However, the number of hours during a year which the whole wind farm at Sleneset is at full production might be calculated to be very few. If this is the case, some hours of overloading in the cable or a decrease in production by the use of regulators might be considered acceptable, instead of investing in a power cable with larger capacity. This discussion is, however, not pursued in this project.

When in addition several node voltages close to the connection point at Nedre Røssåga are unacceptable low, it is clear that Case 2.1 is not an acceptable condition to operate in. On a longer term, overloading a power cable and too low voltages might result in the triggering of protection devices.

Responses considered not being important for the discussion is included in Appendix E. The output file from the steady-state power flow calculation along with the OPTPOW and DYNPOW files are also included in this appendix.

5.2.5 Case 2.2 – DFIG in Voltage Control Mode and SVC at Bardal

5.2.5.1 Description

Case 2.2 describes a situation where a SVC is placed at Bardal. This is done to raise the voltage at the connection point of the radial connection at Nedre Røssåga. It will also reduce the reactive power production of the double-fed induction generators, and thereby reducing the power flow in the radial. The capacity of the SVC is set to 500 MVAR. This is done to avoid making the new SVC the limiting factor.

The steady-state power flow used in Case 1.2 is also employed in this case. This will create a different power flow than the one used in Case 2.1.

Like in Case 2.1 the doubly-fed induction generators are set to control the voltage at the terminals to 0.69 kV. The same increase in wind speed is also used.

The values obtained from the dynamic simulations are based on plotted values and might therefore cause some inaccuracies.

5.2.5.2 Power production

The results from the simulation show that the power production in the wind farms increases to 100% when the wind is increased. The responses from the generators in the wind farms also indicate that the generators have to produce reactive power in order to maintain a terminal voltage of 0.69 kV. The production from DFIG1 is illustrated in Figure 5.20.

It should be noted that the doubly-fed induction generator draws reactive power at 50% production. This is because the generators are trying to maintain a voltage of 0.69 kV at the terminals. If a slightly higher voltage is accepted, this will be avoided.

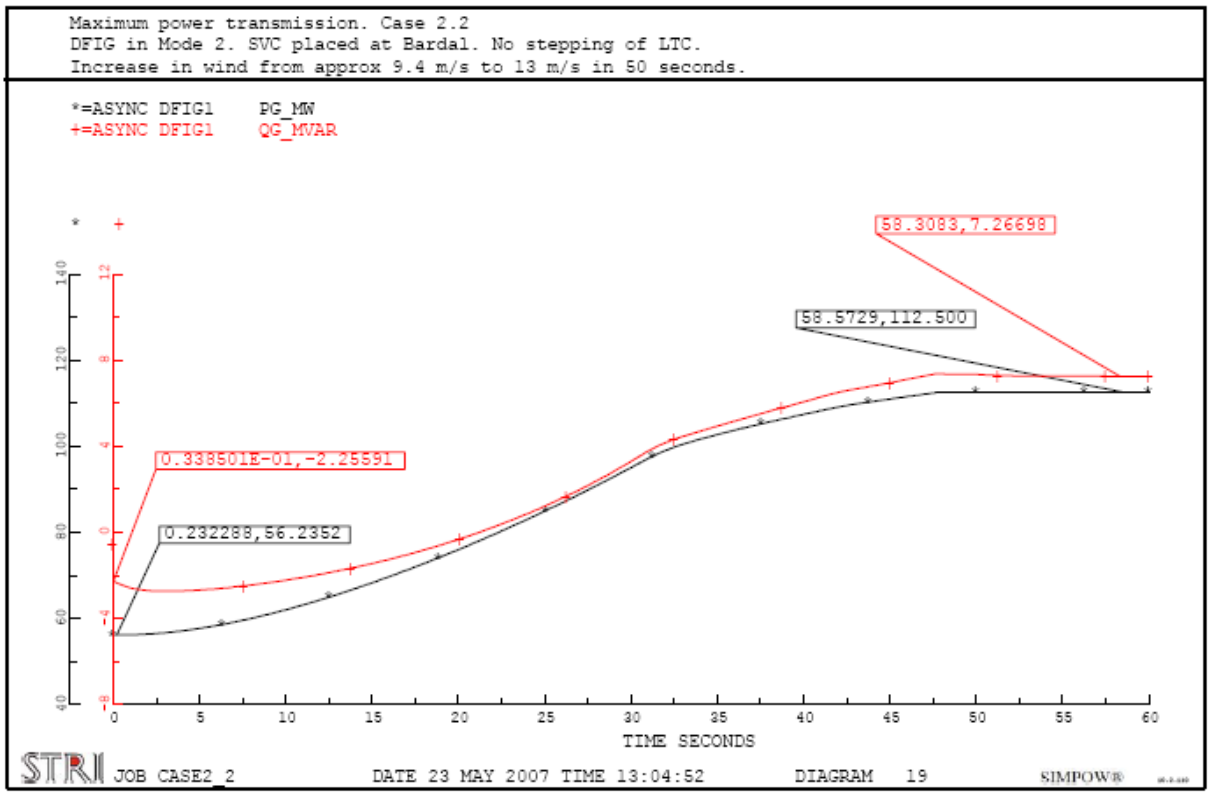

Figure 5.20: Active and reactive power production from DFIG1, Case 2.2

In Table 5.11 the maximum reactive power produced by the doubly-fed induction generators and the SVC at Bardal is presented. In addition the reactive power imported at Nedre Røssåga is given. The row "Total" in the table, describes the total amount of reactive power consumed in the radial. The maximum values all occur when the wind farms are at full active production.

Table 5.11: Reactive power production at full active power production, Case 2.2

Source	Reactive production at full active production [MVAR]
DFIG1	7.3
DFIG2	6.9
DFIG3	5.1
DFIG4	15.2
SVC3	290.4
Imported at N.Røssåga	121.3
Total	446.2

The table shows that the SVC is producing 290.4 MVAR when the wind farms are at full production. This implies that a reactive compensation of 290.4 MVAR is needed in order to maintain a voltage of 133.25 kV at Bardal. The reactive power production increases from 59.4 MVAR at 50% production to 290.4 MVAR at 100% production.

5.2.5.3 Power flow

The power flow through the transformer between the radial towards the wind farms and the main grid at Nedre Røssåga is given in Figure 5.21. It shows that the reactive power drawn from the main grid increases from 7.7 MVAR to 121.3 MVAR when the production is increased from 50% to 100%. Since the doubly-fed induction generators are more than fully compensated, this increase is due to increased reactive losses in transmission lines and transformers.

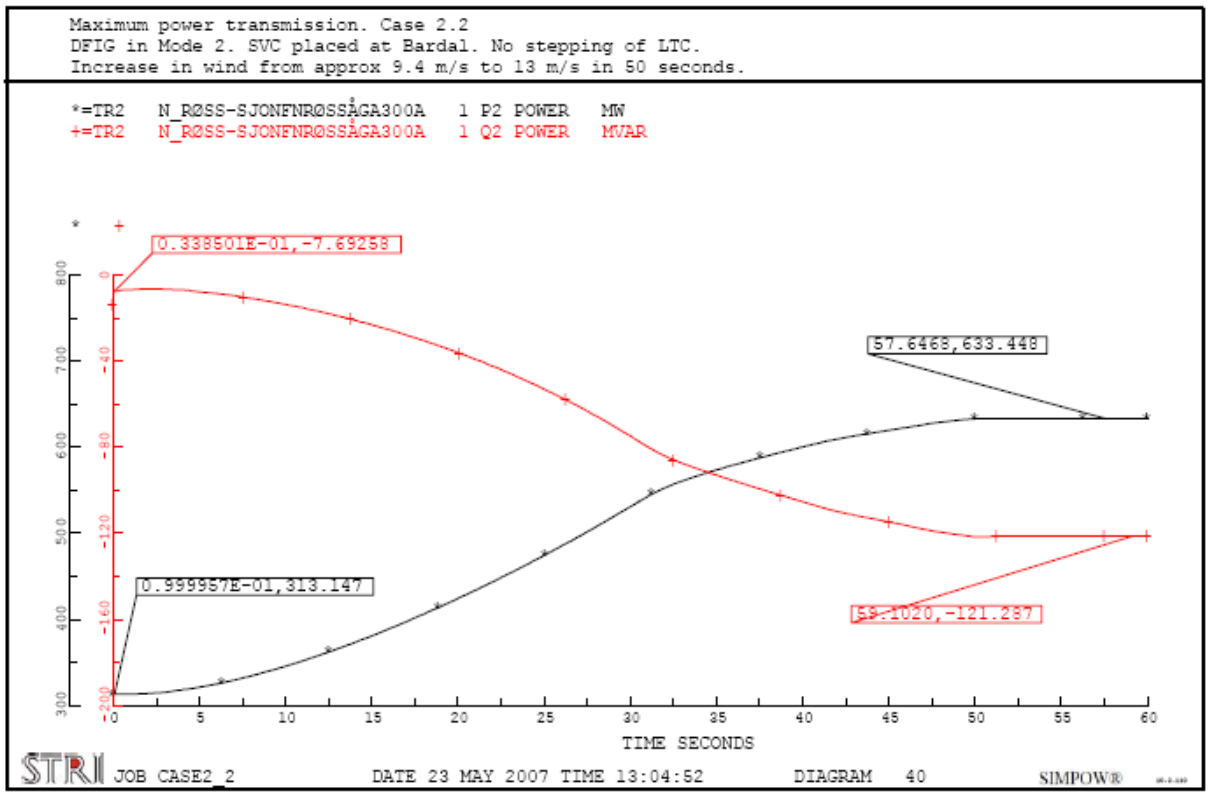

Figure 5.21: Active and reactive power flow through transformer at connection point at Nedre Røssåga, Case 2.2

The reference bus at Tunnsjødal is consuming 1255.3 MW when the wind farms are at full production. The reactive power production increases from 66.5 MVAR to 242.2 MVAR during the given augment in wind. The diagram illustrating the response of the reference bus for Case 2.2 is included in Appendix E.

5.2.5.4 Thermal limits

Table 5.12 shows the maximum currents in the dimensioning lines and power cables between Nedre Røssåga and the wind farms at Sleneset and Sjonfjellet. It also describes the maximum current in the line outside the radial connection with the highest loading. This line is located between Marka and Øvre Røssåga.

Table 5.12: Line loading, Case 2.2

Line	I_{Limit} [kA]	$I_{100\% \text{ production}}$ [kA]	Loading [%]
Bardal – N.Røssåga	6.176	2.927	47.4
Sjo-Alt1_3 - #304656	1.160	0.932	80.4
Sjonfjell132A – Sjonfjell132B	1.160	1.065	91.8
#304633-3662 - #304366	0.970	0.948	97.8
Sleneset132O - Sleneset132V	0.715	0.475	66.4
#300763 - #300788	0.560	0.527	94.0

Table 5.12 illustrates that the power cable between Bardal and Sleneset has the highest loading during full production. The loading increases from 50.5% to 97.8%.

5.2.5.5 Voltage variations

The voltage at the connection point at Nedre Røssåga is given in Figure 5.22. The voltage at the connection point decreases from 129.9 kV to 125.1 kV when the production increases from 50% to 100%.

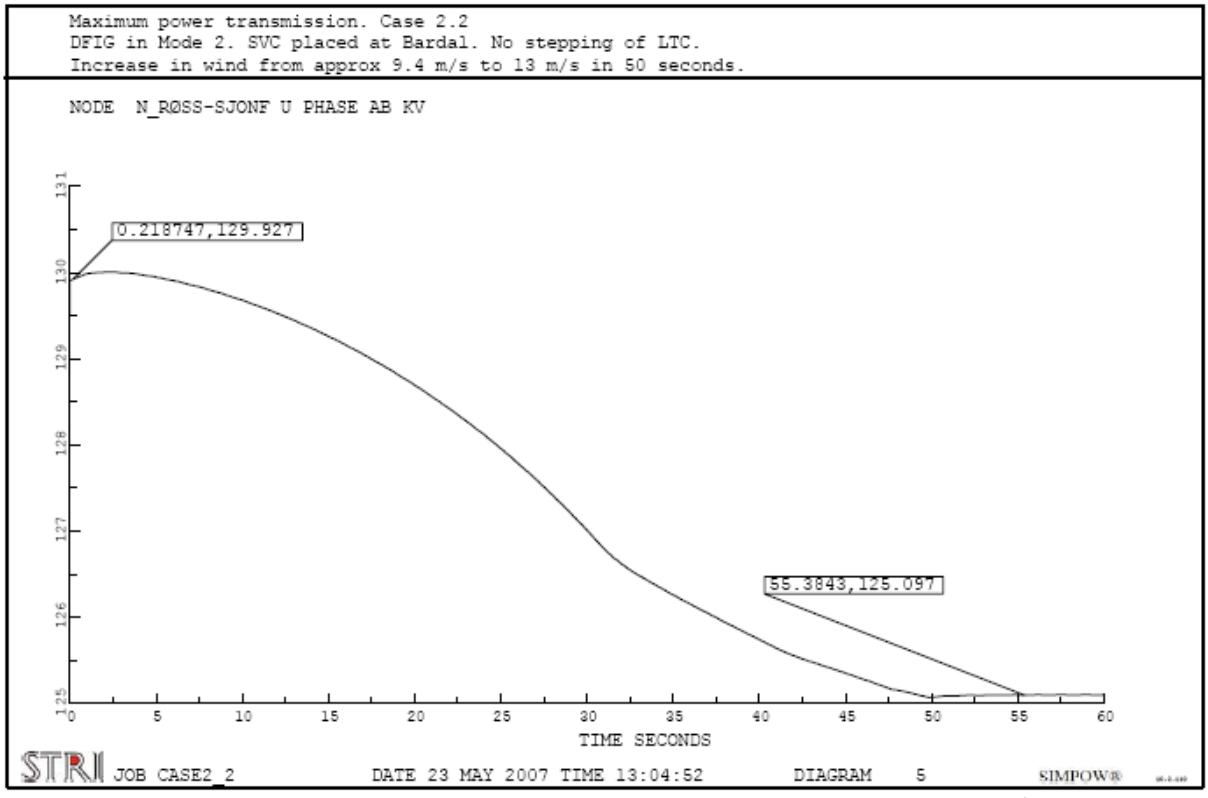

Figure 5.22: Voltage at connection point for wind radial at 132 kV level at Nedre Røssåga, Case 2.2

Figure 5.23 gives an overview over the voltages in the radial connection from Nedre Røssåga to the terminals of DFIG1. It shows that the decrease in voltage is largest at the connection point at Nedre Røssåga. However, all the voltages are well within specified limits.

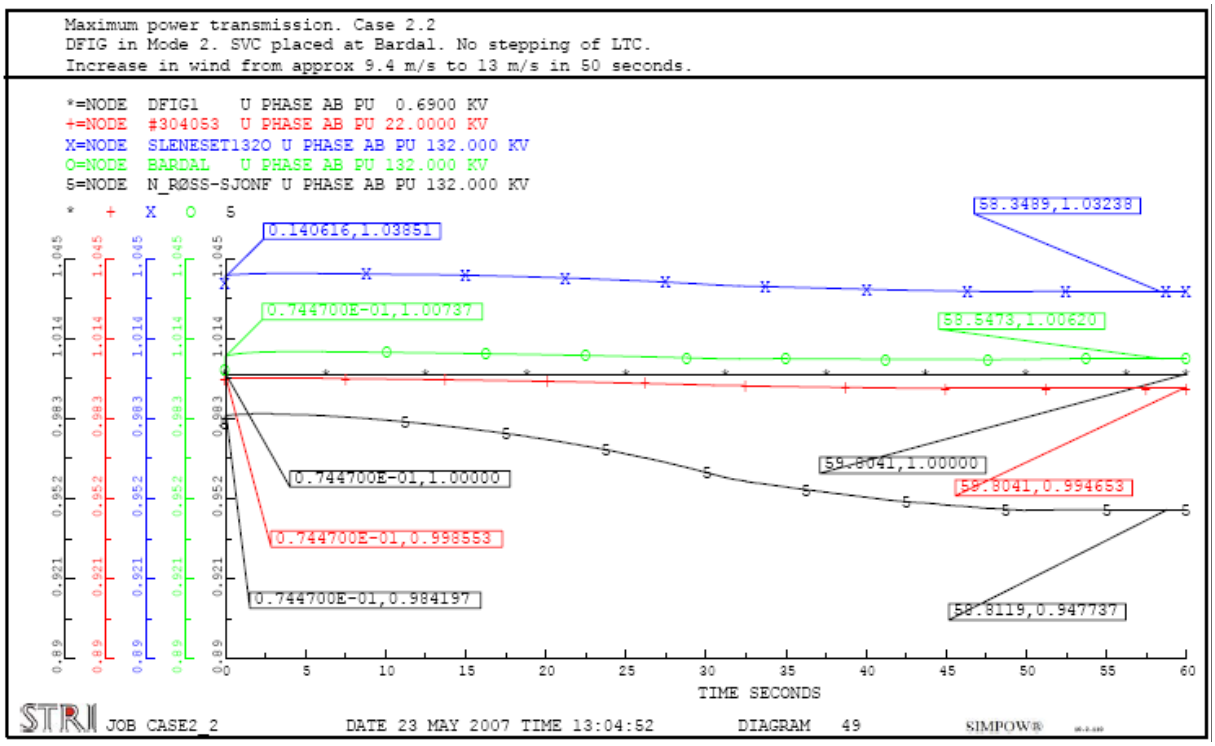

Figure 5.23: Voltages between DFIG1 at Sleneset and connection point at Nedre Røssåga, Case 2.2

The decrease in voltage due to the augmented wind farm production for significant nodes in the grid is described in Table 5.13. The change in voltage is calculated with the initial voltage as a reference.

Table 5.13: Voltage change, Case 2.2

Node	Voltage level [kV]	Min / max voltage [pu]	Voltage at $P_{100\%}$ [pu]	Voltage change [%]
Salten	420	1.00 / 1.00	1.00	-0.01
Rana420	420	0.99 / 1.00	0.99	-1.18
Nedre Røssåga	420	0.98 / 1.00	0.98	-1.60
Nedre Røssåga	300	0.98 / 1.00	0.98	-1.76
N_Røss-Sjonf	132	0.95 / 0.98	0.95	-3.66
DFIG1	0.69	1.00 / 1.00	1.00	0.00
Trofors	300	0.98 / 1.00	0.98	-1.87
Majavatn	300	0.98 / 1.00	0.98	-1.52

5.2.5.6 General

Case 2.2 shows that the production from the wind farms increases to full production when the wind speed is raised to 13 m/s. It also shows that by placing an SVC at Bardal the voltage in the main and regional grid remains within specified limits during the production increase. In order to maintain the specified terminal voltage, the capacity of the SVC has to be above 290 MVAR.

The simulations indicate that a power cable between Sleneset and Bardal is the highest loaded part of the transmission grid at full production in the wind farms. At full production this cable is loaded 97.8% of its full capacity. A power cable within the wind farm at Sjonfjellet is also loaded above 90% of its thermal capacity.

The voltages in the grid decrease as a result of the increased wind power production. As demonstrated by the simulations, the decrease is largest close to the connection point between the wind farm and the main grid. At the northern interface of the model, the decrease in voltage due to increased production is insignificant.

Responses considered not being important for the discussion is included in Appendix E. The output file from the steady-state power flow calculation along with the OPTPOW and DYNPOW files are also included in this appendix.

5.3 Load Tap Changers

5.3.1 Introduction

In order to evaluate how transformers with load tap changers will behave during an increase in production, simulations simulating a relatively slow increase in wind speed are performed. The Beta-regulator for LTC-transformers described in Appendix B is used on the transformers located in the radial connection between Nedre Røssåga and the wind farms.

Transformers with load tap changers placed elsewhere in the grid are not equipped with dynamic regulators in these simulations. This is because the simulations focus upon the impact that the load tap changers directly connected to the wind power production have on the voltage conditions in the radial towards the wind farms, the needed reactive compensation and reactive power drawn from the main grid.

The settings in the transformer regulators are obtained from theory described in chapter 3.2 and are included in the DYNPOW files in Appendix E

The settings used in Case 1.2 and Case 2.2 are used as a basis for the simulations with load tap changers. These cases are chosen because these are the only cases of the ones investigated in this project which allow wind power full production without reaching any specified limits.

5.3.2 Case 3.1 – DFIG in Power Factor Control and SVC at Bardal

5.3.2.1 Description

The applied settings in Case 1.2 are used as a basis for the simulations done in this case. The doubly-fed induction generators are set to control the power factor at the terminals to unity and a SVC is placed at Bardal.

The steady-state power flow is the same as the one in Case 1.2.

The values obtained from the dynamic simulations are based on plotted values and might therefore cause some inaccuracies.

The production is increased by increasing the wind speed from approximately 9.4 m/s to 13 m/s in 600 seconds. After the wind has reached 13 m/s it is kept constant for 200 seconds. This is done to secure that the system has settled and that the simulation is not interrupted while time delays in the transformer regulators are running.

5.3.2.2 Tap-operations

The simulations done in Case 3.1 show that the transformer at the connection point at Nedre Røssåga steps down three times during the wind increase. The tap-operations will increase the voltage on the low-voltage side compared to a situation without tap-changing.

The responses show that both of the transformers at Sleneset steps down a step in order to increase the voltage at the 22 kV side. However, at Sjonfjellet, only the transformer positioned the furthest out on the radial steps down one step. This means that the voltage at transformer located longer in on the radial has a voltage which is within specified limits.

Diagrams describing the positions of the tap changers for the transformers in the wind farm radial are included in Appendix E.

5.3.2.3 Power production

Diagrams illustrating the power production from doubly-fed induction generator show that the production increases to full production and that the reactive production is kept at zero. There are no indications that the power production is affected by the actions of tap changers.

The reactive power production from the SVC at Bardal is illustrated in Figure 5.24. The three tap-operations performed by the transformer at Nedre Røssåga are quite apparent in the diagram. Each step change results in a decrease in reactive power production from the SVC at Bardal. This is because less reactive power is needed to maintain the specified voltage. A direct consequence of this is that the maximum capacity of the SVC can be reduced. For this particular wind increase, a maximum value of 282.9 MVAR is needed to maintain a voltage of 133.25 kV at Bardal. The reactive production from the SVC after the system has stabilized is 260.0 MVAR.

It should be noted that the maximum production from the SVC will depend on how fast the increase in the wind is. However, the value will not be larger than the value obtained in Case 1.2.

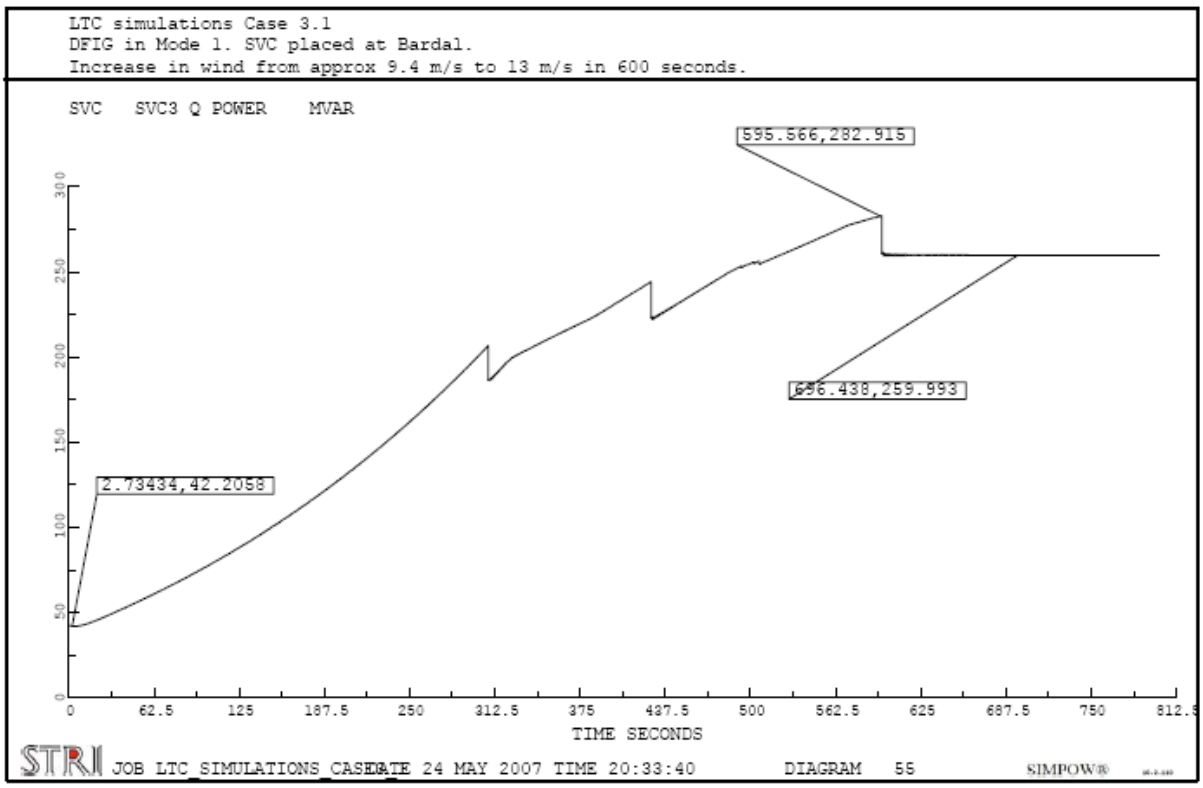

Figure 5.24: Reactive power production from SVC at Bardal, Case 3.1

The tap-operations done by the transformers located between the 132 kV level and the 22 kV level in the wind farms have a much smaller impact on the reactive power production from the SVC at Bardal than the step changes done by the transformer in the connection point. This is because a step change made in these transformers to raise the voltage on the 22 kV level in the wind farms will lead to a smaller change in voltage on the 132 kV side compared with a step change done at Nedre Røssåga to increase the voltage in the 132 kV grid.

The only reactive power consumption on the low-voltage side of the 132 kV / 22 kV transformers in the wind farms are the reactive losses in the transformers. When the transformers in the wind farms step down to increase the voltage on the 22 kV side, the voltage on the 132 kV side should decrease because more reactive power are drawn from the 132 kV grid to raise the voltage. However, the losses in the transformers are reduced due to higher voltage. Since this is the only reactive power consumption, the total reactive power drawn from the 132 kV grid decreases. The reactive power production of the SVC at Bardal is therefore reduced. This is illustrated in Figure 5.25, which shows the reactive power production from the SVC at Bardal. The time plot is zoomed in around the time where the LTC-transformers at Sleneset and Sjonfjellet are regulating the voltage on the 22 kV side.

The power flow through two transformers at Sleneset is given in Figure 5.26, the transformers are connected in series from the 0.69 level and up to the 132 kV level. The power flow is measured at the high-voltage side of the transformers. Figure 5.26 shows that the reactive power drawn from the 132 kV grid decreases when the voltage increases on the 22 kV level in the wind farm.

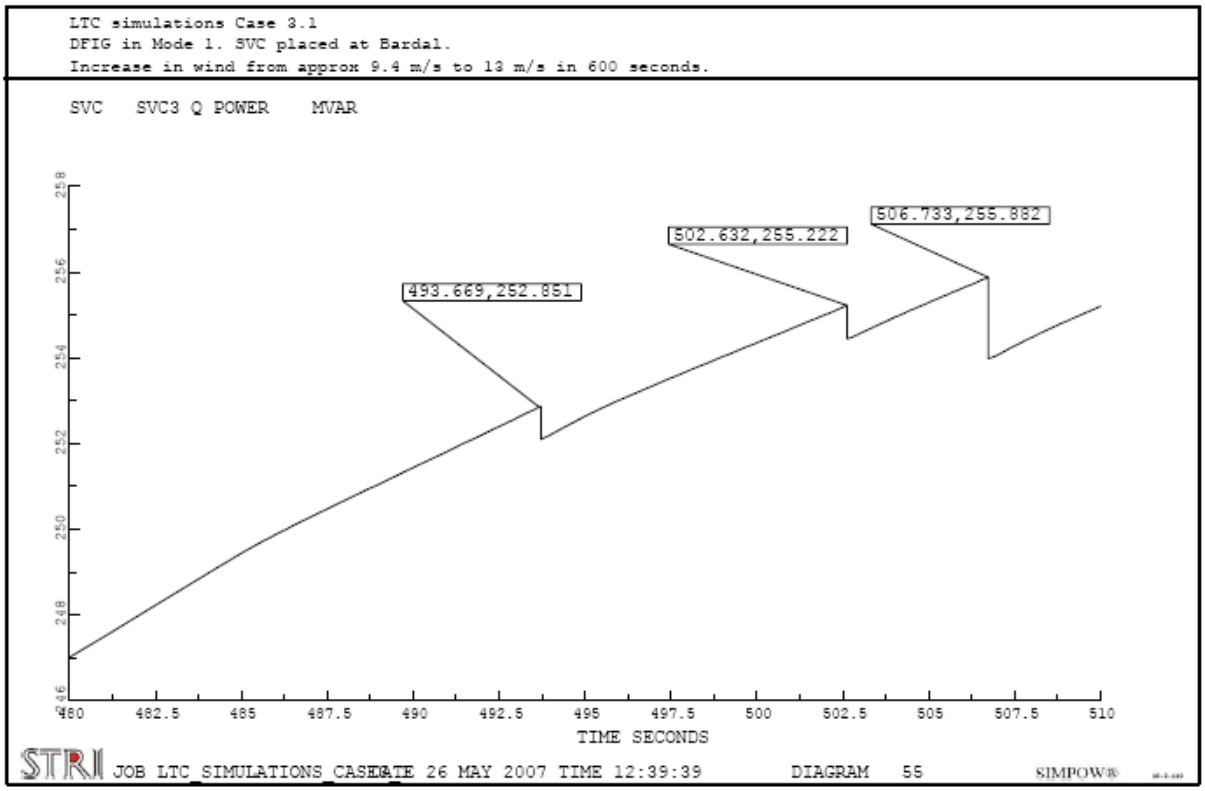

Figure 5.25: Reactive power production from SVC at Bardal, zoomed, Case 3.1

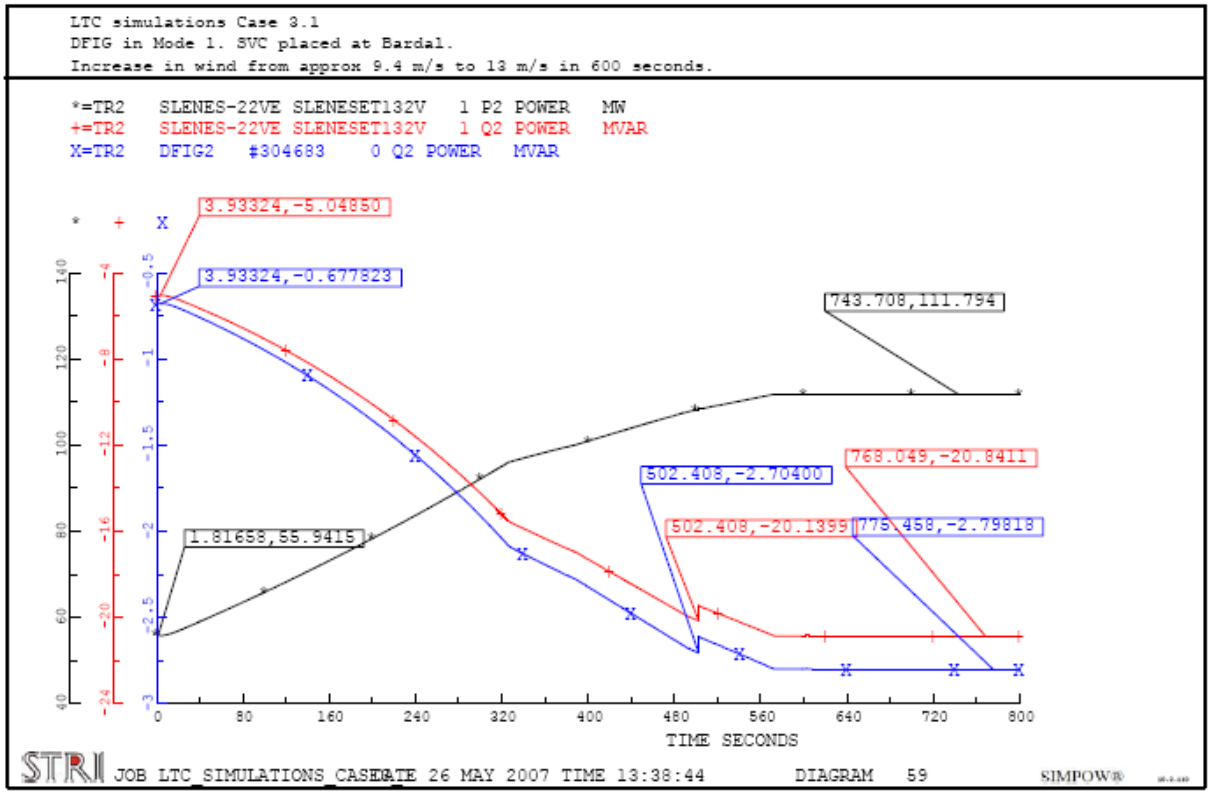

Figure 5.26: Power flow through transformers at Sleneset, Case 3.1

The maximum reactive power produced by the doubly-fed induction generators and the SVC at Bardal is given in Table 5.14. In addition the reactive power imported at Nedre Røssåga is presented. The maximum values all occur when the wind farms are running at full active

production. The row “Total” in the table, describes the total amount of reactive power consumed in the radial.

Table 5.14: Reactive power production at full active power production, Case 3.1

Source	Reactive production at full active production [MVAR]
DFIG1	0
DFIG2	0
DFIG3	0
DFIG4	0
SVC3	260.0
Imported at N.Røssåga	168.1
Total	428.1

5.3.2.4 Power flow

The active and reactive power flow through the transformer between the main grid and the wind farm radial is given in Figure 5.27. It shows that the reactive power drawn from the main grid increases from 5.1 MVAR at 50% production to 168.1 MVAR at full production. It also illustates that when the load tap changer in the transformer at Nedre Røssåga steps down in order to increase the voltage on the low-voltage side, the reactive power drawn from the main grid increases.

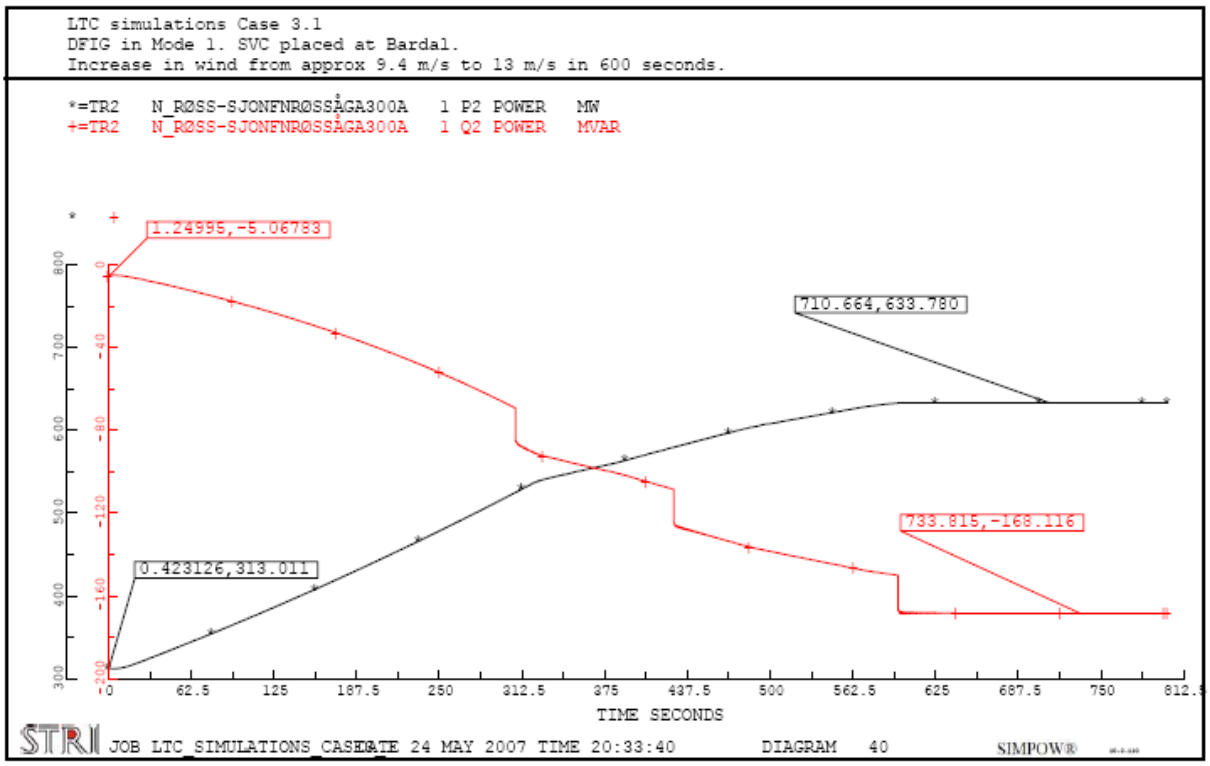

Figure 5.27: Active and reactive power flow through transformer at connection point at Nedre Røssåga, Case 3.1

The active and reactive power flow from the reference bus at Tunnsjødal is given in Figure 5.28. It shows that during the production increase, the active power consumed by the reference bus increases from 938.9 MW to 1257.4 MW, while the reactive power produced by the reference bus increases from 65.1 MVAR to 255.8 MVAR. Figure 5.28 illustrates that the

tap-operations of the transformer at Nedre Røssåga results in increased reactive power production from the reference bus. The tap-operations also results in oscillations in both active and reactive power flow.

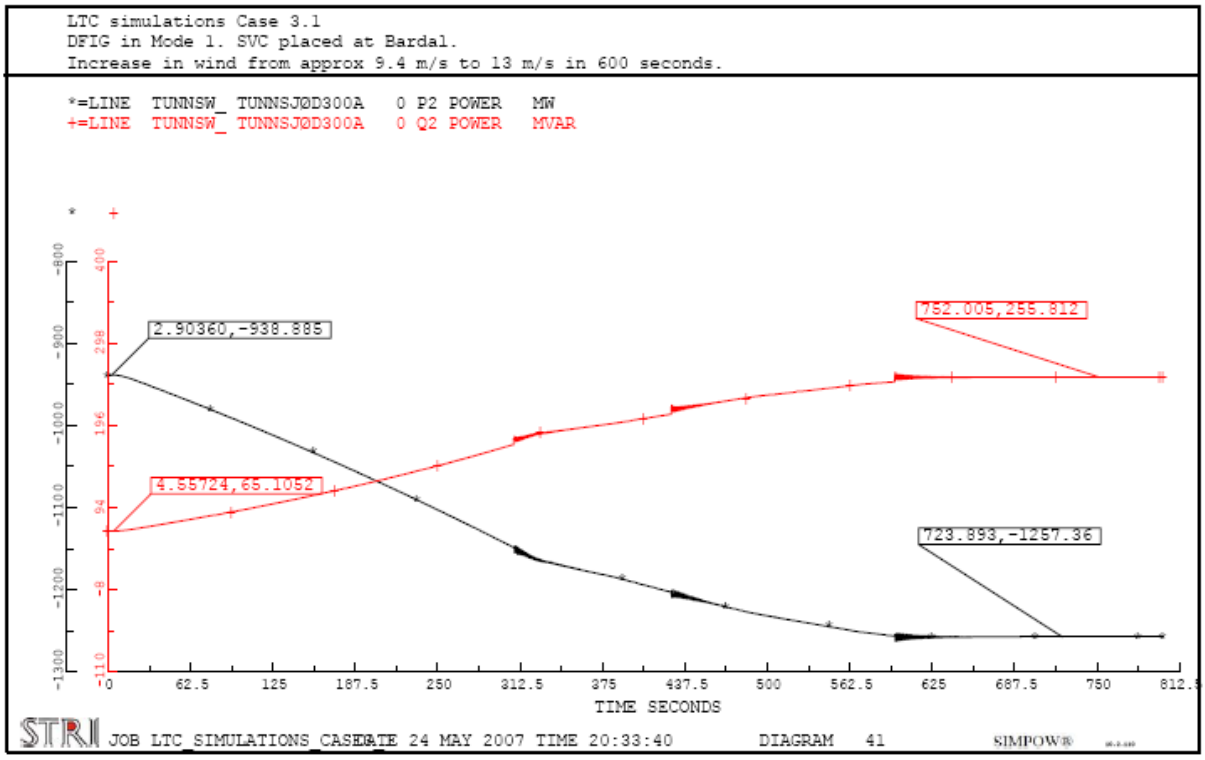

Figure 5.28: Active and reactive power flow from reference bus at Tunnsjødal, Case 3.1

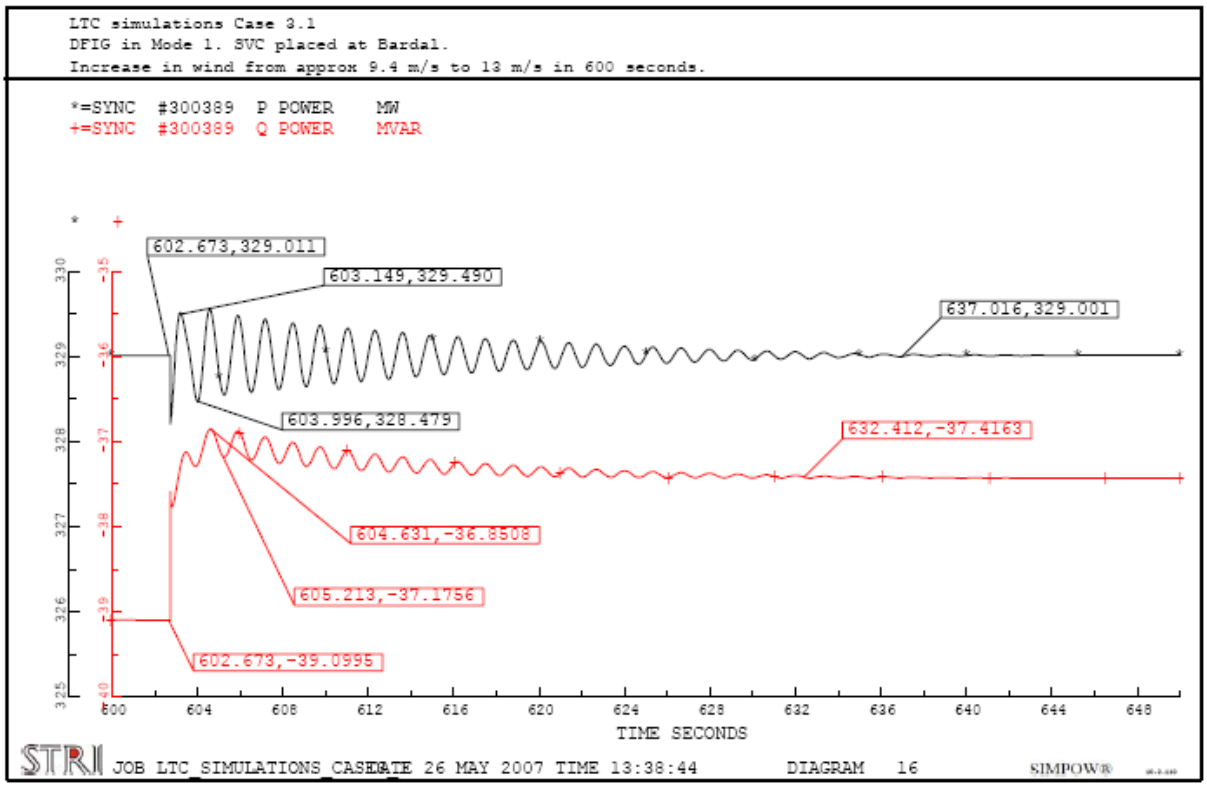

Figure 5.29: Active and reactive power production from Svartisen, zoomed, Case 3.1

In Figure 5.29 the active and reactive power production from the generator at Svartisen is given at the time of the tap-operation of the transformer at Nedre Røssåga. The time plot is zoomed for illustrative purposes.

The figure shows that the tap-operation of the transformer at Nedre Røssåga causes oscillations in active and reactive power production from the generator. This is also the case for other hydro power generators in the model. At Svartisen, the oscillations caused by the tap-operation have a frequency of approximately 0.6 Hz and a maximum peak-to-peak value of approximately 1 MW and 0.3 MVAR.

As seen from the generator at Svartisen, tap-operation of the transformer at Nedre Røssåga can be compared to a sudden increase in reactive load. As a consequence, the generator has to increase its reactive power production to maintain the specified voltage at its terminals.

5.3.2.5 Thermal limits

Table 5.15 shows the current in dimensioning lines and power cables between Nedre Røssåga and the wind farms at Sleneset and Sjonfjellet during full wind power production. It also presents the line outside the radial connection with the highest loading. This line is located between Marka and Øvre Røssåga.

Table 5.15: Line loading, Case 3.1

Line	I_{Limit} [kA]	$I_{100\% \text{ production}}$ [kA]	Loading [%]
Bardal – N.Røssåga	6.176	2.843	46.0
Sjo-Alt1_3 - #304656	1.160	0.938	80.9
Sjonfjell132A – Sjonfjell132B	1.160	1.077	92.8
#304633-3662 - #304366	0.970	0.952	98.1
Sleneset132O - Sleneset132V	0.715	0.483	67.6
#300763 - #300788	0.560	0.528	94.3

Table 5.15 indicates that the power cable between node Bardal and Sleneset has the highest loading during full production. The loading increases from 50.5% to 98.1%.

Figure 5.30 describes the current in the transmission line between Bardal and Nedre Røssåga during the increase in production. The current decreases when the transformer at Nedre Røssåga steps down a step. This is because the reactive power flow from the SVC at Bardal towards Nedre Røssåga is reduced. This decreases the loading on the line.

The maximum current in this transmission line is higher than the current observed when the system has settled at full production. The size of this maximum value will depend on how rapid the increase in the wind speed is. However, even at the maximum value, the line is far from fully loaded.

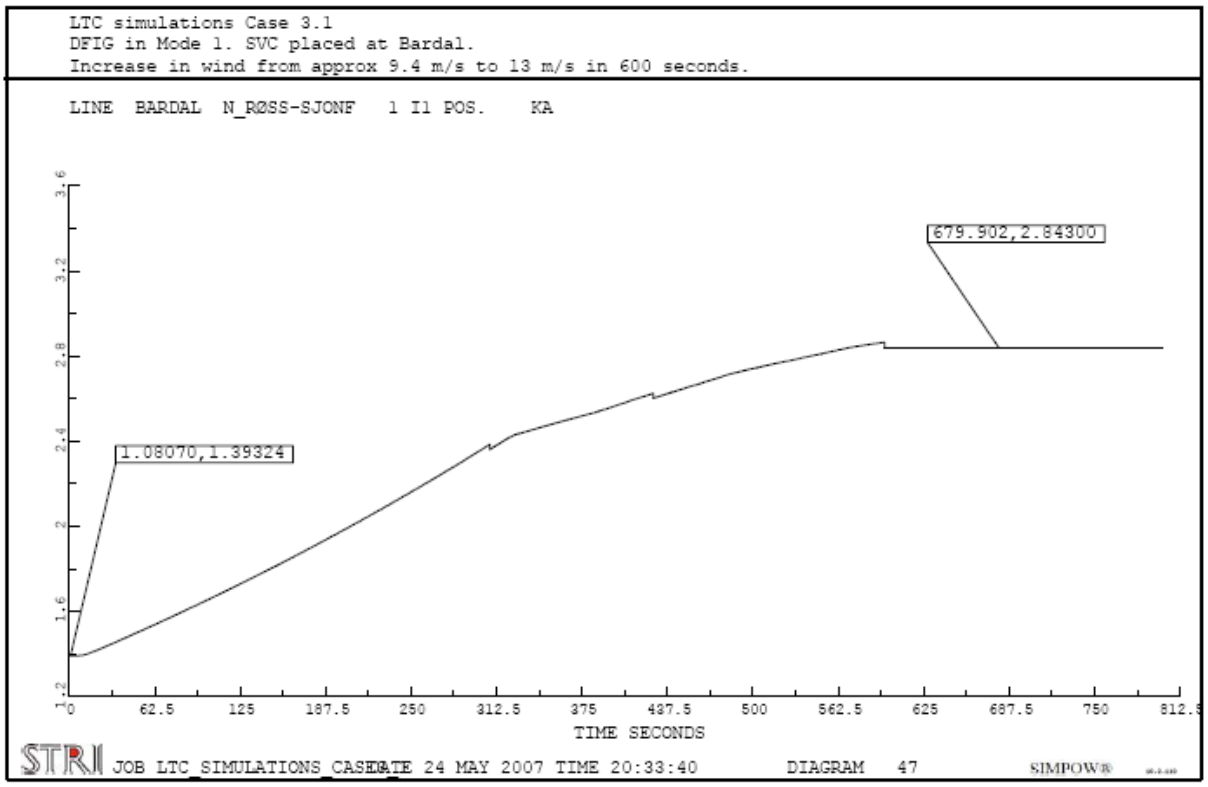

Figure 5.30: Current in transmission line between Bardal and Nedre Røssåga, Case 3.1

The simulations demonstrate that the currents in the lines between Bardal and the two wind farms are not largely affected by the tap change of the transformer at Nedre Røssåga. This is illustrated in Figure 5.31 which shows the current in the power cable between Bardal and Sleneset.

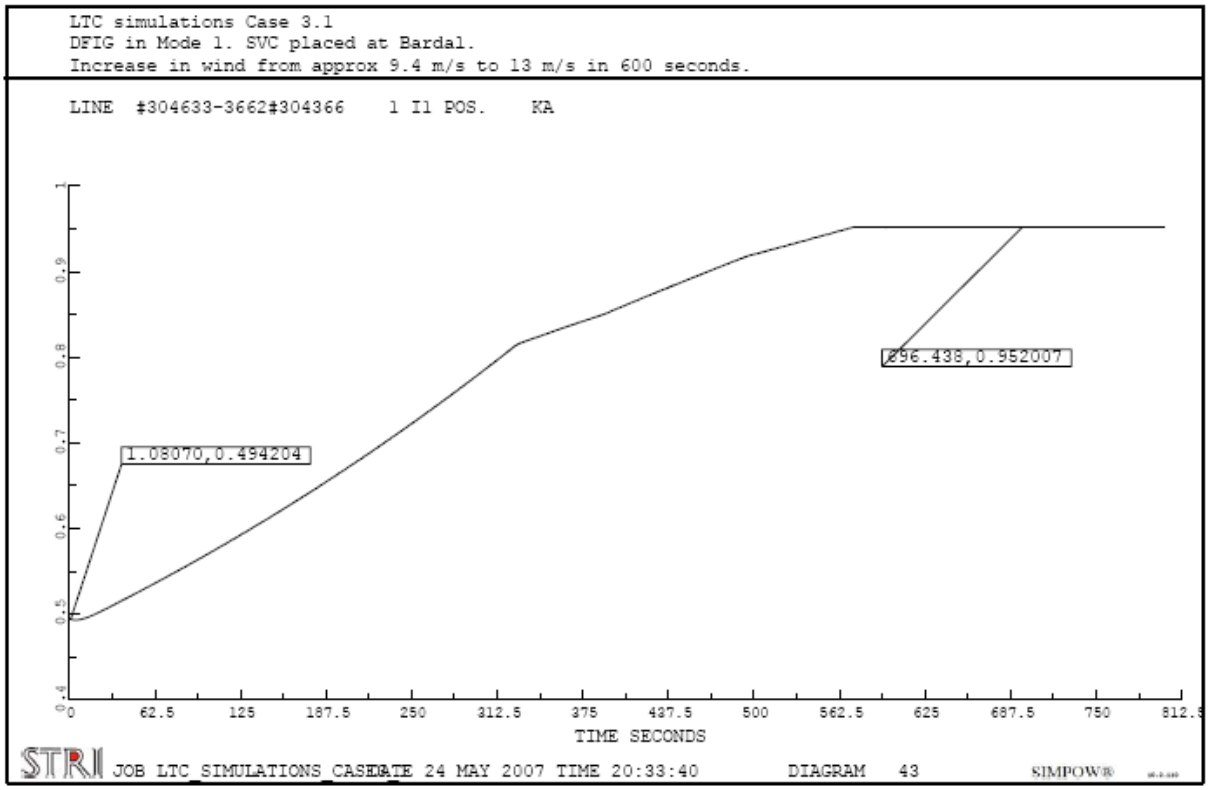

Figure 5.31: Current in highest loaded power cable, located between Bardal and Sleneset, Case 3.1

The figure also shows that the tap-operations of the transformers at Sleneset does not have a significant impact on the current in the power cable. However, since the reactive power flow between Bardal and Sleneset is slightly reduced due to reduced reactive losses in the wind farm transformers, the current will also be slightly reduced compared to a situation without tapping.

5.3.2.6 Voltage variations

The voltage at the 300 kV level at Nedre Røssåga is described in Figure 5.32. It shows that the voltage decreases due to the increased power production. It also shows that the voltage is further reduced when the transformer at the connection point to the radial towards the wind farms steps in order to raise the voltage at the 132 kV level. The voltage is at an acceptable level during full production.

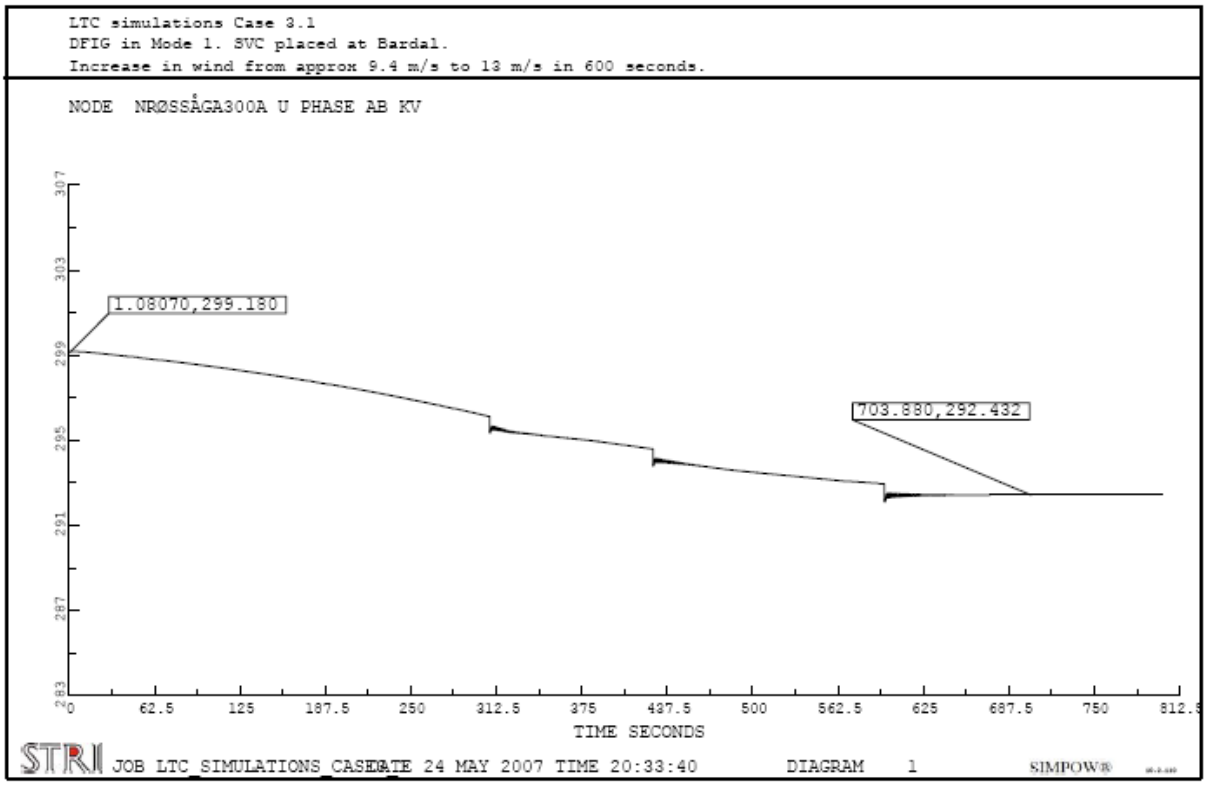

Figure 5.32: Voltage at 300 kV level at Nedre Røssåga, Case 3.1

The voltage at the connection point at Nedre Røssåga is shown in Figure 5.33. The voltage decreases during the production increase and breaches the specified minimum voltage in the transformer regulator at Nedre Røssåga three times. The result is that the transformer steps down three times in order to raise the voltage at the 132 kV level. The minimum voltage during this production increase is 127.4 kV and the end voltage is 128.8 kV. These are acceptable values.

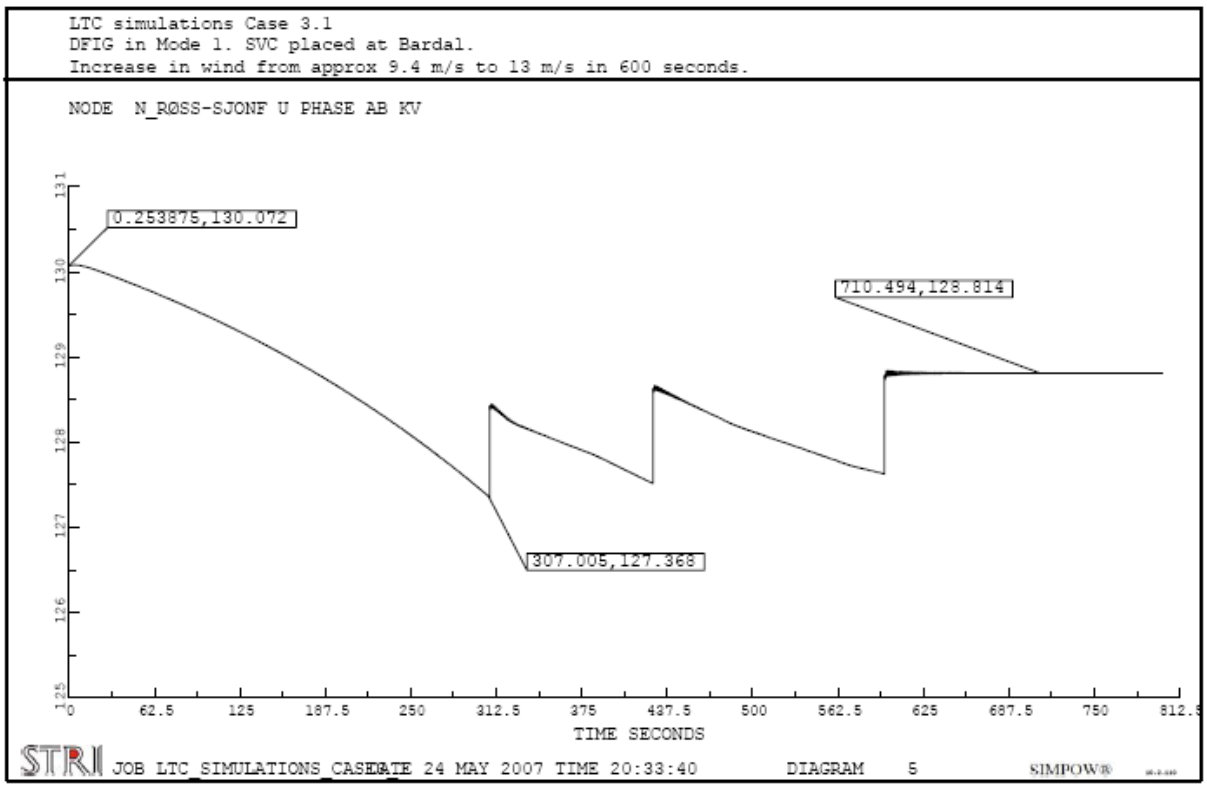

Figure 5.33: Voltage at connection point for wind radial at 132 kV level at Nedre Røssåga, Case 3.1

The voltage at the terminals of DFIG1 is shown in Figure 5.34. It shows that the voltage decreases during the production increase and that it is increased by the tap-operation of the wind farm transformer between 132 kV and 22 kV. The minimum value of the terminal voltage during the production increase is 0.678 kV and the end value is 0.688 kV.

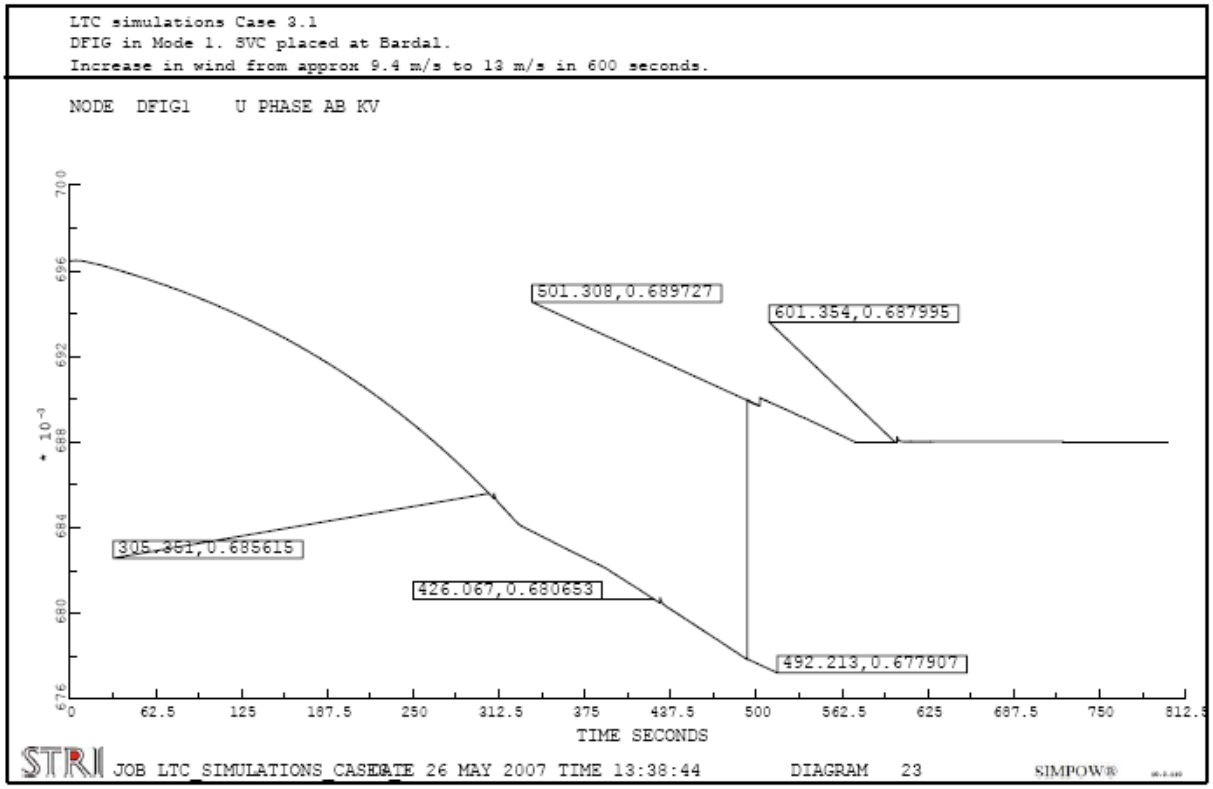

Figure 5.34: Voltage at terminals of DFIG1, Case 3.1

Figure 5.34 illustrates that the terminal voltage of DFIG1 is not significantly affected by the tap-operations of the other four LTC-transformers in the radial connection. However, a small voltage change can be observed on occasions when the other transformers perform a step change. These step changes result in a small increase in voltage at the terminals of DFIG1. This because the reactive power flow between Bardal and Sleneset is reduced as a result of these steps. The voltage loss between Bardal and Sleneset will then be smaller, and the voltage at the DFIG terminals will slightly increase.

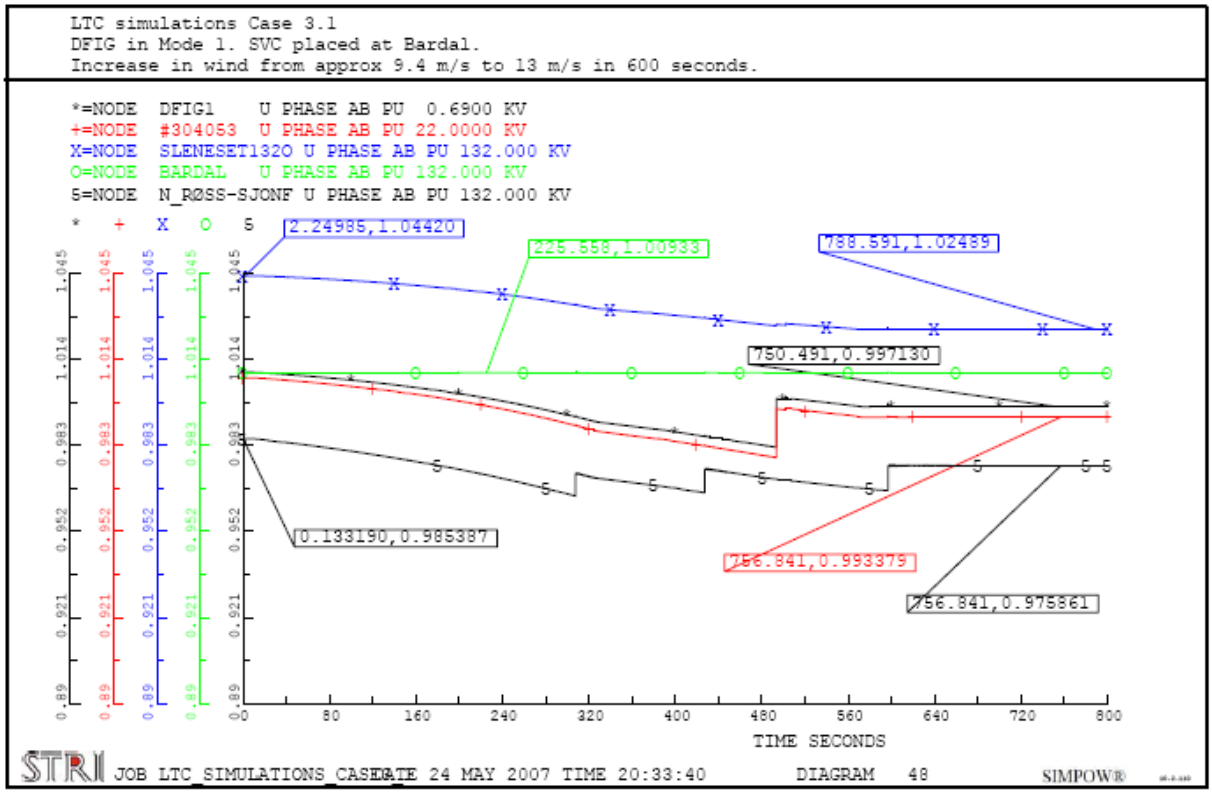

Figure 5.35: Voltages between DFIG1 at Sleneset and connection point at Nedre Røssåga, Case 3.1

The voltages at different nodes between the terminals of DFIG1 at Sleneset and the connection point at Nedre Røssåga are given in Figure 5.35. It shows that all of the voltages are within 0.95 pu and 1.05 pu during the increase in production. It also shows that the voltages on either side of Bardal are not largely affected by each other. This is due to the SVC placed at Bardal which keeps the voltage there close to constant.

The change in voltage for some monitored nodes during the increase in production is given in Table 5.16. It describes the minimum and maximum voltage, the voltage at the end of the simulation and the largest voltage change compared to the voltage at the start of the simulation.

Table 5.16: Voltage changes, Case 3.1

Node	Voltage level [kV]	Min / Max voltage [pu]	End voltage [pu]	Voltage change [%]
Salten	420	1.00 / 1.00	1.00	-0.11
Rana420	420	0.98 / 1.00	0.98	-1.56
Nedre Røssåga	420	0.98 / 1.00	0.98	-2.06
Nedre Røssåga	300	0.97 / 1.00	0.97	-2.27
N_Røss-Sjonf	132	0.96 / 0.99	0.98	-2.06
DFIG1	0.69	0.98 / 1.01	1.00	-2.69
Trofors	300	0.98 / 1.00	0.98	-2.20
Majavatn	300	0.98 / 1.00	0.98	-1.74

5.3.2.7 General

The simulations carried out in Case 3.1 show that the production increases from 50% to 100% when the wind speed is increased from 9.4 m/s to 13 m/s. The simulations also show that the voltages in the grid decreases when the production from the wind farm increases. This is due to increased losses because of the augmented active and reactive power flow.

The transformers with load tap changers located between the main grid and the wind farms improve the voltage conditions in the radial connection by stepping down and thereby increasing the voltage on the low-voltage side. This increased voltage results in less reactive losses compared with a situation without the regulation from load tap changers. There is therefore a decrease in the need for reactive power from the SVC at Bardal. The maximum production of the SVC is 282.9 MVAR. After the system has stabilized, the production at full wind power production is 260.0 MVAR.

The reduced increase in reactive power flow also results in a reduced loading of the transmission lines in the radial connection compared with a situation without load tap changers. The highest loaded part of the radial at full wind power production is a power cable between Bardal and Sleneset which is loaded 98.1% of its full capacity.

The reactive power production from the SVC at Bardal is regulated by a fast regulator. Since the regulator is placed in the middle of the radial connection, changes in voltage or reactive power consumption on either side of Bardal does not to a large extent affect reactive power flow or voltages on the other side.

The tap-operations of the transformer at the connection point at Nedre Røssåga results in an increased reactive power flow from the main grid and into the radial connection. This again results in reduced voltages in the main grid. At full wind power production, the radial draws 168.1 MVAR from the main grid.

Every time the transformer at Nedre Røssåga performs a tap-operation it represents a disturbance for the rest of the grid. This causes oscillations in voltages, reactive and active power flows throughout the grid.

In Case 3.1, dynamic load tap changer regulators were only introduced for the transformers between the wind farms and the main grid. This is a simplification. If dynamic regulators were introduced in all transformers in the system, the end conditions in the grid might be

different. The voltages in the main grid are reduced because of increased losses due to the increased active production. The voltages are further reduced when the transformer at Nedre Røssåga steps down to increase the voltage on the low-voltage side. These voltage reductions could lead to a situation where also other transformers with load tap changers are outside the specified dead band and therefore regulates the voltage. This would cause a further decrease of the voltage in the main grid. However, the voltage reduction is largest close to the connection point at Nedre Røssåga and the likelihood for tap-operations would be largest there. The decrease in voltage will also lead to increased reactive power production from the synchronous generators in the grid. Nodes close to large hydro power plants will therefore not be affected in the same way as nodes far from large hydro power plants. This is because the synchronous generators will try to maintain their terminal voltage.

It should be noted that the minimum values reached for voltages during the production increase depend on how fast the wind increases. This is because the regulators for the load tap changers are equipped with a constant time delay and not with a time delay dependent on the size of the measured voltage difference. A rapid wind increase will therefore result in a lower voltage compared with a slow wind increase.

As explained in chapter 3.2 it is desirable to keep the number of tap-operations as low as possible. The wind increase simulated in Case 3.1 resulted in three tap-operations in the transformer between the main grid and the wind farm radial. In addition, three of the four LTC-transformers in the wind farms performed one tap-operation. However, in this case, a linear increase in wind was simulated. Such a wind increase is unlikely to take place in reality. It is more likely that the wind will fluctuate during a build-up in wind speeds. These fluctuations will result in voltage fluctuations which again can result in an increased number of tap-operations. To simulate this, wind speeds based on real wind measurements should be included. This is not done in this project.

Responses considered not being important for the discussion is included in Appendix E. The output file from the steady-state power flow calculation along with the OPTPOW and DYNPOW files are also included in this appendix.

5.3.3 Case 3.2 – DFIG in Voltage Control and SVC at Bardal

5.3.3.1 Description

The settings used in Case 2.2 are used as a basis for the simulations done in this case. The doubly-fed induction generators are set to control the voltage at the terminals to 0.69 kV and a SVC is placed at Bardal.

The steady-state power flow is the same as the one used in Case 2.2.

The values obtained from the dynamic simulations are based on plotted values and might therefore cause some inaccuracies.

The increase in wind speed is identical to the increase in wind speed applied in Case 3.1

5.3.3.2 Tap-operations

The simulations done in Case 3.2 show that the load tap changer at the transformer at the connection point at Nedre Røssåga steps down three times during the production increase. This is done to increase the voltage on the 132 kV side.

The load tap changers located at the wind farms do not tap during the given production increase. This is natural since the doubly-fed induction generators are set to control the voltage at the terminals. The voltage at the 0.69 kV level in the wind farms will then be constant, and the only voltage decrease at the 22 kV level will be because of an increased voltage drop across the 0.69 kV / 22 kV transformer due to the increased power flow. The simulation indicates that this voltage drop is not sufficient to make the load tap changer between the 22 kV and the 132 kV step.

5.3.3.3 Power production

The active and reactive power production from DFIG1 is described in Figure 5.36. It can be seen from the figure that the active production reaches the full capacity of the generator. At full active production DFIG1 is also producing 6.2 MVAR in order to maintain a terminal voltage of 0.69 kV.

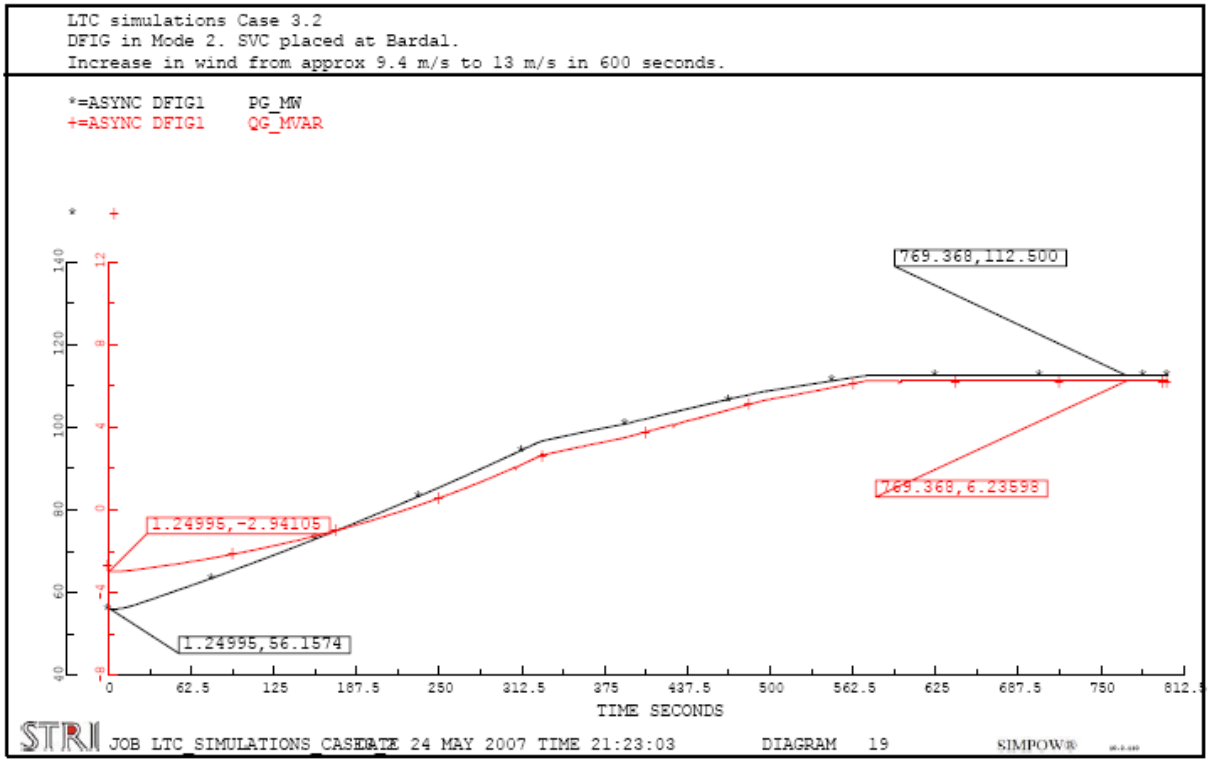

Figure 5.36: Active and reactive power production from DFIG1, Case 3.2

The reactive power production from the SVC located at Bardal is given in Figure 5.37. The reactive power production drops each time the transformer at Nedre Røssåga increases the voltage at the 132 kV side. This is because when the voltage at the 132 kV level at Nedre Røssåga is increased, less reactive power production is needed in order to maintain a terminal voltage of 133.25 kV at Bardal. The maximum production level for this case is 254.4 MVAR. The reactive production from the SVC after the system has settled is 231.5 MVAR.

As mentioned for Case 3.1, the maximum reactive power production from the SVC will depend on how fast the wind increase is.

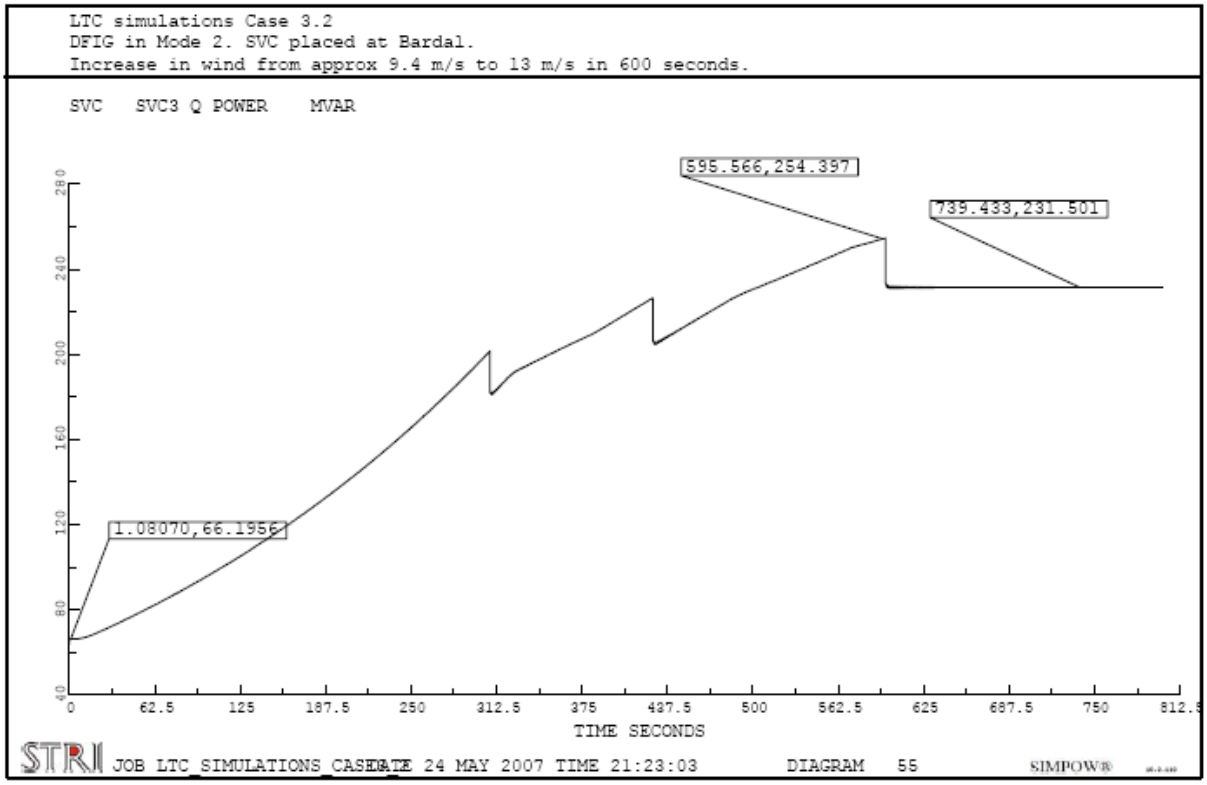

Figure 5.37: Reactive power production from SVC at Bardal, Case 3.2

The maximum reactive power produced by the doubly-fed induction generators and the SVC at Bardal is given in Table 5.17. In addition the reactive power imported at Nedre Røssåga is given. The values are obtained after the system has settled.

Table 5.17: Reactive power production at full active power production, Case 3.2

Source	Reactive production at full active production [MVAR]
DFIG1	6.2
DFIG2	5.9
DFIG3	2.4
DFIG4	12.6
SVC3	231.5
Imported at N.Røssåga	168.1
Total	426.7

5.3.3.4 Power flow

The response of the power flow through the transformer at the connection point at Nedre Røssåga shows approximately the same response as the response from Case 3.1. It shows that each time the LTC-transformer at Nedre Røssåga increases the voltage on the 132 kV side, the reactive power drawn from the main grid increases. During the given production increase in Case 3.2 the reactive power drawn from the main grid increases from 5.0 MVAR to 168.1 MVAR.

The active power consumed by the reference bus increases from 939.7 MW to 1257.5 MW during the wind increase. The reactive production increases from 65.6 MVAR to 255.9 MVAR. This is approximately the same as in Case 3.1

Also in this case the tap-operations of the load tap changer increases the reactive power production from the reference bus and results in oscillations in active and reactive power flow.

The power flows in the connection point at Nedre Røssåga and at Tunnsjødal is included in Appendix E.

A zoomed time plot of the oscillations caused by tap-changing at Nedre Røssåga for the generator at Svartisen is given in Appendix E. It shows approximately an identical response as the one illustrated in Figure 5.29 for Case 3.1.

5.3.3.5 Thermal limits

The current in the dimensioning lines and power cables between Nedre Røssåga and the wind farms during full production are shown in Table 5.18. In addition the loading of the transmission line with the highest loading outside the radial connection is presented. This line is located between Marka and Øvre Røssåga.

Table 5.18: Line loading, Case 3.2

Line	I_{Limit} [kA]	$I_{100\% \text{ production}}$ [kA]	Loading [%]
Bardal – N.Røssåga	6.176	2.843	46.0
Sjo-Alt1_3 - #304656	1.160	0.932	80.3
Sjonfjell132A – Sjonfjell132B	1.160	1.064	91.7
#304633-3662 - #304366	0.970	0.946	97.5
Sleneset132O - Sleneset132V	0.715	0.475	64.4
#300763 - #300788	0.560	0.528	94.3

Also in Case 3.2 the dimensioning power cable between Bardal and Sleneset is the part of the radial which has the highest loading. During full production at Sleneset this cable is loaded with 97.5% of its full capacity.

The time plot for the current between Nedre Røssåga and Bardal for Case 3.2 shows that the response in current to tap-operations at Nedre Røssåga is the same as shown in Figure 5.30 for Case 3.1. The current in the transmission line is reduced due to reduced reactive power flow when the load tap changer increases the voltage at the 132 kV level at Nedre Røssåga.

The time plot for the current in the power cable between Bardal and Sleneset show that the current is not largely affected by the tap-operations at Nedre Røssåga. This was also the outcome in Case 3.1. However, the maximum current is reduced compared to Case 3.1. This is because of the reactive power production from the doubly-fed induction generators. The reactive production reduces the reactive power flow between Bardal and the wind farms.

5.3.3.6 Voltage variations

The voltages in Case 3.2 show approximately the same responses to the production increase as the voltages in Case 3.1. The only changes are at nodes between the SVC at Bardal and the wind farms. The change is due to the introduced reactive power production from the doubly-fed induction generators.

The time plots for the voltages at nodes in the main grid show that the voltage decreases due to the increased production from the wind farms. The voltages are also further reduced when the LTC-transformer step in order to increase the voltage at the wind farm connection point. Nodes close to the connection point at Nedre Røssåga have the largest decrease in voltage.

The voltages at nodes between the terminals of DFIG1 and the connection point at Nedre Røssåga are given in Figure 5.38. It shows that the voltages between DFIG1 and Bardal are kept close to constant during the production increase and that they are not affected by the tap-operations at Nedre Røssåga. All of the voltages in the radial line are between 0.95 and 1.05 pu.

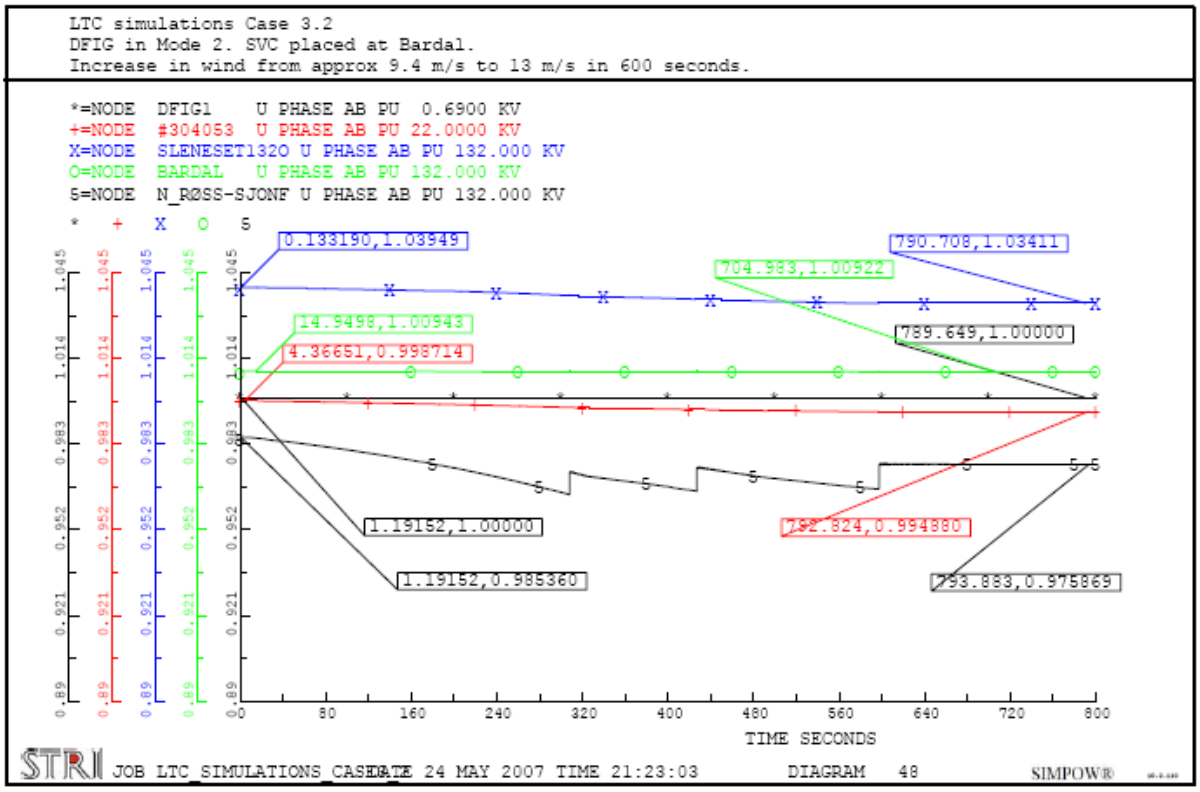

Figure 5.38: Voltages between DFIG1 and connection point at Nedre Røssåga, Case 3.2

The change in voltage for some monitored nodes during the increase in production is given in Table 5.19. It describes the minimum and maximum voltage, the voltage at the end of the simulation and the largest voltage change compared to the voltage at the start of the simulation.

Table 5.19: Voltage changes, Case 3.2

Node	Voltage level [kV]	Min / Max voltage [pu]	End voltage [pu]	Voltage change [%]
Salten	420	1.00 / 1.00	1.00	-0.11
Rana420	420	0.98 / 1.00	0.98	-1.56
Nedre Røssåga	420	0.98 / 1.00	0.98	-2.06
Nedre Røssåga	300	0.97 / 1.00	0.97	-2.25
N_Røss-Sjonf	132	0.96 / 0.99	0.98	-2.04
DFIG1	0.69	1.00 / 1.00	1.00	0.00
Trofors	300	0.98 / 1.00	0.98	-2.19
Majavatn	300	0.98 / 1.00	0.98	-1.75

5.3.3.7 General

The simulations in Case 3.2 show that the production increases from 50% to 100% when the wind speed is increased from 9.4 m/s to 13 m/s. The simulations also demonstrate that the voltages in the grid decreases when the production from the wind farm increases. This is due to increased losses because of the increased active and reactive power flow.

The voltage conditions in the radial connection are improved compared with the conditions in Case 3.1. This is because voltage control is introduced at the terminals of the doubly-fed induction generators. This also results in reduced reactive power flow between the SVC at Bardal and the wind farm generators. As a result, the size of the SVC at Bardal can be reduced. The total amount of reactive power consumed in the radial connection is slightly less than the amount consumed in Case 3.1.

The reduced reactive power flow in the radial reduces reactive losses and line loading. The highest loaded power cable is loaded 97.5% of its maximum capacity.

However, as seen from the main grid, Case 3.2 and Case 3.1 are two almost an identical situations. The amount of reactive power drawn from the grid at full active production in the wind farms are in both cases 168.1 MVAR. This reactive power consumption, along with increased losses due to increased power flow, reduces the voltages in the main grid. The voltages are further reduced by tap-operations at Nedre Røssåga.

With the introduction of voltage control at the generator terminals the tap-operations from the transformers in the wind farms are eliminated. If the objective is to reduce the number of tap-operations, the situation is improved in Case 3.2 compared to Case 3.1. The LTC-transformer at the connection point to the main grid performs three tap-operations during the given production increase. This is the same as in Case 3.1. However, as explained in Case 3.1 the number of tap-operations will most likely be larger in a real-case scenario. This is because a linear wind increase is used in the simulation.

The simplification that was done in Case 3.1 by only adding dynamic load tap changer regulators to the LTC-transformers between the main grid and the wind farms is also done in Case 3.2. The consequences of this are described for Case 3.1.

Responses considered not being important for the discussion is included in Appendix E. The output file from the steady-state power flow calculation along with the OPTPOW and DYNPOW files are also included in this appendix.

5.4 Reactive Power Control

5.4.1 Introduction

It is desirable to minimize the negative impacts that wind farms might have on the rest of the grid. As described in section 3.4, the regulator controlling the wind park should be able to operate in two different modes in the connection point. These modes are voltage control and power factor control. Power factor control often means to minimize the reactive power drawn by the wind farm at the connection point. One way to resolve this is to introduce a regulator which regulates the reactive power flow through a specified transmission line. The power flow can then be set to a specified level, provided that the grids on both sides are able to fulfil the specified requirement.

In this project such a regulator is introduced in the SVC at Bardal as a secondary regulator.

The values of the input parameters used in this project for the regulator are described in Appendix D.

A dummy transmission line is inserted at the high-voltage side of the transformer at Nedre Røssåga. All power flow between the main grid and the wind farms will have to go through this line. The regulator is set to control the reactive power flow through this line. In this way, the regulator also compensates for the reactive losses in the transformer between the wind farm radial and the main grid. The impedance in the transmission line is set low in order to minimize the effects from this line on the power flow.

In these simulations, the wind is increased from approximately 9.4 m/s to 13.0 m/s in 50 seconds. Transformers with load tap changers are disregarded. First a simulation is done with the doubly-fed induction generators in power factor control, then a simulation with voltage control is carried out.

Both conditions in the radial connection towards the wind farms and in the rest of the system are monitored.

5.4.2 Case 4.1 – DFIG in Power Factor Control

5.4.2.1 Description

Since the amount of reactive power drawn from the grid can be expected to be reduced in this simulation, the production from the SVC at Bardal can be expected to increase. This will increase the voltages in the radial. Preliminary simulations show that the voltage level in the radial will rise above the accepted value of 1.1 pu. Therefore, the voltage level in the radial is lowered in the steady-state power flow in order to be able to cope with this voltage increase. This will create a new steady-state power flow. The voltage is lowered by reducing the terminal voltage of the SVC at Bardal and reducing the controlled voltage of the transformer at Nedre Røssåga.

Except for the voltage changes, the settings used in Case 1.2 are used as a basis for the simulations done in this case. The doubly-fed induction generators are set to control the power factor at the terminals to unity.

The reactive power regulator of the SVC at Bardal is set to keep the reactive power flow through the monitored transmission line to the same value as the reactive power flow in the steady-state simulation. This power flow is not zero. However, compared to the active power flow, the reactive power flow is insignificant.

The values obtained from the dynamic simulations are based on plotted values and might therefore cause some inaccuracies.

After the wind has reached 13 m/s it is kept constant in 50 seconds. This is done to secure that the system has settled.

The simulation results from the simulations with the same voltages in the radial as in Case 3.1 are given in Appendix E.

5.4.2.2 Power production

Diagrams describing the production increase of the DFIGs for the simulated scenario in Case 4.1 shows that the active power production increases from approximately 50% to 100% for the given wind increase. The reactive power production is kept at zero. These diagrams are included in Appendix E.

The reactive power production from the SVC at Bardal is described in Figure 5.39. The SVC is producing 412.5 MVAR when there is full active production in the wind farms.

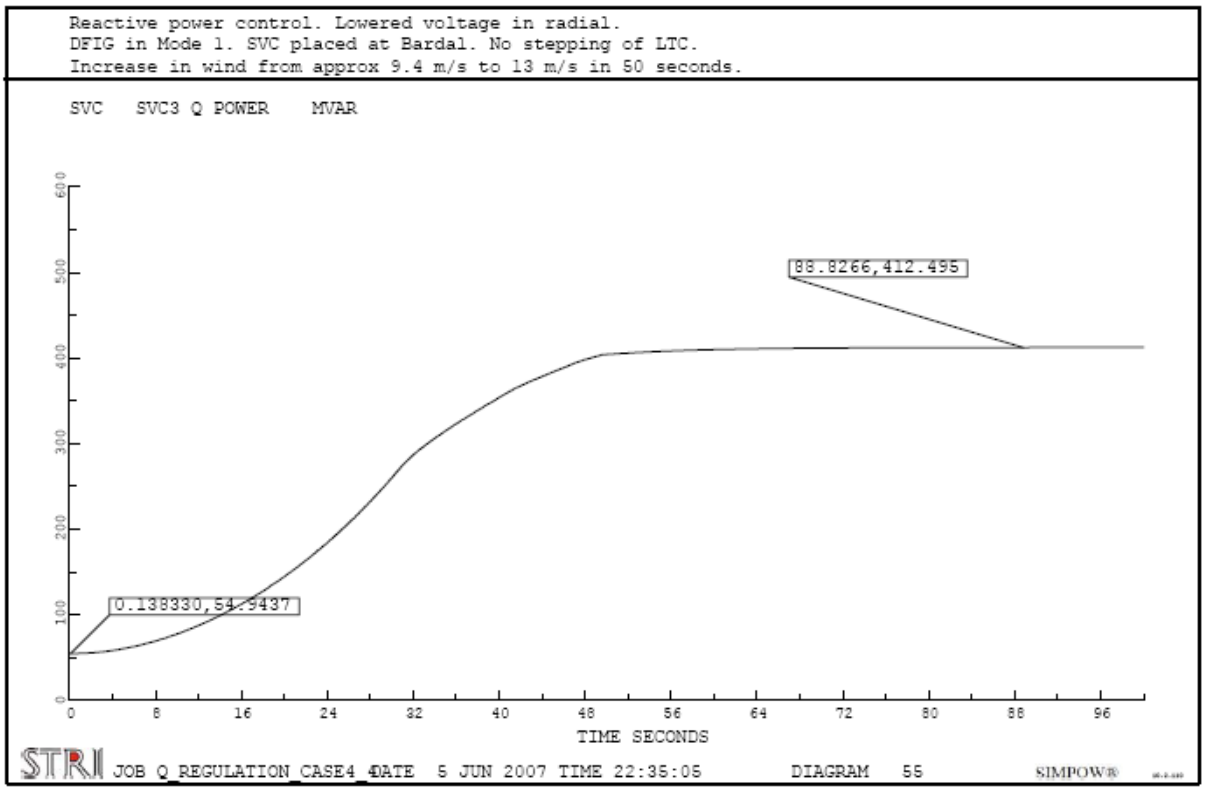

Figure 5.39: Reactive power production from SVC at Bardal

The reactive power production connected to the wind farm radial and the amount of reactive power drawn from the main grid are given in Table 5.20.

Table 5.20: Reactive power production at full active production, Case 4.1

Source	Reactive production at full active production [MVAR]
DFIG1	0
DFIG2	0
DFIG3	0
DFIG4	0
SVC3	412.5
Imported at N.Røssåga	3.6
Total	416.1

5.4.2.3 Power flow

The active and reactive power flow through the transmission line controlled by the reactive power regulator at Bardal is given in Figure 5.40. It shows that the maximum reactive power drawn from the main grid occurs at 31.9 seconds. At that time, 31.5 MVAR are drawn from the main grid. Though, due to the large active power flow at the time, the power factor is close to unity.

The increased reactive power flow in the regulated transmission line is due to the large gradient of the increase in wind power production. As shown in Figure 5.40, the regulator eventually regulates the reactive power flow to a level close to the initial level.

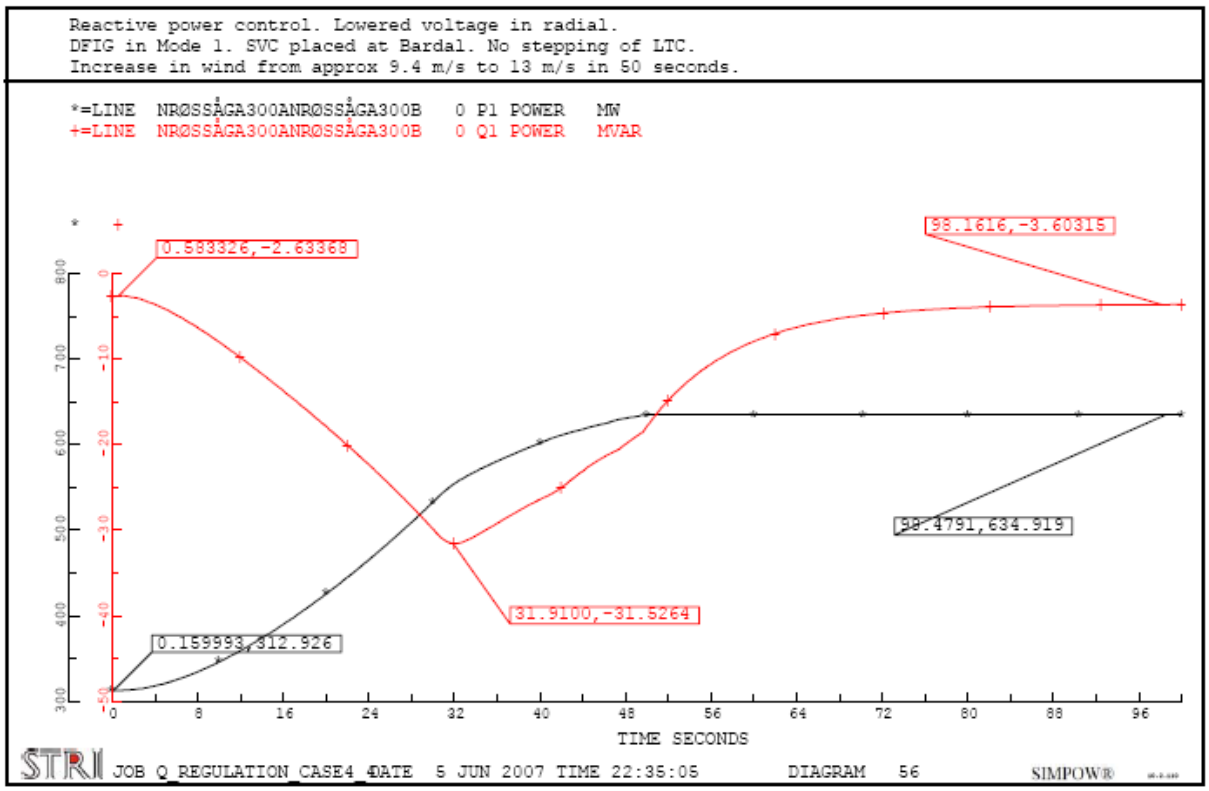

Figure 5.40: Power flow between wind farm radial and main grid at Nedre Røssåga, Case 4.1

The active and reactive power flow from the reference bus at Tunnsjødal is described in Figure 5.41. It shows that the reactive production of the reference bus increases from 64.6 MVAR to 208.1 MVAR during the production increase in Case 4.1. Compared to the reactive production from the reference bus in Case 1.2 this is a decrease of 37.0 MVAR. However, it is important to note that the steady-state power flow in Case 4.1 is different.

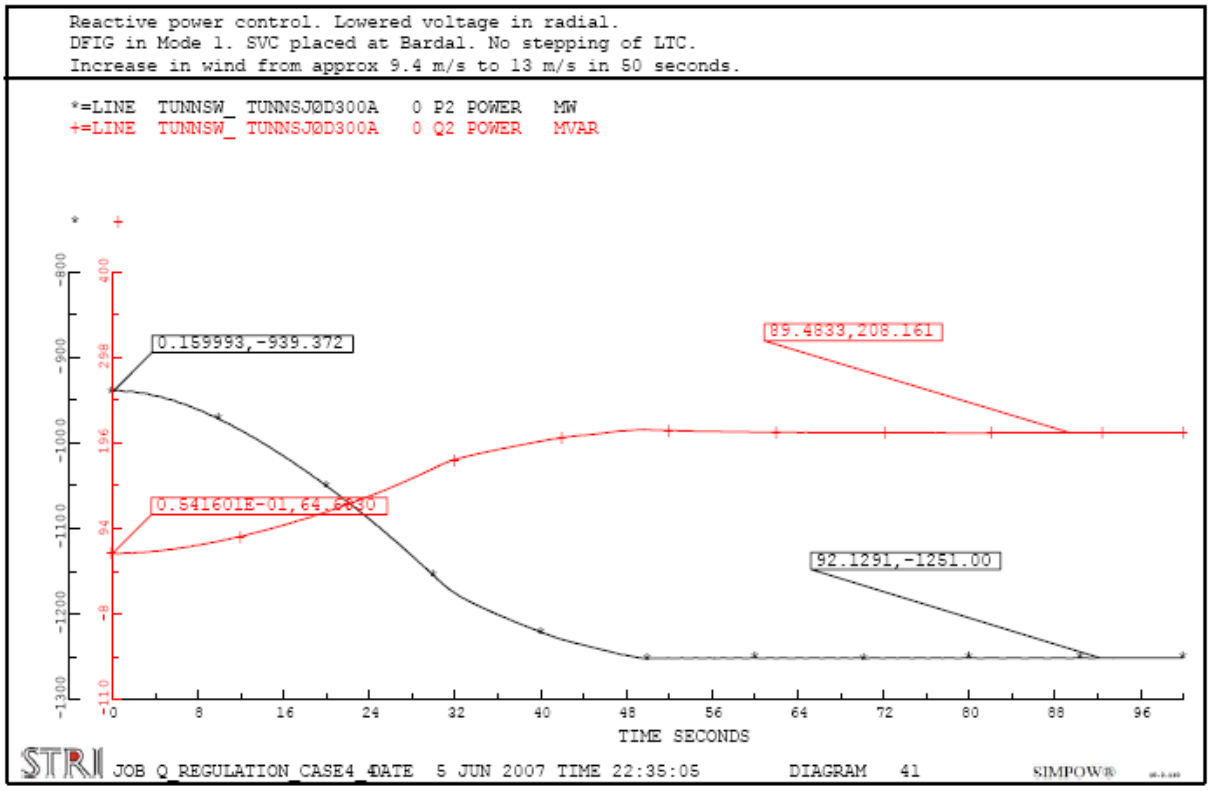

Figure 5.41: Active and reactive power flow from reference bus at Tunnsjødal, Case 4.1

5.4.2.4 Thermal limits

The current in dimensioning lines and power cables between Nedre Røssåga and the wind farms during full production are shown in Table 5.21. In addition the maximum current in the transmission line with the highest loading outside the radial connection is given. This line is located between Marka and Øvre Røssåga.

Table 5.21: Line loading, Case 4.1

Line	I_{Limit} [kA]	$I_{100\% \text{ production}}$ [kA]	Loading [%]
Bardal – N.Røssåga	6.176	2.940	47.6
Sjo-Alt1_3 - #304656	1.160	0.877	75.6
Sjonfjell132A – Sjonfjell132B	1.160	1.006	86.7
#304633-3662 - #304366	0.970	0.893	92.1
Sleneset132O - Sleneset132V	0.715	0.450	62.9
#300763 - #300788	0.560	0.524	93.6

Table 5.22 shows that the loading in the transmission lines and power cables between Bardal and the wind farms are reduced in Case 4.1 compared to Case 1.2. The loading is reduced due to reduced losses because of the increased voltage in the radial.

The power cable between Bardal and Sleneset is the part of the radial with the highest loading. During full wind power production, this cable is loaded with 92.1% of its maximum capacity.

The transmission line between Bardal and Nedre Røssåga has an increased loading compared to Case 1.2. This is due to the increased reactive power flow from Bardal towards Nedre Røssåga.

The line with highest loading in the grid is the line between Marka and Nedre Røssåga. This line is loaded with 93.6% of its maximum capacity. However, as explained previously, the loading of this line is not greatly affected by the increase in wind power production.

5.4.2.5 Voltage variations

The voltage at the terminals of DFIG3 is given in Figure 5.42. This is the generator with the highest terminal voltage. The voltage passes 1.05 pu (0.7245 kV) after 38.3 seconds. A voltage above 1.05 pu over a longer period at the terminals of a generator can be considered to be unacceptable. At full production the voltage reaches 1.08 pu.

All of the doubly-fed induction generators have a terminal voltage above 1.05 pu at full production.

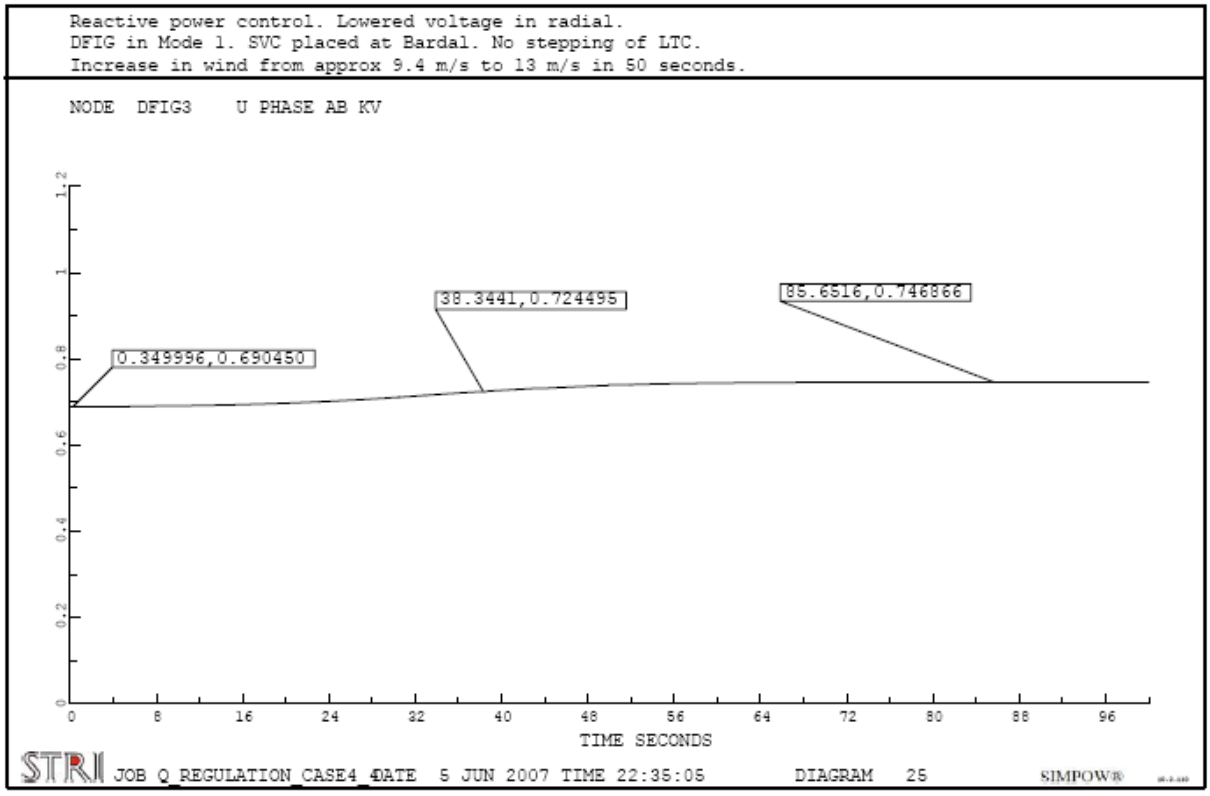

Figure 5.42: Terminal voltage DFIG3, Case 4.1

In Figure 5.43 the voltages between the terminals of DFIG1 and the connection point at Nedre Røssåga are given. It shows that the SVC at Bardal increases the voltage in order to hold the reactive power flow at the 300 kV level of the connection point constant. This results in increased voltages elsewhere in the radial. The increase is largest at the 132 kV level at

Sleneset. At full production the voltage is just below 1.10 pu. The voltages at Sleneset are the highest voltages in the radial. No voltage increases above 1.1 pu for the given wind increase.

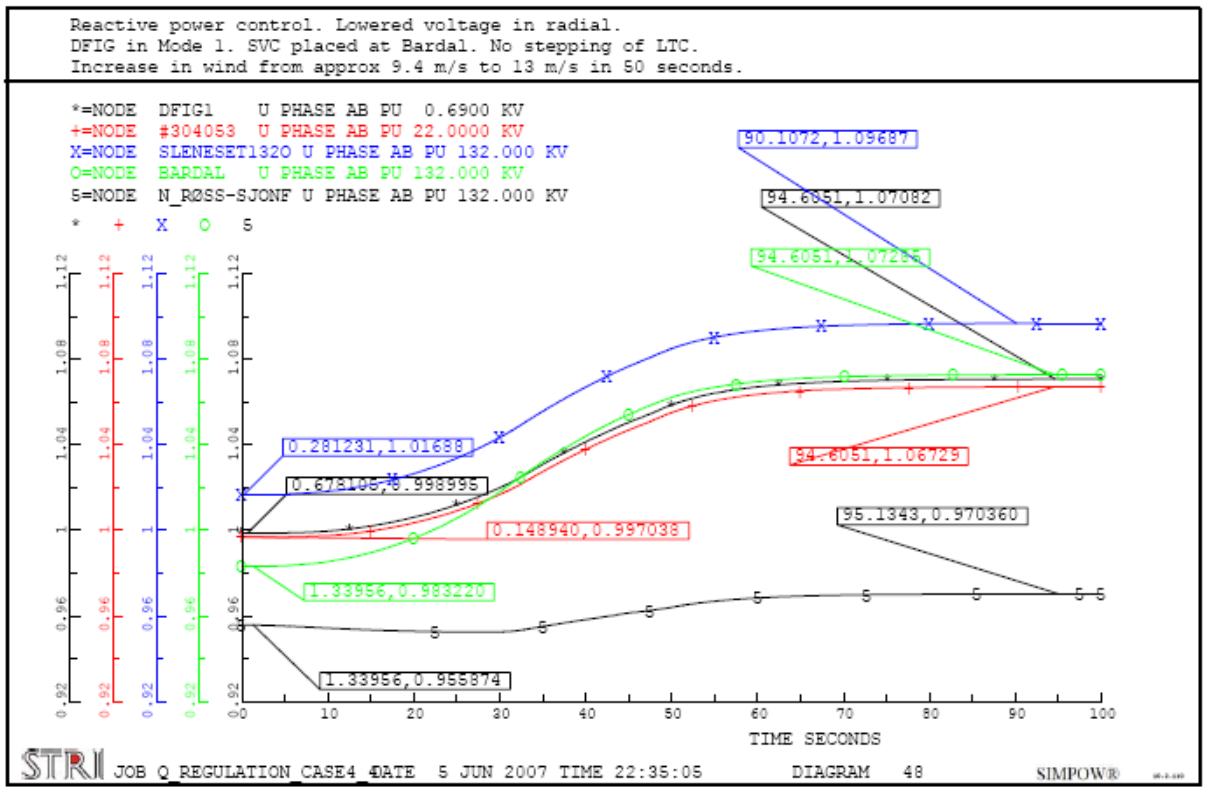

Figure 5.43: Voltage between DFIG1 and Nedre Røssåga, Case 4.1

The change in voltage for some monitored nodes during the increase in production is given in Table 5.22. It describes the minimum and maximum voltage, the voltage at the end of the simulation and the largest voltage change compared to the voltage at the start of the simulation.

Table 5.22: Voltage changes, Case 4.1

Node	Voltage level [kV]	Min / Max voltage [pu]	End voltage [pu]	Voltage change [%]
Salten	420	1.00 / 1.00	1.00	-0.08
Rana420	420	0.99 / 1.00	0.99	-0.56
Nedre Røssåga	420	0.99 / 1.00	0.99	-0.76
Nedre Røssåga	300	0.99 / 1.00	0.99	-0.83
N_Røss-Sjonf	132	0.95 / 0.97	0.97	1.44
DFIG1	0.69	1.00 / 1.07	1.07	7.18
Sleneset132O	132	1.02 / 1.10	1.10	8.00
Trofors	300	0.99 / 1.00	0.99	-1.32
Majavatn	300	0.99 / 1.00	0.99	-1.15

5.4.2.6 General

The simulations done in Case 4.1 show that the reactive power exchange between the radial connection with the wind farms and the main grid can be minimized by implementing a reactive power regulator at the SVC at Bardal. During this rapid wind increase the maximum

imported reactive power from the main grid is 31.9 MVAR. After the system has stabilized at full wind power production, the reactive power drawn from the main grid is reduced to 3.6 MVAR. Compared to Case 1.2, the amount of reactive power drawn from the main grid at full wind power production is reduced with 112.1 MVAR.

The reduced amount of imported reactive power results in a need for increased reactive power production in the wind farm radial. The reactive power production from the SVC at Bardal is therefore increased. The maximum production from the SVC is 412.5 MVAR. This is 77.7 MVAR more than in Case 1.2.

The increased reactive power production results in increased voltages in the radial. The simulations show that the terminal voltage of the doubly-fed induction generators increases above 1.05 pu. This is not an acceptable operational situation over a longer period of time. It is possible that the voltages could have been further reduced in the steady-state power flow. However, it can be expected that transformers with load tap changers will improve the voltages at the 0.69 kV level and that the voltage will be only temporary above this level. As described in section 4.3.2.7, this can be accepted for a limited amount of time. A further reduction of the voltages in the steady-state calculation will result in voltages in the radial below 0.95 pu during 50% wind power production.

The production from the wind farms are at 93.5% when the voltage at the terminals of DFIG3 reaches 1.05 pu.

The change in voltage in the main grid is reduced in Case 4.1 compared to Case 1.2. This is due to the reduced reactive power exchange between the main grid and the wind farm radial. The voltages are well within specified limits. However, the voltages in the grid are still reduced because of the increased transmission losses.

Responses considered not being important for the discussion is included in Appendix E. The output file from the steady-state power flow calculation along with the OPTPOW and DYNPOW files are also included in this appendix.

5.4.3 Case 4.2 – DFIG in Voltage Control

The settings used in Case 2.2 are used as a basis for the simulations done in this case. The doubly-fed induction generators are set to control voltage at the terminals to 0.69, and a SVC is placed at Bardal. The maximum capacity of the SVC at Bardal is increased to 600 MVAR. This is done to secure that the size of the SVC does not become the limiting factor.

The reactive power regulator of the SVC at Bardal is set to keep the reactive power flow through the monitored transmission line at the same value as the reactive power flow in the steady-state simulation. This power flow is not zero. However, compared to the active power flow, the reactive power flow is insignificant.

The values obtained from the dynamic simulations are based on plotted values and might therefore cause some inaccuracies.

After the wind has reached 13 m/s, it is kept constant for 50 seconds. This is done to secure that the system has stabilized.

5.4.3.1 Power production

The simulations done in Case 4.2 show that the active production in the wind farms increases to 100% production for the given wind increase. The active and reactive power production from DFIG1 is described in Figure 5.44.

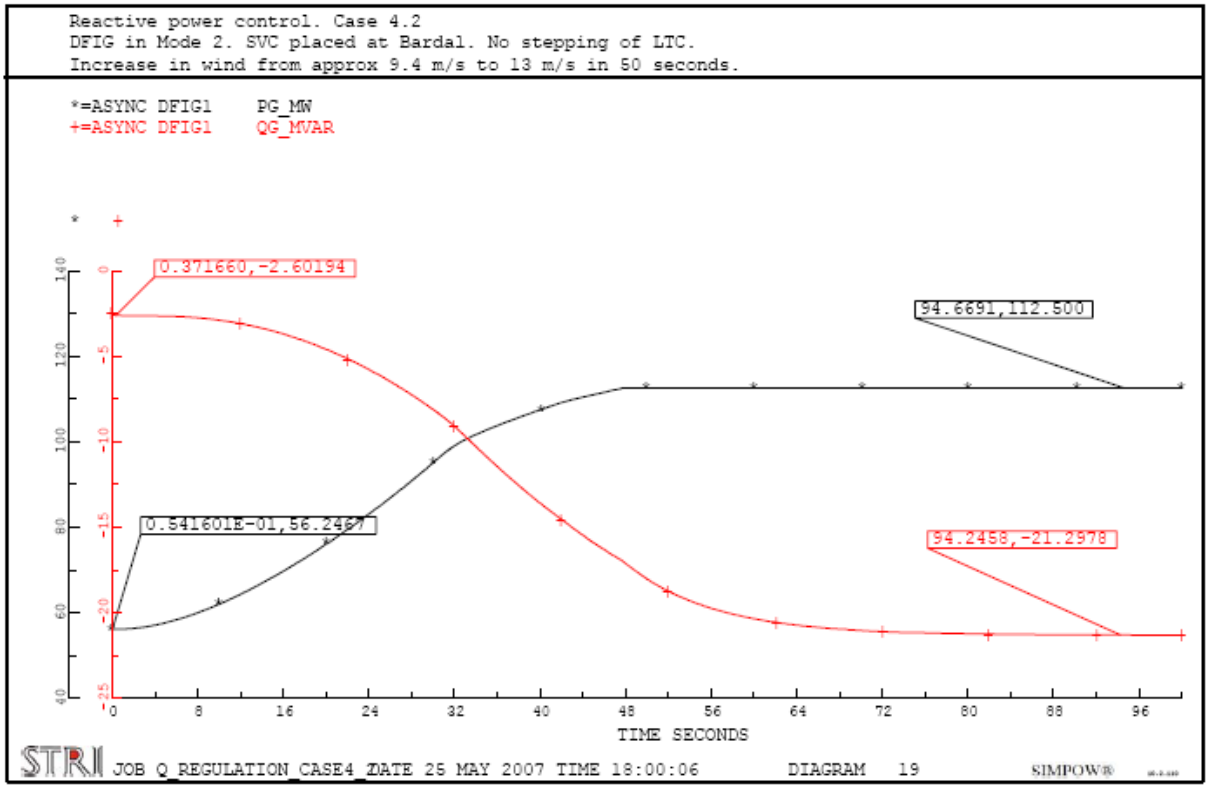

Figure 5.44: Active and reactive power production DFIG1, Case 4.2

Figure 5.44 shows that DFIG1 has to consume 21.3 MVAR at full production in order to maintain a terminal voltage of 0.69 kV.

The reactive power production from the SVC at Bardal is given in Figure 5.45. It shows that at full wind active power production in the wind farms, the SVC is producing 589.8 MVAR. Compared to Case 2.2 this is an increase of almost 300 MVAR.

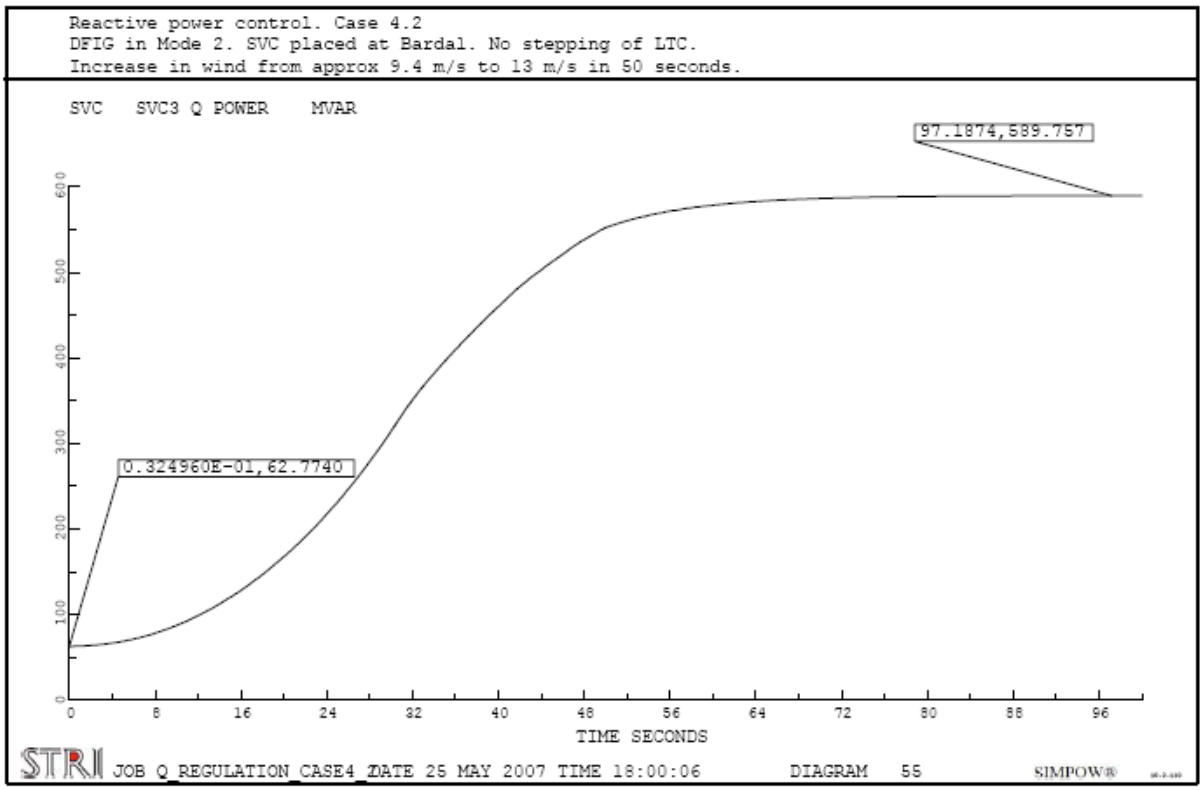

Figure 5.45: Reactive power production from SVC at Bardal, Case 4.2

The reactive power production connected to the wind farm radial and the amount of reactive power drawn from the main grid are given in Table 5.23.

Table 5.23: Reactive power production at full active production, Case 4.2

Source	Reactive production at full active production [MVAR]
DFIG1	0
DFIG2	0
DFIG3	0
DFIG4	0
SVC3	589.8
Imported at N.Røssåga	7.2
Total	597.0

The reactive power production of the doubly-fed induction generators is set to zero in Table 5.23. This is done to illustrate the total amount of reactive power fed into the radial. As shown by Figure 5.44 the generators are consuming reactive power in order to keep the voltage at the terminals down.

At full active production, DFIG2 is consuming 21.1 MVAR, DFIG3 is consuming 71.1 MVAR and DFIG4 is consuming 56.1 MVAR. DFIG3 will have a power factor of 0.93.

5.4.3.2 Power flow

The power flow in the transmission line controlled by the reactive power regulator at Bardal is given in Figure 5.46. It shows that the power flow between the main grid and the wind farm radial has the same form as in Case 4.1, however the amount of reactive power drawn from

the grid is slightly larger in Case 4.2. This is due to the difference in steady-state power flow. The maximum reactive power drawn from the main grid is 32.8 MVAR.

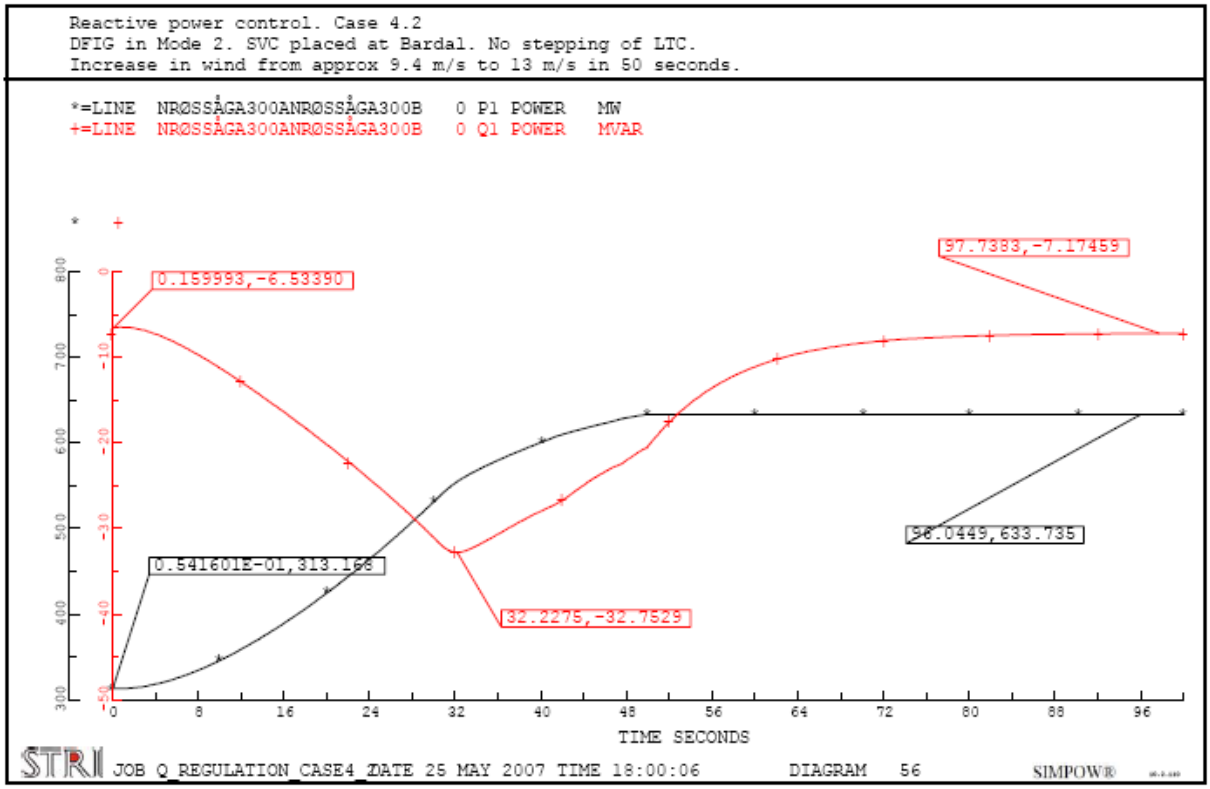

Figure 5.46: Power flow between wind farm radial and main grid at Nedre Røssåga, Case 4.2

The response of the reference bus during the wind speed increase is given in Appendix E, together with other diagrams describing the power flow in monitored lines.

The reactive production of the reference bus increases from 66.0 MVAR to 208.5 MVAR. Compared to the result obtained in Case 2.2 this is a reduction of 33.7 MVAR.

5.4.3.3 Thermal limits

The current in the dimensioning lines and power cables between Nedre Røssåga and the wind farms during full production are shown in Table 5.24. In addition, the maximum current in the transmission line with the highest loading outside the radial connection is given. The line is located between Marka and Øvre Røssåga.

Table 5.24: Line loading, Case 4.2

Line	I_{Limit} [kA]	$I_{100\% \text{ production}}$ [kA]	Loading [%]
Bardal – N.Røssåga	6.176	2.842	46.0
Sjo-Alt1_3 - #304656	1.160	0.963	83.0
Sjonfjell132A – Sjonfjell132B	1.160	1.091	94.1
#304633-3662 - #304366	0.970	0.913	94.1
Sleneset132O - Sleneset132V	0.715	0.479	67.9
#300763 - #300788	0.560	0.524	93.6

During full wind power production, both the power cables between Bardal and Sleneset and within Sjonfjellet are operating at 94.1% of their capacity. However, due to the reactive power consumption of the doubly-fed induction generators, the power cable between Bardal and Sleneset is in this case not delivering reactive power in both ends. This can result in a large difference in current between the two sides of the cable. At full production, the current on the wind farm side is 0.959 kA. This is 98.8% of full capacity. Therefore this cable is the part in the radial which operates closest to its maximum capacity. This is discussed further in Case 5.2

As mentioned above, cases 4.1 and 4.2 have approximately the same influence on the rest of the modelled grid. This result is supported by the fact that the loading in the highest loaded line outside the radial connection is in both cases equal.

5.4.3.4 Voltage variations

The voltages between the terminals of DFIG1 and the 132 kV side of the connection point at Nedre Røssåga are given in Figure 5.47. It shows that the SVC at Bardal increases the voltage to 1.09 pu at full wind power production. The voltage at the 132 kV side of the transformer at Nedre Røssåga also increases when the wind power production increases. This is because the SVC at Bardal is compensating for the increasing reactive power loss within the transformer at the connection point.

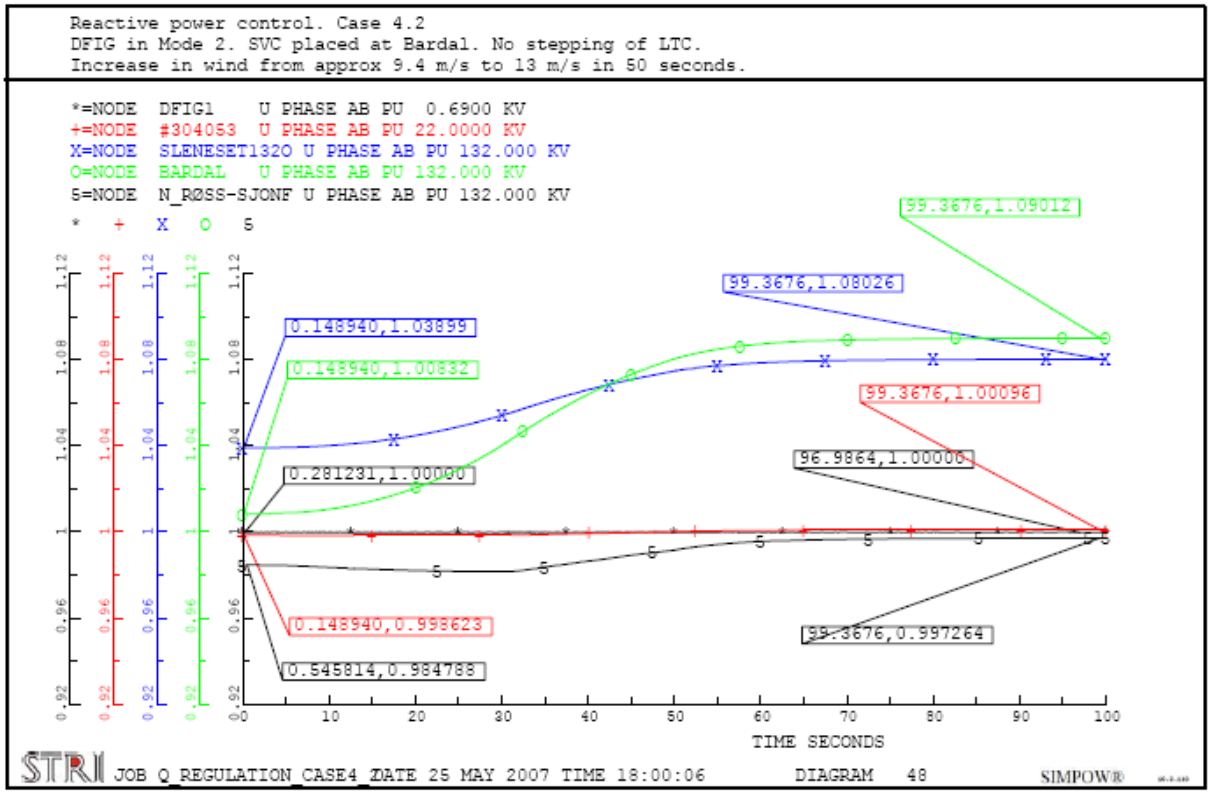

Figure 5.47: Voltages between DFIG1 and connection point at Nedre Røssåga, Case 4.2

The figure also shows that the voltage at the terminals of DFIG1 is held constant at 1.00 pu or 0.69 kV. The voltage at the 132 kV level at Sleneset reaches a maximum voltage of 1.08 pu or 142.6 kV during full wind power production.

The highest voltage in the radial is at Bardal. The voltage there reaches 1.09 pu at wind full power production This equals 143.9 kV.

The minimum, maximum and end voltages for some monitored nodes are presented in Table 5.25. In addition the largest voltage change compared to the initial value is given.

Table 5.25: Voltage changes, Case 4.2

Node	Voltage level [kV]	Min / Max voltage [pu]	End voltage [pu]	Voltage change [%]
Salten	420	1.00 / 1.00	1.00	-0.06
Rana420	420	0.99 / 1.00	0.99	-0.54
Nedre Røssåga	420	0.99 / 1.00	0.99	-0.72
Nedre Røssåga	300	0.99 / 1.00	0.99	-0.80
N_Røss-Sjonf	132	0.98 / 1.00	1.00	1.56
DFIG1	0.69	1.00 / 1.00	1.00	0.00
Sleneset132O	132	1.04 / 1.08	1.08	4.12
Trofors	300	0.99 / 1.00	0.99	-1.26
Majavatn	300	0.99 / 1.00	0.99	-1.14

As mentioned above, the difference between the results in Case 4.1 and Case 4.2 as seen from the grid is small. However, due to differences in the steady-state power flow, some variations occur.

5.4.3.5 General

The simulations done in Case 4.2 show that the reactive power flow between the wind farms and the rest of the grid can be controlled by implementing a reactive power regulator at the SVC at Bardal. The maximum reactive power drawn from the grid during the given wind increase is 38.2 MVAR. After the system has settled at full wind power production, the reactive power drawn from the main grid is reduced to 7.2 MVAR. Compared with Case 2.2, the amount of reactive power drawn from the main grid at Nedre Røssåga at full wind power production is reduced with 114.1 MVAR.

The reduced import of reactive power from the main grid to the radial connection results in an increased need for reactive production from the SVC at Bardal. During the given wind increase, the SVC needs to produce 589.8 MVAR of reactive power in order to control the reactive power drawn from the grid. This is an increase of 299.4 MVAR compared with Case 2.2 and an increase of 177.3 MVAR compared with Case 4.1.

The reason for this large increase in production from the SVC is the introduction of voltage control at the terminals of the doubly-fed induction generators. The voltage control regulators for the generators are set to control the terminal voltage to 0.69 kV. Due to the increased power transfer, the SVC at Bardal increases its reactive production to compensate for the increased reactive losses. The result of this increase is that the voltage at Bardal increases. What is more, the voltage at the DFIG terminals will also start to increase. However, since the voltage regulator at the terminals controls the voltage, the doubly-fed induction generators starts to consume reactive power. The size of the consumption from the DFIG will depend on the amount of reactive power flow needed in order to create a sufficiently large voltage drop between Bardal and the different wind power generators.

Other compensating equipment, like for instance shunt reactors, can be used to consume the desired reactive power if the doubly-fed induction generators are unable to do it.

The size of the reactive power transfer can be reduced by allowing the voltage at the terminals of the DFIG to increase. This is illustrated by Case 4.1. An allowed voltage increase at the DFIG terminals will both reduce the amount consumed by the DFIG and the amount produced by the SVC at Bardal. This option is further investigated in Case 5.3 where also load tap changers also are included.

The line loadings in Case 4.2 shows that compared to Case 4.1, the transmission lines in the wind farm radial between Bardal and the wind farms operate closer to their thermal limits. This is due to the increased reactive power flows between the SVC and the doubly-fed induction generators. The line between Bardal and Nedre Røssåga has a reduced loading in Case 4.2. This is because the voltage level is lower in Case 4.1 and as a consequence, the losses are larger.

Compared to Case 2.2, some of the lines in the radial in Case 4.2 are more loaded and some are less. This is because there are two factors influencing the current in opposite direction; the current is reduced due to the voltage increase at Bardal and it is increased because of the increased power flow between Bardal and the wind farms. At nodes close to Bardal and the connection point at Nedre Røssåga the voltage increase is at its largest compared to the result in Case 2.2. The lines close to and between these nodes will therefore have a reduction in line loading. At nodes close to the generator terminals, where the voltage is kept constant, the increase in losses due to increased power flow will be dominating. The increase in loading in these lines will therefore be larger compared with Case 2.2.

The voltage conditions within the radial connection leading towards the wind farms are improved compared with the voltage conditions observed in Case 4.1. All the voltages are within specified limits. This is due to the voltage control at the DFIG terminals which reduces the voltage by consuming reactive power.

Compared with Case 2.2, the voltage conditions in the main grid are improved. The reduction in voltage is reduced by controlling the reactive power exchange with the wind farms to a constant value. However, like in Case 4.1, the voltages in the main grid are reduced due to the increased power flow between Nedre Røssåga and Tunnsjødal.

Responses considered not being important for the discussion is included in Appendix E. The output file from the steady-state power flow calculation along with the OPTPOW and DYNPOW files are also included in this appendix.

5.5 Reactive Power Control and Load Tap Changers

5.5.1 Introduction

Simulations with both a reactive power regulator and a dynamic load tap changer regulator are performed. This is done to illustrate how the reactive power regulator at Bardal will influence the behaviour of the LTC-transformers in the radial connection, and how eventual tap-operations will influence the production from the SVC at Bardal.

Also in these simulations, only transformers with load tap changers placed between the main grid and the wind farms are equipped with dynamic regulators. This is because these simulations focus upon how the impact from the load tap changers directly connected to the wind power production affect the voltage conditions in the radial towards the wind farms, the needed reactive compensation and the reactive power drawn from the main grid.

The settings for the dynamic load tap changer regulator and the reactive power regulator are respectively described in Appendix E and Appendix D.

The wind speed is increased from approximately 9.4 m/s to 13 m/s in 600 seconds in all the simulated cases. The wind speed is then held constant to secure that the system has stabilized and that the simulation is not stopped while, due to time delays, the transformer regulators are still running.

5.5.2 Case 5.1 – DFIG in Power Factor Control

5.5.2.1 Description

The basis for this case is the settings used in Case 4.1. The doubly-fed induction generators are set to keep the power factor at the terminals to unity and a SVC is placed at Bardal. The voltage in the wind farm radial is lower compared with in the steady-state power flow in Case 1.2.

The SVC at Bardal is set to keep the reactive power flow through the transmission line located at the high-voltage side of the transformer at the connection point to the level given by the steady-state power flow. The reactive power flow through this line in the steady-state calculation is not exactly zero. However, considering the size of the active power flow, no effort is made to reduce it further.

The values obtained from the dynamic simulations are based on plotted values and might therefore cause some inaccuracies.

5.5.2.2 Tap-operations

The results from Case 5.1 show that the transformer at the connection point steps up one time during the given wind increase. This is done in order to reduce the voltage at the 132 kV level in the radial. During the same wind increase all of the four LTC-transformers located at the wind farms steps up three times in order to reduce the voltage at the 22 kV level.

The diagrams showing the position of the taps in the load tap changers in Case 5.1 are given in Appendix E.

5.5.2.3 Power production

The active power production from the wind farms increases to full production for the given wind speed increase. The reactive power production is kept at zero. There is no indication in the diagrams describing the power production from the doubly-fed induction generators that the generators are affected by the tap change of transformers.

The active and reactive power production from the doubly-fed induction generators is given in Appendix E

The reactive power production from the SVC at Bardal is given in Figure 5.48. The reactive power production increases as a result of the tap-operation of the transformer in the connection point.

The reactive production from the SVC reaches 440.4 MVAR at full active production in the wind farms.

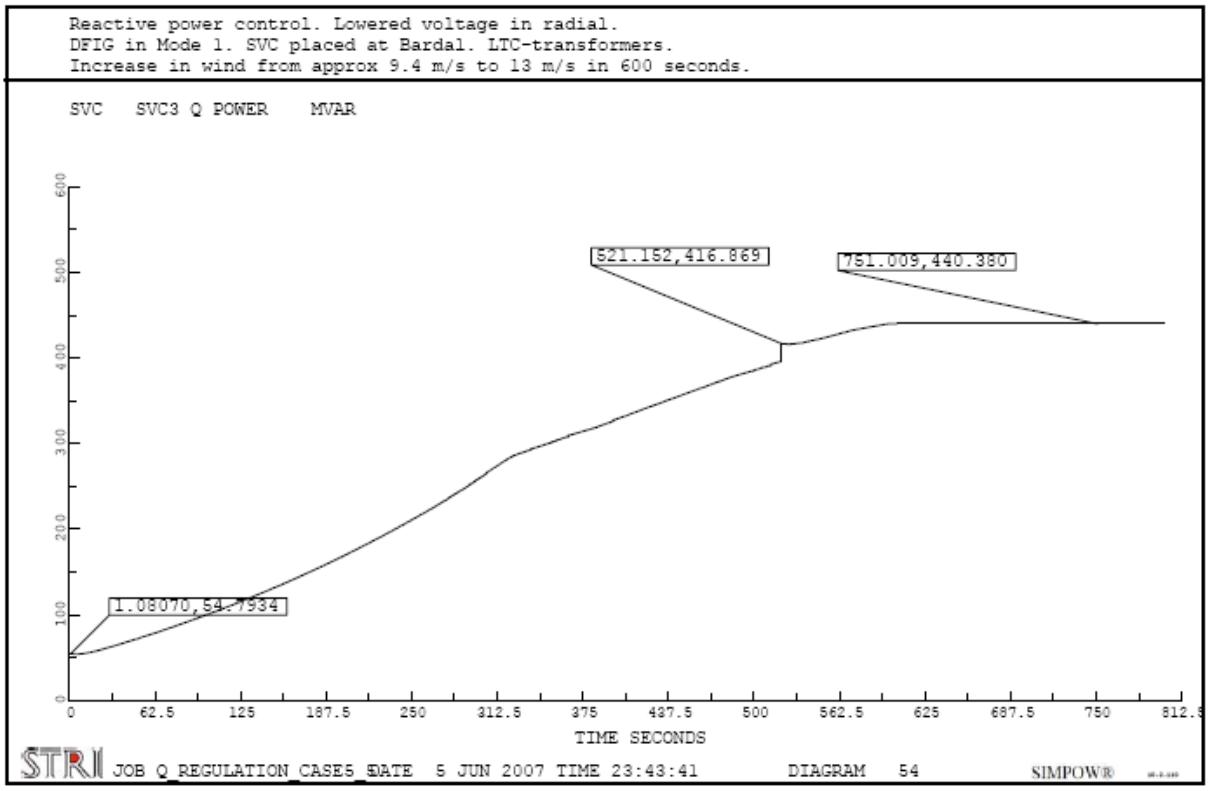

Figure 5.48: Reactive power production from SVC at Bardal, Case 5.1

The reactive power production from the SVC increases when the transformer at Nedre Røssåga reduces the voltage on the 132 kV side. The increase is a consequence of the tap-operation. When the transformer regulator decreases the voltage, the losses in the grid increase due to higher currents. This increase will decrease the voltage in the radial even more. In order to meet this increase in losses, the reactive production is increased. However an increase in reactive power production large enough to maintain the voltage at Bardal after the tap-operation will result in a change in reactive power flow in the line monitored by the secondary controller of the SVC. The secondary controller will therefore limit this production increase and allow a sag in voltage at Bardal.

The reactive power production from the SVC at Bardal also increases when the LTC-transformers at the wind farms step up in order to reduce the voltage at the 22 kV level. Production increases because the losses on the transformers in the wind farms will increase when the voltage is reduced. It is difficult to observe this from Figure 5.48, therefore a diagram where it is zoomed in at the time of a tap-operation in the wind farms is provided in Appendix E.

The reactive power produced by the doubly-fed induction generators and the SVC at Bardal at full wind power production is presented in Table 5.26. In addition the reactive power imported at Nedre Røssåga is given.

Table 5.26: Reactive power production at full wind power production, Case 5.1

Source	Reactive production at full active production [MVAR]
DFIG1	0
DFIG2	0
DFIG3	0
DFIG4	0
SVC3	440.4
Imported at N.Røssåga	3.5
Total	443.9

5.5.2.4 Power flow

The active and reactive power flow through the transmission line controlled by the reactive power regulator at Bardal is given in Figure 5.49. The maximum amount of reactive power drawn from the main grid is 5.8 MVAR. At full wind power production the wind farms draw a total of 3.5 MVAR from the main grid at Nedre Røssåga.

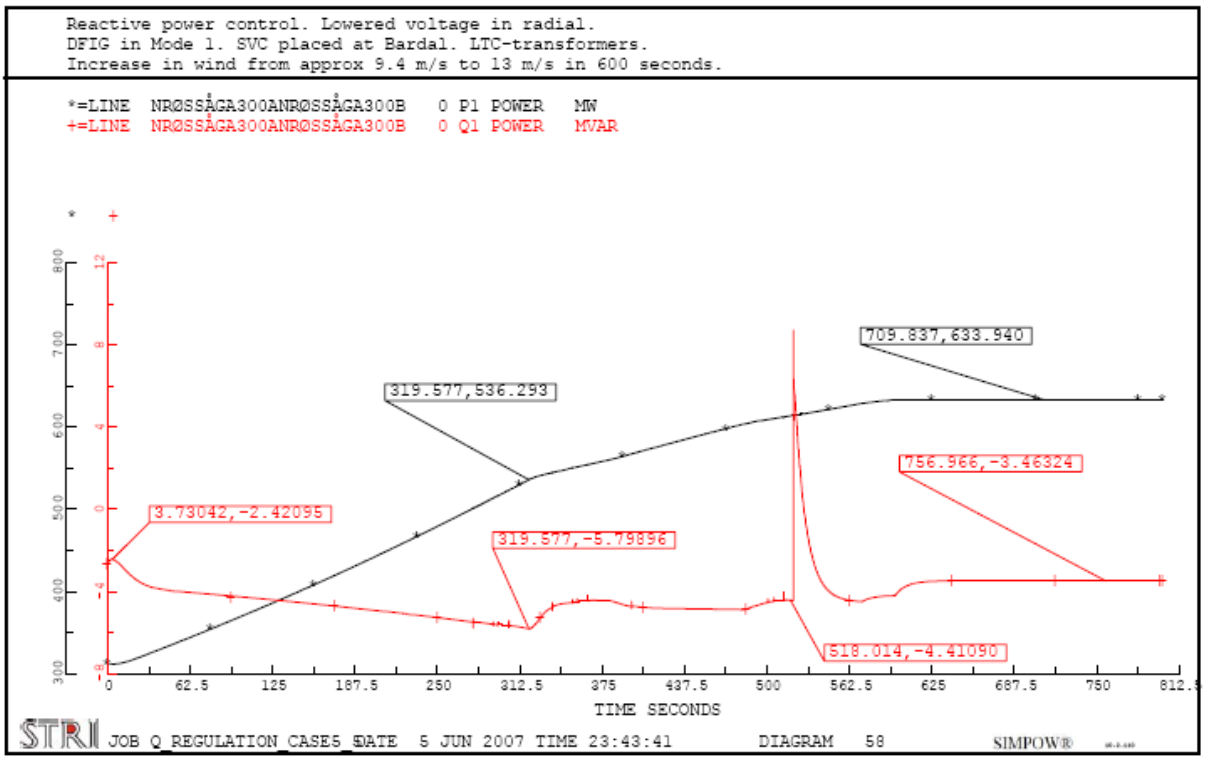

Figure 5.49: Power flow between wind farms and main grid at Nedre Røssåga, Case 5.1

Compared with Case 4.1 it is clear that the reactive power regulator in this case copes better with the rate of the wind speed increase. The regulator manages to keep the power flow during the wind increase to a more constant level. The differences in end values are, however, insignificant.

The tap-operation of the transformer at Nedre Røssåga results in a leap in the reactive power flow in the transmission line from -4.4 MVAR to 9.0 MVAR. This leap is a consequence of the different reaction times of the two regulators in the SVC at Bardal. The primary voltage regulator is fast and will try to limit the voltage sag at Bardal by increasing the production. This will lead to an increased reactive power flow from the wind farm radial into the main grid. The slower secondary regulator will limit this production increase in order to maintain a constant reactive power flow through the monitored transmission line. Since the reactive power regulator is slower than the voltage regulator, the result is an increase in the reactive power flow that is flowing towards the grid until the secondary regulator manages to limit the production increase.

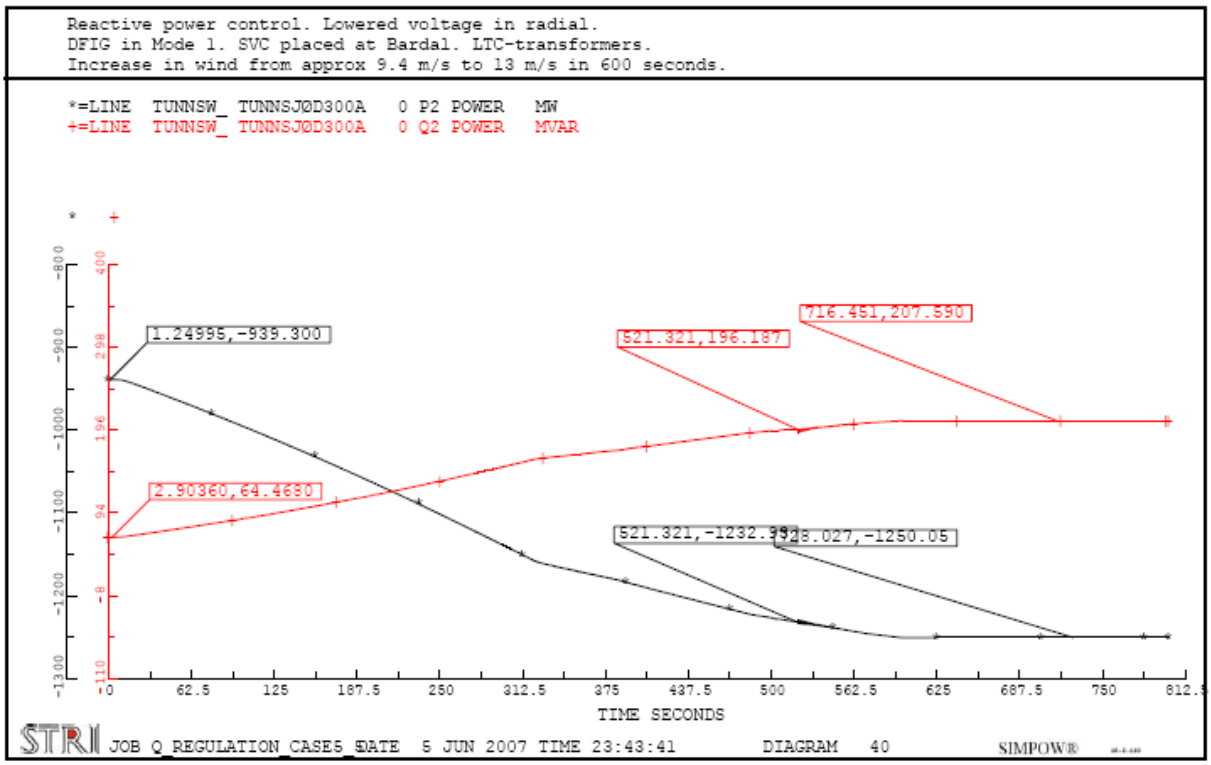

Figure 5.50: Active and reactive power flow from reference bus at Tunnsjødal, Case 5.1

The active and reactive power flow from the reference bus at Tunnsjødal is given in Figure 5.50. It shows that the reference bus is consuming 1250.1 MW and producing 207.6 MVAR when the wind farms are at full production.

As in Case 3.1 the tap-operation at Nedre Røssåga results in oscillations in active and reactive power throughout the grid.

The disturbance caused by the tap-operation is illustrated in Figure 5.51. It shows the active and reactive power production from the generator at Svartisen. The diagram is zoomed in at the exact time when the tap-operation occurs. It shows that the tap-operation causes a sudden increase in reactive power consumption. This is because the voltage at Nedre Røssåga increases suddenly when the reactive power flow at the connection point changes direction and reactive power is inserted into the main grid. In this case the generators in the grid will have to decrease their reactive power production in order to maintain their terminal voltage. This can also be observed in Figure 5.50 for the reference bus.

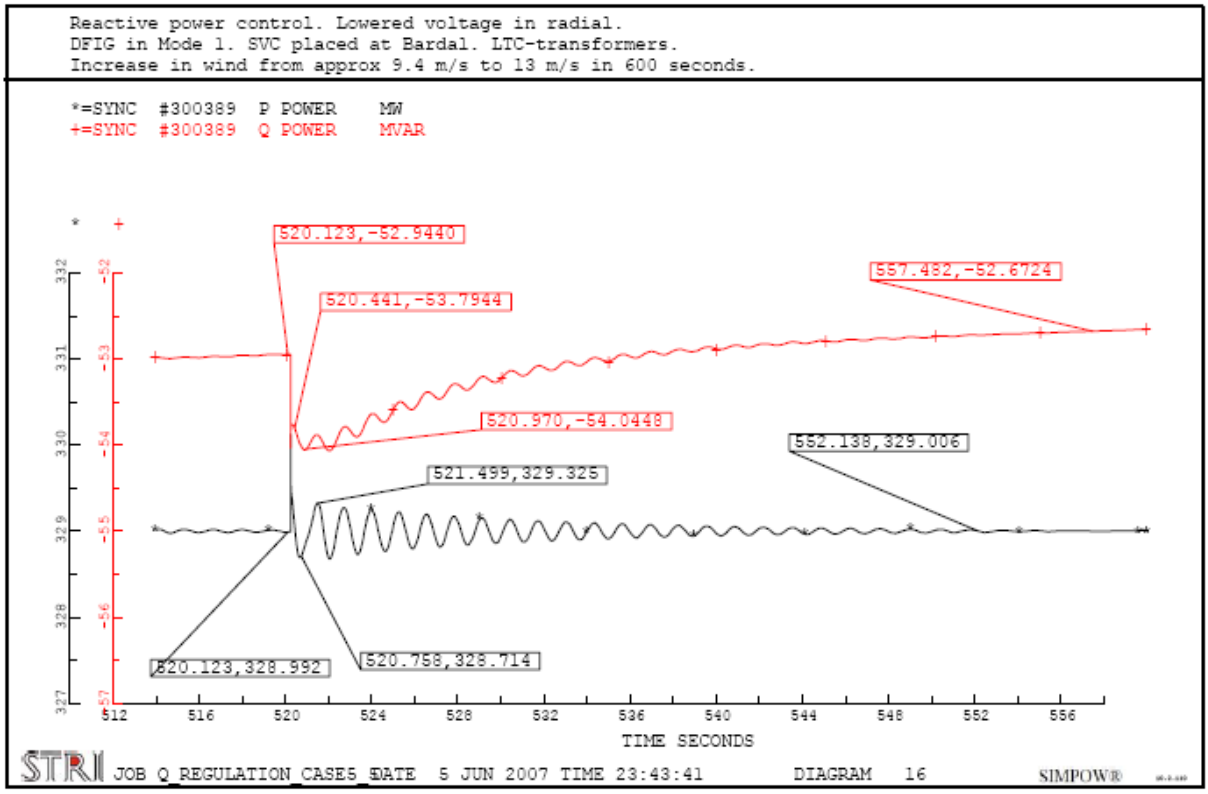

Figure 5.51: Active and reactive power production Svartisen, zoomed, Case 5.1

The oscillations caused by the tap-operation at Nedre Røssåga have a frequency of approximately 0.7 Hz and a maximum peak-to-peak value of 0.6 MW and 0.3 MVAR.

5.5.2.5 Thermal limits

Table 5.27 shows the current in dimensioning lines and power cables between Nedre Røssåga and the wind farms at Sleneset and Sjonfjellet during full wind power production. It also presents the current the line outside the radial connection with the highest loading. This line is located between Marka and Øvre Røssåga.

Table 5.27: Line loading, Case 5.1

Line	I_{Limit} [kA]	$I_{100\% \text{ production}}$ [kA]	Loading [%]
Bardal – N.Røssåga	6.176	2.982	46.8
Sjo-Alt1_3 - #304656	1.160	0.888	76.6
Sjonfjell132A – Sjonfjell132B	1.160	1.021	88.0
#304633-3662 - #304366	0.970	0.902	93.0
Sleneset132O - Sleneset132V	0.715	0.456	63.8
#300763 - #300788	0.560	0.524	93.6

Also in Case 5.1 it is the power cable between Bardal and Sleneset which is closest to its thermal capacity limit within the wind farm radial. During full production this cable is loaded with 93.0% of its total capacity.

The transmission line with the highest loading in the model is the line between Øvre Røssåga and Marka. This line is loaded with 93.6% of its total capacity. However, as explained earlier,

this line is not greatly affected by the production increase. The line has only an increase of 0.4% in loading during the production increase in Case 5.1.

Compared to Case 3.1, where the secondary regulator is not introduced, the maximum current in the line between Øvre Røssåga and Marka is reduced. This is because there is a reduced reactive power flow in this line due to reduced reactive power drawn by the wind farms at Nedre Røssåga. Compared to Case 4.1 the loading is the same.

5.5.2.6 Voltage variations

Figure 5.52 shows the voltage on the low-voltage side of the transformer at the connection point at Nedre Røssåga. As the production from the wind farms increases, the voltage at Nedre Røssåga increases. This is because the reactive power regulator is set to control the reactive power flow on the high-voltage side of the transformer at Nedre Røssåga. This means that the SVC at Bardal has to compensate for the increased losses in the transformer at the connection point. Therefore, as the losses in the transformer increases, the voltage on the 132 kV side increases. Due to this voltage increase, the load tap changer regulator decreases the voltage on the low-voltage side by performing a tap-operation on the high-voltage side.

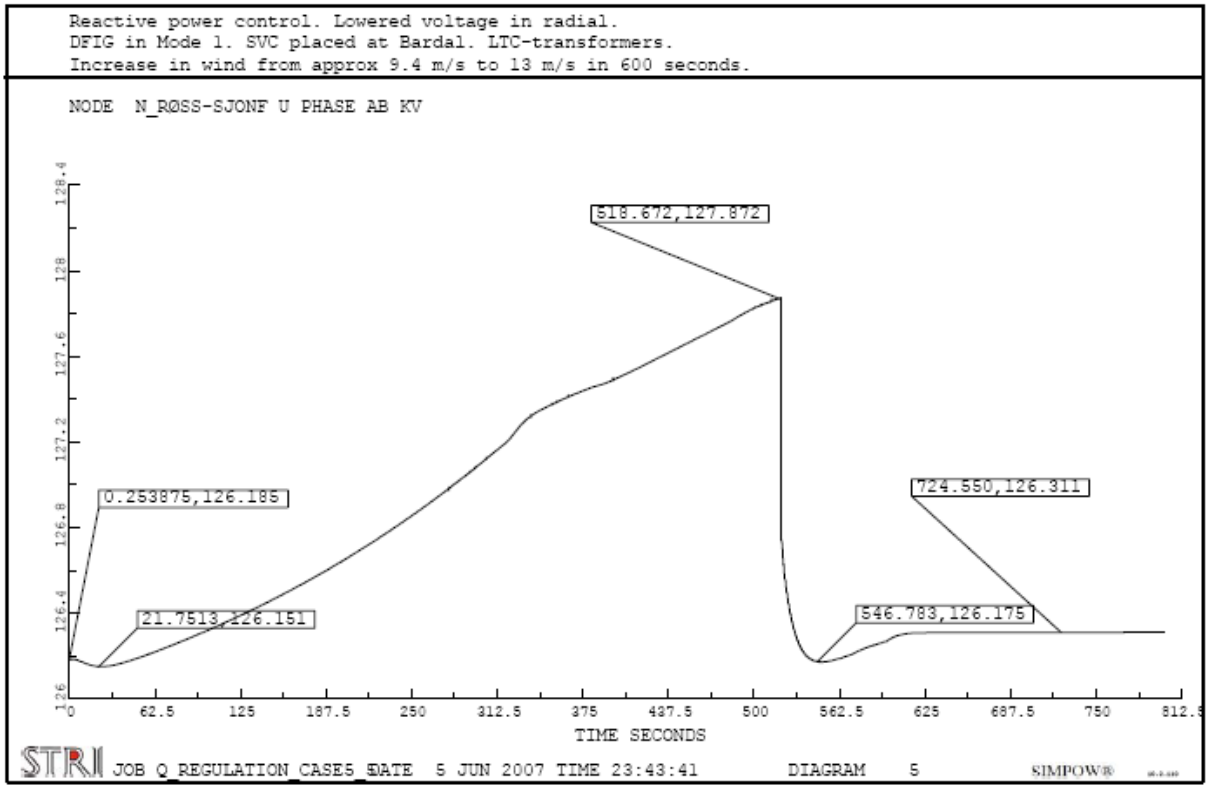

Figure 5.52: Voltage at 132 kV level at connection point at Nedre Røssåga, Case 5.1

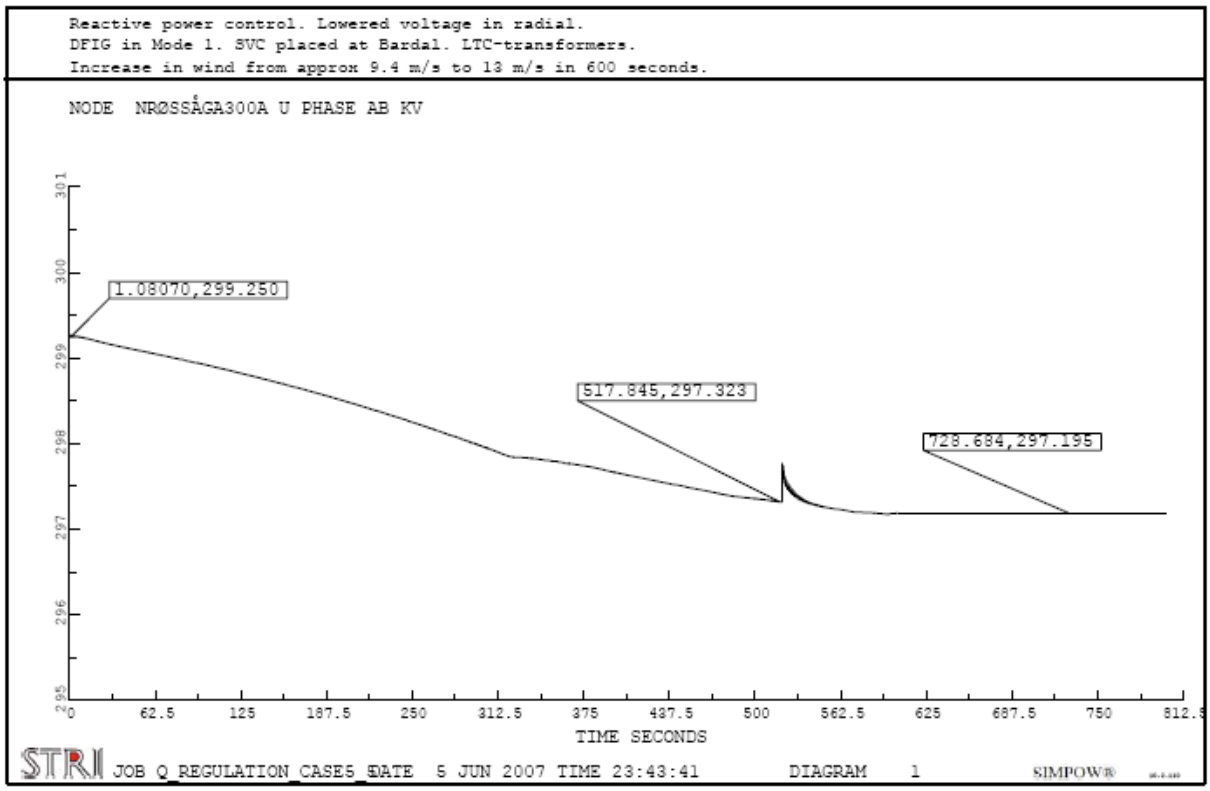

Figure 5.53: Voltage at 300 kV level at Nedre Røssåga, Case 5.1

The voltage on the high-voltage side of the transformer at the connection point at Nedre Røssåga is given in Figure 5.53. It shows that the voltage decreases due to increased power flows in the main grid. When the transformer at Nedre Røssåga steps up, the voltage at the 300 kV level experiences an increase in voltage. This increase is a result of the reactive power inserted into the main grid at the wind park connection point when the load tap changer decreases the voltage at the 132 kV level.

The voltages between the terminals of DFIG1 and the connection point at Nedre Røssåga are given in Figure 5.54. It shows, like in Case 4.1, that the voltages are increased when the production from the wind farm increases. However, the voltage at the terminals of DFIG1 is reduced by tap-operations in the transformer between the 132 kV and 22 kV level at Sleneset. These tap-operations keep the terminal voltage below 1.05 pu during the entire production increase. None of the other three doubly-fed induction generators experiences a voltage above 1.05 pu.

The voltage at the terminals of DFIG1 is not largely affected by the tap-operations performed by the transformer above DFIG2 at Sleneset. However, when the 132 kV / 22 kV transformer above a DFIG reduces the voltage, there will be increased losses in the 22 kV / 0.69 kV transformer above the generator. This will again result in a small voltage decrease at the 132 kV level in the wind farm, and therefore also on the terminals of the other aggregated DFIG in the same wind farm. This situation is difficult to observe in Figure 5.54, but can be observed in the diagrams illustrating terminal voltage for the doubly-fed induction generators. These are provided in Appendix E.

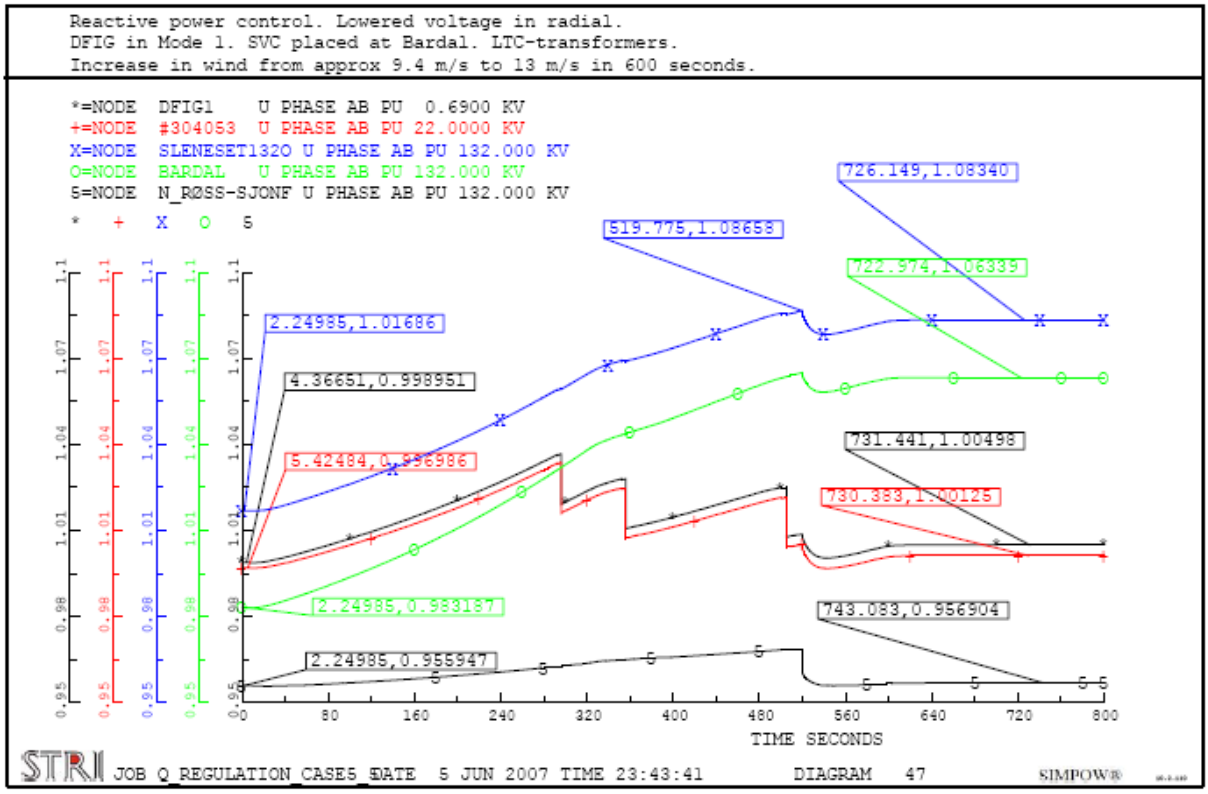

Figure 5.54: Voltages between DFIG1 and Nedre Røssåga, Case 5.1

As shown in Figure 5.54, after approximately 520 seconds, all of the voltages in the radial are affected by the tap-operation at Nedre Røssåga. This reduces the voltage level in all nodes in the radial. The situation is different from Case 3.1 where the voltages between Bardal and the wind farms were not affected by the tap-operations at Nedre Røssåga to a large degree. This difference is a result of the secondary regulator added in the SVC at Bardal in Case 5.1. Adding a secondary regulator allows the voltage to vary at Bardal. As a consequence, the voltages at the wind farms will be more affected by voltage variations in the connection point.

Figure 5.54 shows that the voltage at node Sleneset132O is below the maximum allowed voltage of 1.1 pu during the given wind increase. It should be noted that due to the constant time delay in the load tap changer regulators, the maximum voltage will depend on the increase rate of the wind speed. However, the voltage will not become higher than in Case 4.1.

None of the voltages are outside the specified limits.

The change in voltage for some monitored nodes during the increase in production is given in Table 5.28. It describes the minimum and maximum voltage, the voltage at the end of the simulation and the largest voltage change that occurs compared with the voltage at the start of the simulation.

Table 5.28: Voltage change, Case 5.1

Node	Voltage level [kV]	Min / Max voltage [pu]	End voltage [pu]	Voltage change [%]
Salten	420	1.00 / 1.00	1.00	0.06
Rana420	420	0.99 / 1.00	0.99	-0.46
Nedre Røssåga	420	0.99 / 1.00	0.99	-0.63
Nedre Røssåga	300	0.99 / 1.00	0.99	-0.69
N_Røss-Sjonf	132	0.96 / 0.97	0.96	1.28
DFIG1	0.69	1.00 / 1.04	1.04	3.77
Sleneset132O	132	1.02 / 1.09	1.08	6.95
Trofors	300	0.99 / 1.00	0.99	-1.23
Majavatn	300	0.99 / 1.00	0.99	-1.09

5.5.2.7 General

The simulations done in Case 5.1 show that the reactive power exchange between the wind farms and the main grid is significantly reduced and almost constant compared to a situation without a reactive power regulator. During the given production increase the reactive power exchange varies between -5.8 MVAR and 9.0 MVAR. Compared with the power flow in Case 4.1, it is clear that the reactive power regulator copes better with a slow wind increase. At full wind power production, the wind farms are drawing 3.5 MVAR from the main grid. This is approximately the same as in Case 4.1 and 164.6 MVAR less than Case 3.1.

The implementation of the reactive power regulator at Bardal results in a voltage increase at the 132 kV level at Nedre Røssåga. This voltage increase leads to a tap-operation at Nedre Røssåga in order to decrease the voltage. This tap-operation results in a short-term turn in the direction of the reactive power flow between the wind farms and the main grid. This injection of reactive power into the main grid leads to a short-term voltage increase. The injection is short-term because it is limited by the slow reactive power regulator.

The reduction of voltage by the load tap changer at Nedre Røssåga results in higher losses in the radial. In order to maintain a constant reactive power flow at the connection point, the SVC at Bardal has to increase its reactive production. The production of the SVC at maximum wind production is 440.4 MVAR. Compared to Case 4.1 this is an increase of 27.9 MVAR. Compared to Case 3.1, it is an increase of 180.4 MVAR.

The voltage levels at the terminals of the doubly-fed induction generators are improved compared to the voltage levels observed in Case 4.1. This is due to the tapping of transformers at the wind farms. The voltage levels are within the desired limits of ±5% of rated voltage during the given production increase.

The voltage changes in the main grid are smaller in Case 5.1 than in both Case 3.1 and Case 4.1. The changes are smaller than Case 3.1 because of the reduced reactive power drawn from the main grid at Nedre Røssåga. Compared to Case 4.1 the voltage reduction is only slightly smaller. This is because of the larger increase rate of the production in Case 4.1.

The loading of the line between Bardal and Nedre Røssåga is increased in Case 5.1 compared to Case 3.1. This is because the decrease in voltage caused by the tap changer regulator at Nedre Røssåga causes a higher reactive power flow and an increased current. The reactive

power flow in this line is also increased compared to Case 3.1 because the SVC at Bardal has to compensate for the reactive losses in the transformer at Nedre Røssåga. It is important to note that the steady-state power flows for these two cases are different and that this difference also will create some variations between the results of the two cases.

Compared with Case 4.1 the loading in the line between Bardal and Nedre Røssåga is increased due to the decrease in voltage caused by the tap-operation at Nedre Røssåga.

The lines and power cables between the wind farms and the SVC at Bardal experience a higher loading than in Case 4.1, though lower than in Case 3.1. This is because the reactive power consumption between Bardal and the wind farms only consists of reactive losses in transmission lines and transformers. Since the voltage levels are higher within the radial connection than in Case 3.1, these losses will be lower. However, the tap change of transformers at the wind farms reduces the voltage at the 22 kV and 0.69 kV levels. The loading is therefore higher than the loading in Case 4.1 where no dynamic LTC-transformers were introduced.

As seen from the main grid, Case 5.1 is quite similar to Case 4.1. The largest difference is the disturbance caused by the load tap changer at Nedre Røssåga which results in a sudden injection of reactive power into the main grid. Compared to Case 3.1, the number of tap-operations at the connection point to the main grid is reduced. This results in fewer disturbances. From a maintenance perspective this would also be positive.

The number of tap-operations at the wind farms is increased compared with Case 3.1. This could mean more maintenance and thereby less availability of the wind farms. However, it should be noted that maintenance which requires de-energizing of the transformer at Nedre Røssåga will result in a stop in the production from of both wind farms. This will not be the case for maintenance on the wind farm transformers.

Responses considered not being important for the discussion is included in Appendix E. The output file from the steady-state power flow calculation along with the OPTPOW and DYNPOW files are also included in this appendix.

5.5.3 Case 5.2 – DFIG in Voltage Control

5.5.3.1 Description

The basis used in this case contains the same settings as the one used in Case 4.2. This means that the doubly-fed induction generators are set to control the terminal voltage to 0.69 kV. An SVC placed at Bardal is set to control the voltage at Bardal and the reactive power flow at the connection point at Nedre Røssåga.

The steady-state power flow is the same as the one applied in Case 4.2

The values obtained from the dynamic simulations are based on plotted values and might therefore cause some inaccuracies.

5.5.3.2 Tap-operations

The results from the simulation done in Case 5.2 show that the transformer at the connection point at Nedre Røssåga performs one tap-operation during the production increase. After approximately 545 seconds the transformer steps up in order to decrease the voltage on the 132 kV side of the transformer. During the same production increase, the four LTC-transformers at the wind farms does not step a single time.

The diagrams showing the position of the taps in the load tap changers in Case 5.2 are given in Appendix E.

5.5.3.3 Power production

When the wind increases from approximately 9.4 m/s to 13 m/s, the active power production from the wind farms increases from approximately 50% to 100%.

The active and reactive power production from DFIG1 is given in Figure 5.55. It shows that the generator has to consume reactive power in order to maintain a terminal voltage of 0.69 kV. The tap-operation at Nedre Røssåga results in a decrease in the reactive power consumption because of a lowered voltage level. The maximum amount of consumed reactive power occurs right before the tap-operation. DFIG1 is then consuming 20 MVAR. At full active power production the generator is consuming 17.8 MVAR.

The power production from the other three generators is given in Appendix E. At full active production DFIG2 is consuming 17.6 MVAR, DFIG3 is consuming 61.7 MVAR and DFIG4 is consuming 47.3 MVAR. DFIG3 will have a power factor of 0.95.

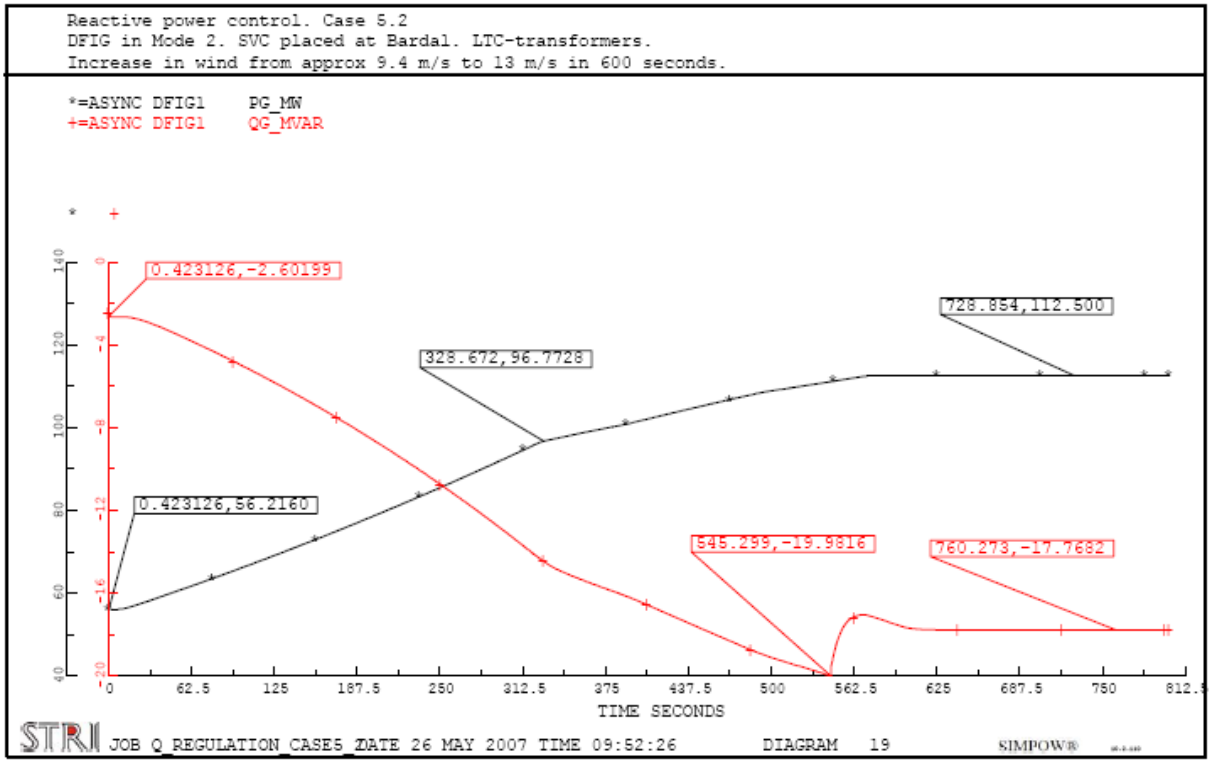

Figure 5.55: Active and reactive power production from DFIG1, Case 5.2

The reactive power production from the SVC at Bardal is described in Figure 5.56. It shows that at full wind power production, the SVC is producing 573.1 MVAR. The maximum production occurs right before the tap-operation at Nedre Røssåga. At this moment, the SVC is producing 575.6 MVAR.

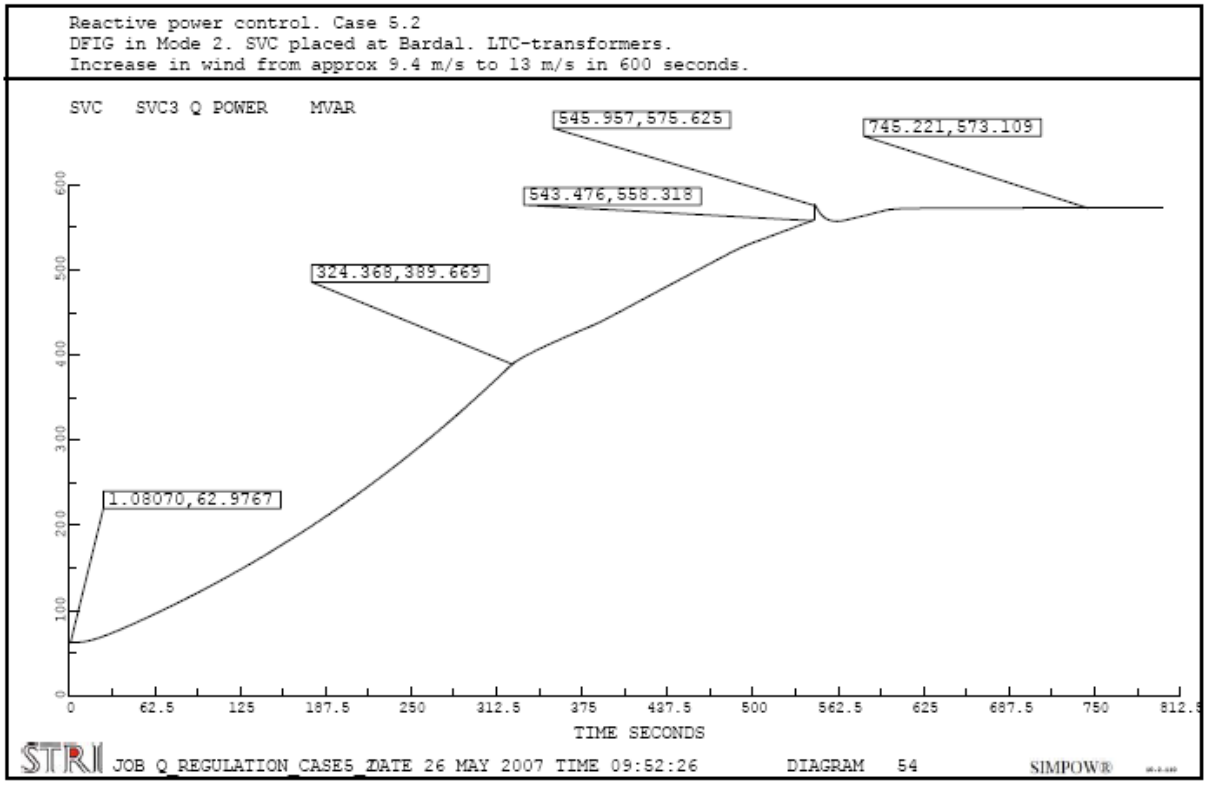

Figure 5.56: Reactive power production from SVC at Bardal, Case 5.2

Compared to Case 3.2, the SVC at Bardal is producing 341.7 MVAR more at full wind power production than in Case 5.2. However, compared to the production in Case 4.2, the tap-operation at Nedre Røssåga results in a decrease in reactive production of 16.7 MVAR when the wind farms operate at full wind power production.

At the time of the tap-operation at Nedre Røssåga the production from the SVC increases. This is because the fast voltage regulator in the SVC tries to minimize the voltage sag. The voltage regulators of the doubly-fed induction generators are slower than the SVC regulator. They will therefore use longer time to adjust their reactive power consumption to the new voltage level caused by the tap-operation. The reactive power regulator, which is the slowest of the three regulators, will eventually adjust the production level of the SVC to maintain a constant reactive power flow through the monitored transmission line. In total, this causes the reactive power production response to the tap-operation at Nedre Røssåga which is described in Figure 5.56.

The reactive power produced by the doubly-fed induction generators and the SVC at Bardal at full wind power production is given in Table 5.29. In addition, the reactive power imported at Nedre Røssåga is given.

Table 5.29: Reactive power production at full wind power production, Case 5.2

Source	Reactive production at full active production [MVAR]
DFIG1	0
DFIG2	0
DFIG3	0
DFIG4	0
SVC3	573.1
Imported at N.Røssåga	7.0
Total	580.1

The reactive power production of the doubly-fed induction generators is set to zero in Table 5.29. This is done to illustrate the total amount of reactive power fed into the radial. As shown by Figure 5.55 the generators are consuming reactive power to keep the voltage at the terminals at 0.69 kV

5.5.3.4 Power flow

The power flow in the transmission line controlled by the reactive power regulator at Bardal is given in Appendix E. It shows that the power flow between the main grid and the wind farms is similar to the power flow in Case 5.1. However, since the steady-state power flow is different in the two cases, there will also be some variation in the two responses. The maximum reactive power drawn from the main grid is 9.2 MVAR. At full wind power production the wind farms are drawing 7.0 MVAR from the main grid. The tap-operation at Nedre Røssåga results in a short-term injection of reactive power into the main grid. The maximum amount of reactive power injected into the main grid is 4.3 MVAR. This is the same as in Case 5.1. The reason for this spike-response is, as explained in Case 5.1, the different time constants for the different regulators.

At full wind power production the reference bus at Tunnsjødal is producing 208.4 MVAR. This is a decrease of 47.5 MVAR compared to Case 3.2.

As in Case 5.1, the tap change of the transformer at Nedre Røssåga results in oscillations in the grid. The response in active and reactive power production for the generator at Svartisen to the tap-operation at Nedre Røssåga is given in Appendix E. The diagram is zoomed in at the time of the tap change.

5.5.3.5 Thermal limits

The current at 100% wind power production is given Table 5.30 for dimensioning transmission lines and power cables within the wind farm radial. It also shows the transmission line outside the radial connection with the highest loading. This line is located between Marka and Øvre Røssåga.

Table 5.30: Line loading, Case 5.2

Line	I_{Limit} [kA]	$I_{100\% \text{ production}}$ [kA]	Loading [%]
Bardal – N.Røssåga	6.176	2.889	46.8
Sjo-Alt1_3 - #304656	1.160	0.953	82.2
Sjonfjell132A – Sjonfjell132B	1.160	1.083	93.4
#304633-3662 - #304366	0.970	0.915	94.3
Sleneset132O - Sleneset132V	0.715	0.477	66.7
#300763 - #300788	0.560	0.524	93.6

The current in the line between Øvre Røssåga and Marka at full wind power production equals 93.6% of the thermal capacity in this line. However, as explained earlier, the loading in this line is not largely affected by the increase in wind production.

The line between Bardal and Nedre Røssåga has a higher loading in Case 5.2 than in Cases 3.2 and 4.2. The loading is higher than in Case 3.2 because the implementation of the reactive power regulator at Bardal results in a larger reactive flow in this line.

Compared to Case 4.2, the loading is higher because the transformer at Nedre Røssåga reduces the voltage in the wind farm radial. This will result in larger reactive losses in the transmission line and in the transformer at Nedre Røssåga. The lines and power cables between Bardal and the wind farms are less loaded in Case 5.2 than in Case 4.2. This is because the reactive consumption of the doubly-fed induction generators decreases when the voltage in the radial is decreased.

In the long power cable between Bardal and Sleneset the loading seems to be reduced compared with Case 3.2, even though the reactive power flow is larger. The other power cables in the radial have a larger loading in Case 5.2 than in Case 3.2. The long power cable generates reactive power because it is loaded below its surge impedance loading. In Case 3.2 the reactive power flow is so low that the cable delivers reactive power at both ends. In Case 5.2 the doubly-fed induction generators are consuming reactive power. As a consequence, reactive power has to be transferred across the power cable because the reactive production in the cable is insufficient. Due to the reactive power production in the cable, the reactive power flow from the cable at the wind farm side will be larger than the reactive power input at the other side. The measured current on the side towards Sleneset will therefore also be higher than on the other side, towards Bardal. The current during full production measured at the wind farm side is 0.955 kA or 98.4 % of thermal capacity. This is a higher loading than in Case 3.2 and it shows that the increased reactive power production in the cable due to the increased voltage in Case 5.2 does not weigh up for the increased reactive consumption from the generators. Measured on either side, this is the part of the radial closest to its thermal capacity.

The difference in current on different sides of the power cables will be largest for the cable discussed in the section above. This is because it is by far longest cable in the radial. The difference in measured current will be largest in simulations where reactive power is transferred across the cable. This is the situation for Cases 4.2 and 5.2.

All of the other power cables and transmission lines between Bardal and the wind farms have a higher loading in Case 5.2 than in Case 3.2. This is due to the increased reactive power flow.

Compared with Case 5.1, the transmission lines and power cables between Bardal and the wind farms are closer to their capacity limit. This is because of the large reactive power flow between the SVC and the doubly-fed induction generators.

5.5.3.6 Voltage variations

The voltages between DFIG1 and the 132 kV side of the connection point at Nedre Røssåga are described in Figure 5.57. It shows that the SVC at Bardal increases the voltage in order to maintain a constant power flow at the 300 kV side of the connection point. At full wind power production, this voltage is at 1.08 pu. The maximum voltage at Bardal is 1.09 pu and occurs just before the tap-operation at Nedre Røssåga.

The voltage response at the 132 kV side of the connection point at Nedre Røssåga is given in Appendix E. The response is similar to the response in Case 5.1. However, the voltage is at a higher level in Case 5.2 due to the decreased steady-state voltage in the radial in Case 5.1.

Figure 5.57 also shows that the voltage at the terminals of DFIG1 is kept constant during the production increase. A consequence of this is that the voltage at the 22 kV level at the wind farm is also kept close to constant.

As in Case 5.1, the voltages at the 132 kV level at the wind farms are reduced when the load tap changer at Nedre Røssåga reduces the voltage on the 132 kV side. This is a result of the reactive power regulator at Bardal which allows the voltage at the SVC terminals to change.

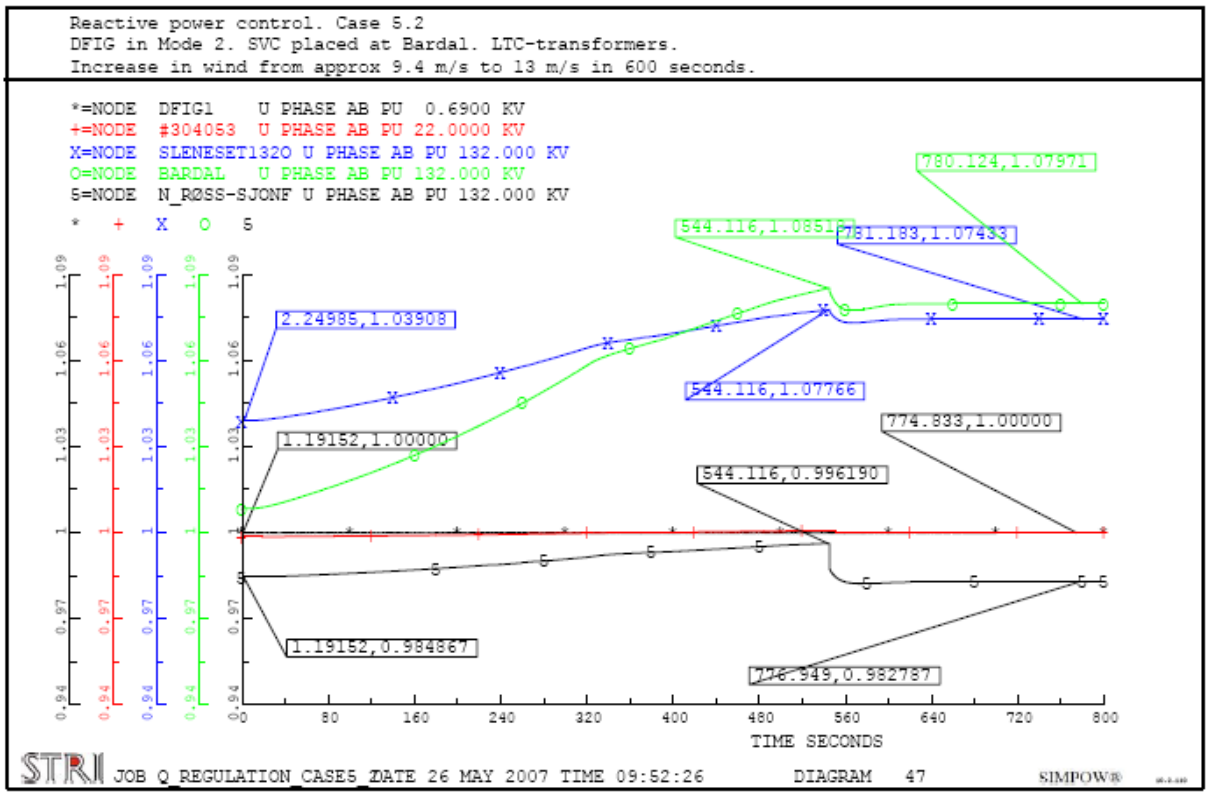

Figure 5.57: Voltages between DFIG1 and connection point at Nedre Røssåga, Case 5.2

The change in voltage for some monitored nodes during the increase in production is given in Table 5.31. It describes the minimum and maximum voltage, the voltage at the end of the

simulation and the largest voltage change compared to the voltage at the start of the simulation.

Table 5.31: Voltage changes, Case 5.2

Node	Voltage level [kV]	Min / Max voltage [pu]	End voltage [pu]	Voltage change [%]
Salten	420	1.00 / 1.00	1.00	0.09
Rana420	420	0.99 / 1.00	0.99	-0.45
Nedre Røssåga	420	0.99 / 1.00	0.99	-0.61
Nedre Røssåga	300	0.99 / 1.00	0.99	-0.68
N_Røss-Sjonf	132	0.98 / 1.00	0.98	1.15
DFIG1	0.69	1.00 / 1.00	1.00	0.00
Sleneset132O	132	1.04 / 1.08	1.07	3.86
Trofors	300	0.99 / 1.00	0.99	-1.22
Majavatn	300	0.99 / 1.00	0.99	-1.08

5.5.3.7 General

The simulations done in Case 5.2 show that the reactive power exchange between the main grid and the wind farms can be controlled by adding a reactive power regulator in the SVC at Bardal. Compared to Case 4.2, it is clear that the slow reactive power regulator copes better with the smaller wind increase rate in Case 5.2. The reactive power flow in the controlled dummy line in Case 5.2 is different from the power flow in Case 5.1. This is due to the difference in the steady-state power flows. This difference is, however, considered to be insignificant in these analyses and the influence on the rest of the grid is approximately the same for these two cases.

The voltage in the radial leading towards the wind farms increases when the wind power production increases. This is because the SVC at Bardal has to increase the terminal voltage in order to maintain a constant reactive power flow at the connection point. The voltage does not increase above 1.1 pu during the given wind increase. The difference from Case 5.1 is that the voltage is reduced by the reactive consumption of the doubly-fed induction generators.

The tap-operation at Nedre Røssåga reduces the voltages in the radial. This gives increased losses, but the total reactive production decreases compared to Case 4.2. This is because the doubly-fed induction generators have to consume less reactive power in order to maintain a terminal voltage of 0.69 kV. The maximum reactive power production of the SVC at Bardal is 573.1 MVAR. Compared to Case 4.2, this is a reduction of 16.7 MVAR.

The voltage changes in the main grid are smaller in Case 5.2 than in both Case 3.2 and Case 4.2. They are smaller than Case 3.2 because of the reduced reactive power drawn from the main grid at Nedre Røssåga. Compared to Case 4.2, the voltage reduction is only slightly smaller. This is because of the larger increase rate of the production in Case 4.2. The larger increase rate results in a larger value for the maximum reactive power drawn from the main grid at Nedre Røssåga. This gives a lower minimum voltage compared to Case 5.2. Compared to Case 5.1, the voltages in the main grid are approximately the same.

As shown in Case 3.2, the introduction of voltage control at the wind farms removes the need for automatic load tap changers in the transformers at the wind farms during the wind increase.

As described in Case 5.1, the introduction of the reactive power regulator at Bardal reduces the number of tap-operations for the transformer at Nedre Røssåga. However, it is likely that the number of tap-operations will increase during a real wind increase.

Responses considered not being important for the discussion is included in Appendix E. The output file from the steady-state power flow calculation along with the OPTPOW and DYNPOW files are also included in this appendix.

5.5.4 Case 5.3 – Increased Terminal Voltage of DFIGs

5.5.4.1 Description

Case 5.3 describes a situation where the terminal voltage at the doubly-fed induction generators has been increased to 1.04 pu or 0.7176 kV. In addition, the dynamic load tap changer regulators in the wind farms have been disabled. Beyond that, the settings are the same as the ones used in Case 5.2.

The steady-state power flow is given in Appendix E.

The values obtained from the dynamic simulations are based on plotted values and might therefore cause some inaccuracies.

5.5.4.2 Tap-operations

The results from Case 5.3 show that the transformer at Nedre Røssåga steps up one time during the given production increase in order to reduce the voltage in the wind farm radial.

5.5.4.3 Power production

The active and reactive power production from DFIG1 is given in Figure 5.58. It shows that the active production increases from 50% to 100% during the given wind increase.

In order to maintain a terminal voltage of 1.04 pu, the generator has to produce 10.6 MVAR at 50% active production. At full production, the generator is consuming 6.2 MVAR.

The three other generators show a similar response in reactive power production during the wind increase. At full active power production, DFIG2 is consuming 6.3 MVAR, DFIG3 28.8 MVAR and DFIG4 17.6 MVAR.

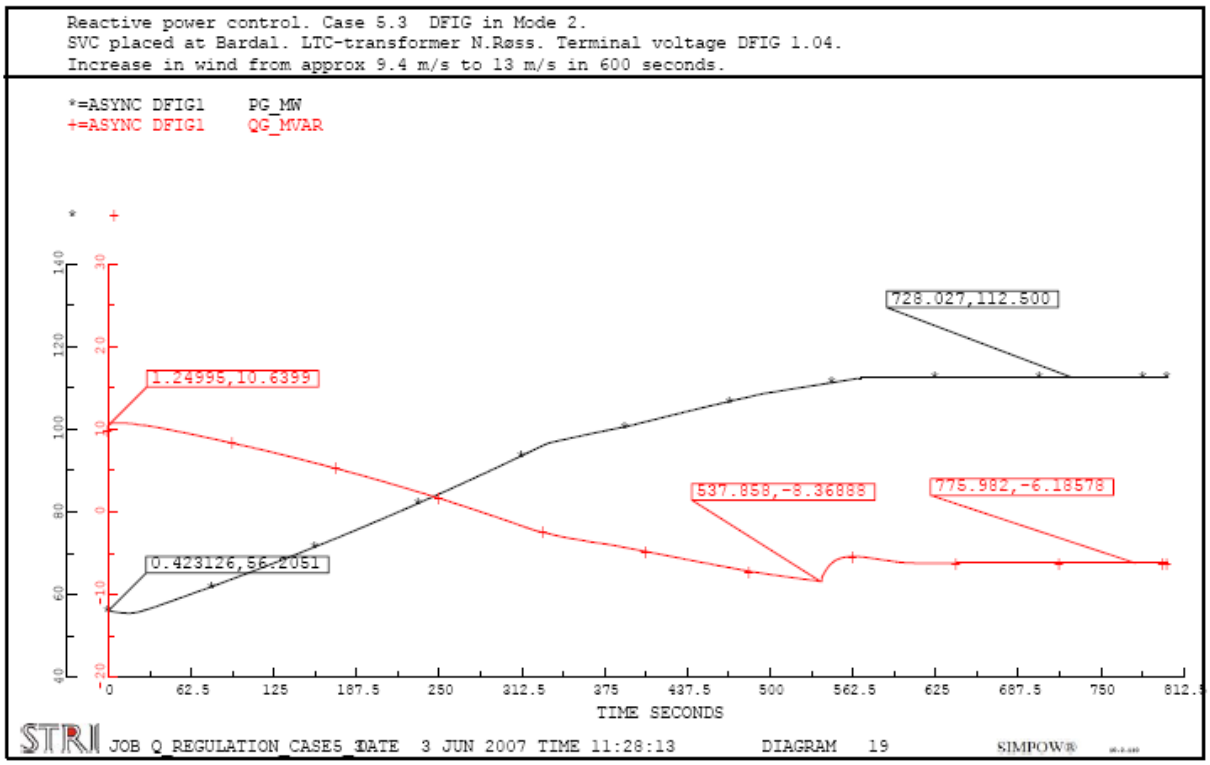

Figure 5.58: Active and reactive power production from DFIG1, Case 5.3

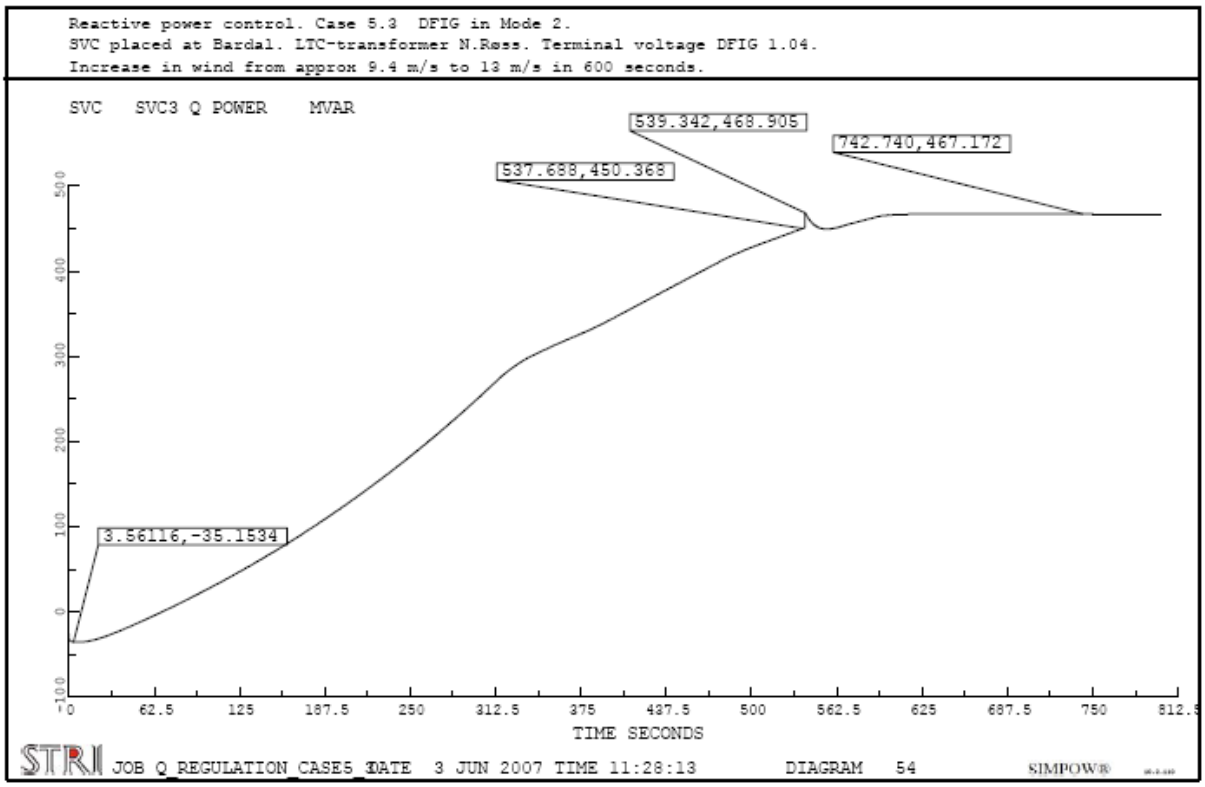

Figure 5.59: Reactive power production from SVC at Bardal, Case 5.3

The reactive power production from the SVC at Bardal is given in Figure 5.59. During full active production the SVC at Bardal has to produce 467.1 MVAR in order to maintain a constant power flow at the connection point at Nedre Røssåga.

The reactive power production from the doubly-fed induction generators and the SVC at Bardal show the same response to the tap-operation at Nedre Røssåga as the response in Case 5.2.

The reactive power produced by the doubly-fed induction generators and the SVC at Bardal at full wind power production is given in Table 5.32. In addition the reactive power imported at Nedre Røssåga is presented.

Table 5.32: Reactive power production at full wind power production, Case 5.3

Source	Reactive production at full active production [MVAR]
DFIG1	0
DFIG2	0
DFIG3	0
DFIG4	0
SVC3	467.2
Imported at N.Røssåga	7.0
Total	474.2

5.5.4.4 Power flow

The power flow in the transmission line monitored by the reactive power regulator is the same as in Case 5.2. The consequence of this is that the production increase has the same impact on the rest of the grid as in Case 5.2.

The power flow in monitored lines during the production increase in 5.3 is given in Appendix E.

5.5.4.5 Thermal limits

Table 5.33 shows the current in dimensioning lines and power cables between Nedre Røssåga and the wind farms at Sleneset and Sjonfjellet during full wind power production. It also shows the line outside the radial connection with the highest loading. This line is located between Marka and Øvre Røssåga.

Table 5.33: Line loading, Case 5.3

Line	I_{Limit} [kA]	$I_{100\% \text{ production}}$ [kA]	Loading [%]
Bardal – N.Røssåga	6.176	2.893	46.8
Sjo-Alt1_3 - #304656	1.160	0.897	77.3
Sjonfjell132A – Sjonfjell132B	1.160	1.025	88.4
#304633-3662 - #304366	0.970	0.911	93.9
Sleneset132O - Sleneset132V	0.715	0.455	63.6
#300763 - #300788	0.560	0.524	93.6

The long power cable between Bardal and Sleneset is the part of the radial leading towards the wind farms which is closest to its thermal capacity limit. It is loaded with 93.9% of its total capacity.

5.5.4.6 Voltage Variations

The voltages between DFIG1 and the 132 kV side of the connection point at Nedre Røssåga are given in Figure 5.60. It shows that the SVC at Bardal increases the voltage in order to maintain a constant reactive power flow at the connection point at Nedre Røssåga. At full wind power production the voltage at the terminals of the SVC is 1.080 pu. The maximum voltage at the terminals is 1.085 pu and occurs right before the tap-operation at Nedre Røssåga. This tap-operation reduces the voltage at all nodes in the radial except at the terminals of the doubly-fed induction generators.

The maximum voltage in the radial is at the 132 kV level at Sleneset. Right before the transformer at Nedre Røssåga taps, the voltage at Sleneset132O is 1.097 pu.

No voltage increases above 1.1 pu for the given production increase.

Compared to Case 5.2, the voltages within the radial connection have increased. This is due to the increase in terminal voltage for the doubly-fed induction generators.

It should be noted that according to Figure 5.60, the voltage at the DFIG terminals is constant at 1.00 pu during the simulation. However, in this case, 1.00 pu equals 0.7176 kV. This is because the base voltage of the DFIG terminals had to be altered in order to get the voltage regulator of the doubly-fed induction generators to control the voltage to a different value than 0.69 kV.

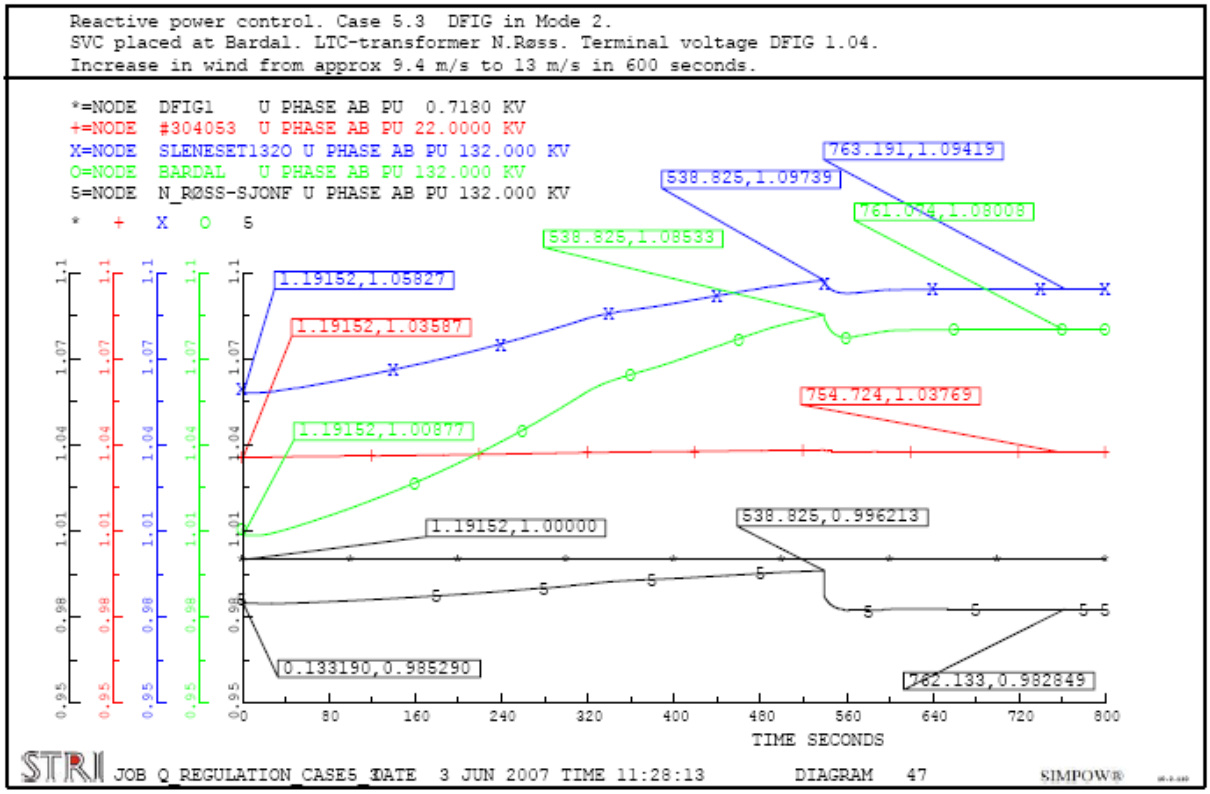

Figure 5.60: Voltages between DFIG1 and connection point at Nedre Røssåga, Case 5.3

The change in voltage for some monitored nodes during the increase in production is given in Table 5.31. It describes the minimum and maximum voltage, the voltage at the end of the simulation and the largest voltage change compared to the voltage at the start of the simulation.

Table 5.34: Voltage changes, Case 5.3

Node	Voltage level [kV]	Min / Max voltage [pu]	End voltage [pu]	Voltage change [%]
Salten	420	1.00 / 1.00	1.00	0.09
Rana420	420	0.99 / 1.00	0.99	-0.47
Nedre Røssåga	420	0.99 / 1.00	0.99	-0.63
Nedre Røssåga	300	0.99 / 1.00	0.99	-0.70
N_Røss-Sjonf	132	0.98 / 1.00	0.98	1.10
DFIG1	0.69	1.04 / 1.04	1.04	0.00
Sleneset132O	132	1.06 / 1.10	1.09	3.91
Trofors	300	0.99 / 1.00	0.99	-1.23
Majavatn	300	0.99 / 1.00	0.99	-1.10

5.5.4.7 General

The simulations done in Case 5.3 show that the reactive power production from the SVC at Bardal can be reduced by increasing the terminal voltage at the doubly-fed induction generators. By increasing the voltage to 1.04 pu, the reactive power production at Bardal at full wind power production is reduced to 467.2 MVAR. Compared with the results obtained in Case 5.2, this is a reduction of 105.9 MVAR. However, the doubly-fed induction generators now have to produce reactive power during 50% in order to maintain the terminal voltage.

The increased terminal voltage results in increased voltage levels throughout the radial connection. Simulations done without load tap changers show that with a terminal voltage of 1.04 pu, the voltage at the 132 kV level at Sleneset reaches a voltage of 1.10 pu at full wind power production. This is shown in Appendix E.

Compared to Case 5.2, the lines between Bardal and the wind farms less loaded in Case 5.3. This is because the reactive power flow between the SVC at Bardal and the doubly-fed induction generators is reduced.

The loading of the line between Bardal and Nedre Røssåga and Marka and Øvre Røssåga is approximately the same as the loading in Case 5.1 and 5.2.

As seen from the rest of the grid, the increase in terminal voltage in Case 5.3 has no significant effects on the voltages or the power flows.

6 Discussion

6.1 Introduction

A summary of the results obtained from the simulations and a general discussion regarding these is given in this chapter. The most important results are presented in Table 6.1.

The value of the production level specified in Table 6.1 is the actual production level at both wind farms at the instant in the simulations when a limit was reached. The production level indicates total production at both wind farms at that particular moment in time, even though the limitation might be connected to only one of the wind farms.

The total reactive power production describes the reactive power produced by the doubly-fed induction generators, the SVC at Bardal and the amount of reactive power imported at Nedre Røssåga. Except for Case 1.1, the values are obtained after the system has stabilized at full production. This means that the thermal and voltage limits are neglected in the reading of these values. In Case 1.1, the values are measured at the instant the first generator is disconnected due to unacceptable low terminal voltage.

In cases 4.2, 5.2 and 5.3 the doubly-fed induction generators are consuming reactive power. The values are, however, not included in the reactive power production column in Table 6.1. If these values were to be added, total reactive power production would be reduced, something which would improve these cases compared with the result of other cases.

Table 6.1: Summary simulation results

Case	Production level [%](1)	Limitation	Total reactive power production [MVAR](2)	Largest voltage change in main grid [%](3)
1.1	63.8	CRC-limit(4)	192.0	-1.57
1.2	100.0	-	450.5	-1.84
2.1	93.5	Thermal capacity limit power cable	530.7	-2.83
2.2	100.0	-	446.2	-1.87
3.1	100.0	-	428.1	-2.27
3.2	100.0	-	426.7	-2.25
4.1	93.5	Terminal voltage above 1.05 pu	416.1	-1.32
4.2	100.0	-	597.0(5)	-1.26
5.1	100.0	-	443.9	-1.23
5.2	100.0	-	580.1(5)	-1.22
5.3	100.0	-	474.2(5)	-1.23

(1) Referred to maximum capacity.
(2) Sum of reactive power production from DFIGs, SVC at Bardal and import at Nedre Røssåga.
(3) Referred to the initial voltage value.
(4) CRC-limit is the specified voltage limit at which the frequency converter of the DFIGs is disconnected.
(5) DFIGs are consuming reactive power.

6.2 No SVC at Bardal

The simulations done in Case 1.1 and Case 2.1 show the need for additional reactive power compensation in addition to compensation in the wind farms. Without extra reactive power production in the radial between Nedre Røssåga and the wind farms, it is not possible to reach full wind power production without reaching any of the specified limits.

In Case 1.1, the wind turbines are fully compensated. However, the voltages at the terminals of the doubly-fed induction generators still become unacceptable low during a production increase. The limit is set to 0.90 pu. If the limit were set to 0.95 pu, the maximum production would be even lower.

Whether or not the voltage at the generator terminals should be allowed to deviate more than ±5% of the rated voltage will depend on the characteristics of the chosen generator. Normally, a deviation of ±10% is allowed in a power system, however, from an electric machine perspective an operating situation with a deviation in voltage of more than ±5% is considered to be unacceptable for the machine. [25] In some cases, it would be preferable to allow a temporary voltage deviation between ±5-10%. This could for instance be the case while waiting for a transformer equipped with a load tap changer to regulate, as this would reduce the need for fast reactive power control. Such a situation is illustrated by the results from Case 4.1.

Considering the voltage changes observed at the generator terminals during simulations with the generators in *power factor control* and the observed consequences of a disconnection of the frequency converters. In this case it seems natural to set the voltage limits for the crow-bar control regulator respectively to 0.9 and 1.1 pu. According to [17], the doubly-fed induction generator equipped with crow-bar resistors is typically disconnected from the grid when the voltage falls below 0.7-0.8 pu. This indicates that the settings used in this project are conservative. However, no fault-ride through capability analyses are performed on the DFIGs in the present grid model and a operational situation with a terminal voltage below 0.9 pu is not accepted, regardless of the crow-bar control setting. The maximum production level obtained in Case 1.1 can therefore be considered as valid for the grid configuration in question.

In Case 2.1, where *voltage control* is introduced at the wind farms, the limit to the increase in production level is the thermal capacity of the long power cable between Bardal and Sleneset. A higher production level could be reached if the existing power cable was replaced by a cable with a higher thermal capacity. However, with this configuration, the amount of reactive power production from the doubly-fed induction generators and the amount of reactive power production imported from the main grid is considerable. At full wind power production DFIG3 is producing reactive power at a power factor of 0.90 and 283.8 MVAR is imported from the main grid at Nedre Røssåga. This would be the largest amount of import in all cases investigated. If it is not possible for the chosen generator to produce reactive power to such an amount that it operates at a power factor as low as 0.90, additional compensating devices could be added at the wind farms.

The large import of reactive power results in a large voltage drop in the grid. During the production increase in Case 2.1, the voltage at the 300 kV level at Nedre Røssåga decreases with 2.83%. The voltage at the 132 kV side of the connection point at Nedre Røssåga falls below 0.9 pu. This would also be unacceptable.

6.3 SVC in Voltage Control Mode

In cases 1.2 and 2.2, reactive power compensation is added at Bardal. Bardal was considered to be a good location for the compensation, since it is the meeting point for the radial connections that are leading towards the wind farms. Cases where the doubly-fed induction generators are set to control the terminal voltage to a specified value can in many ways be regarded as equivalent to other forms of fast reactive power compensation at the wind farms. It was therefore decided unnecessary to place additional compensation there. Similarly regarding the question whether compensation should be placed at the connection point at Nedre Røssåga. Because there already were two SVCs connected to the main grid at Nedre Røssåga and since the production in cases 1.1 and 2.1 were not able to reach 100%, it was considered to be inadequate to add further reactive compensation there.

When reactive power compensation is introduced at Bardal, the wind farms are able to reach full production without reaching any of the specified voltage or thermal limits. In this project, the compensation is in the form of a SVC. However, it could be replaced by for instance switched shunt capacitors with small steps. Whether or not this would be acceptable would depend on the tolerance for voltage variations in the radial, the demand for reactive power flow control in the connection point and the possible settings of the shunt capacitors. The voltage will most likely fluctuate more with shunt capacitors than with a SVC. [5]

It is important to note that there is no local load connected to the radial connection that leads towards the wind farms. The tolerance for voltage variations in the 132 kV grid can therefore be expected to be larger in this radial than in the rest of the grid. This is especially the case if voltage control is introduced at the wind farms so that the voltage there is not allowed to vary beyond specified limits.

With an SVC at Bardal there are much smaller differences between when the generators operate in power factor control and when they operate in voltage control. The SVC at Bardal helps to maintain the voltages at an acceptable level in the radial. The main difference in the results from the two operating modes of the DFIGs is that the voltages are kept more constant at the wind farms with the DFIGs in voltage control. The capacity of the SVC at Bardal can also be reduced due to the reactive power production in the wind farms. The reactive power production from the DFIGs in voltage control results in reduced reactive power flow. As a consequence, the loading of transmission lines and power cables are reduced.

As seen from the grid, the two cases are approximately identical. Due to the reactive power production in the wind farms, the voltage level at Bardal is slightly reduced when DFIGs are in voltage control. This reduction results in a slightly larger reactive power import at Nedre Røssåga and a slightly larger voltage reduction in the main grid.

In cases 3.1 and 3.2 transformers with load tap changers are introduced in the dynamic simulation. LTC-transformers might have improved the situation in both Case 1.1 and Case 2.1 by performing tap-operations. The voltage at the DFIG terminals could have been increased by tap-operations at both Nedre Røssåga and at the wind farms in Case 1.1, and the voltage at the connection point at Nedre Røssåga could have been increased by tap-operations in Case 2.1. The latter would have decreased the reactive power production of the DFIGs and reduced the power flow and loading in the power cables. However, since the situation in both cases was quite far beyond the specified limits and since the grid configurations would not be able to handle rapid wind changes, they were considered to be unacceptable, also in a

situation with load tap changers. The configuration with an SVC at Bardal was therefore used in the simulations with load tap changers (cases 3.x and 5.x).

In Case 3.1, the doubly-fed induction generators are in *power factor control mode*. In order to maintain an acceptable voltage profile during the production increase, both the transformers at the wind farms and the transformer at the connection point at Nedre Røssåga increases the voltage on their low-voltage sides. This results in an increase in imported reactive power at Nedre Røssåga and a decrease in reactive power production from the SVC at Bardal. The load tap changers connected to the wind farms are therefore increasing the negative impact on the main grid compared to a situation without load tap changers. Case 3.1 is the case among the acceptable cases in this project that has the largest voltage reduction in the main grid when wind power production is between 50% and 100% wind power production.

With *voltage control* at the wind farms transformers with load tap changers at the wind farms is redundant. This is the case at least for the production increase simulated in cases 3.2, 4.2, 5.2 and 5.3. However, in situations where the reactive power capacity of the voltage control unit at the wind farms becomes a limiting factor, LTC-transformers can be used to limit the demand for reactive power production at the wind farms. This is not investigated further in this project.

The simulations in Case 3.2 show that the impacts on the main grid are approximately the same when the doubly-fed induction generators are in voltage control as when they are in power factor control. Also in the former case, the transformer at Nedre Røssåga has to perform tap-operations in order to increase the voltage at the 132 kV level. The voltage reduction and the amount of reactive power drawn from the main grid are more or less identical to what could be observed in Case 3.1. The results are approximately the same because the difference in conditions at the wind farms that can be observed between Case 3.2 and Case 3.1 is compensated by the fast voltage regulator in the SVC at Bardal. As long as the SVC at Bardal is within its capacity limits, a disturbance like a tap-operation at the connection point will not largely affect the conditions on the wind farm side of the SVC.

The tap-operations at Nedre Røssåga result in oscillations in voltages and reactive power flows throughout the grid. A tap-operation is equivalent to a sudden change in reactive load for the generators in the grid. They therefore have to adjust their excitation to adapt to the new loading. Since the hydro power generators are modelled as physical generators, a sudden step in excitation is not possible. Oscillations are therefore created as the generators adapts to the new situation. The results from the simulations in Case 3.1 indicate that the tap-operations at Nedre Røssåga causes oscillations with a frequency of 0.6 and a maximum peak-to-peak value of 1 MW and 0.3 MVAR at the generator at Svartisen.

The frequency, size and damping of the oscillations will depend on the disturbance, the grid configuration and the parameters of the generators in the grid. Since standardized parameters have been used for the hydro power generators in the model, the oscillations will most likely be different compared with the oscillations in the real power grid. Oscillations have therefore not been studied further in detail in this project.

Oscillations in reactive power also cause oscillations in active power. This is because the active power of a bus load is altered when the inserted reactive power and hence the bus voltage is altered. [6]

The results from the simulations show that the oscillations after one tap change can last up to 40 seconds. It is likely that the damping could be increased by introducing power system stabilizers (PSS) to the voltage regulators of the hydro power generators. Due to time limitations and since in the simulations, the system stabilizes before the next incident occurs in the grid, it was chosen to not include PSS in this project. This should not have an impact on the final steady-state values as long as the system is stable. Designing and applying PSS is not simple and often requires individual settings for the different regulators. What is more, a badly designed PSS could be the source of undesired oscillations. [9]

6.4 SVC in Reactive Power Control Mode

The simulation results from Case 4.1 show that when a secondary regulator is introduced in the SVC at Bardal, the amount of reactive power drawn from the grid at the connection point can be significantly reduced. This again reduces the voltage depression in the grid. This can be seen from Table 6.1. However, since the SVC at Bardal then has to compensate for the entire reactive power consumption in the radial, the reactive production from the SVC increases. This again increases the voltage levels in the radial. During the rapid wind increase in Case 4.1 the load tap changers are not included, and the voltages at the terminals of the generators increase above 1.05 pu. If an increase of above +5% of rated voltage at the generator terminals is not accepted, the production level will only reach 93.5%. It should also be noted that the voltage at the 132 kV level in the wind farms approaches 1.1 pu when the production approaches 100%. This occurs even if the voltages in the steady-state power flow have been reduced compared to the previous cases.

The results from the simulations done with a slower increase in wind speeds and when LTC-transformers are included, show that during the wind increase, the load tap changers at the wind farms manage to maintain a voltage at the terminals of the doubly-fed induction generators well within ±5% of the rated value.

The tap-operation at Nedre Røssåga results in a decrease in voltage in the radial and an increase in reactive power production from the SVC at Bardal. If the voltage in the radial had increased above 1.1 pu, it would have been necessary to try to reduce the voltage in the radial. However, when the voltage conditions are acceptable during a simulation without load tap changers, a relevant question will be if there is a need for the automatic load tap changer at Nedre Røssåga. Especially in configurations were there are no local loads connected to the radial. The load tap changer reduces the voltage and thereby increases the reactive power production from the SVC. This results in a larger need for reactive compensation than in a case without a load tap changer at the connection point. A possible solution to this can be to adjust the dead band in the load tap changer in the connection point to only perform tap-operations if the voltage is about to increase above 1.1 pu. This is not pursued any further in this project.

With the doubly-fed induction generators in *voltage control*, the voltages in the radial leading towards the wind farms are kept within specified limits in situations with a rapid wind increase. This is because the generators are consuming reactive power in order to maintain the predefined terminal voltage. The consumption of reactive power from the generators results in a large reactive power production from the SVC at Bardal. At full wind power production the SVC is producing 589.8 MVAR. This is the largest reactive production in all the cases observed in this project. As seen from the grid, the differences between when the doubly-fed induction generators are in voltage or in power factor control are insignificant.

In Case 5.2 and Case 5.3 a dynamic load tap changer regulator is only included at Nedre Røssåga. As in Case 5.1, the load tap changer will perform a tap-operation in order to decrease the voltage in the radial. However, as opposed to Case 5.1, the tap-operation leads to a reduction in the reactive power production of the SVC at Bardal. This is because the voltage reduction results in a decrease in reactive power consumption at the wind farms.

In Case 5.3 simulations are performed with increased terminal voltages at the doubly-fed induction generators. This is done in order to illustrate that the need for reactive power production from the SVC at Bardal decreases when the terminal voltages in the wind farms increases. By increasing the voltage level at the generator terminals from 1.00 to 1.04 pu, the production of the SVC at Bardal decreases from 573.1 MVAR to 467.2 MVAR. It is, however, important to note that this increases the voltage level in the 132 kV grid in the radial when the wind farms are at full production. This will also increase the amount of reactive power production from the DFIGs when the wind speeds are low. A simulation describing the conditions during decreasing wind speeds is given in Case 5.4 in Appendix E.

It is possible that the reactive power production from the SVC at Bardal could be further reduced when the DFIGs are in voltage control. This could be done by using the steady-state power flow used in cases 4.1 and 5.1. This is not investigated further because of numerical difficulties in SIMPOW when the DFIGs were in voltage control and the radial voltage was lowered. This was not resolved within the time-frame of this project.

The reactive power regulator is a relatively slow generator. This can be seen from the observed difference in controlled reactive power flow at the connection point between cases with a fast wind increase and cases with a slower wind increase. The regulator is able to hold the reactive power flow more constant when the wind is increased during a longer period of time. In Appendix E, with the time plots from Case 5.2, a curve describing the power flow at the connection point when the speed of the reactive power regulator is increased is included. The curve shows that the reactive power flow is kept more constant when the speed of the regulator is increased. In such a situation the regulator also decreases the amplitude of the spike caused by the tap-operation at Nedre Røssåga. However, the initial and end conditions are the same as in the case with the slow regulator.

What the settings for this regulator should be will depend on the demand for control of reactive power exchange at the connection point. No time-frame for the measuring of the power factor at the connection point is specified in [16]. If the regulator is fast it will be able to compensate for fluctuations in reactive power with higher frequency. However, this will also cause more and faster fluctuations in voltage in the radial connection. If local loads are connected to the radial leading towards the wind farms, reduced voltage quality can be expected with this solution. In this project no local loads are connected to the radial. As a consequence, the tolerance for voltage fluctuations can be expected to be larger than in configurations with local load.

6.5 General Observations

In some of the cases oscillations can be observed at the start of the simulations. This is due to a mismatch between the specified power output in OPTPOW and the power output based on the calculated mechanical torque, which again is based on the calculated wind speed in DYNPOW. This will create oscillations until the system has stabilized. However, these oscillations are considered to be small and insignificant for the end results. [38]

The wind in this project is increased linearly by the use of tables. Such a situation is, however, unlikely to occur in reality. In reality, the wind will fluctuate more during a wind increase. This will again create more fluctuations in power flows and voltages and might also result in more tap-operations from the load tap changers. However, the increase used in this project is considered to be sufficient to illustrate the end values and also to illustrate principal differences between regulating methods.

The simulations done in Case 4.1 and Case 5.1 show that by reducing the voltage in the radial in the steady-state simulation, the voltage conditions are kept within specified limits during the given wind increase. This indicates that the grid within the radial is sensitive for voltage changes. This is important to note from an operational point of view.

The needed maximum reactive power capacity of the SVC at Bardal might be considered to be too high from an economical point of view in some of the cases. A possible way to reduce the size of the SVC is to buy reactive power compensation from a reactive power source located outside the radial and thereby allow a larger import in reactive power. That this will reduce the needed maximum size of the SVC, can be seen by comparing the reactive power production and import in Cases 3.1 and 3.2 with Cases 5.1, 5.2 and 5.3. However, whether or not this is an economically profitable solution is not pursued in this project.

Compared with the guidelines for grid connection of wind farms presented in chapter 3.4 and [16], the simulations show that it is possible to implement two different control strategies for reactive power compensation without major changes in the configuration. However, if reactive power flow is controlled, this requires significantly more reactive power capacity and the voltage levels within the radial increases.

Traditional fault analyses are not performed in this project. However, based on the results from the simulations performed in Case 1.1 and in Appendix A, it can be expected that the doubly-fed induction generator used in this project will not be able to stay connected during the voltage dips illustrated in chapter 3.4.3. This is supported by [17].

In chapter 3.5 it is concluded that voltage control should be used for as many grid supporting machines as possible. A relevant question on whether voltage or reactive power flow control is preferable for the SVC at Bardal is if the SVC should be able to support the grid with reactive power. This discussion is not pursued any further in this project.

For all of the cases, the simulations show that the largest decrease in voltage in the main grid is located in the area between Nedre Røssåga and Trofors. This is due to the reactive power drawn by the wind farm radial and due to the transmission losses in the main grid. The voltage at Tunnsjødal is kept constant by the reference bus. The voltage at Salten is less affected since the power flow mainly is increased between Nedre Røssåga and Tunnsjødal.

7 Conclusions and Recommendations for Further Work

7.1 Conclusions

Analyses are performed on a dynamic model which describes the power system between Tunnsjødal and Salten. This has been done in order to illustrate the impacts from wind power production under different control alternatives.

The model includes the wind farms at Sleneset (225 MW) and Sjonfjellet (428 MW).

The basis for the dynamic model is a steady-state model developed by NORSEC, describing grid connection of the wind farms to Nedre Røssåga. The time is set to January 2009.

This model is converted to SIMPOW in order to perform dynamic analyses. The comparison between the two models shows differences in reactive power flows. However, these differences are considered to be acceptable considering the size of the model and the changes that have been made.

The wind farms are modelled as aggregated doubly-fed induction generators. Simulations are performed with the wind farms in both power factor control and voltage control.

The simulations performed in this project indicates that reactive power compensation is needed between the wind farms and the connection point at Nedre Røssåga in order to reach full wind power production in both wind farms. By adding a static VAR compensator at Bardal, the wind farms are able to reach full wind power production within specified system limits in all of the presented simulation scenarios, except one.

The simulations show that an increase in wind power production results in a decrease in voltage levels throughout the grid. This decrease is largest when the SVC at Bardal operates in voltage control and dynamic load tap changers are introduced for the transformers in the radial connection towards the wind farms. With the doubly-fed induction generators in power factor control the largest decrease in voltage in the main grid is 2.27%. This is during a wind production increase from 50% to 100%. The decrease in voltage is due to an increase in reactive losses because of the raise in power flow.

When the SVC at Bardal is in *voltage control*, simulations show that the tap-operations from load tap changers in the radial improve the voltage conditions and reduce the need for reactive power compensation within the radial. However, they also increase the amount of reactive power imported from the main grid, and thereby augment the negative impact from the wind farms on the rest of the power system.

By introducing a *secondary reactive power flow regulator* to the SVC at Bardal, simulations indicate that the reactive power flow between the wind farms and the main grid can be controlled. As seen from the main grid during normal operating conditions, the reactive power regulator reduces the impact from the wind farms and the radial connection on the rest of the grid. However, simulations demonstrate that voltage levels are still reduced due to increased power flow between Nedre Røssåga and Tunnsjødal.

Simulations illustrate that the voltage levels within the radial connection towards the wind farms will increase with increasing wind power production when a reactive power flow regulator is included at Bardal.

When the doubly-fed induction generators operate in *voltage control*, the voltages within the radial stays within acceptable limits. However, the reactive production from the SVC at Bardal is considerable. Simulations indicate that the needed reactive power production can be reduced by increasing the terminal voltages of the wind farm generators. By increasing the terminal voltage from 1.00 pu to 1.04 pu the needed reactive production of the SVC at Bardal is reduced with 105.9 MVAR.

When the doubly-fed induction generators operate in *power factor control* and the SVC operates in reactive power control, simulations show that the voltages within the radial need to be reduced. The reduction is necessary in order to maintain acceptable voltages during full wind power production. This issue is in this project resolved by reducing the terminal voltage of the SVC at Bardal and the desired voltage of the regulating transformer at Nedre Røssåga in the steady-state model.

Results from the simulations carried out in this project indicate that the number of tap-operations from the load tap changer at the connection point is reduced when a reactive power flow regulator is included in the SVC at Bardal. However, since a linear wind increase is included in the simulations, it can be expected that in a real-life scenario the number of tap-operations will be increased in reality. This increase can be expected to take place both with and without a reactive power flow regulator.

The results from the simulations imply that with the doubly-fed induction generators in *power factor control* and the SVC at Bardal in reactive power control, load tap changers at the connection point increase the needed reactive power capacity within the radial. When the voltages are within specified limits without tap-operations, the need for tap changers in the connection point should be evaluated. Load tap changers are, however, necessary at the wind farms in order to maintain a terminal voltage below 1.05 pu during a production increase.

When *voltage control* is introduced at the wind farms and reactive power control at the SVC, simulations indicate that tap-operations from the LTC-transformer decrease the needed reactive power capacity within the radial. This is due to a reduction in reactive power consumption in the wind farms.

The simulations demonstrate that the largest decrease in voltage in the main grid is located in the area between Nedre Røssåga and Trofors. This applies for all the simulations performed in this project.

Simulations carried out on a small test grid indicate that the dynamic TREGLTCUAC-regulator for load tap changers included in SIMPOW is not suitable for dynamic load tap changer simulations conducted on large models. This is because it is necessary to manually alter parameters between the steady-state simulation and the dynamic simulation.

Test simulations performed to evaluate the crow-bar control function of the doubly-fed induction generator model in SIMPOW indicate that the fault ride-through capability of the DFIGs in this model is limited.

7.2 Recommendations for Further Work

Due to problems encountered during the set-up of the steady-state and dynamic models, some of the initial goals and expectations for this project were not reached or could not be investigated further within the given time-frame of this project. What is more, during the course of the project, interesting topics beyond the scope of the initial project have arisen. A section describing recommendations for possible further work is therefore included below.

The suggestions listed below are suggestions which do not demand large changes in the dynamic model.

The steady-state model used as a basis for the simulations in this project is based on a heavy load situation. In order to observe the impacts from the wind farms in question during periods with lower loading, a light load steady-state model should be established.

Simulations examining the system's response to disturbances are not performed in this project. This would, however, be a natural part of a continuation of this project. Such simulations should include scenarios where the response of the wind farms are investigated during faults elsewhere in the model. An important assignment would be to map what kind of disturbances that will cause voltage variations at the wind farm connection point at which the wind farms should be able to ride through.

During such analyses it could be interesting to investigate how different generator solutions respond differently to disturbances. This could be useful in the process of choosing generator solutions for the wind power production.

Additional disturbances which could be interesting to examine are the system's response to a sudden loss of wind power production or the system's response to a sudden loss of reactive power compensation.

Ideally, real wind speed models obtained from statistical wind data from the planned sites should also be included in future analyses. During such analyses it would be natural to monitor how the load tap changers behave during a realistic wind increase. It would also be useful to map which oscillations in voltage and active and reactive power flow that can be expected from a realistic wind scenario. This should be investigated during different control scenarios at the wind farms and at the SVC at Bardal.

References

[1] Nordel, *The Transmission Grid in the Nordic Countries*, revision date: 01-04-2006, www.nordel.org

[2] L. Davik, *Nettilknytning av vindkraftparkene Sjonfjell og Sleneset*. (Preliminary report, KSP 18-2006, Norsk Systemplan og Enøk AS – NORSEC, Oct. 2006)

[3] S. S. Helland (Project manager NNV), *Konsesjonssøknad med konsekvensutredninger for Sleneset Vindkraftverk og tilhørende nettilknytning i kommunene Lurøy og Rødøy*, (Nord-Norsk Vindkraft AS, Nov 2005), www.nve.no

[4] S. S. Helland (Project manager NNV), *Melding om planlegging av Sjonfjellet Vindkraftverk og tilhørende nettilknytning i kommunene Nesna og Rana*, (Nord-Norsk Vindkraft AS, Jul 2006)

[5] T. B. Solvang, *Large-scale wind power integration in Troms*. (Norwegian University of Science and Technology, Faculty of Information Technology, Mathematics and Electrical Engineering, Department of Electrical Engineering, Des. 2006)

[6] O. I. Elgerd, *Electric Energy Systems Theory*, McGraw-Hill Inc., 1982

[7] M. Larsson, "Coordinated Tap Changer Control – Theory and Practice", (Doctoral dissertation, Lund Institute of Technology, 1997)

[8] P. Kundur, *Power System Stability and Control,* McGraw-Hill Inc., 1994

[9] J. Machowski, J. W. Bialek, J. R. Bumby, *Power System Dynamics and Stability*, John Wiley & Sons Ltd, 1997

[10] S. Persson, T. Thorsen, *Spenningsregulering av krafttransformatorer*, (P.M. nr. 20-1989, Samkjøringen av kraftverkene i Norge, May 1989)

[11] J. J. Grainger, W.D. Stevenson, *Power system analysis*, McGraw-Hill Inc., 2006

[12] OPTPOW Power Flow Analysis User Manual, SIMPOW® Power System Simulation Software, revision date: 05-04-29, STRI AB 2004, www.stri.se/simpow

[13] A. Petterson, "Analysis Modelling and Control of Doubly-Fed Induction Generators for Wind turbines", (Doctoral dissertation, Chalmers University of Technology, 2005)

[14] S. Seman, J. Niiranen, S. Kanerva, A. Arkkio, J. Saitz, "Performance Study of a Doubly-Fed Wind-Power Induction Generator Under Network Disturbances", IEEE Transactions on Energy Conversion, Vol. 21, Issue 4, Dec. 2006, Pages: 883-890

[15] J. Eek, K. Uhlen, T. Gjengedal, "Transient Stability Studies Comparing Synchronous and Doubly-fed Induction Generators", Paper presented at CIGRE Symposium: Power Systems with Dispersed Generation, Athens 2005

[16] I.H. Vognhild (editor), *Veiledende systemkrav til anlegg tilknyttet regional og sentralnettet i Norge*, (Statnett SF, revision date: 16.12.2005), www.statnett.no/

[17] C. Zahn, C. D. Baker, "Fault Ride-through Capability Investigation of a Doubly-fed Induction Generator with an Additional Series-connected Voltage Source Converter", The 8th. IEE International Conference on AC and DC Power Transmission, ACDC 2006, Mar. 2006, Pages: 79 - 84

[18] J. Morren, S. W. H. de Haan, "Ridethrough of Wind Turbines with Doubly-Fed Induction Generator During a Voltage Dip", IEEE Transactions on Energy Conversion, Vol. 20, Issue 2, Jun. 2005, Pages: 435-44

[19] SIMPOW® Power System Simulations Software User Manual (Beta release), revision date: 06-09-29, STRI AB 2004, www.stri.se/simpow

[20] J.D. Hurley, L.N. Bize, C.R. Mummert, "The Adverse Effects of Excitation System VAR and Power Factor Controllers", IEEE Transactions on Energy Conversion, Vol. 14, Issue 4, Dec. 1999, Pages: 1636-1645

[21] C. W. Taylor, "Line Drop Compensation, High Side Voltage Control, Secondary Voltage Control – Why Not Control a Generator like a Static VAR Compensator?", IEEE Power Engineering Society Summer Meeting, Vol. 1, Jul. 2000, Pages: 307-310

[22] U. Kolstad (Project manager), *Vindkraft i Nord-Norge, konsekvenser for sentralnettet*, (UA-notat 04-53, Statnett SF, Dec. 2004), www.statnett.no

[23] DYNPOW Dynamic Simulation User Manual, SIMPOW® Power System Simulation Software, revision date: 05-04-29, STRI AB 2004, www.stri.se/simpow

[24] T. Toftevaag, Personal Communication, Mar. 28, 2006

[25] J. O. G. Tande, *Retningslinjer for nettilkobling av vindkraftverk*, (SINTEF Energiforskning AS, TR A5329, EBL-K 17-2001, Mar 2001), www.nve.no

[26] IEC 60034-1, Ed. 11.0, *Rotating Electrical Machines – Part 1: Rating and performance*, Apr. 2004

[27] P. Rosas, "Dynamic Influences of Wind Power on the Power System", (Doctoral dissertation, Technical University of Denmark, Mar. 2003)

[28] P. M. Anderson, A. A. Fouad , *Power System Control and Stability*, IEEE Press, 1997

[29] L. Lindquist (lars.lindquist@stri.se), May 10. 2007, RE: DFIG:ustabilitet i spenning ved simulering i voltage-control, E-Mail to T. Toftevaag (trond.toftevaag@sintef.no)

[30] T. Toftevaag (trond.toftevaag@sintef.no), Apr. 24. 2007, *Modell for spennings-regulator*, Email to T. B. Solvang (tarjeibe@stud.ntnu.no)

[31] B. Franken (bengt.franken@stri.se), May 21. 2007, Fwd: *DFIG: testnet som gir uforklarlig problem*, E-Mail to T. Toftevaag (trond.toftevaag@sintef.no)

[32] M. Þ. Pálsson, *QREG – Sekundærregulator for SVC – Settpunktsregulering*, (Preliminary report, SINTEF Energiforskning AS, Archive code: 020801936902080110222O, Jan. 2002)

[33] A. Palesjö, *Tap Changer Control*, (ABB Power Systems, TRH, May 12. 2000)

[34] B. Franken (bengt.franken@stri.se), May 11. 2007, FW: *[Fwd: RE: DFIG: ustabilitet i spenning ved simulering i voltage-control mode]*, E-Mail to T. Toftevaag (trond.toftevaag@sintef.no)

[35] J.F. Manwell, J.G. McGowan, A.L. Rogers, *Wind Energy Explained*, John Wiley & Sons Ltd., 2002

[36] R. Datta, V. T. Ranganathan, "Variable-Speed Wind Power Generation Using Doubly-Fed Wound Rotor Induction Machine - A Comparison with Alternative Schemes," IEEE Transactions on Energy Conversion, Vol. 17, Sep. 2002 Issue 3, Pages: 414–421

[37] J. Eek, K. Uhlen, *TET 15 Vindkraft i det Norske Energisystemet*, Lecture hand-outs, Sep 8. 2006, NTNU

[38] B. Franken (bengt.franken@stri.se), May 21. 2007, *[Fwd: DFIG - sprang i produksjon mellom optpow og dynpow]*, E-Mail to T. Toftevaag (trond.toftevaag@sintef.no)

Appendix index

Appendix A

Test of Crow-Bar Control Regulator

Description

The doubly-fed induction generator is, as described in chapter 3.3, equipped with a crow-bar control system. This system should disconnect the power electronic equipment in the generator if large changes in voltage were to occur.

In order to illustrate how the DFIG model in SIMPOW behaves during disturbances which causes the crow-bar control system to act, some simulations are done on a small test grid.

The test grid is shown in Figure A 1. It includes one reference bus, one DFIG, one load and two transmission lines. The DFIG is located at 0.69 kV and the load is connected at 22 kV.

The input values of the different grid components are considered to be of minor importance. The simulation is only done for illustrative purposes. In Appendix E the files used for this simulation is given.

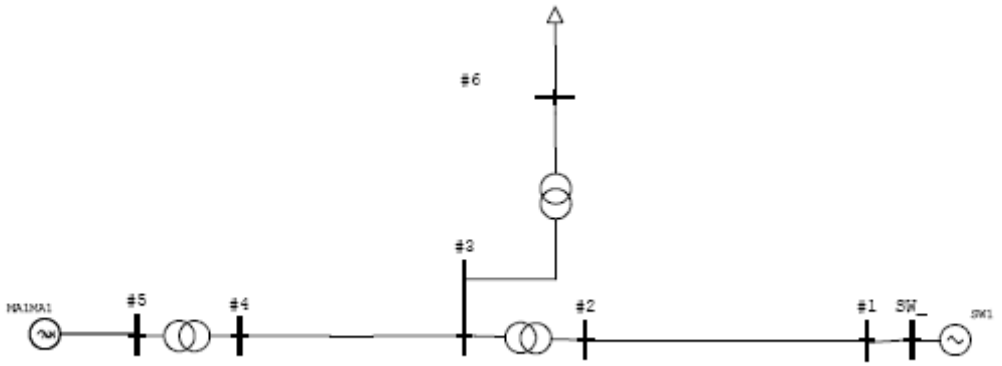

Figure A 1: DFIG test grid

The voltage at the reference bus terminals is altered in order to create controlled disturbances.

Case 0

Case 0 represent a case where the disturbance is not large enough to create a disconnection of the power electronic equipment. By reducing the voltage at the reference bus in DYNPOW to 0.92 pu in 3 seconds, the voltage at the terminals of the DFIG is reduced to a level just above 0.9 pu. The minimum allowed voltage level specified in crow-bar control is 0.9 pu. This disturbance in voltage should therefore not be large enough to cause the crow-bar control to act. To better illustrate what happens during a disturbance, the length of the disturbance is set as long as 3 seconds.

Figure A 2 shows the voltage at the terminals of the DFIG, and the status of the crow-bar resistor. As mentioned in chapter 3.3.4, the status of the resistor is switched from 0 to 1 if the rotor is short-circuited.

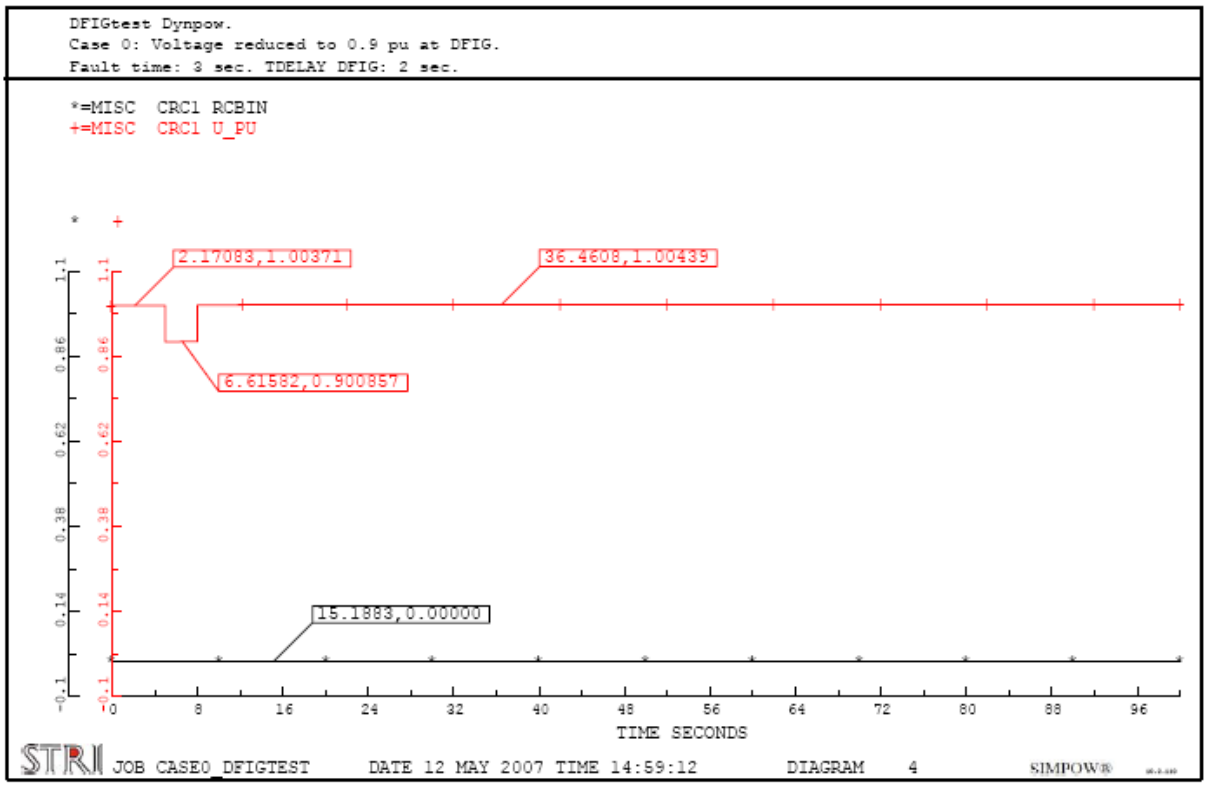

Figure A 2: Voltage at DFIG terminals and status of crow-bar resistor, Case 0

It is obvious from Figure A 2 that this disturbance does not cause the crow-bar control to interfere. The value of R_{cbin} is constant at zero during the whole simulation and the voltage at the DFIG terminals is restored when the reference bus voltage is restored. This is therefore not a disturbance which causes a disconnection of the frequency converter. A voltage just above 0.9 pu at the machine terminals might still be considered to be unacceptable low and damaging for the machine in other ways. However, this is not focus of the simulations in this part of the project and will consequently not be discussed here.

Figure A 3 presents the active and reactive power production from the generator during the disturbance. The active power production is constant during the entire simulation and the reactive power production is at zero in order to keep the power factor at the terminals at unity.

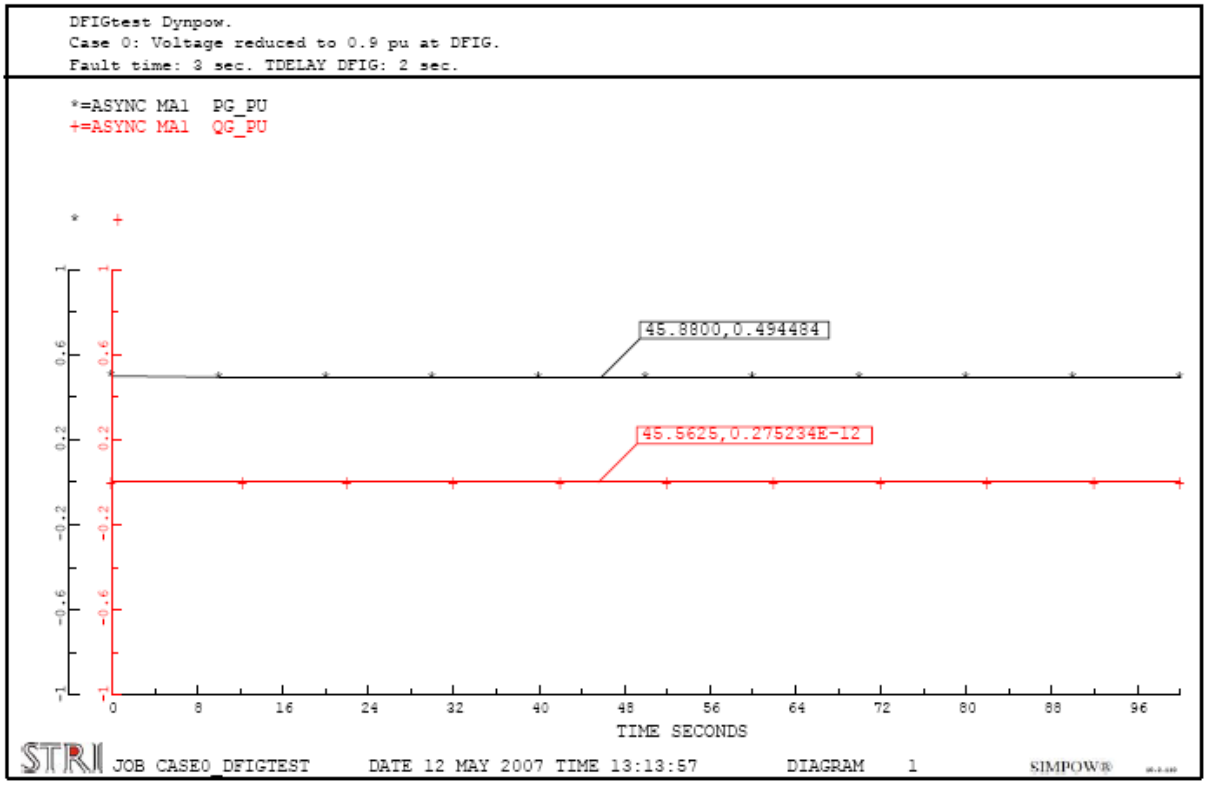

Figure A 3: Active and reactive power production from DFIG during disturbance, Case 0

Case 1

In Case 1 the voltage at the reference bus is reduced to 0.914 pu for 3 seconds. Afterwards, the voltage is restored to 1.0 pu.

The voltage at the DFIG terminals and the status of the crow-bar resistor during this disturbance is illustrated in Figure A 4.

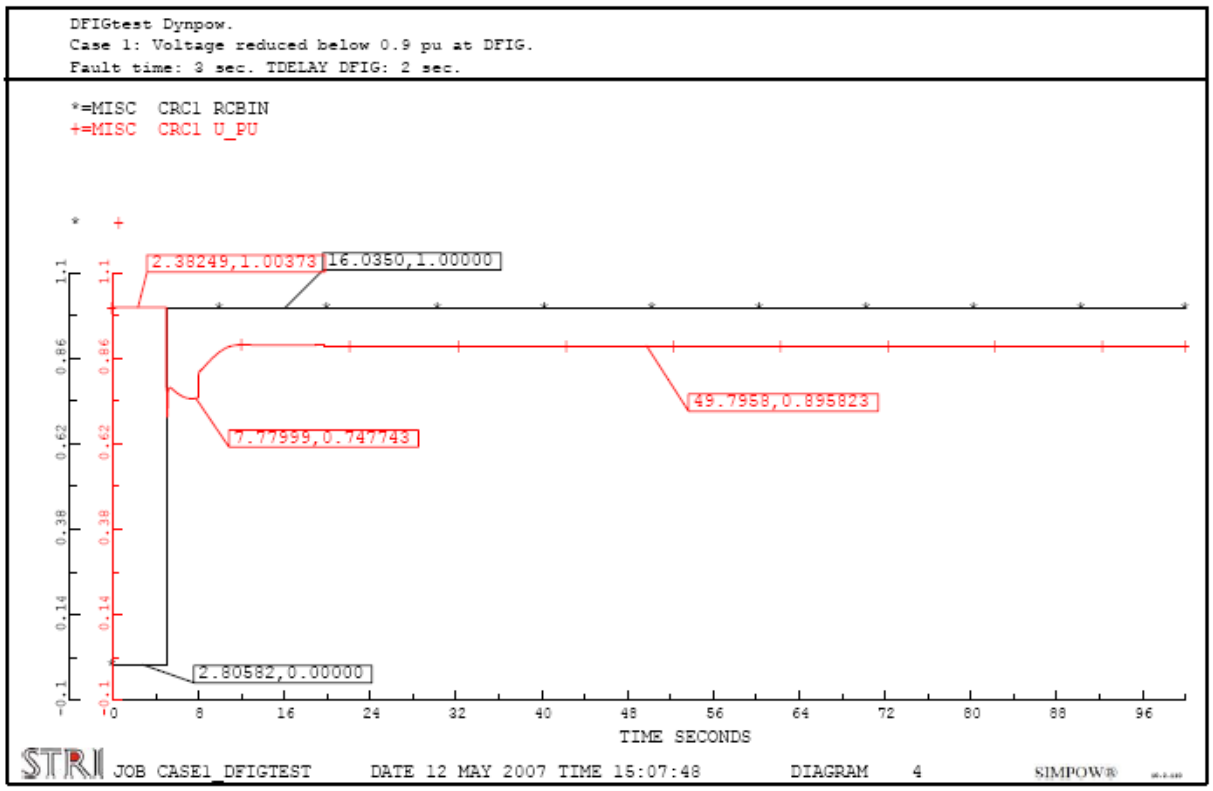

Figure A 4: Voltage at DFIG terminals and status of crow-bar resistor, Case 1

When the disturbance occurs and the voltage at the terminals falls below 0.9 pu, the crow-bar resistor is connected and the frequency converter disconnected. Figure A 4 shows that the voltage at the DFIG terminals does not recover to a value above 0.9 pu after the voltage at the reference bus has recovered to its original value. A consequence of this is that the frequency converter remains disconnected.

Figure A 5 illustrates the active and reactive power production from the DFIG. When the frequency converter is disconnected and the rotor short-circuited, the generator starts to consume reactive power. This coincides with the theory presented in chapter 3.3 where it is stated that a doubly-fed induction generator behaves like a squirrel-cage induction generator if the rotor is short-circuited. The consumption of reactive power is the reason why the voltage at the DFIG terminals is still below 0.9 pu after the voltage at the reference bus has been restored.

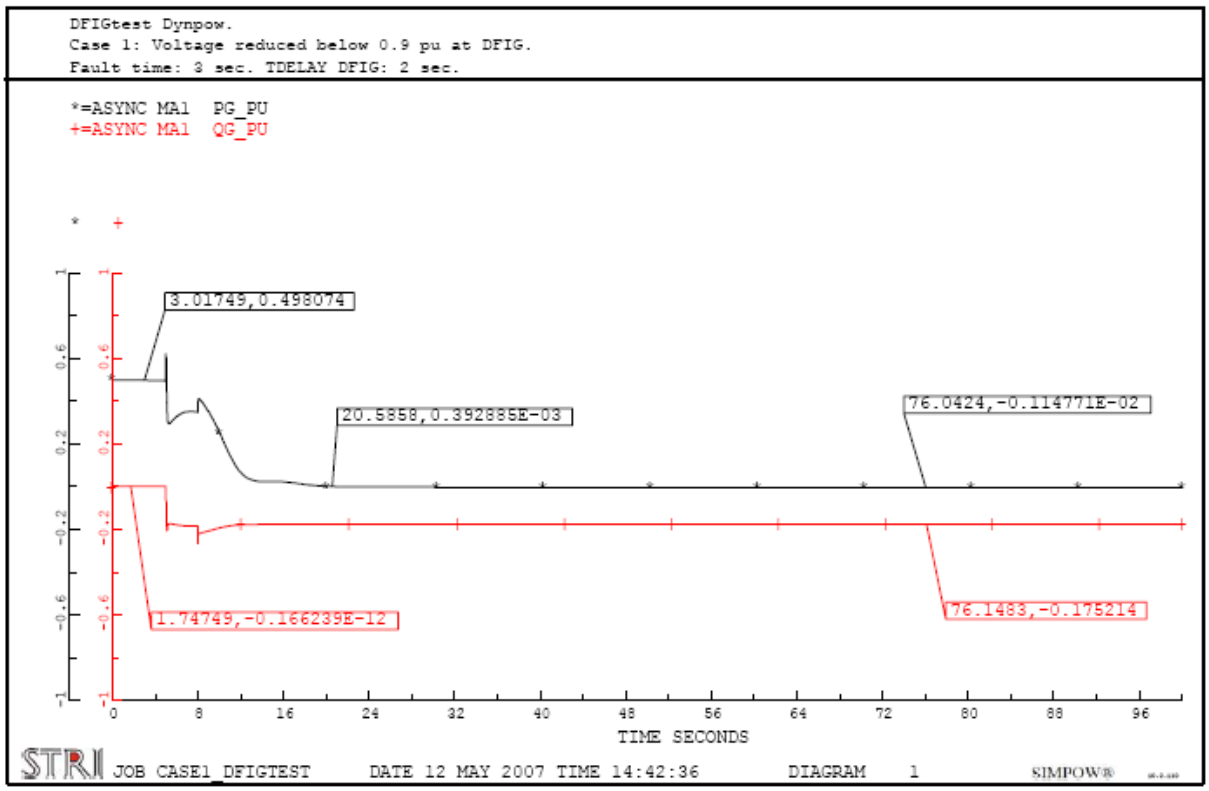

Figure A 5: Active abd reactive power production from DFIG during disturbance, Case 1

Figure A 5 also shows that the active power production goes to zero after approximately 20 seconds. This is due to the pitch control regulator. Figure A 6 describes the blade angle, β, during the simulation.

When a disturbance large enough to create a disconnection of the frequency converter occurs, the speed control system will also be disconnected. In this case, the only speed regulating capability left is the pitch control. This is a fairly slow regulator compared with the speed control regulator. The maximum allowed blade angle change should be between 1 and 2 degrees per second. In these simulations, the allowed change is set to 2 degrees per second. [34]

The pitch control regulator starts to increase the blade angle when the frequency converter is disconnected. This is done to obtain the maximal wind turbine efficiency at the given wind speed. [19]

The pitch control system does not succeed in controlling the turbine speed before it reaches its maximum allowed angle of 27 degrees. This can be seen from Figure A 6. When beta reaches 27 degrees, the mechanical torque reaches zero. [34] This can be seen from the default C_p-curves given in [19].

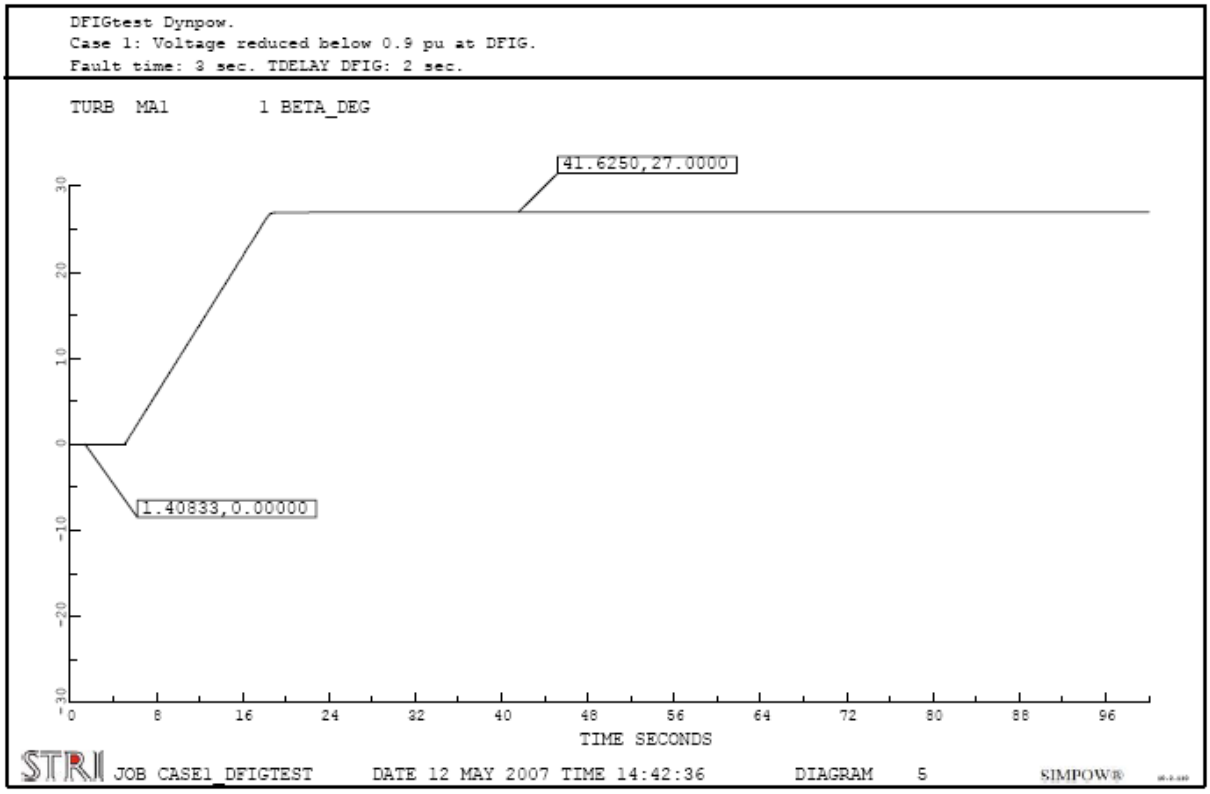

Figure A 6: Blade angle, Case 1

Case 2

From Case 1 it is clear that it is necessary to increase the voltage to a higher level than 1.0 pu after the disturbance in order to raise the voltage at the DFIG terminals to a level above 0.9 pu. The voltage curve of the reference bus in case 2 is shown in Figure A 7. The voltage is first lowered to 0.914 pu for 3 seconds and then raised to 1.08 pu for seven seconds. The time lapse is obtained from trial simulations and is chosen to illustrate the disconnection and connection of the frequency converter.

When the voltage at the terminals of the DFIG has passed 0.9 pu after a disturbance, a timer is started. The timer represents the time delay between the time where the voltage becomes acceptable and the reconnection of the frequency converter. This delay should be between 1 and 10 seconds. [34] In the simulations performed here, the time delay is set to 2 seconds.

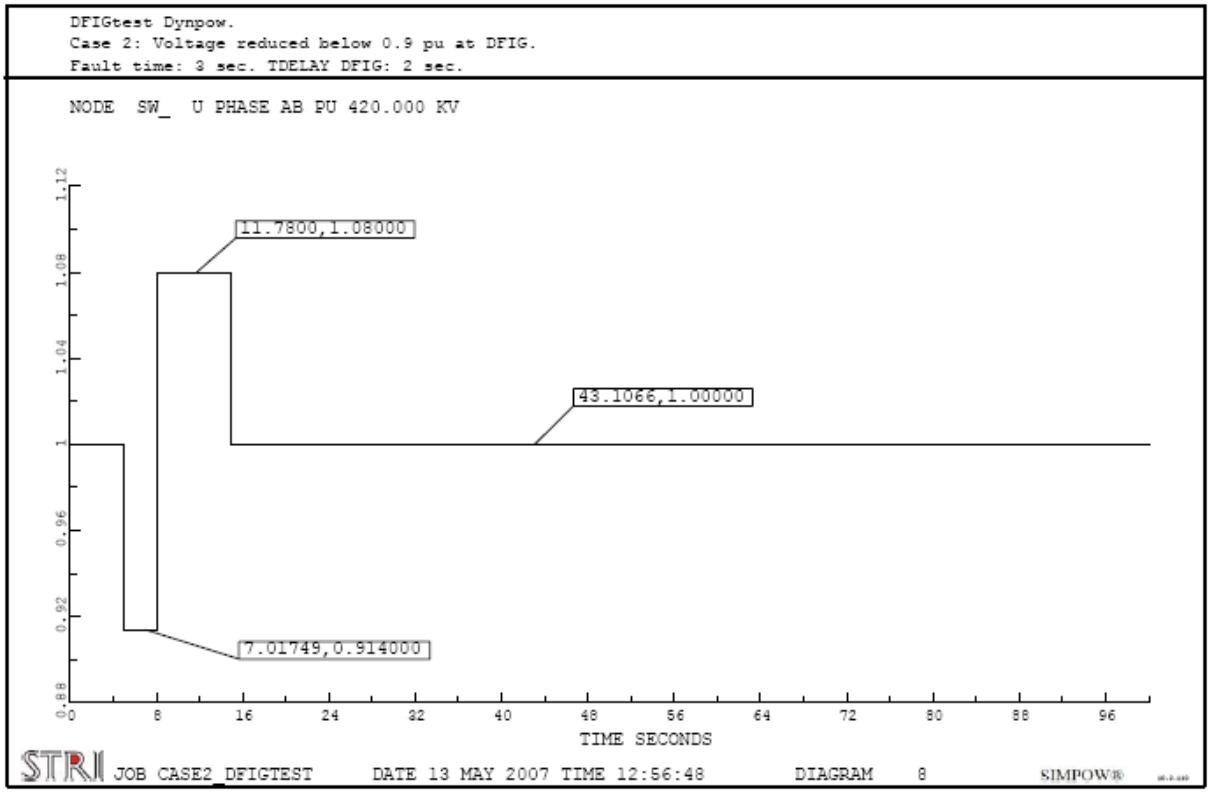

Figure A 7: Reference bus voltage, Case 2

Figure A 8 shows the voltage and the status of the crow-bar resistor before, during and after the disturbance. Like in Case 1, the drop in voltage causes the connection of the crow-bar resistor. However, due to the leap in voltage to 1.08 pu at 8 seconds, the voltage at the DFIG terminals passes 0.9 pu and the status of R_{cbin} is switched back to 0.

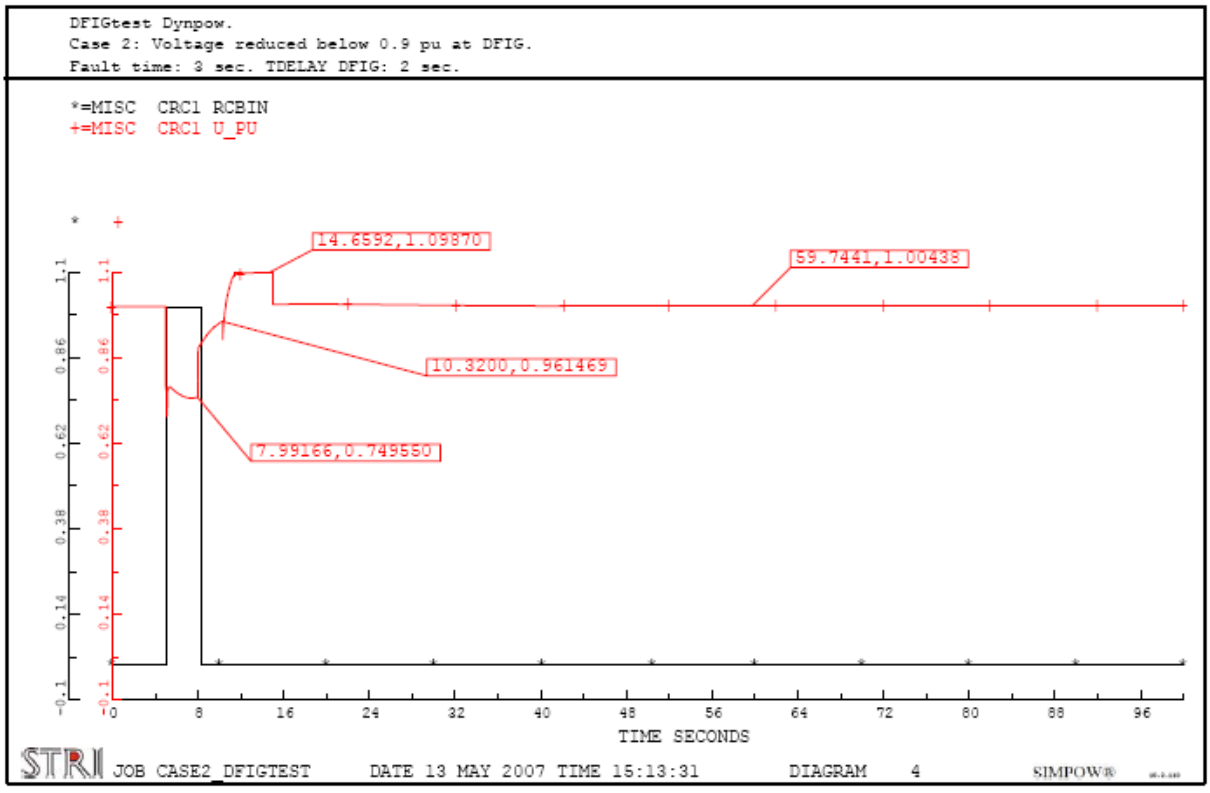

Figure A 8: Voltage at DFIG terminals and status of crow-bar resistor, Case 2

Figure A 9 describes the active and reactive power production from the generator during the simulated time. It should be noted that the frequency converter does not connected when the status of R_{cbin} is changed just after 8 seconds, but waits the specified time delay before it connects. When the frequency converter is connected there is leap in both active and reactive power. The reactive power goes to 0 in order to keep the demand of unity power factor at the DFIG terminals. The leap in active power results in a small drop in voltage at the voltage terminals. This can be seen as a spike at approximately 10.3 seconds in Figure A 8. The drop in voltage can be quite critical because it might result in a voltage at the terminals below 0.9 pu. This will then lead to another disconnection of the frequency converter.

It is also important that the increase in voltage is not too high. If this becomes the case, the voltage at the DFIG terminals after the reconnection of the frequency converter might reach the upper specified limit in the crow-bar control regulator. This will also lead to a new disconnection.

The time delay described above is in this case essential. The time delay will allow the voltage to increase above 0.9 pu before the frequency converter is reconnected.

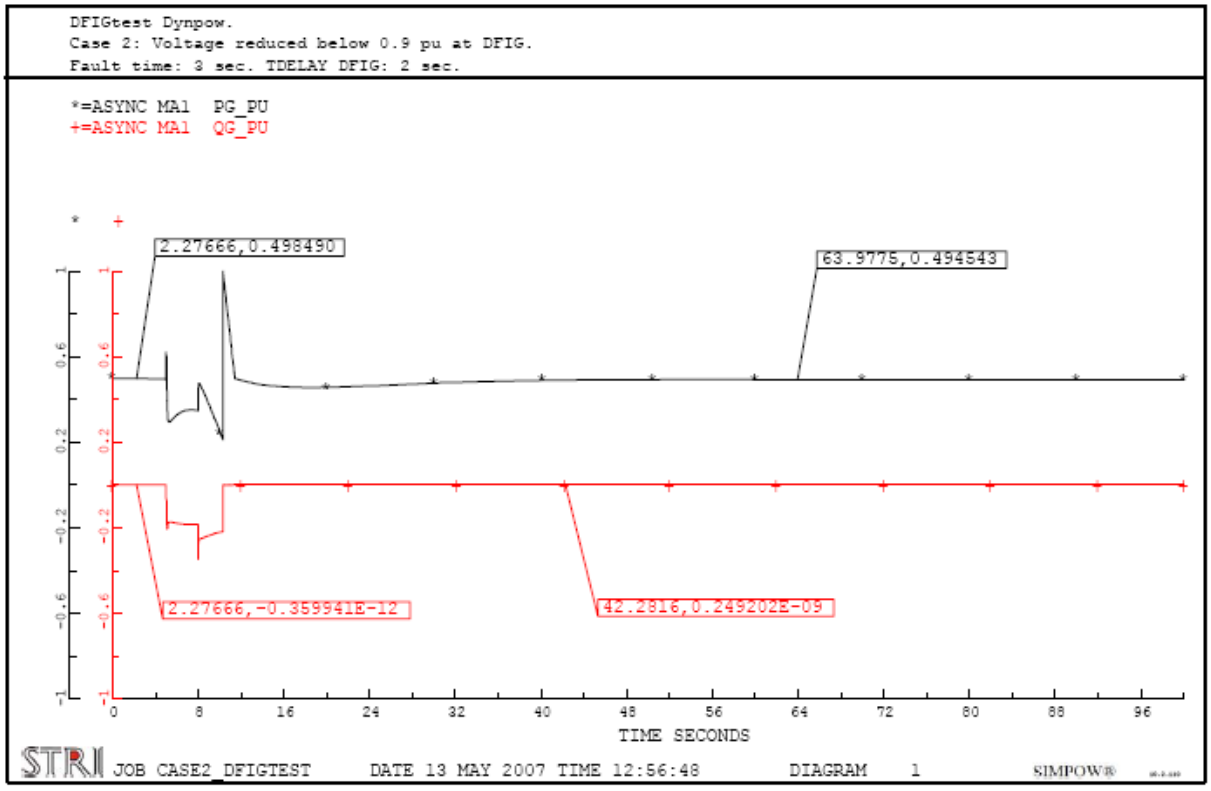

Figure A 9: Active and reactive power production from DFIG during disturbance, Case 2

The increase in reactive power consumption at 8 seconds is due to the leap in voltage described in Figure A 8. This will result in a higher current and higher reactive losses in the generator.

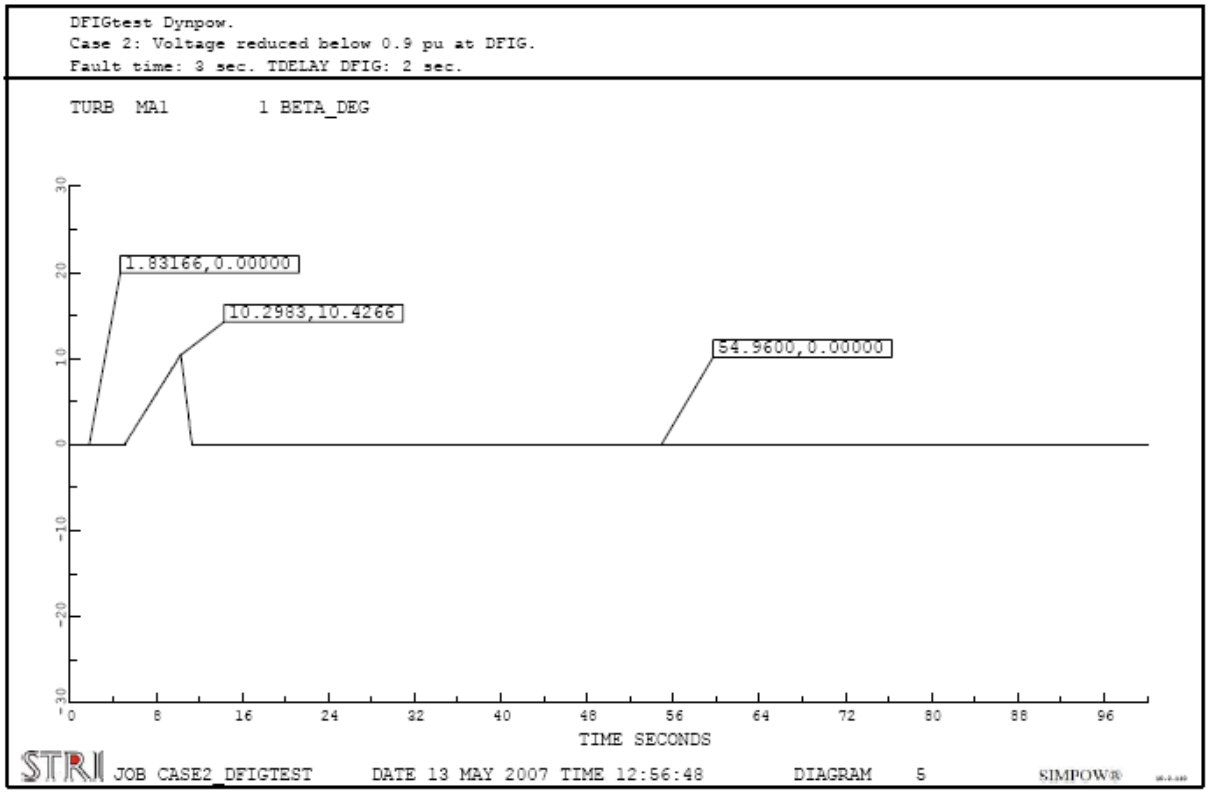

Figure A 10: Blade angle, Case 2

The blade angle is described in Figure A 10. It shows that at approximately 10.3 seconds, the increase in the blade angle is stopped and decreases towards 0. This is because the frequency converter is reconnected and the speed control is being handled by the speed control system.

General

These simulations are carried out to illustrate the behaviour of the doubly-fed induction generator during a drop in voltage at the generator terminals. The simulations have shown that if the DFIG is operated in the unity power factor mode, it has no capability to support the grid if the disturbance is large enough. To the contrary, it can in fact make the situation worse by reducing the voltage even more.

The simulations have also shown that it might not be sufficient to restore the voltages in the grid to their pre-fault values in order to reconnect the frequency converter. This is because in a situation with a disconnected frequency converter, the voltage at the DFIG terminals will be lowered by the reactive consumption of a DFIG. This will, however, depend on the pre-fault values and how much the voltage at the terminals is lowered.

Appendix B

Test of DYNPOW Load Tap Changer Regulators

Description

In the DYNPOW manual, a regulator which can be used in dynamic simulations regarding load tap changers is described. This regulator is called the TREGLTCUAC-regulator. There is also an "unofficial" load tap changer regulator available. This one is not described in the SIMPOW manual, but a description is given in [33]. In order to decide which regulator which is suitable to use in the dynamic model, an evaluation of the two regulators on a small test-grid is performed.

The test grid is made up by a reference bus, a transmission line, a transformer with a load tap changer and a load. A single line diagram from the grid is shown in Figure B 1.

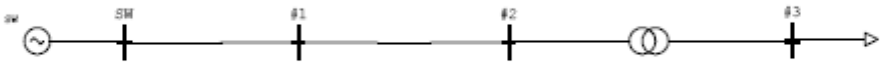

Figure B 1: Test grid for load tap changer transformer regulator

The reference bus and transmission line lies at a voltage level of 22 kV, while the load lies at 0.69 kV.

The transformer has a turn ratio of 22 kV± 8x1.67 % / 0.69 kV. The transformer regulator in OPTPOW is trying to control the voltage at the load to 0.69 kV.

The parameters chosen for the transmission line, transformer and load are typical values in a power grid. Specific sizes are considered to be of minor importance since the purpose of these simulations is to illustrate eventual differences between the two transformer regulators.

The input parameters used for components in this grid can be found in the OPTPOW and DYNPOW files included in Appendix E.

During the test simulations, both the voltage at the reference bus and the load size is varied. The voltage at each side of the transformer will be monitored.

TREGLTCUAC-regulator

The principle for the TREGLTCUAC-regulator is illustrated by Figure B 2. The voltage is controlled by comparing a measured voltage, U, with a reference value, U_0. The difference, ΔU, is compared with a given allowed voltage change, ΔU_s. [23]

If $\Delta U \geq \Delta U_s$, then a step of the tap changer is triggered that decreases the number of winding turns on the tap side in order to increase the voltage on the load controlled side. If $\Delta U \leq \Delta U_s$, a step that will decrease the voltage on the controlled side is triggered. [23]

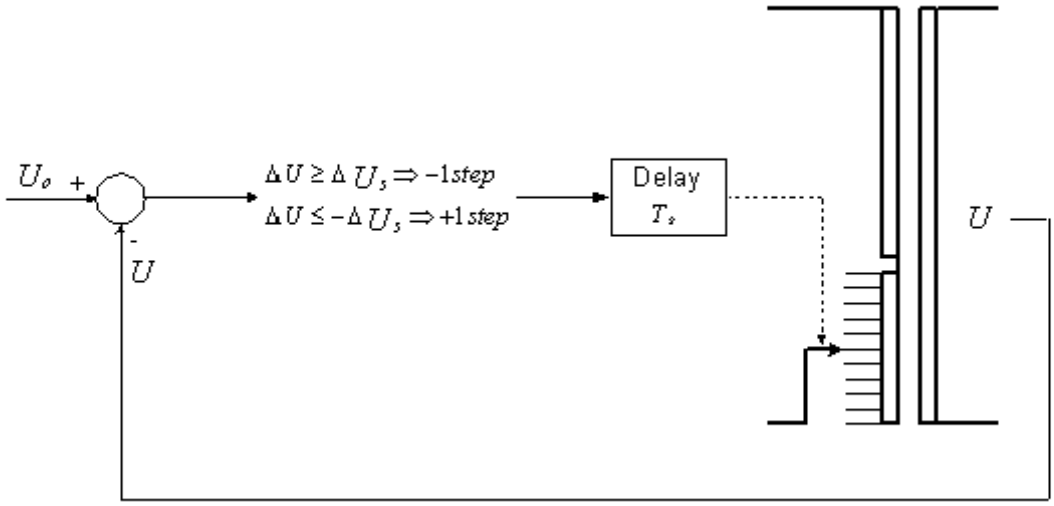

Figure B 2: Control principle for TREGLTCUAC-regulator, from [23]

The regulator model also includes time delays for completing a step. This is done to reduce the number of steps due to short term voltage variations and to illustrate the physical movement of the tap changer. If the step in question is the first step, the time delay will also include a start-up of the motor that manoeuvres the tap changer mechanically. However, if the motor is still operating after a previous step, the time delay will not include this motor start-up, and hence it will be smaller. [23]

For further description of this regulator, see [23].

Test-simulations

The simulations are done on the grid specified in Figure B 1.

The specified allowed voltage change, ΔU_s, is specified in pu of the nominal voltage on the tap side. The size is set to 2 % of the controlled voltage. Since the nominal voltage on the low voltage side is 0.690 kV, this means an allowed voltage change of 0.0138 kV. Referred to the high voltage side the input value is 0.0006273 pu.

The initial time delay is set to 10 seconds whereas the following time delay is set to 4 seconds.

For further details regarding the regulator settings, see Appendix E.

These regulator values are not values that are typical regulator values in a power system with load tap changers at different voltage levels. However, these simulations are for illustrative

purposes only and the exact settings are of minor importance. For details around transformers with load tap changers in power systems, see chapter 3.2.

Case 1.0

In this case the load draws 2 MW and 1 MVAR from the grid.

Table B 1 shows the voltages in the test grid for Case 1.0.

Table B 1: Results from steady-state calculation from Case 1.0

Node	Voltage [kV]
#1	22.0000
#2	21.2418
#3	0.6872

The transformer has stepped two steps down in order to increase the voltage at the load.

More details from the static power flow for this test-grid can be found in the result file from OPTPOW, located in Appendix E.

In the dynamic simulation, the voltage at the reference bus terminals is increased from 1.0 pu to 1.03 pu in a time span of 250 seconds.

The dynamic time lapses for the voltage on both sides of the transformer are shown in Figure B 3 and Figure B 4.

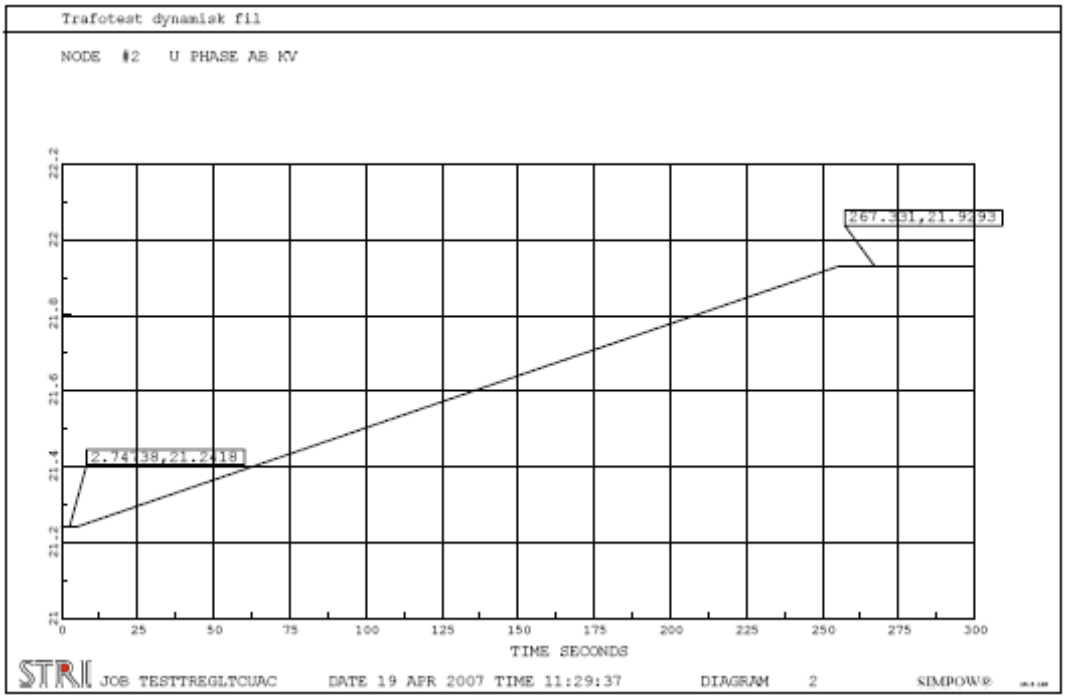

Figure B 3: Voltage on high-voltage side of transformer, Case 1.0

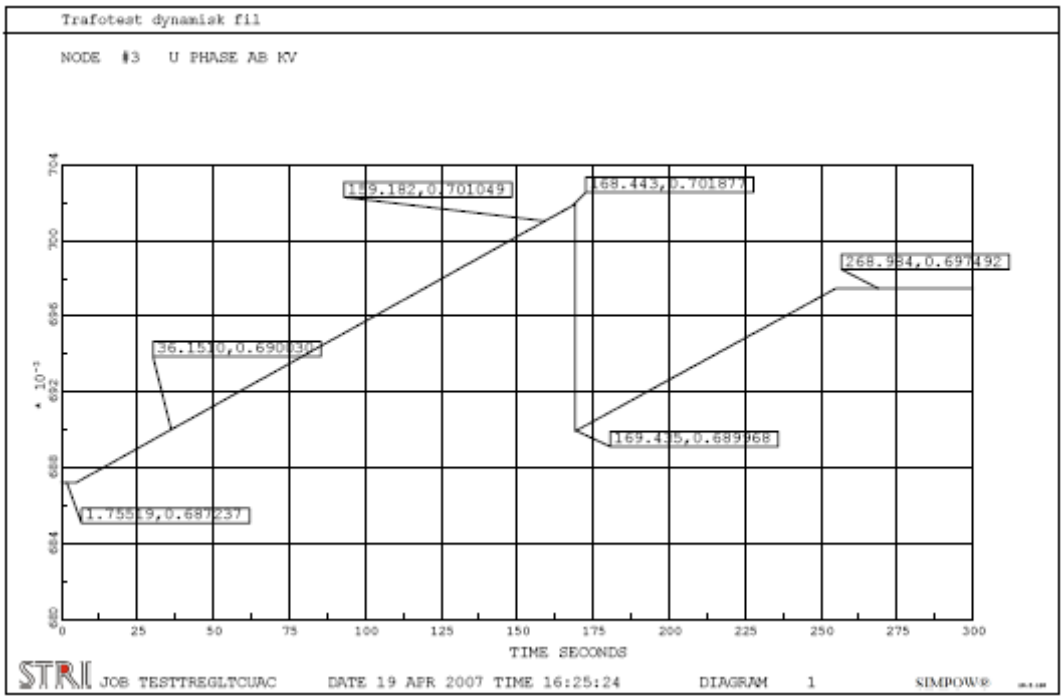

Figure B 4: Voltage on load side of transformer, Case 1.0

The dynamic response on the load-side of the transformer starts at the voltage given by the steady-state power flow. When the voltage reaches 0.7019 kV, the load tap changer steps up one step in order to reduce the voltage on the load side. The end voltage is at an acceptable voltage of 0.6975, which is 1.0109 pu.

The load voltages until the first step is made are shown in Table B 2.

Table B 2: Load voltages, Case 1.0

	Voltage [kV]	Distance to stepping point [kV]
Stepping point	0.7019	-
Starting point	0.6872	0.0147
Reference in OPTPOW	0.6900	0.0119

Table B 2 shows that the TREGLTCUAC-regulator does not consider the specified voltage reference from OPTPOW. The size of the allowed voltage change was set to 0.0138 kV. For this case, the difference in voltage between the OPTPOW-reference and the stepping point was 0.0119 kV. Since there is a time delay on the tap changer, the voltage difference between the stepping point and the used voltage reference has to be larger or equal to the specified allowed voltage change.

Case 1.1

In Case 1.1 the load is increased to 6 MW and 4 MVAR.

Table B 3 shows the voltages in the test-grid for Case 1.1.

Table B 3: Results from steady-state calculations from Case 1.1

Node	Voltage [kV]
#1	22.0000
#2	18.1691
#3	0.6496

The transformer has stepped 8 steps down in order to increase the voltage at the load. This is the maximum number of steps available. The voltage on the 22 kV side of the transformer is unacceptable low and the voltage on the 0.69 kV side is below the specified reference value of 0.69 kV in OPTPOW.

More details from the static power flow for this test-grid can be found in the result file from OPTPOW, located in Appendix E.

In an attempt to restore the voltage levels, the reference bus voltage is increased from 1.0 pu to 1.08 pu in a time span of 250 seconds in the dynamic simulation.

The dynamic time lapses for the voltage on both sides of the transformer are shown in Figure B 5 and Figure B 6.

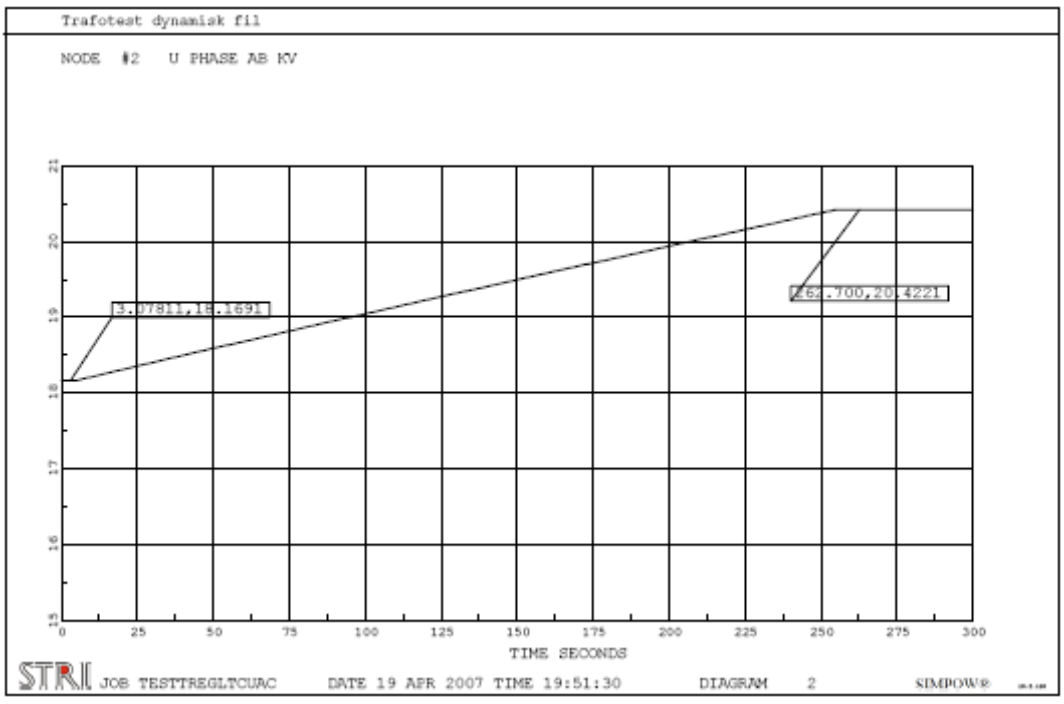

Figure B 5: Voltage on high-voltage side of transformer, Case 1.1

The voltage increase at the reference bus results in an increase in voltage at the high-voltage side of the transformer. If a voltage deviation of 10 % from the nominal voltage is accepted, the voltage goes from an unacceptable level to an acceptable level. This is illustrated by Figure B 6.

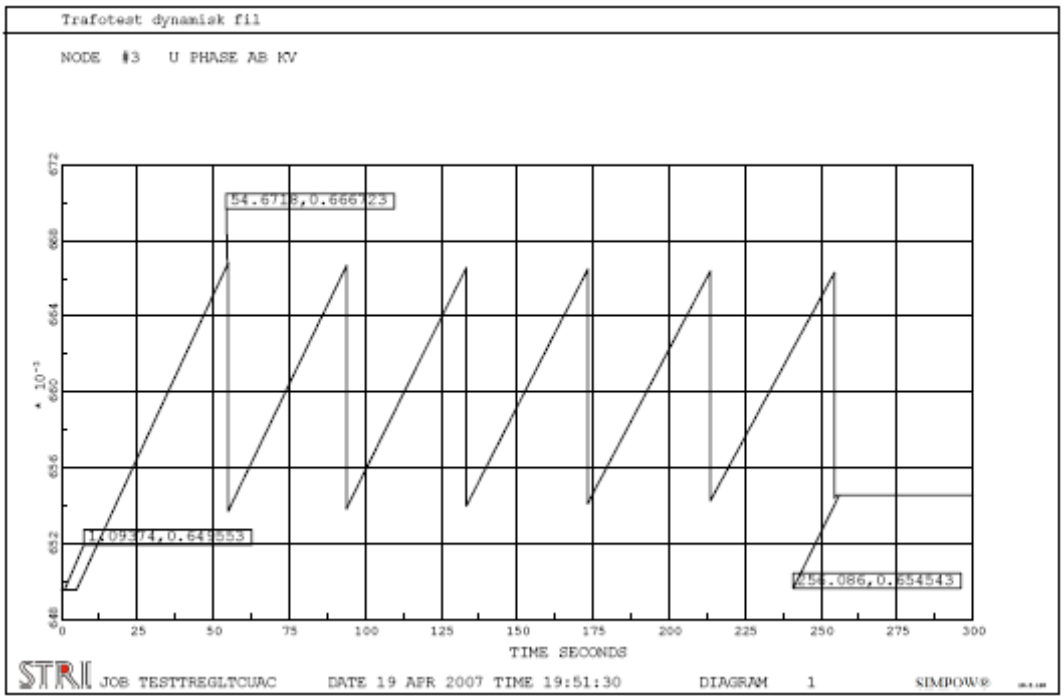

Figure B 6: Voltage on load side of transformer, Case 1.1

As explained in Case 1.0 the TREGLTCUAC-regulator does not use the voltage reference specified for the transformer in the steady-state analysis. Instead, it uses the value calculated in the steady-state-analysis. In cases where the transformer has reached its maximum number of steps in the steady-state analysis, this might have serious consequences in the dynamic simulations.

Table B 4: Load voltages, Case 1.1

	Voltage [kV]	Distance to stepping point [kV]
Stepping point	0.6667	-
Starting point	0.6496	0.0172
Reference in OPTPOW	0.6900	-0.0233

As shown in Figure B 6 and Table B 4, the transformer steps up in order to reduce the voltage on the load before it reaches the reference value specified in OPTPOW. This result in an end voltage that is only slightly improved compared to the situation at the start of the simulation.

Table B 4 shows that the distance between the stepping point and the starting point is larger than in Case 1.0. This is because the increase rate in voltage in Case 1.1 is larger. The time delay is the same in both cases.

Case 1.2

Case 1.2 is based on the same steady-state situation as Case 1.1. The results from the static power flow are given in Table B 3.

More details from the static power flow for this test-grid can be found in the result file from OPTPOW, located in Appendix E.

The DYNPOW-file is also the same as the one used in Case 1.1. However, in this case the dynamic simulation is stopped after the pre-simulation. The reference value, U_0, in the transformer regulator is then changed from the result value in OPTPOW to 0.69 kV (1.0 pu). The voltage responses on both sides of the transformer are given in Figure B 7 and Figure B 8.

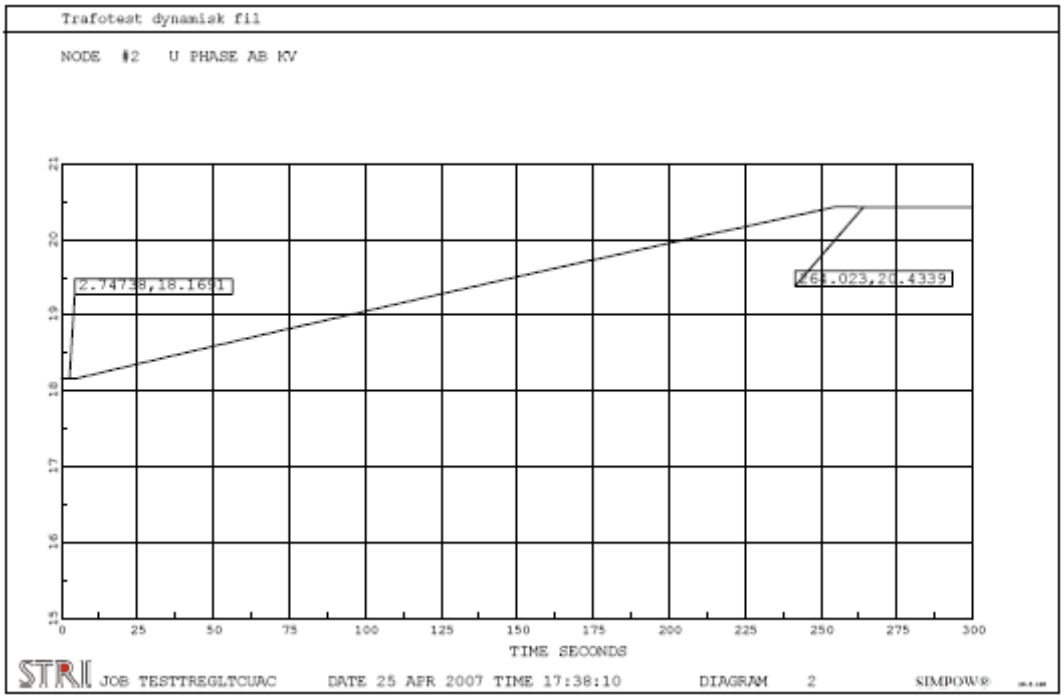

Figure B 7: Voltage on high-voltage side of transformer, Case 1.2

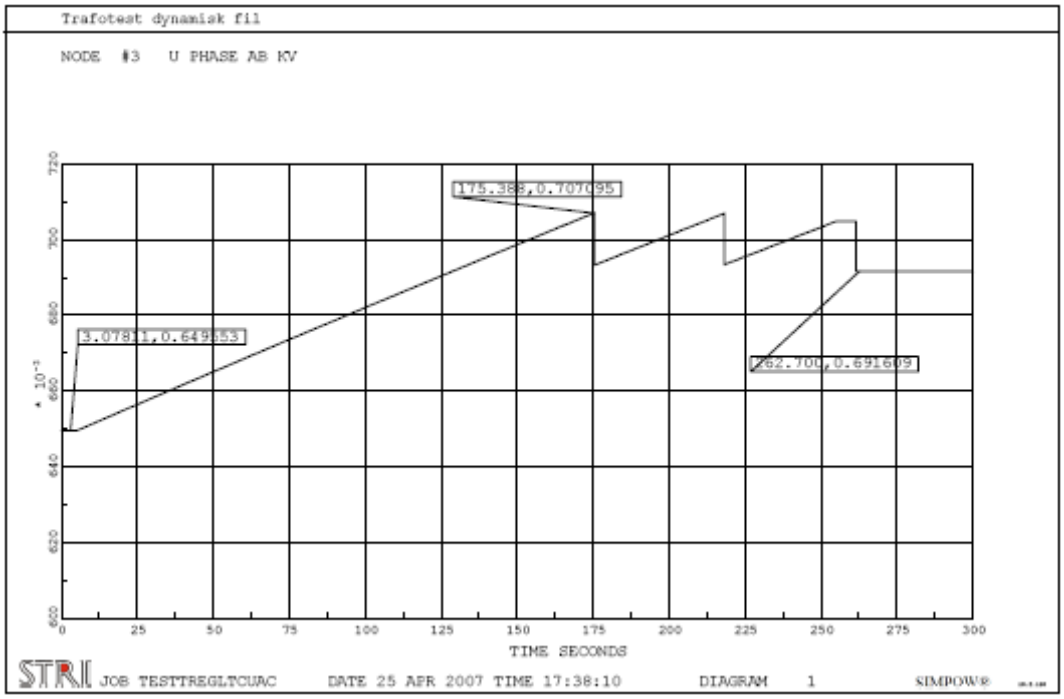

Figure B 8: Voltage on load side of transformer, Case 1.2

When the reference value, U_0, is altered the regulator responds in the desired way. As shown by Figure B 8, the voltage ends up at 0.6916 kV or 1.002 pu, which is close to the reference value.

Table B 5: Load voltages, Case 1.2

	Voltage [kV]	Distance to stepping point [kV]
Stepping point	0.7071	-
Starting point	0.6496	0.0575
Reference in OPTPOW	0.6900	0.0171

It should be noted that if the model is larger than the one used in this case and there is a large number of LTC-transformers, the method applied here would be very inefficient. A specific regulator has to be implemented for each transformer and the reference value for each regulator has to be altered between pre-simulation and simulation. In addition, this has to be done for every simulation.

Beta-regulator

The regulator measures the voltage on the controlled side and compares it to a reference value. If the measured value is within a specified dead band around the reference value, the tap changer is inactive. However, when the voltage is outside the dead band, a timer is started. If the voltage is still outside the dead band after the timer has reached a specified initial timer value, an order to step is given to the tap changer control. The step is performed after a time delay which represents the mechanical delay of the tap changer. If, after the first step, the voltage is still outside the dead band, another step will follow within a smaller time delay than the delay in time before the first step. If the voltage after the second step remains outside the dead band the same procedure is valid for the following steps. [33]

A significant difference between the Beta-regulator and the TREGLTCUAC-regulator is that for the former, it is possible to specify the reference value for the controlled voltage in DYNPOW. This, however, means that a unique regulator must be specified for each transformer, unless several transformers are identical and have the same target voltage. [23] [33]

For further description of the Beta-regulator, see [33].

Test-simulations

The simulations are done on the grid specified in Figure B 1.

The maximum voltage change from the target voltage is set to 2 %. This is the same as the maximum allowed voltage change in the TREGLTCUAC-regulator and gives a dead band of 0.0138 kV in each direction from the target voltage of 0.69 kV.

The initial time delay is set to 10 seconds. The following time delay is set to 4 seconds.

For further details regarding the regulator settings, see Appendix E.

The regulator values applied here are not values that are typical regulator values in a power system with load tap changers at different voltage levels. However, these simulations are for illustrative purposes only and the exact settings are of minor importance. For details around transformers with load tap changers in power systems, see chapter3.2.

Case 2.0

In this case the load draws 2 MW and 1 MVAR from the grid.

The static power flow in Case 2.0 is identical to the static power flow in Case 1.0. The voltages from Case 2.0 can therefore be seen in Table B 1.

The transformer has stepped two steps down in order to increase the voltage at the load.

More details concerning the static power flow for this test-grid can be found in the result file from OPTPOW, located in Appendix E.

In the dynamic simulation, the voltage at the reference bus terminals is increased from 1.0 pu to 1.03 pu in a time span of 250 seconds.

The dynamic time lapses for the voltage on both sides of the transformer are shown in Figure B 9 and Figure B 10.

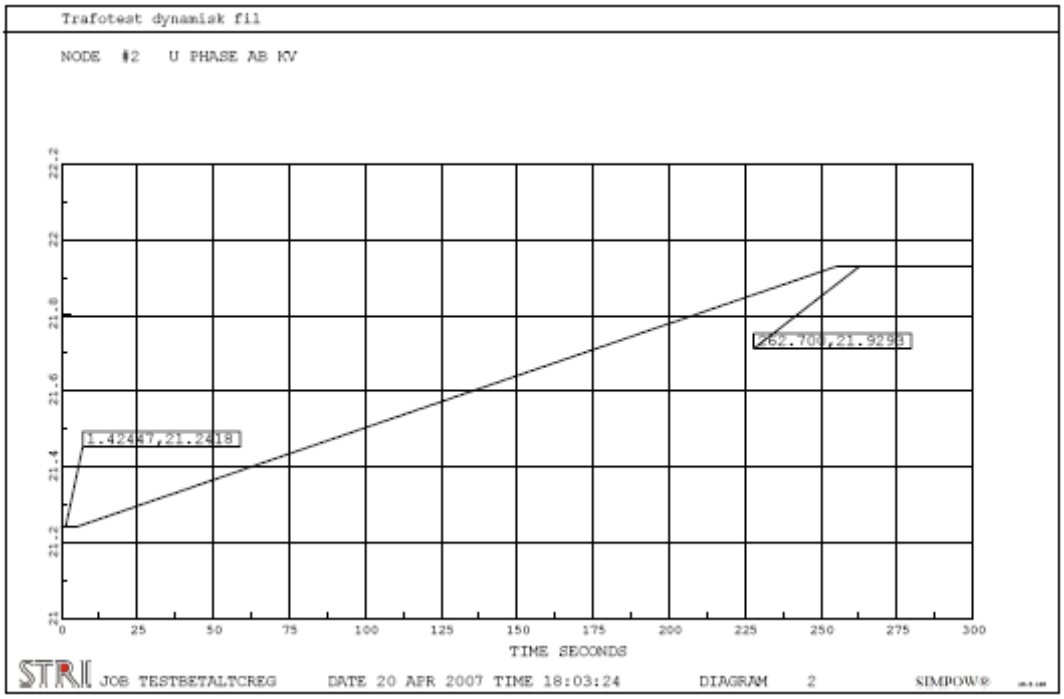

Figure B 9: Voltage on high-voltage side of transformer, Case 2.0

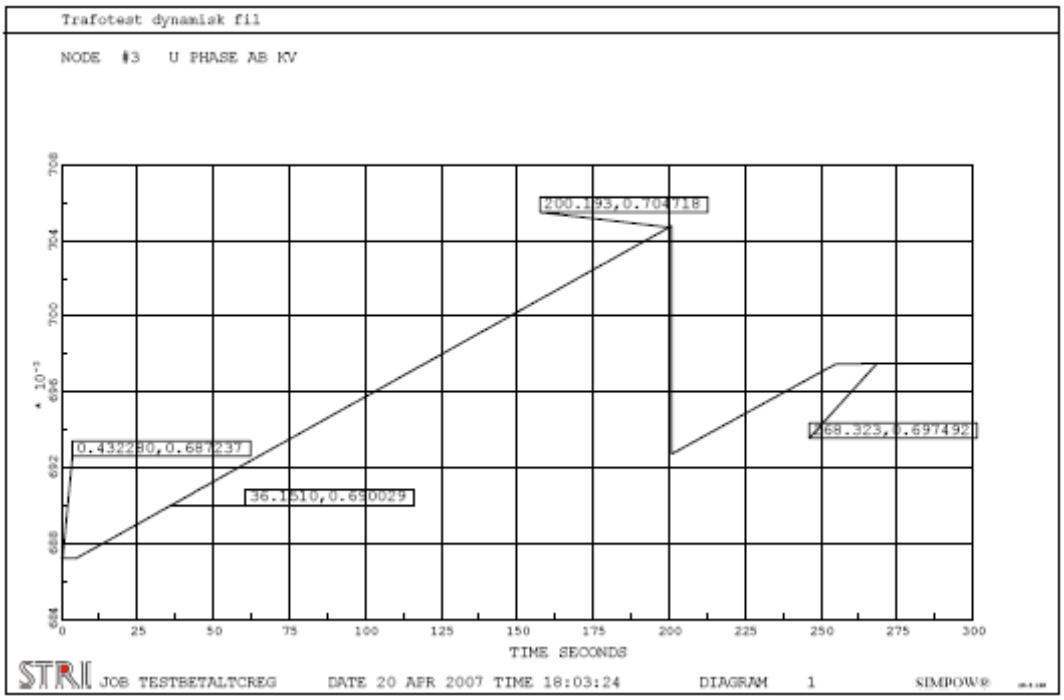

Figure B 10: Voltage on load side of transformer, Case 2.0

Like in Case 1.0, the voltage on the load-side of the transformer starts at the value calculated in the static power flow. When the voltage reaches the value of 0.7047 kV, the load tap changer is stepping up a step in order to reduce the voltage on the load side. The end voltage is at an acceptable voltage of 0.6975 kV, which is equal to 1.0109 pu.

The start, reference and stepping voltages are shown in Table B 6.

Table B 6: Load voltages, Case 2.0

	Voltage [kV]	Distance to stepping point [kV]
Stepping point	0.7047	-
Starting point	0.6872	0.0175
Reference in OPTPOW	0.6900	0.0147

The results from the dynamic simulation in Case 2.0 show that the load tap changer does not step before the voltage has passed the specified reference value and given dead band.

Case 2.1

In Case 2.1 the load is set to consume 6 MW and 4 MVAR. This is equal to Case 1.1.

The results from the power flow are shown in Table B 3 under Case 1.1.

The transformer has in this case stepped 8 steps down in order to increase the voltage at the load. This is the maximum number of steps available. At this tap position, the voltage on the 22 kV side of the transformer is unacceptable low, and the voltage on the 0.69 kV side is below the specified reference value of 0.69 kV in OPTPOW.

More details from the static power flow for this test-grid can be found in the result file from OPTPOW, located in Appendix E.

In the dynamic simulation, the voltage at the reference bus terminals is increased from 1.0 pu to 1.08 pu in a time span of 250 seconds.

The dynamic time lapses for the voltage on both sides of the transformer are shown in Figure B 11 and Figure B 12.

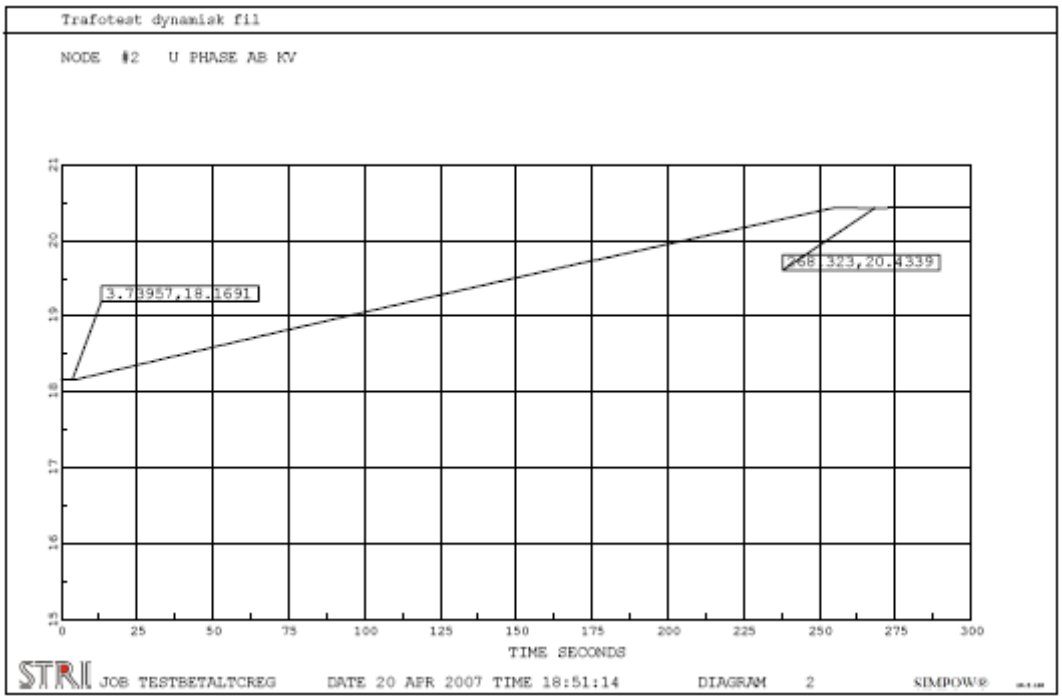

Figure B 11: Voltage on high-voltage side of transformer, Case 2.1

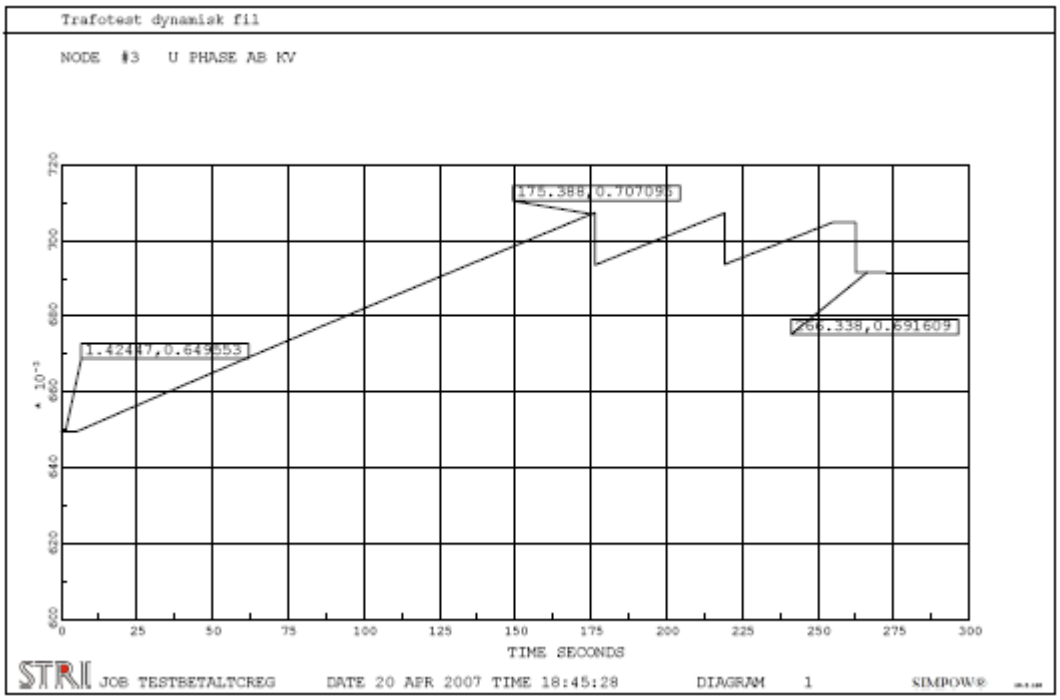

Figure B 12: Voltage on load side of transformer, Case 2.1

The load voltages before the first step is performed are given in Table B 7.

Table B 7: Load voltages, Case 2.1

	Voltage [kV]	Distance to stepping point [kV]
Stepping point	0.7071	-
Starting point	0.6496	0.0575
Reference in OPTPOW	0.6900	0.0171

From Table B 7 it is obvious that this regulator does not use the starting point for the dynamic simulation as a reference for calculating the maximum allowed voltage change.

The distance between the reference point and the stepping point is larger than in Case 2.0. This is because the increase in voltage in Case 2.1 is larger than in Case 2.0.

Figure B 11 shows that the end voltage on the high-voltage side of the transformer is 20.434 kV or 0.929 pu. This is a low, but acceptable voltage if a deviation of 10 % is allowed. On the load-side, Figure B 12 show that the voltage ends up at 0.692 kV or 1.002 pu.

General

Compared with the TREGLTCUAC-regulator, the Beta-regulator seems to be better at improving the voltage on the controlled side if the grid is heavily loaded in the steady-state analysis. As shown in Case 1.2 it would be possible to use both regulators, but in a large model the Beta-regulator is more efficient to use.

Appendix C

Aggregation of Wind Turbines

The basis for the aggregation is the example of a wind turbine given in [19]. The specific size of the turbine is of minor importance. It is the ratio between nominal power, blade length and turbine speed which is interesting.

The aggregation is based on equation (B.1) given in [35]. This equation describes the power output from the captured wind power.

$$P_{out} = \frac{1}{2}\rho\pi R^2 v^3 \left(\eta_{mech} C_P\right) \tag{B.1}$$

Where:

P_{out} = Power in W.

ρ = Air density in kg/m^3.

R = Blade length in m.

v = Wind speed in m/s.

C_P = Rotor power coefficient.

η_{mech} = Mechanical (including electrical) efficiency.

The air density and wind speed will be the same for the aggregated turbine and a real wind turbine. The mechanical efficiency and power coefficient are assumed to be the same if you sum together several turbines. A result of this is that the increase in power output from an aggregated turbine result in an increase in the blade length.

The power coefficient, C_P, is a function of the tip speed ratio, λ, and the blade tip angle, β. In SIMPOW several default $C_P\lambda$-curves for different values of β is specified. These are used in this project.

In order to get the right C_P-value for the aggregated turbines, the value for λ has to be the same as for a single turbine. The value of λ is given by equation (B.2) from [35].

$$\lambda = \frac{\Omega R}{v} \tag{B.2}$$

Where:

Ω = Rotational speed in rpm.

R = Blade length in m.

v = Wind speed in m/s.

The only way to keep the same λ-function at different wind speeds when the blade length is altered, is to alter the rotational speed.

The aggregation of the different turbines is shown below. The nominal power of the aggregated wind turbines are set to be equal to S_N. This is done because no decision is made regarding the choice of generators in the wind farms. It is assumed that the ratio of S_N between the aggregated turbine and the basis turbine will be equal to the ratio of rated power, P_N. Equation (B.1) can then be used to calculate the blade length and rotational speed of the aggregated turbines.

Basis turbine

S_N = 2.05 MVA

Ω = 18.0 rpm

R = 36.0 m

Sleneset

DFIG1 = DFIG2

S_N = 112.5 MVA

Blade length:

$$\frac{P_{Sleneset}}{P_{Basis}} = \frac{0.5\rho\pi R_{Sleneset}^2 v^3 \eta_{mech} C_P}{0.5\rho\pi R_{Basis}^2 v^3 \eta_{mech} C_P} = \frac{R_{Sleneset}^2}{R_{Basis}^2} \tag{B.2}$$

$$R_{Sleneset} = \sqrt{R_{Basis}^2 \frac{P_{Sleneset}}{P_{Basis}}} = 266.69m \tag{B.3}$$

Rotational speed:

$$\lambda = \frac{\Omega_{Basis} R_{Basis}}{v} = \frac{\Omega_{Sleneset} R_{Sleneset}}{v} \tag{B.4}$$

$$\Omega_{Sleneset} = \frac{\Omega_{Basis} R_{Basis}}{R_{Sleneset}} = 2.43rpm \tag{B.5}$$

Sjonfjellet

DFIG3:

S_N = 185 MVA

Blade length:

$$\frac{P_{DFIG3}}{P_{Basis}} = \frac{0.5\rho\pi R_{DFIG3}^2 v^3 \eta_{mech} C_P}{0.5\rho\pi R_{Basis}^2 v^3 \eta_{mech} C_P} = \frac{R_{DFIG3}^2}{R_{Basis}^2} \tag{B.6}$$

$$R_{DFIG3} = \sqrt{R_{Basis}^2 \frac{P_{DFIG3}}{P_{Basis}}} = 341.99m \tag{B.7}$$

Rotational speed:

$$\lambda = \frac{\Omega_{Basis} R_{Basis}}{v} = \frac{\Omega_{DFIG3} R_{DFIG3}}{v} \tag{B.8}$$

$$\Omega_{DFIG3} = \frac{\Omega_{Basis} R_{Basis}}{R_{DFIG3}} = 1.89rpm \tag{B.9}$$

DFIG4:

S_N = 243 MVA

Blade length:

$$\frac{P_{DFIG4}}{P_{Basis}} = \frac{0.5\rho\pi R_{DFIG4}^2 v^3 \eta_{mech} C_P}{0.5\rho\pi R_{Basis}^2 v^3 \eta_{mech} C_P} = \frac{R_{DFIG4}^2}{R_{Basis}^2} \tag{B.10}$$

$$R_{DFIG4} = \sqrt{R_{Basis}^2 \frac{P_{DFIG4}}{P_{Basis}}} = 391.95m \tag{B.11}$$

Rotational speed:

$$\lambda = \frac{\Omega_{Basis} R_{Basis}}{v} = \frac{\Omega_{DFIG4} R_{DFIG4}}{v} \tag{B.12}$$

$$\Omega_{DFIG4} = \frac{\Omega_{Basis} R_{Basis}}{R_{DFIG4}} = 1.65rpm \tag{B.13}$$

Appendix D

Regulator Parameters

Voltage regulator, synchronous machines:

The input values for the voltage regulator for the synchronous machines are given in Table D 1. This regulator is employed in all the dynamic simulations. For parameters not listed, default values are used.

Table D 1: Voltage regulator parameters, synchronous generators

Parameter	
Regulator gain, KA [pu/pu]	30
Regulator amplifier time constant, TA [s]	0.055
Exciter time constant, TE [s]	0.36
Initial value of VR, VR [pu]	0
Regulator stabilizing circuit gain, KF [pu/pu]	0.125
Regulator stabilizing circuit time constant, TF [s]	1.8
Maximum exciter output voltage, UEMAX [pu]	4.0
Minimum exciter output voltage, UEMIN [pu]	-4.0
Saturation Se at Ue=UEMAX, SEMAX	0.4127188
Saturation Se at Ue=0.75·UEMAX, SE75	0.14086

Regulators included in the doubly-fed induction generators:

The input values for the regulators controlling the doubly-fed induction generators are given in the tables below.

Table D 2: Pitch control regulator for DFIG

Parameter	
Gain factor for power control, KPP [pu/pu]	150
Gain factor for in integration of power control, KPC [pu/pu]	3
Gain factor for speed deviation control, KIP [pu/pu]	25
Gain factor in integration of speed deviation control, KIC [pu/pu]	30
Filter time constant, TP [s]	0.3
Maximum blade angle, BMAX [deg]	27
Minimum blade angle, BMIN [deg]	0
Maximum derivative of blade angle, DBDTMAX [deg/s]*	2
Minimum derivative of blade angle, DBDTMIN [deg/s]*	-2
Block of pitch control, BLOCK	0

*In Case 1.1 DBDTMAX is set to 10 deg/s and DBDTMIN is set to -10 deg/s.

Table D 3: Speed control regulator for DFIG

Parameter	
Proportional constant, KS [pu/pu]	0.6
Integration time constant, TPC [s]	0.05
Proportional constant, KP [pu/pu]	3.0
Minimum power order, PMIN [pu]	0.1
Maximum power order, PMAX [pu]	1.0
Minimum time derivative of the power order, DPMIN [pu/s]	-0.45
Maximum time derivative of the power order, DPMAX [pu/s]	0.45
Minimum speed, WMIN [pu]	0.70
Maximum speed, WMAX [pu]	1.50
Coefficient, A2	-0.631
Coefficient, A1	1.379
Coefficient, A0	0.524

Table D 4: Crow-bar control regulator for DFIG

Parameter	
Minimum voltage limit, UMIN [pu]	0.9
Maximum voltage limit, UMAX [pu]	1.1
Time delay at connection of crow-bar resistor, INDELAY [s]	0.0
Block of crow-bar control, BLOCK	0

Table D 5: AC voltage control regulator for DFIG

Parameter	
Gain factor in the controller, KA [pu]	4
Time constant in integrator, TA [s]	0.02
Gain factor in proportional part, KP [pu]	10
Maximum voltage limit, QMAX [pu]	0.3
Minimum voltage limit, QMIN [pu]	-0.3
Block of AC voltage control, BLOCK*	0 / 1

*In cases where the DFIG is operating in power factor control the voltage regulator is blocked.

Regulator employed in static VAR compensators:

SVC regulator employed at Nedre Røssåga, in cases between Case 1.1 and Case 3.2, and at Bardal in Case 1.2 and 2.2.

Table D 6: SVC regulator Nedre Røssåga and Bardal

Parameter	
Maximum value for susceptance, BMAX [pu]	1.2
Minimum value for susceptance, BMIN [pu]	-1.2
Proportional gain, KP [pu]	10
Adaption gain, KA [pu susceptance/pu voltage signal]	15
Filter time constant, TF [s]	0.01
Maximum value VP, VPMAX [pu]	12
Minimum value VP, VPMIN [pu]	-12
Lead time constant, T1 [s]	1.0
Lag time constant, T2 [s]	10

SVC regulator at Bardal, in cases between 3.1 and 5.3, also included in SVCs at Nedre Røssåga in cases between 4.1 and 5.3

Table D 7: SVC regulator at Nedre Røssåga and Bardal

Parameter	
Maximum value for susceptance, BMAX [pu]	1.2
Minimum value for susceptance, BMIN [pu]	-1.2
Proportional gain, KP [pu]	100
Adaption gain, KA [pu susceptance/pu voltage signal]	15
Filter time constant, TF [s]	0.0001
Maximum value VP, VPMAX [pu]	12
Minimum value VP, VPMIN [pu]	-12
Lead time constant, T1 [s]	1.0
Lag time constant, T2 [s]	10

Secondary SVC regulator at Bardal in cases between 4.1 and 5.3

Table D 8: Secondary SVC regulator at Bardal

Parameter	
Gain, KQ [pu]	10
Lead time constant, TC [s]	1.0
Lag time constant, TB [s]	1000
YMAX	0.5
YMIN	-0.5

Appendix E

Electronic appendix.